Two-Dimensional Vibrations of Inflated Geosynthetic Tubes Resting on a Rigid or Deformable Foundation

By

Stephen A. Cotton

Thesis submitted to the Faculty of
Virginia Polytechnic Institute and State University
in partial fulfillment of the requirements for the degree of

MASTER OF SCIENCE
IN
CIVIL ENGINEERING

Approved by:

_____

Raymond H. Plaut, Chairman

_____

George M. Filz

_____

Thomas E. Cousins

April 2003
Blacksburg, Virginia

Keywords: Flood control, flood-fighting devices, geomembrane tube, geotextile, geosynthetic tube, numerical modeling, soil-structure interaction, dynamic response, vibrations

Two-Dimensional Vibrations of Inflated Geosynthetic Tubes Resting on a Rigid or Deformable Foundation

By

Stephen A. Cotton

Dr. Raymond H. Plaut, Chairman

Charles E. Via, Jr. Department of Civil and Environmental Engineering

(ABSTRACT)

Geosynthetic tubes have the potential to replace the traditional flood protection device of sandbagging. These tubes are manufactured with many individual designs and configurations. A small number of studies have been conducted on the geosynthetic tubes as water barriers. Within these studies, none have discussed the dynamics of unanchored geosynthetic tubes.

A two-dimensional equilibrium and vibration analysis of a freestanding geosynthetic tube is executed. Air and water are the two internal materials investigated. Three foundation variations are considered: rigid, Winkler, and Pasternak. Mathematica 4.2 was employed to solve the nonlinear equilibrium and dynamic equations, incorporating boundary conditions by use of a shooting method.

General assumptions are made that involve the geotextile material and supporting surface. The geosynthetic material is assumed to act like an inextensible membrane and bending resistance is neglected. Friction between the tube and rigid supporting surface is neglected. Added features of viscous damping and added mass of the water were applied to the rigid foundation study of the vibrations about the freestanding equilibrium configuration.

Results from the equilibrium and dynamic analysis include circumferential tension, contact length, equilibrium and vibration shapes, tube settlement, and natural frequencies. Natural frequencies for the first four mode shapes were computed. Future models may incorporate the frequencies or combinations of the frequencies found here and develop dynamic loading simulations.

Acknowledgements

I would like to express my sincere gratitude to my primary advisor, Dr. Raymond H. Plaut, for providing immeasurable guidance and assistance. Also, the benefit and opportunity of working with Dr. Plaut has encouraged me to grow more academically and approach all angles of a given topic. I would also like to thank Dr. George M. Filz for his geotechnical insight and research suggestions. I thank Dr. Thomas Cousins, for his presence on my committee and the practical aspect he possesses.

I greatly appreciate the financial support provided by the National Science Foundation under Grant No. CMS-9807335.

Looking back on the work that was accomplished here and the trials that were surpassed, I thank and appreciate my fellow structural engineering students for their ideas and friendship. I would also like to thank my two Tennessee Tech roommates, Josh Sesler and Brad Davidson, for their captivating philosophies and support.

A special thanks is reserved for my fiancée, Gina Kline. All of her patience, support, and encouragement is experienced daily by myself and is treasured tenfold.

Last but certainly not least, I would like to thank my family for all the support, encouragement, and confidence.

Table of Contents

List of Figures

List of Tables

Chapter 1: Introduction and literature review

1.1 Introduction

Water is a calm life-sustaining element commonly used for bathing, quenching of thirst, and generating power. Water composes 75% of our human body and the world. However, when produced by torrential rainstorms with a high intensity of precipitation in relatively small intervals, the element of water transforms into a whole new entity called the flood. Flooding has puzzled the minds of engineers and created some of the most fascinating inventions. Frequently, floods surpass the 100-year storm that practicing hydrologic engineers consider in site design. What can be done in preventing floods after design limits are considered? The concept is simple: control these floods in a manner that minimizes the damage experienced by housing, businesses, loss of life, and the people that rely on the tame bodies of water for a source of revenue.

Flood season in the mid-western United States typically starts in July and ends in September. Also, in low temperature climates, the melting of ice and snow creates a potential for serious flood concerns. Taking into account the minimal indications of flash-flood warnings and thunderstorm watches, the general public has no other means of preparing for a disastrous flood. Many different methods and systems exist that can be used to prevent and protect from flooding. The variety of these systems includes permanent steel structures, earth levees, concrete dams, and temporary fixtures. All techniques have their favorable aspects and opposing attributes. An in-depth look at a temporary fixture that uses self-supporting plastics will be discussed.

In our present society, sandbagging is the most common flood-fighting method of choice. Sandbagging is labor intensive, expensive, and has no reusable components but serves its purpose as being a successful water barrier. Producing a successful sandbag system requires manpower, construction time, and a readily available supply of bags, filling material, shovels, and transport vehicles (Biggar and Masala 1998). Entire communities must come together and stack these sandbags in order to overcome hazards the flood can

inflict. Once constructed and after the flood has subsided, significant time is required to clean the site and dispose of the waste.

The engineering society has identified a new ground-breaking replacement for sandbags. Using geosynthetics (also known as geotextiles or geomembranes) as a water barrier is one efficient method to protect from flooding and prevent destruction to property and loss of life. A source of both ease with regards to installation and efficiency with regards to reuse, geosynthetic tubes are an economical alternative to sandbagging and other flood protection devices (Biggar and Masala 1998). The geosynthetic tubes or sand sausages studied by Biggar and Masala (1998) range in size from 0.3 to 3 m in diameter and can hold back roughly 75% of the tube's height in water. These water barriers can be filled with water, air, or a slurry mixture composed of concrete, sand, or mortar. Currently, there are five configurations offered by the industry. Attached apron supported, single baffle, double baffle, stacked, and dual interior tubes with an exterior covering make up the different types of geosynthetic designs available. Case studies have proven the barriers to be a secure alternative for flood protection.

The evolution of geosynthetic tubes owes it origin to its larger more permanent ancestor, the anchored inflatable dam. "Fabridams" were conceived by N. M. Imbertson in the 1950's and produced by Firestone Tire and Rubber. These dams are anchored along one or two lines longitudinally and used primarily as permanent industrial water barriers (Liapis et al. 1998). Over the years, the evolution of geosynthetics has developed into a more damage resistant material with UV inhibitors and durable enhancements. Liapis et al. (1998) specifies a 30-year life expectancy in lieu of deteriorating ultraviolet rays and floating debris.

Today, geosynthetics have merited their own organization, the Geosynthetic Material Association (GMA). Over 30 companies devoted to producing and researching geosynthetic goods and methods are registered with GMA (2002). Presently, geosynthetics is one of the fastest growing industries.

This thesis analytically studies the dynamics of geosynthetic tubes resting on rigid and deformable foundations. The Winkler soil model was incorporated initially and then upgraded to a Pasternak model, which includes a shear resistance component. The study has been conducted to find "free vibrations" or "natural vibrations" using a freestanding model of both water and air-filled geosynthetic tubes. Once known, these "free vibrations" will predict the frequency and shape of a tube set in a given mode. Future models may incorporate the frequencies found here and develop dynamic loading simulations.

1.2 Literature Review

A small number of studies have been conducted on geosynthetic tubes as water barriers. Within these studies, none have discussed the dynamics of geosynthetic tubes. Growing in popularity, these barriers have the potential to be the only solid choice in flood protection. The following literature review discusses the geosynthetic material, advantages and disadvantages of its use, applications of this material, and results of previous research and analyses.

1.2.1 Geosynthetic Material

Geosynthetics is the overall classification of geotextiles and geomembranes. Geotextiles are flexible, porous fabrics made from synthetic fibers woven by standard weaving machinery or matted together in a random, or nonwoven, manner (GMA 2002). Geomembranes are rolled geotextile sheets that are woven or knitted and function much like geosynthetic tubes. Accounts of in-situ seam sewn sheets are found in Gadd (1988). He recommends that the seam strength should be no less than 90% of the fabric strength. Dependent on the application, the types of base materials used include nylon, polyester, polypropylene, polyamide, and polyethylene. The primary factors for choosing a type of fabric are the viscosity of the slurry acting as fill, desired permeability, flexibility, and of course cost.

Physical properties of these water barriers include the geometry of material, internal pressure, specific weight (950 kg/m^3 in the example in Huong 2001), and Young's modulus (modulus of elasticity). When considering geosynthetic tubes as a three-dimensional form, two quantities represent Young's modulus in orthogonal directions. Three studies that have analyzed or used the modulus of elasticity for a particular geomembrane include: Filz et al. (2001), Huong (2001), and Kim (2003). Filz et al. conducted material property tests at Virginia Tech and concluded that an average modulus of elasticity is 1.1 GPa longitudinally (when stress is under 10 MPa) and 0.34 GPa transversely (when stress is from 10 MPa to 18 MPa). Huong (2001) chose a value of 1.0 GPa, which was derived from Van Santvoort's results in 1995. Kim (2003) studied the effect of varying the modulus of elasticity. Her results conclude that varying Young's modulus does not significantly affect the deformation of the cross-section. Typical geometric dimensions consist of thicknesses ranging from 0.0508 mm to 16 mm, lengths commonly 15.25, 30.5, and 61 m (custom lengths are available), and circumferential lengths typically 3.1 to 14.6 m (www.aquabarrier.com, Biggar and Masala 1998, Huong 2001, Freeman 2002, and Kim 2003).

Geosynthetics can be permeable or impermeable to liquid, depending on their required function. It follows that these tubes can be filled with concrete slurry, sand, dredged material, waste, or liquid and still retain their form. Impermeable geosynthetics are not entirely perfect and some seepage will occur. Huong (2001) stated that the material's permeability rates range from $5x10^{-13}$ to $5x10^{-9}$ cm/s. When permeable, this material may also function as a filter. In the majority of applications, these geosynthetic tubes are exposed to the elements of nature. Gutman (1979) suggested that thin coats of polyvinyl chloride or acrylic be applied to prevent fiber degradation by ultraviolet rays.

As mentioned earlier, five unique designs are currently used as geosynthetic tubes for flood control. The attached apron design consists of a single tube with an additional sheet of geotextile material bonded at the crest of the tube and extending on the ground under the floodwater. The purpose of the apron is to prevent sliding or rolling of the tube. The concept is that, with enough force (produced by the weight of external water)

acting on the extended apron, friction retains the tube in place. A single baffle barrier uses a vertical stiff strip of material placed within the tube. Having a vertical baffle within a thin-walled membrane limits the roll-over and sliding effects by the internal tension of the baffle. The double baffle follows the same concept, only there are two baffles in an A-frame configuration. Stacked tubes are three or more single tubes placed in a pyramid formation. The friction between the tubes and the tube/surface interface counteract the sliding and rolling forces. The sleeved or dual interior tubes consist of two internal tubes contained in an external tube. The interfaces and base of a two-tube configuration produce enough friction between surface and tube that sliding is resisted.

These characteristics of geosynthetic devices can be seen in the goods produced by the following manufacturers: Water Structures Unlimited of Carlotta, California (www.waterstructures.com), Hydro Solutions Inc. headquartered in Houston, Texas (www.hydrologicalsolutions.com), U.S. Flood Control Corporation of Calgary, Canada (www.usfloodcontrol.com), and Superior Dams^{TM}, Inc. (www.superiordam.com).

1.2.2 Advantages and Disadvantages of Geosynthetics

All over the world, floods remain second only to fire as being the most ruinous natural occurrence. A solution to blocking water levels less than 2 m is employing geosynthetic tubes instead of sandbags. Sandbagging may appear inexpensive; yet, tax dollars cover the delivered sand and sandbag material (Landis 2000). Possessing desired attributes, such as quick installation and recyclable materials, these water barriers may dominate the market for the need of controlling floods. Aqua Barrier^{TM} (2002) quotes data from a U.S. Army Corps of Engineers report that installation time of a 3-foot high by 100-foot long tube is 20 minutes compared to the same dimensioned sandbag installment at four hours. The construction of the geosynthetic tube is manned by two personnel, and a five-man crew is needed to assemble the sandbagging system. Geosynthetic units also possess the capability to be repaired easily in the field, and once drained and packed, they provide for compact storage and transport. Liapis et al. (1998) attested that the geosynthetic material

can experience extreme temperature changes and be applied to harsh conditions, yet perform effectively.

Currently, geosynthetic barriers are commonly produced with the following dimensions: one to nine feet high by 50, 100, and 200 foot lengths with an option for custom lengths and variable purpose connectors. Connectors can be created to conform to any arbitrary angle and allow multiple units to be joined in a tee configuration or coupled as an in-line union. The key element of flexibility accommodates positioning the geosynthetic structure on any variable terrain. Using a stacked formation, the level of protection can be increased one tube at a time. With practically unlimited product dimensions, the geosynthetic tube can bear fluid, pollutant, or dredged material at almost any job site (Landis 2000).

While geosynthetic tubes may prove to be the next method to stop temporary flooding, there are a few setbacks. Geosynthetic material is not puncture resistant and therefore circumstances such as hurling tree trunks, vandalism, or problems due to transport may damage them (Pilarczyk 1995). Though the air and water-filled barriers do not possess the problem of readily available filling material, the slurry-filled tubes do. Rolling, sliding, and seepage rank as the top failure modes of installed barriers. The uses of UV inhibitors are necessary to combat the tubes' exposure. Low temperatures freeze the water within the tubes and cause damage if shifted prematurely. The large base, due to its size, may present a problem when placed in a confined area. One true test of geosynthetic tubes was the 1993 Midwest Flood. There are two accounts that describe failures of the sleeved and single configurations. In Jefferson City, Missouri, single design tubes were not tied down adequately and deflected, causing water to pass. The sleeved tube formation in Fort Chartres, Illinois rolled and failed under external water pressure (Turk and Torrey 1993). However, with proper installation and maintenance, these geosynthetic tubes could have a long and successful life, combating the toughest floods.

1.2.3 Geosynthetic Applications

One pioneering solution that uses strong synthetic material was developed fifty years ago by Karl Terzaghi. Using a flexible fabric-like form, Terzaghi poured concrete to construct the Mission Dam in British Columbia, Canada (Terzaghi and LaCroix 1964). Other advantages specific to applications of geosynthetics include: the ability to recharge groundwater, divert water for irrigation, control water flow for hydroelectric production, and prevent river backflows caused by high tides (Liapis et al. 1998). The evolution and adaptation of this geosynthetic material is both outstanding and, in the age of plastics, sensible. Many applications have stemmed from this idea. Geosynthetic material has assisted in water control devices, such as groins, temporary levees, permanent dikes, gravity dams, and underwater pipelines. For recreational purposes, geosynthetic tubes have aided in the forming of breakwaters and preventing beach erosion. An example of preventing beach erosion occurred in 1971 when the Langeoog Island experienced severe eroding of the northwestern beach and barrier dune. The solution was to restore the damage by beach nourishment. Three kilometers of geosynthetic tube were installed 60 m in front of the eroded dune toe. This method worked well for a number of years and only parts of the tubes sank due to the waves' scouring effect (Erchinger 1993). An article in Civil Engineering reported that sand-filled geotextile tubes dampen the force of the waves as they strike the shore at Maryland's Honga River (Austin 1995). In 1995, the U.S. Army Corps of Engineers used two geotubes of woven and nonwoven material for offshore breakwaters serviced in the Baltimore District Navigation Branch. The Sutter Bypass north of Sacramento, California experienced two 100-year floods striking the area in the same month (Landis 2000). Emergency measures were needed, so the U.S. Army Corps of Engineers installed a three-foot-high, 800 feet long geotextile dam. The total duration of saving the Sutter Bypass took seven hours.

Alternate applications include flexible forms for concrete structures, tunnel protection, and grass reinforcement. Geosynthetic tubes have also aided in diverting pollution and containing toxic materials (Koerner and Welsh 1980, Liapis et al. 1998). River isolation, performed for the purpose of contaminated sediment removal, is outlined by Water Structures Unlimited. They produce dual internal tubes encompassed by a larger

superficial tube (www.waterstructures.com). The use of two track-hoes and one 100-foot tube was the removal solution for the contaminated sediment in Pontiac, Illinois.

Water Structures Unlimited is one of several manufacturers in the industry. Hydro Solutions Inc., headquartered in Houston, Texas, is the producer of the Aqua-Barrier system which is comprised of a single baffle or double baffle formation (www.hydrologicalsolutions.com). Aqua-Barrier's system was utilized in a dewatering effort for a construction site at West Bridgewater, Massachusetts in July of 2002. The U.S. Flood Control Corporation makes use of the Clement system of flood-fighting. Gerry Clement, a native of Calgary, Canada has demonstrated his invention by protecting north German museums (www.usfloodcontrol.com). Superior Dams^{TM}, Inc. specializes in producing the VanDuzen Double Tube (www.superiordam.com). The unique design of NOAQ consists of a tube with an attached apron for resisting rollover and sliding which can be exclusively filled with air (www.noaq.com). All designs with the exception of NOAQ's attached apron system needs a heavy fill material, such as water or a slurry mix, to counteract the tube's ability to roll and slide. In the general sense, these types of tubes act as gravity dams. (This list of manufacturers and their designs are not the entire spectrum of the geosynthetic tube industry. Only examples of each individual and unique system were addressed.)

Additional testimonies of the geosynthetic product have been published to describe successful results. For example, these water barriers were used when El Nino hit the Skylark Shores Motel Resort in northern California's Lake County. The manager, Chuck Roof, installed two fronts of these geosynthetic barriers. One three x 240 foot water barrier was installed between the lake and the motel and the second boundary, a four-ft x 100-ft water barrier, was erected in front of the resort's lower rooms. These two water walls not only prevented water from destroying the resort but also made it the only dry property in the area. This accessibility made it possible for the Red Cross and the National Guard to use the resort as a headquarters during their flood relief efforts (Landis 2000). When flood water needs to be controlled, geosynthetic tubes can often perform well (if the water isn't too high).

1.2.4 Previous Research and Analyses

The first system investigated was the inflatable dam, which is a two-point supported structure. A number of analytical and experimental studies have been conducted using this system. Authors include Hsieh and Plaut (1990), Plaut and Wu (1996), Mysore et al. (1997, 1998), and Plaut et al. (1998). Similar assumptions carry over to the formulation of the freestanding geosynthetic tubes. Almost all previous models of geosynthetic devices associate the membrane material with negligible bending resistance, inextensibility, and negligible geosynthetic material weight (water making up the majority of the weight). Most previous models also assume long and straight configurations where the changes in cross-sectional area are neglected. These last two assumptions facilitate the use of a two-dimensional model. Several dynamic studies were conducted by Hsieh et al. (1990) in the late 1980's and early 1990's. Similar to the freestanding tube formulation conducted in this thesis and others, inflatable dams were usually assumed to exhibit small vibrations about the equilibrium shape. Using the finite difference method and boundary element method, the first four mode shapes were calculated. Hsieh et al. (1990) discussed the background of equilibrium configurations and inflatable dam vibration studies in detail.

In Biggar and Masala (1998), a comparison chart of various manufactured product specifications is presented. The length, width, and height of the tube, as well as the maximum height of retained water and the material weight, are presented in this chart. Evaluated in this table are tubes from seven manufacturers with all five previously mentioned designs (apron supported, sleeved, single baffle, double baffle, and stacked tubes). Biggar and Masala (1998) go further to recommend the Clement stacked system (with its ability to extend the system's height) to be the best overall method for fighting floods.

Two studies have been conducted here at Virginia Tech. FitzPatrick et al. (2001) conducted experiments on the attached apron, rigid block supported, and sleeved

formations. Results examine the deformation and stability of tubes under increasing external water levels. Also, physical testing of a 2-1 (2 bottom tubes, 1 top tube) stacked tube configuration and interface tests of reinforced PVC were described by Freeman (2002). Results from the 13 stacked tube trials executed include critical water height and criteria for successful strapping configurations. Individual testing of these water barriers has also been conducted by all previously mentioned manufacturers, which produce specification charts and manuals of their respected product.

Two studies have been conducted using Fast Lagrangian Analysis of Continua (FLAC), a finite difference and command-driven software developed by ITASCA Consultants (Itasca Consulting Group 1998). Huong (2001) modeled a single freestanding tube supported by soft clay. It was found that stresses in the tube were a function of the consistency or stiffness of the soil. Huong also studied the effects of varying pore pressures underneath the tube, and one-sided external water to simulate flooding. In addition, Huong studied the effects of varying soil parameters using a Mohr-Coulomb soil model. Stationary rigid blocks were employed to restrain the freestanding tube configuration from sliding (Huong et. al. 2001). From these models, their shapes, heights, circumferential tension, and ground deflection were reported. Kim (2003) was the second student to employ FLAC. Her studies included the apron supported, single baffle, sleeved, and stacked tube designs. Kim determined critical water levels of the tubes by applying external water.

Seay and Plaut (1998) used ABAQUS to perform three-dimensional calculations
The results obtained consist of the three-dimensional shape of the tube, the amount of contact between the tube and its elastic foundation, the mid-surface stresses that form in the geotextile material, and the relationship between the tube height and the amount of applied internal hydrostatic pressure.

Freeman (2002), comparing his Mathematica coded apron data with FLAC analysis and FitzPatrick's physical apron tests, found that all are in close agreement. Plaut and Klusman (1998) used Mathematica to perform two-dimensional analyses of a single tube,

two stacked tubes, and a 2-1 stacked formation. Friction between tubes and tube/foundation interface was neglected. External water on one side of the single tube and 2-1 formation was considered, and like Huong's (2001) model, stationary rigid blocks were employed to prevent sliding. Two-dimensional shapes, along with heights, circumferential tensions, and ground deflections, were tabulated. A stacked configuration including a deformable foundation was modeled with varying specific weights of the top and bottom tubes. A 2-1 configuration was considered with the two base tubes supported by a deformable foundation. Levels of water in the top tube were varied. An increase in tension and height always accompanies an increased internal pressure head. An increase in the foundation stiffness causes an increase in the total height of the structure and a decrease in tension (Klusman 1998). Models developed by Plaut and Suherman (1998) incorporate rigid and deformable foundations, in addition to an external water load. As seen, many models have been developed and tests were conducted. The tasks of this thesis are to continue the research and explore dynamic effects.

1.2.5 Objective

A powerful mathematical program, Mathematica 4.2, was used to develop the two numerical models (Wolfram 1996). In conjunction with Mathematica 4.2, Microsoft Excel was used extensively as a graphing tool and elementary mathematical solver. The two-dimensional models developed take into consideration water and air-filled tubes, dynamic motion, damping, added mass (where applicable), and deformable foundations. A parametric study was conducted with these two models.

Two freestanding tube models were developed to analyze free vibrations of different internal elements, water and air. For the internal water situation, internal pressure head values specified were 0.2, 0.3, 0.4, and 0.5 and for the internal air case internal pressure values specified were 1.05, 2, 3, 4, and 5. These are normalized values. Both water and air situations were similar in formulation and execution.

The tube itself is assumed to be long and straight, i.e., the changes in cross-sectional area along the tube length are neglected. These two assumptions facilitate the use of a two-dimensional model. With the thickness of the geotextiles being used in these tubes, the weight of material was neglected in the water-filled case and the tube was assumed to act like an inextensible membrane.

The first task was to calculate an initial equilibrium configuration of the tube in the absence of external floodwaters. An internal pressure head, h, was specified and the results from the equilibrium configuration were the contact length, b, between tube and surface, and the membrane tensile force, qe. These values for b and qe were confirmed with the results from Freeman (2002). Once we knew the project was going in the correct direction, we enhanced the model with the introduction of dynamics. Vibrations about the equilibrium shape could be analyzed and the mode shapes and natural frequencies were calculated. Due to the structure's ease to form shapes with lower frequencies the lowest four mode shapes were computed. These four mode shapes are denoted First symmetrical, First nonsymmetrical, Second symmetrical, and Second nonsymmetrical. The set values for the vibration configuration were h, b, and qe. Once the mode shapes were found for their respected h, b, and qe values, extensions to the Mathematica program were developed.

Additional aspects of the internal water model include added mass, damping, and a deformable foundation. The added mass, a, is an approximated account of the resistance of the water internally. Viscous damping, with coefficient ??is attributed to the motion of the material internally. For the deformable foundation, first a tensionless Winkler behavior was assumed, which exerts a normal upward pressure proportional to the downward deflection with stiffness coefficient, k. In the internal air model, damping and a deformable foundation were also incorporated in the same respect. Added mass would not be applicable for the air-filled tube as we defined air as weightless and therefore it would not cause any added mass effect.

Using information discovered in creating the previous literature review, the objective of this research was to analytically study the dynamics of geosynthetic tubes resting on rigid and deformable foundations. Winkler and Pasternak soil models were incorporated to study the effects of placing freestanding water barriers upon deformable foundations. The major goal has been to find the “free vibrations” or “natural vibrations” using a freestanding model of both water and air-filled geosynthetic tubes. Once known, these free vibrations will predict the frequency and shape of a tube set in a given mode. Future models may incorporate the frequencies found here and develop dynamic loading simulations.

Chapter 2: Tube with internal water and rigid foundation

2.1 Introduction

This chapter presents the formulation and results of a water-filled geosynthetic tube resting on a rigid foundation. A number of manufacturers produce geosynthetic tubes with the intention of using water as the fill material. These examples are presented within the Literature Review in section 1.2.3 entitled Geosynthetic Applications.

The analytical tools utilized to develop this model and subsequent models are mathematical, data, and pictorial software. Mathematica 4.2 was used to solve boundary value problems and obtain membrane properties. In Mathematica 4.2 an accuracy goal of five or greater was used in all calculations. The Mathematica 4.2 solutions were transferred (via text file written by the Mathematica code) to Microsoft Excel where they were employed to graph property relationships, equilibrium shapes, and shapes of the vibrations about equilibrium. AutoCAD 2002 was also used in presenting illustrations of free body diagrams and details of specific components of the formulation. All derivations within were performed by Dr. R. H. Plaut.

In section 2.2, the geosynthetic material and the tube's physical assumptions are presented. Section 2.3 defines variables and pictorially displays the freestanding tube considered, laying out the basic equilibrium concepts for arriving at reasonable nondimensional solutions in section 2.4. Once equilibrium is understood and the results are known, the dynamic system is introduced and discussed in section 2.5 with assumptions followed by the formulation layout. Damping and added mass are the two features added to the vibrating structure and are discussed in sections 2.5.1 and 2.5.2, respectively. The results, along with a dimensional case study example, are presented and discussed in section 2.6.

2.2 Assumptions

A freestanding geosynthetic tube filled with water and supported by a rigid foundation is considered. The tube itself is assumed to be long and straight, i.e., the changes in cross-sectional area along the tube length are neglected. These two assumptions facilitate the use of a two-dimensional model. With the small thickness of the geotextiles being used in these tubes, the weight of material is neglected. It also follows that water makes up the majority of the entire system's weight, justifying the assumption to neglect the membrane weight. The geosynthetic material is assumed to act like an inextensible membrane and bending resistance is neglected. Because the tubes have no bending stiffness, it is assumed that they are able to conform to sharp corners.

2.3 Basic Equilibrium Formulation

Consider Figure 2.1, the equilibrium geometry of the geosynthetic tube resting on a rigid foundation. Plaut and Suherman (1998), Klusman (1998), and Freeman (2002) begin with similar equilibrium geometry. The location of the origin is at the right contact point between the tube and supporting surface (point O). Horizontal distance X and vertical distance Y represent the two-dimensional coordinate system. The symbol ? signifies the angular measurement of a horizontal datum to the tube membrane. The measurement S corresponds to the arc length from the origin following along the membrane. X, Y, and ? are each a function of the arc length S. Y_{max} denotes the maximum height of the tube and W represents the complete width from left vertical tangent to right vertical tangent. The character B represents the contact length between the tube material and foundation, and L represents the circumferential length of the entire membrane. Common circumferential lengths range from 3.1 to 14.6 meters (www.aquabarrier.com).

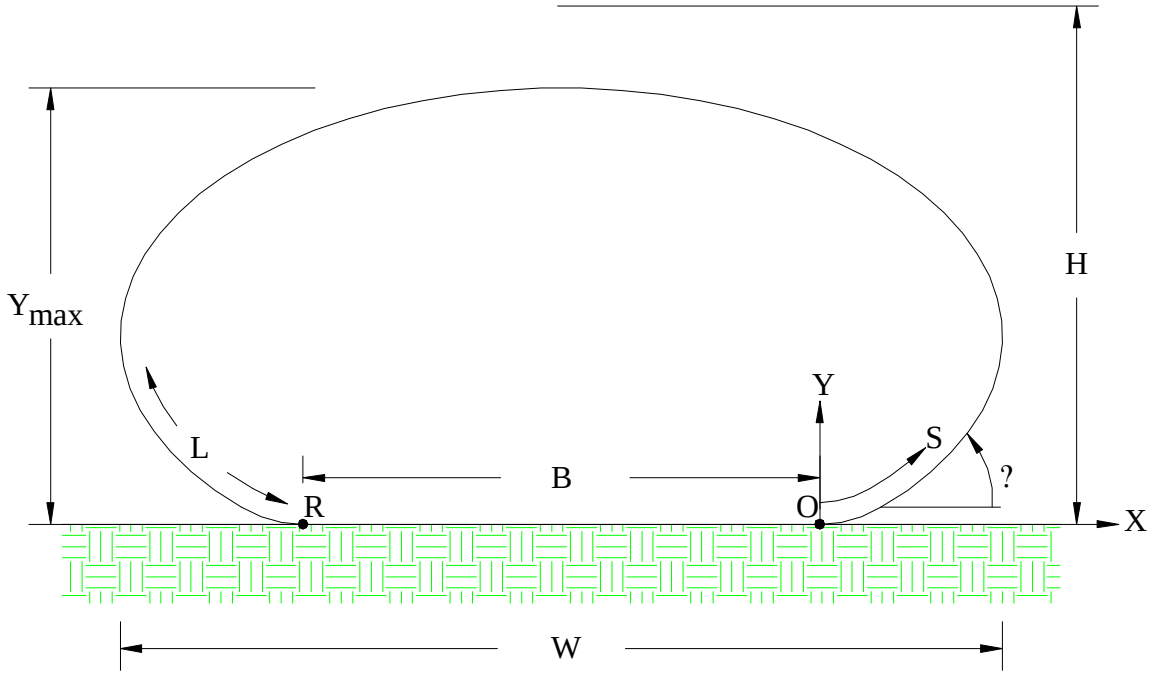

Figure 2.1 Equilibrium configuration

As stated in the literature review, geosynthetic tubes may be filled with air, water, or a slurry mixture (air is modeled in the next chapter). For this reason, the symbol $?_{int}$ represents the specific weight of the fill material (or fluid), which is assumed to be incompressible. Slurry mixtures are generally 1.5 to 2.0 times the specific weight of water (Plaut and Klusman 1998). The internal pressure head H is a virtual measurement of a column of fluid with specific weight $?_{int}$ that is required to give a specified pressure. P_{bot} and P_{top} are the pressure at bottom and top of the tube, respectively. P represents the pressure at any level in the tube. The tension force in the membrane per unit length (into the page) is represented by the character Q.

To relate pressure with the internal pressure head, the two fundamental equations are

$$P ? P_{bot} ? ?_{int} Y, \qquad \text{where } P_{bot} ? ?_{int} H \qquad (2.1, 2.2)$$

Figure 2.2 presents a physical representation of the linear hydrostatic pressure model used.

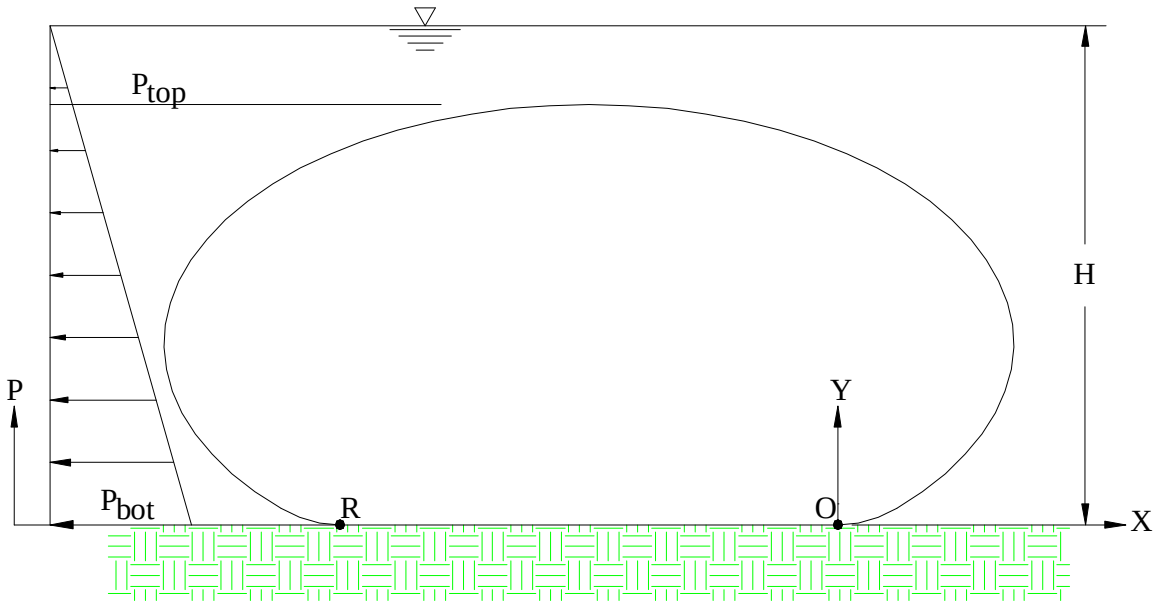

Figure 2.2 Equilibrium hydrostatic pressure

Taking a segment of the two-dimensional tube in Figure 2.1, the following can be derived, where the subscript e denotes equilibrium values:

$$\frac{dX_e}{dS} ? \cos?_e, \qquad \frac{dY_e}{dS} ? \sin?_e, \qquad \frac{d?_e}{dS} ? \frac{?_{int}(H ? Y_e)}{Q_e} \qquad (2.3, 2.4, 2.5)$$

Equations 2.3 through 2.5 describe the geometric configuration of a freestanding geosynthetic tube. Given a differential element the arc length becomes a straight hypotenuse. For example, a change in X would simply be the cosine of the angle between the horizontal coordinate and the arc length. Nondimensional quantities are employed to support any unit system. (An example of using the SI system of units is discussed in section 2.7) This is possible by dividing the given variable by the circumference of the tube or a combination of $?_{int}$ and L:

$$x ? \frac{X}{L}, \qquad y ? \frac{Y}{L}, \qquad s ? \frac{S}{L}, \qquad b ? \frac{B}{L}$$

$$h ? \frac{H}{L}, \qquad q_e ? \frac{Q_e}{?_{\text{int}} L^2}, \qquad p ? \frac{P}{?_{\text{int}} L}, \qquad p_{bot} ? h ? \frac{P_{bot}}{?_{\text{int}} L} ? \frac{H}{L}$$

From Plaut and Suherman (1998), Klusman (1998), and Freeman (2002), the controlling equations become

$$\frac{dx_e}{ds} ? \cos ?_e, \qquad \frac{dy_e}{ds} ? \sin ?_e, \qquad \frac{d?_e}{ds} ? \frac{(h ? y_e)}{q_e} \qquad (2.6, 2.7, 2.8)$$

Alternately to Klusman (1998) and Freeman (2002), a more simplistic approach to derive solutions uses the shooting method. Once governing differential equations are known, the shooting method utilizes initial guesses (set by the user) at the origin and through an iteration process the system "shoots" for the boundary conditions at the left contact point. The shooting method is able to use continuous functions of x, y, and ? to describe the tube's shape. This approach of calculating the equilibrium shapes was efficiently completed with the use of Mathematica 4.2 (Wolfram 1996). With the inclusion of a scaled arc length t, it is possible to begin at $t ? 0$ (at the origin point O) and "shoot" to where $t ? 1$ (point R) making a complete revolution. Therefore, the following equations are derived:

$$t ? \frac{s}{(1 ? b)}, \qquad \frac{dx}{dt} ? (1 ? b)\cos[? (t)] \qquad (2.9, 2.10)$$

$$\frac{dy}{dt} ? (1 ? b)\sin[? (t)], \qquad \frac{d?}{dt} ? (1 ? b)\frac{(h ? y(t))}{q_e} \qquad (2.11, 2.12)$$

The two-point boundary conditions for a single freestanding tube resting on a rigid foundation are as follows:

For the range $0 ? s ? 1 ? b$

@ $s ? 0$ (point O): $x_e ? 0$, $y_e ? 0$, $?_e ? 0$

@ $s ? 1 ? b$ (point R): $x_e ? ? b$, $y_e ? 0$, $?_e ? 2?$

These values are presented in Figure 2.4 and 2.6. The Mathematica program is presented and commented in Appendix A.

2.4 Equilibrium Results

This section covers the results obtained from the previous formulation and execution of the Mathematica file presented in Appendix A. As stated above, the shooting method was used in order to solve the complex array of equations. The evaluation of this equilibrium program required two initial variables to be estimated, contact length b and membrane tension q_e. After a trial and error approach, an initial guess was found to converge. The next step was to record the result and begin the next execution with slightly different initial estimates. Extrapolation was used to some degree when choosing the next guesses of b and q_e. Convergence of the next estimates might depend sensitively on the difference between previous results and the next estimates. To arrive at convergent solutions, a low value for the accuracy goal was taken initially. For instance, an accuracy goal of three was commonly used in the beginning of an initial run, and then the results of this run were taken as the initial guess for the next run with a higher accuracy goal. Due to this repetitive exercise of guessing, a "Do loop" was explored and found to be unsuccessful. The concept of iteration in the shooting method does not lend itself well to the use of a "loop."

Below is a comparison of results from this study (present) and the values obtained from the analysis of Freeman (2002):

	Maximum Tube Height		Contact Length		Membrane Tension	
h	Freeman	present	Freeman	present	Freeman	present
0.2	0.176	0.176	0.306	0.305	0.010	0.010
0.3	0.221	0.221	0.234	0.234	0.021	0.021
0.4	0.246	0.246	0.185	0.185	0.034	0.034
0.5	0.261	0.261	0.152	0.152	0.048	0.048

Table 2.1 Freeman equilibrium parameter comparison (nondimensional)

The parameters are classified by the dependent value of internal water head. The first column of like heading values represents the values from Freeman (2002) and the second column represents the resulting values from this study. All three components are in good agreement with Freeman's previous study, which used a direct integration approach.

This confirmation leads to confident results displayed here and in other subsequent sections and chapters.

Values of h from 0.2 to 0.5 were chosen to compare to previous research. Figure 2.3 displays the different equilibrium shapes with varying internal pressure heads.

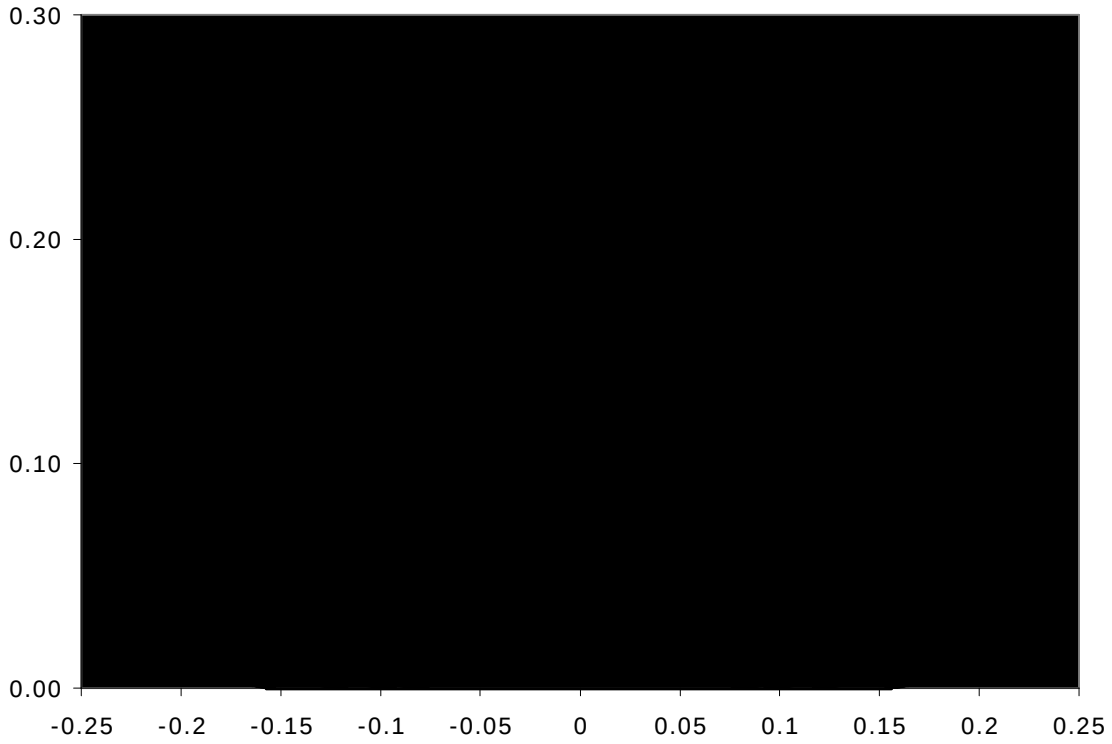

Figure 2.3 Equilibrium configuration

The following are results displayed in graphical form with the abscissas being the set internal pressure head. As discussed in the literature review, the height of external water to be retained by a given geosynthetic tube is a function of the tube's overall height, y_{max} (approximately 75% of the overall height of the tube can be retained). Figures 2.4 and 2.5 illustrate key components that are needed in deciding what tube to select for a particular purpose. The force of the membrane relates to what material composition to choose, i.e., nylon, polyester, polypropylene, polyamide, or polyethylene. The maximum height of the tube relates to what internal pressure is required so that a given height of

retention will be achieved. Intuitively, the tube height y_{max}, membrane tension at origin q_o increase as the internal pressure increases. However, the precise curve could not have been predicted due to the nonlinearity of the governing equations.

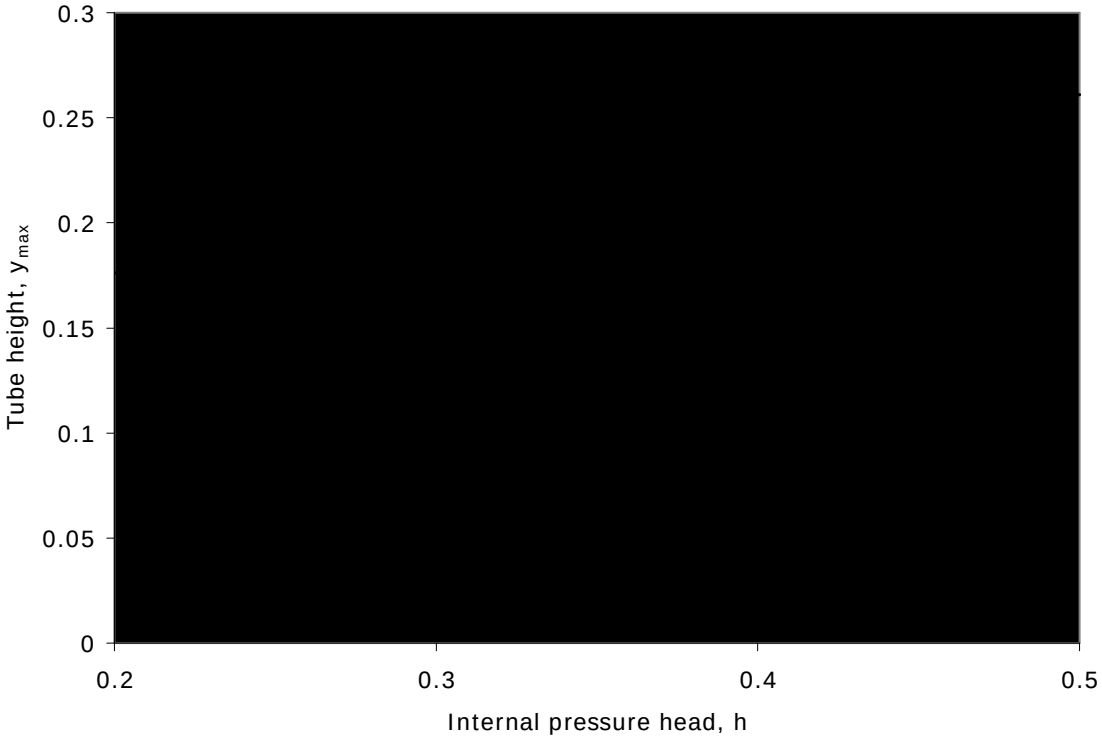

Figure 2.4 Tube height versus internal pressure head

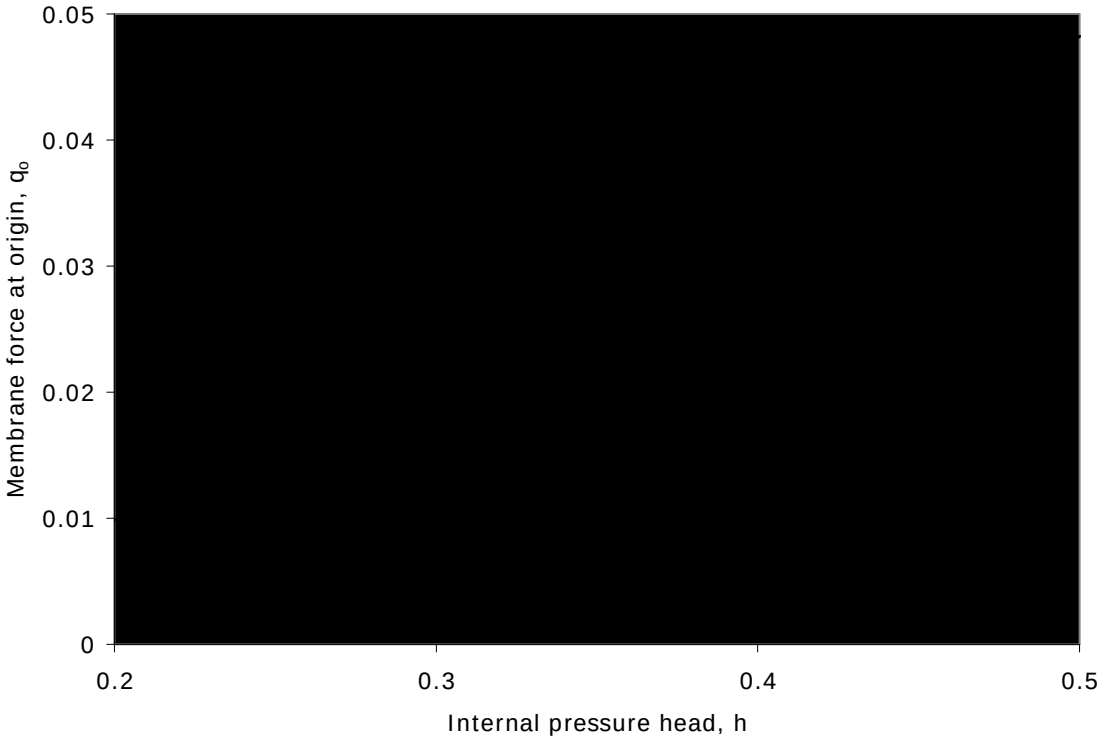

Figure 2.5 Membrane force at origin versus internal pressure head

Figure 2.6 displays the decrease in contact length of the tube with the supporting surface. It is important to know the contact length, since failures often occur when there is not enough friction developed or the tube's supporting base is not broad enough to resist the tube's disposition to roll or slide. The force produced by the weight of the water is greater when a larger contact length is observed. Thus, the smaller the internal pressure head the lower the developed friction force. By the results displayed, it is safe to assume that an internal pressure head higher than 0.5 will result in a lower contact length.

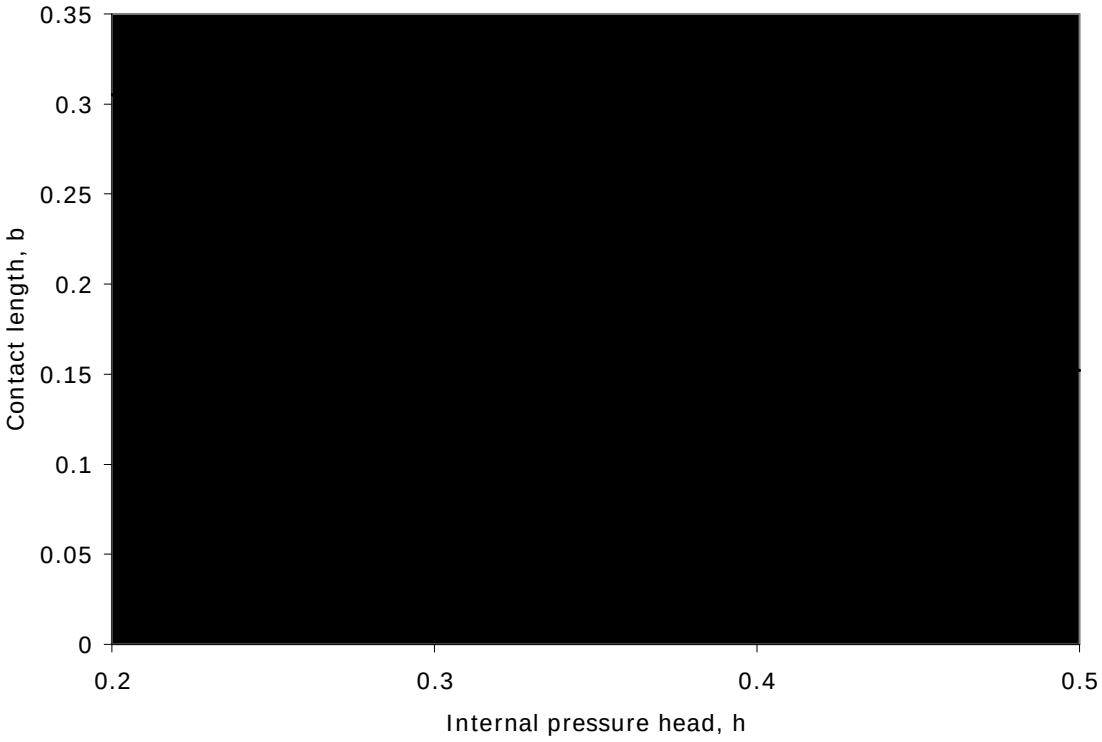

Figure 2.6 Contact length versus internal pressure head

2.5 Dynamic Formulation

The primary goal of vibration analysis is to be able to predict the response, or motion, of a vibrating system (Inman 2001). In this study, consider the free body diagram below in Figure 2.7. D'Alembert's Principle states that a product of the mass of the body and its acceleration can be regarded as a force in the opposite direction of the acceleration (Bedford and Fowler 1999). This results in kinetic equilibrium.

It is important to note that initially in this vibration study damping of the air, fluid, and material are neglected. Later additions to the dynamic model will include viscous damping and an added mass component. These two additions aid in modeling the behavior of the water in a dynamic state. To adequately represent a model of water in a dynamic system, far too many variables would be needed to consider this behavior.

Therefore, to compensate for the complexity of a thorough water model, viscous damping and added mass are introduced.

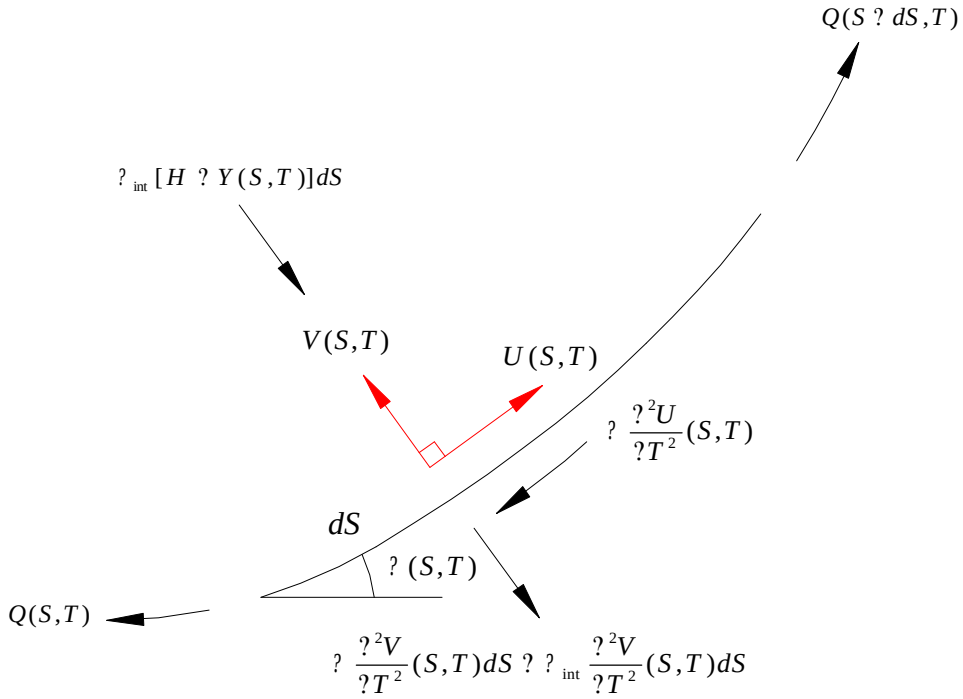

Figure 2.7 Kinetic equilibrium diagram

In the kinetic equilibrium diagram, four new variables are introduced. U and V are the tangential and normal deflections from the equilibrium geometry, respectively. The symbols ? and $?_{int}$ are the mass per unit length of the tube and internal material (in this study water is the internal material), respectively. As in equilibrium, Q represents the membrane tension and ? is the angle of an element. All expressions are a function of the arc length S and time T. The second derivatives of the displacement are the accelerations. Multiplying their accelerations by their respective mass gives a force acting in the opposite direction of this acceleration.

In order to analyze the vibrations about the equilibrium configuration of a single freestanding tube resting on a rigid foundation, consider the element shown in Figure 2.7. Hsieh and Plaut (1989) along with Plaut and Wu (1996) have discussed the dynamic analysis of an inflatable dam which is modeled as a membrane fixed at two points.

Hsieh, Wu, and Plaut's work closely resembles the results produced in the following section. Other than the two anchor points (which support and restrict the inflatable dam to move laterally), motion of an anchored inflatable dam is similar to the motion of a freestanding geosynthetic tube resting on a rigid foundation except for the first mode of the anchored dam (nonsymmetric with one node) which does not occur for the freestanding tube.

When displaced due to vibrations, the change of the X component of the membrane yields

$$X(S,T) ? X_e(S) ? U(S,T)\cos? (S,T) ? V(S,T)\sin? (S,T)$$

and the change in the Y component of the membrane yields

$$Y(S,T) ? Y_e(S) ? U(S,T)\sin? (S,T) ? V(S,T)\cos? (S,T)$$

When vibrations are induced, the changes in pressure can be represented by

$$H ? Y(S,T) ? H ? Y_e(S) ? U(S,T)\sin? (S,T) ? V(S,T)\cos? (S,T)$$

Due to the assumption of inextensibility, the tangential strain is equal to zero. This is described by the expression $\frac{?U}{??} ? V$ (Firt 1983).

Using the chain rule, the above equation becomes

$$\frac{?U}{?S}\frac{?S}{??} ? V \qquad \frac{?U}{??} ? V\frac{??}{?S} \tag{2.13}$$

Now take the kinetic equilibrium diagram (Figure 2.8) and sum the forces in the U and V direction. This respectively produces

$$? \frac{?^2U}{?T^2} ? \frac{?Q}{?S}, \qquad (? \; ? \; ?_{int})\frac{?^2V}{?T^2} ? Q\frac{??}{?S} ? ?_{int}[H ? Y] \tag{2.14, 2.15}$$

Substituting the equation for inextensibility (2.13) into the summation of forces in the V direction (2.15) yields

$$(? \; ? \; ?_{\text{int}})\frac{?^2V}{?T^2} ? \frac{Q}{V}\frac{?U}{?S} ? ?_{\text{int}}[H ? Y] \tag{2.16}$$

Equations 2.13 through 2.16 describe the dynamics of a geosynthetic tube and are considered the equations of motion for this system. For further derivation, it is convenient to nondimensionalize the following quantities:

$$u ? \frac{U}{L}, \qquad v ? \frac{V}{L}, \qquad t ? T\sqrt{\frac{?_{\text{int}}}{?}}, \qquad q ? \frac{Q}{(?_{\text{int}}L^2)}$$

The inertia of the internal material $?_{\text{int}}$ is neglected for now.

Using the nondimensional expressions above, equations 2.14 through 2.16 are written in terms of $\frac{?u}{?s}$, $\frac{?v}{?s}$, $\frac{??}{?s}$, and $\frac{?q}{?s}$. The membrane tension q multiplies the geometric derivatives $\frac{?u}{?s}$, $\frac{?v}{?s}$, and $\frac{??}{?s}$. This process yields

$$q\frac{?u}{?s} ? v[\frac{?^2v}{?t^2} ? h ? y_e ? u\sin? \; ? v\cos? \;] \tag{2.17}$$

$$q\frac{?v}{?s} ? q\sin(? \; ? ?_e) ? u[\frac{?^2v}{?t^2} ? h ? y_e ? u\sin? \; ? v\cos? \;] \tag{2.18}$$

$$q\frac{??}{?s} ? \frac{?^2v}{?t^2} ? h ? y_e ? u\sin? \; ? v\cos? \tag{2.19}$$

$$\frac{?q}{?s} ? \frac{?^2u}{?t^2} \tag{2.20}$$

In the formulation of 2.18, the geometric equation 2.21 was employed, and 2.18 resulted by substituting 2.19 into 2.21, where

$$\frac{?v}{?s} ? \sin(? \; ? ?_e) ? u\frac{??}{?s} \tag{2.21}$$

At this point, it is appropriate to introduce $?$ as the nondimensional frequency. To incorporate dimensions to $?$, the following formula should be used, where $?$ is the dimensional frequency:

$$? \; ? \; ? \sqrt{\frac{?}{?_{\text{int}}}} \tag{2.22}$$

The following set of equations describe the total effect of motion on the equilibrium configuration, where the subscript d represents "dynamic":

$$x(s,t) ? x_e(s) ? x_d(s)\sin ? t, \quad y(s,t) ? y_e(s) ? y_d(s)\sin ? t, \quad ? (s,t) ? ? _e(s) ? ? _d(s)\sin ? t$$

$$u(s,t) ? u_d(s)\sin ? t, \qquad v(s,t) ? v_d(s)\sin ? t, \qquad q(s,t) ? q_e(s) ? q_d(s)\sin ? t$$

The two-point boundary conditions for a single freestanding tube are as follows:

For the range $0 ? s ? 1 ? b$

$$@ s ? 0: \qquad x_d ? 0, \qquad y_d ? 0, \qquad ?_d ? 0, \qquad v_d ? 0$$

$$@ \; s ? 1 ? b: \quad x_d ? 0, \qquad y_d ? 0, \qquad ?_d ? 0, \qquad v_d ? 0$$

In this study we assume infinitesimal vibrations. Therefore, nonlinear terms in the dynamic variables are neglected. For example, the products of two dynamic deflections are approximately zero ($u_d v_d ? 0$ and $v_d v_d ? 0$). It follows that this assumption of small vibrations, along with the substitution of the total geometric expressions above into equations 2.17 through 2.20, produces the following equations:

$$q_e \frac{du_d}{ds} ? (h ? y_e)v_d \tag{2.23}$$

$$q_e \frac{dv_d}{ds} ? q_e ?_d ? (h ? y_e)u_d \tag{2.24}$$

$$q_e \frac{d?_d}{ds} ? ? q_d \frac{(h ? y_e)}{q_e} ? ? ^2 v_d ? u_d \sin ?_e ? v_d \cos ?_e \tag{2.25}$$

$$\frac{dq_d}{ds} ? ?? ^2 u_d \tag{2.26}$$

Equations 2.23 through 2.26 along with 2.7 and 2.8 were written into a Mathematica program and with the boundary conditions above, convergent solutions were calculated. Separate versions of the program were used to obtain symmetric modes and nonsymmetric modes. The concept associated with the differences in symmetrical and nonsymmetrical modes and the Mathematica programs are both presented in Appendix A.

2.5.1 Viscous Damping

The free body diagram in Figure 2.8 includes viscous damping forces. To simulate the presence of damping in the tube and the internal material (in this case water), a nondimensional viscous damping coefficient ? accompanied the original Mathematica code. This subcritical damping is the simplest model from a theoretical perspective. The viscous damper is a device that opposes the relative velocity between its ends with a force that is proportional to the velocity (Inman 2001). The expression for this force is

$$F_c \; ? \; C\frac{?X}{?T} \qquad 2.27)$$

where X is some displacement in any direction. Therefore, F_c is the damping force resulting from the motion of the system and C (kg/s) is the multiplier that relates the force to the velocity.

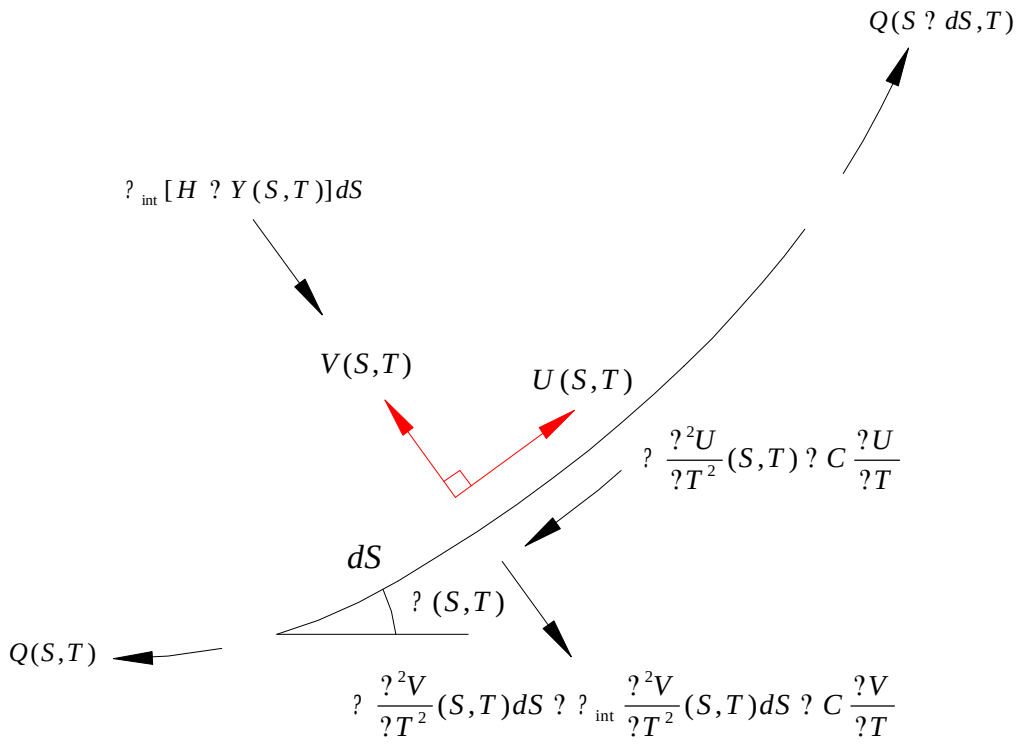

Figure 2.8 Kinetic equilibrium diagram with damping component

In order to apply dimensions to the damping coefficient, the following relation was derived:

$$? \ ? \frac{C}{\sqrt{? \ _{int} \ ?}} \tag{2.28}$$

By replacing the term $? \ ^2$ in equations 2.23 through 2.26 with $? \ ^2 ? \ i? \ ?$, it is possible to incorporate viscous damping in the system.

2.5.2 Added Mass

A second feature was added to model the effect of the inertia of the internal water. If the water field oscillates in the same phase as the tube, the translating membrane will behave dynamically as if its mass had increased by that of the vibrating water (Pramila 1987). Moreover, the water particles are assumed to move only in a plane perpendicular to the

transverse direction of the tube. The nondimensional "added mass" is defined here as

$$a ? \frac{? _{int}}{?} \tag{2.29}$$

However, there is no known precise value for a given fill material and tube property. The added mass component a is only a coefficient representation of this phenomenon.

2.6 Dynamic Results

The following section displays and discusses the results of this vibration study. The plots and tables below represent the lowest four mode shapes for the water-filled case. The four mode shapes fall into two categories: symmetric and nonsymmetric. Symmetric and nonsymmetric refers to the dynamic shape of the tube being symmetrical or nonsymmetrical about the centerline of the equilibrium configuration. This concept is illustrated in Figures 2.10 through 2.13 and is discussed in Appendix A.

As stated earlier, once the equilibrium results (contact length b and membrane tension q_e) are known (via the shooting method described in section 2.4 and presented in Appendix A) the vibration about the original configuration can be calculated. The results from this dynamic computation include the frequency ? ?tangential deflection u at s = 0 (i.e., $u ? u_d(0)$), and Cartesian coordinates x and y. Similar to the procedure in obtaining the contact length and membrane tension at the origin, the dynamic problem also employed the shooting method with the unknown parameters ? and u. The Mathematica code used to calculate the dynamic parameters is presented in Appendix A. Table 2.2 presents the calculated frequencies for the given internal water heads.

h	1st Sym. Mode	1st Nonsym. Mode	2nd Sym. Mode	2nd Nonsym. Mode
0.2	1.160	1.629	2.123	2.623
0.3	1.359	2.096	2.806	3.486
0.4	1.577	2.512	3.384	4.202
0.5	1.769	2.881	3.906	4.831

Table 2.2 Frequencies (?) for tube with internal water and rigid foundation

The results are plotted in Figure 2.9. As the height of the tube increases, the frequencies rise nearly linearly. Figures 2.10 through 2.13 show the mode shapes (in black) transcribed over the equilibrium configuration (in red) for the cases h = 0.2, 0.3, 0.4, and 0.5, respectively. Damping is not considered. A coefficient, c, was used in order to obtain an amplitude of the vibration mode which would provide an appropriate separation between the equilibrium shape and the dynamic shape.

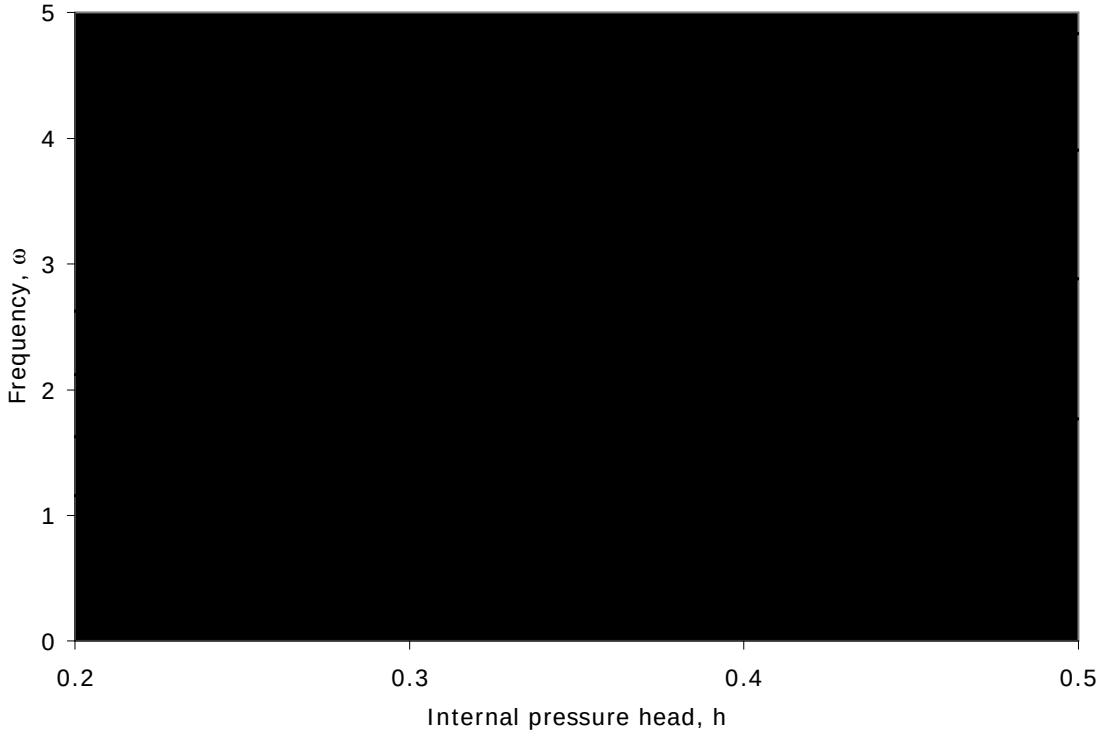

Figure 2.9 Frequency versus internal pressure head

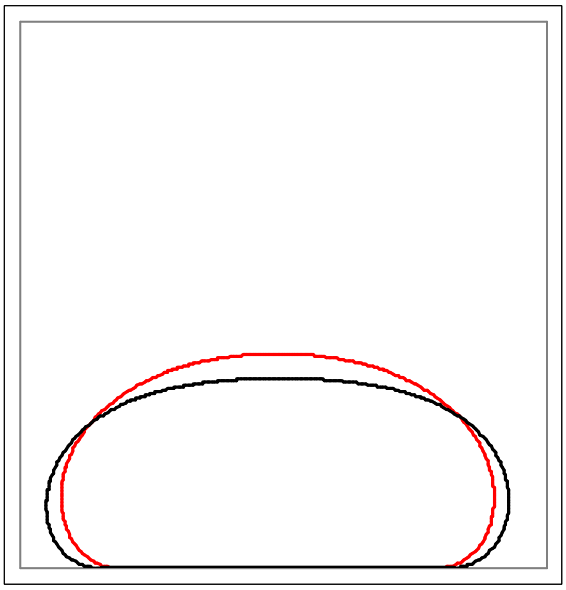

(a) 1st symmetrical mode

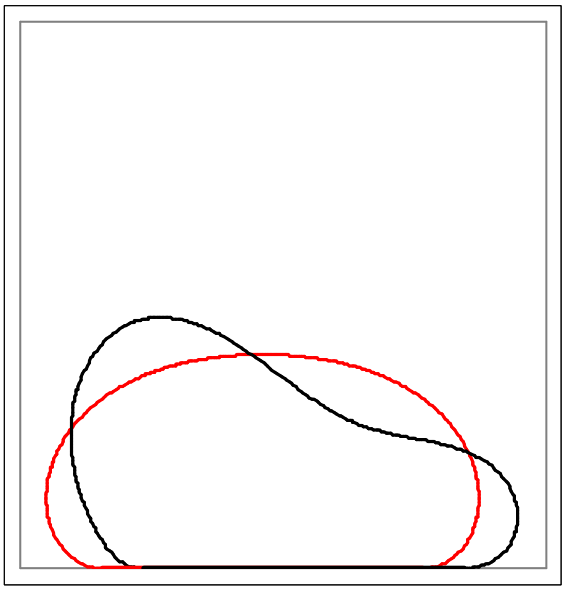

(b) 1st nonsymmetrical mode

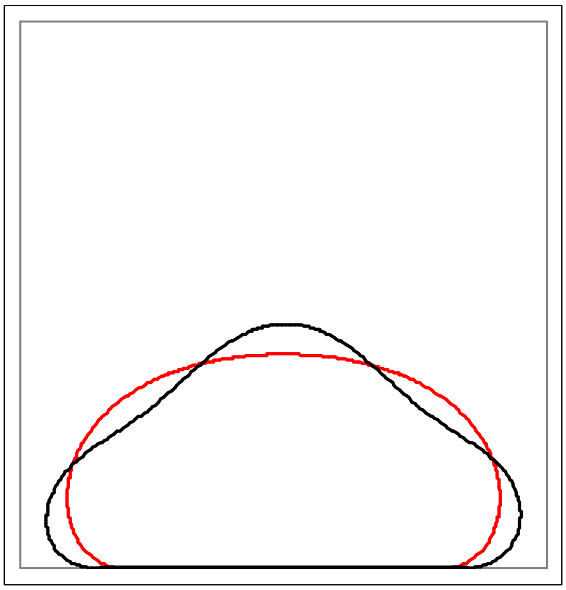

(c) 2nd symmetrical mode

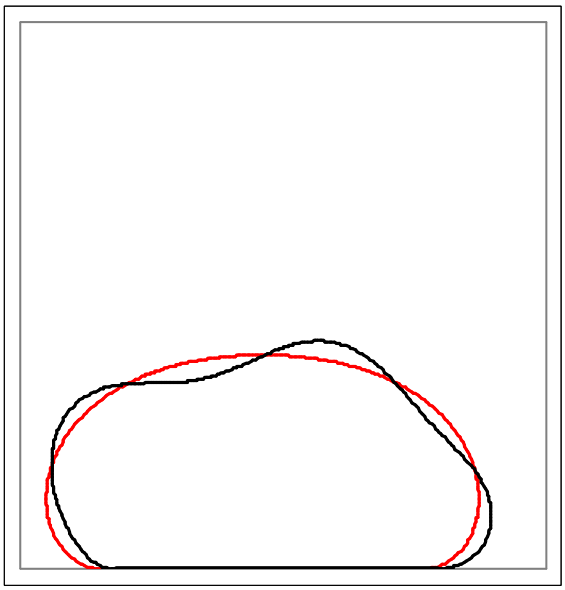

(d) 2nd nonsymmetrical mode

Figure 2.10 Mode shapes for h = 0.2

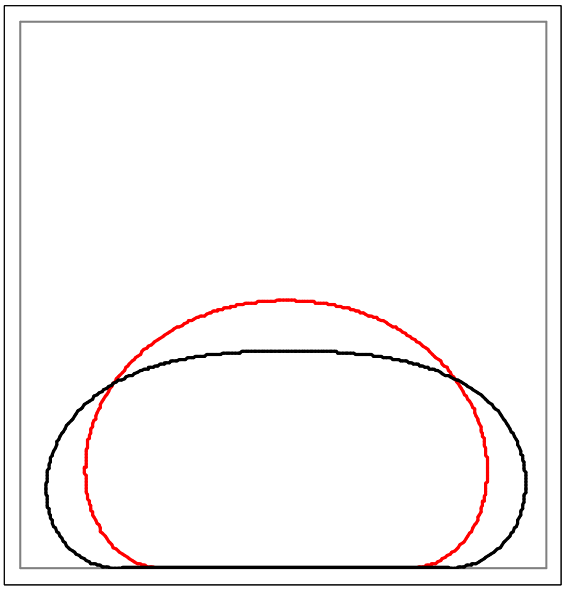

(a) 1st symmetrical mode

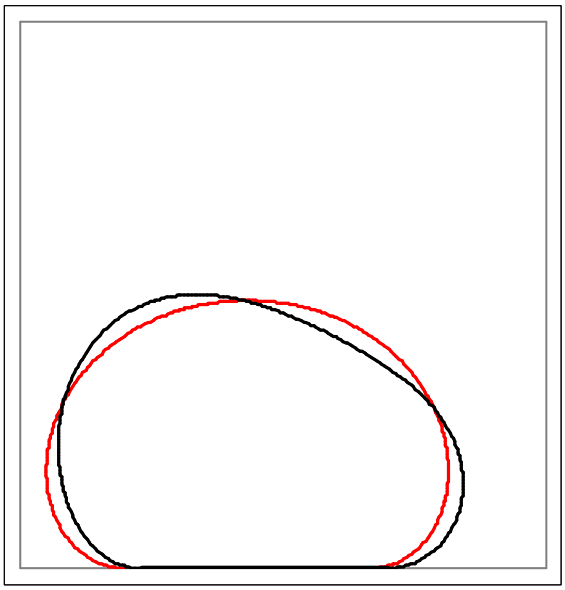

(b) 1st nonsymmetrical mode

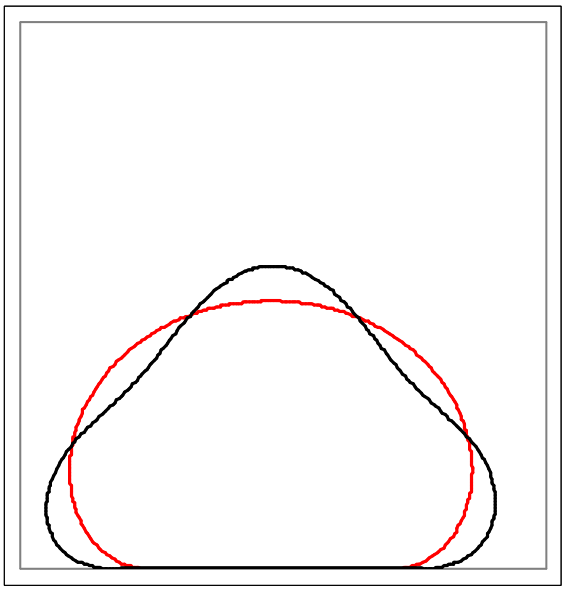

(c) 2nd symmetrical mode

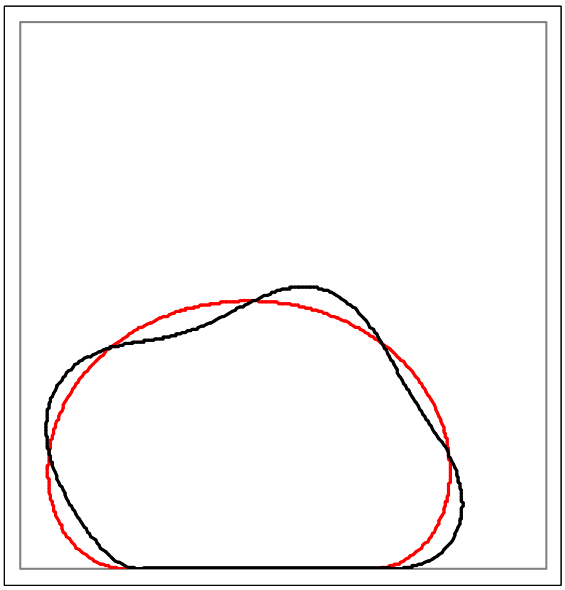

(d) 2nd nonsymmetrical mode

Figure 2.11 Mode shapes for h = 0.3

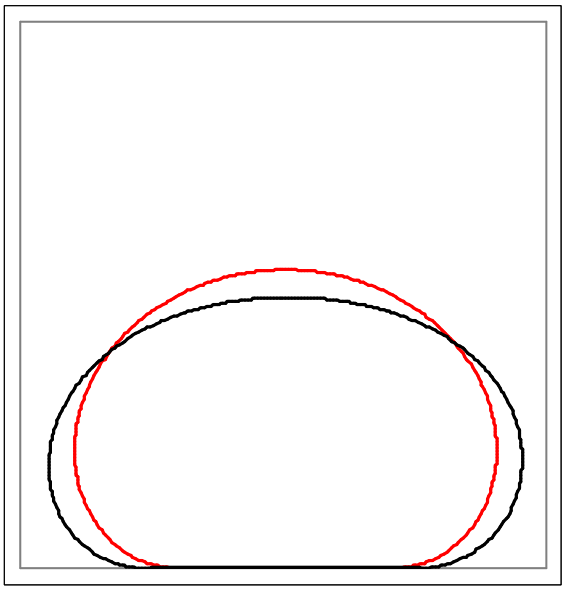

(a) 1st symmetrical mode

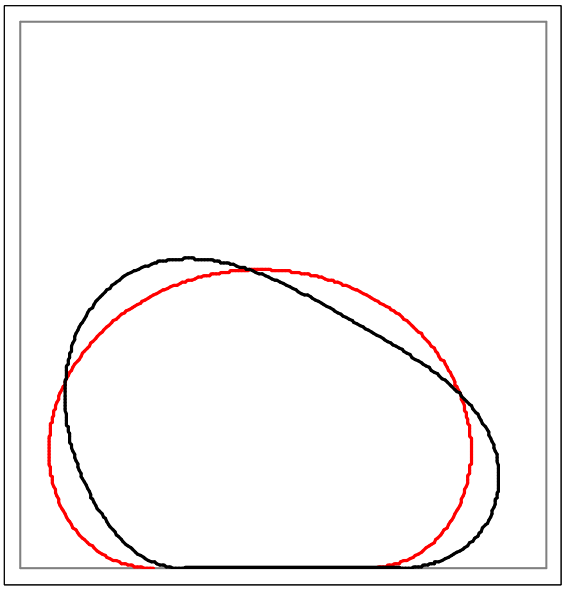

(b) 1st nonsymmetrical mode

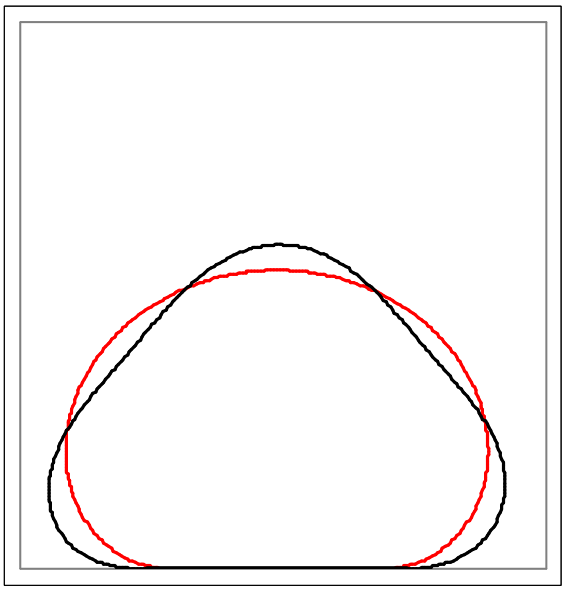

(c) 2nd symmetrical mode

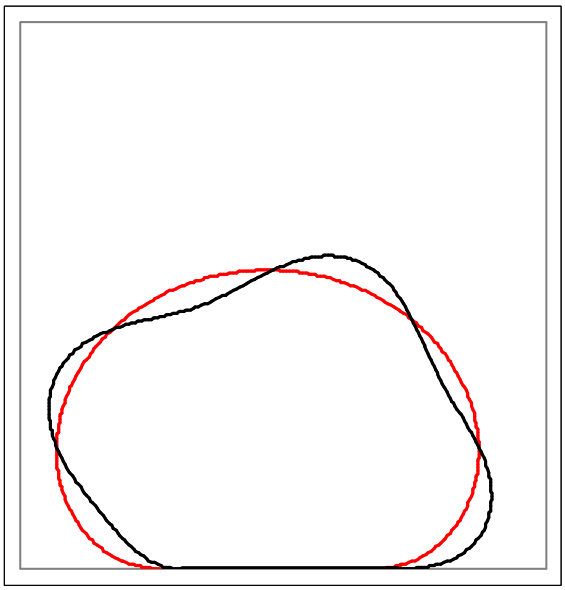

(d) 2nd nonsymmetrical mode

Figure 2.12 Mode shapes for h = 0.4

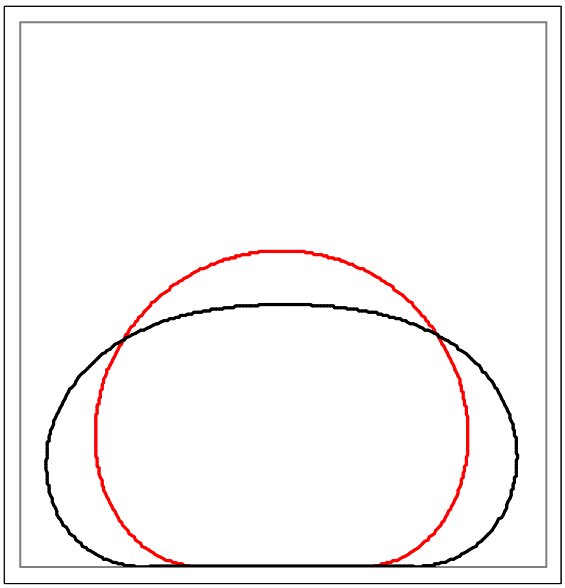

(a) 1st symmetrical mode

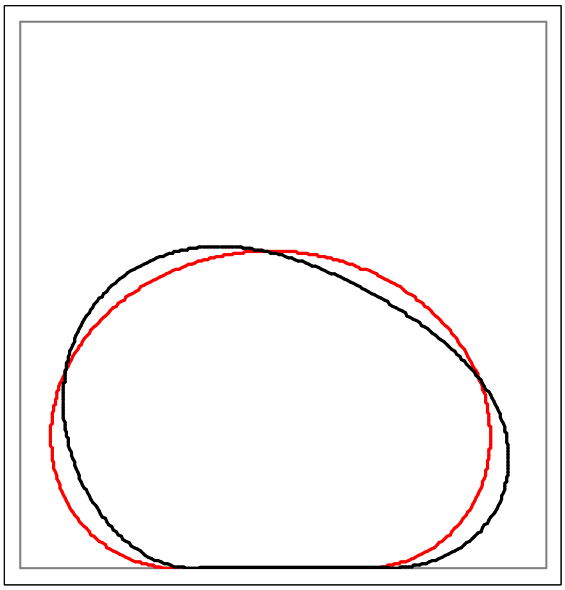

(b) 1st nonsymmetrical mode

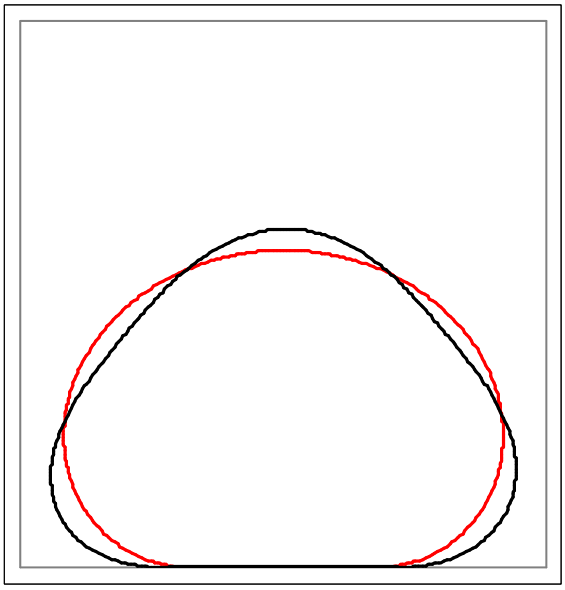

(c) 2nd symmetrical mode

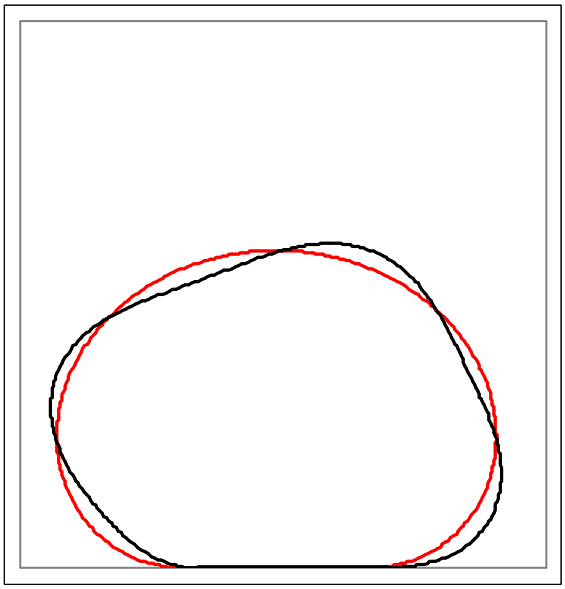

(d) 2nd nonsymmetrical mode

Figure 2.13 Mode shapes for h = 0.5

2.6.1 Damping Results

Consider Figures 2.14 through 2.17. If an internal pressure head is set and the mode chosen, there is a specific curve that the frequency follows as damping coefficient values increase from zero to a state of zero oscillation (where the frequency reaches zero). Overall, a higher internal pressure head takes a greater value of damping coefficient to eliminate oscillations (where frequency is zero).

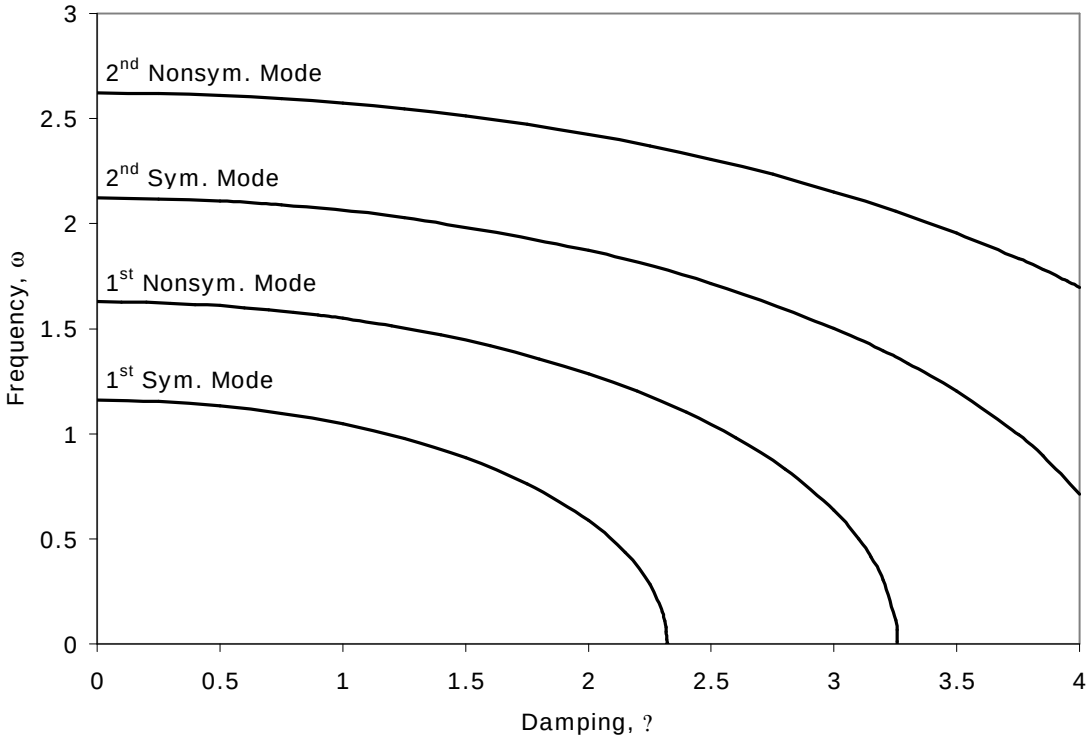

Figure 2.14 Frequency versus damping coefficient with h = 0.2 and no added mass

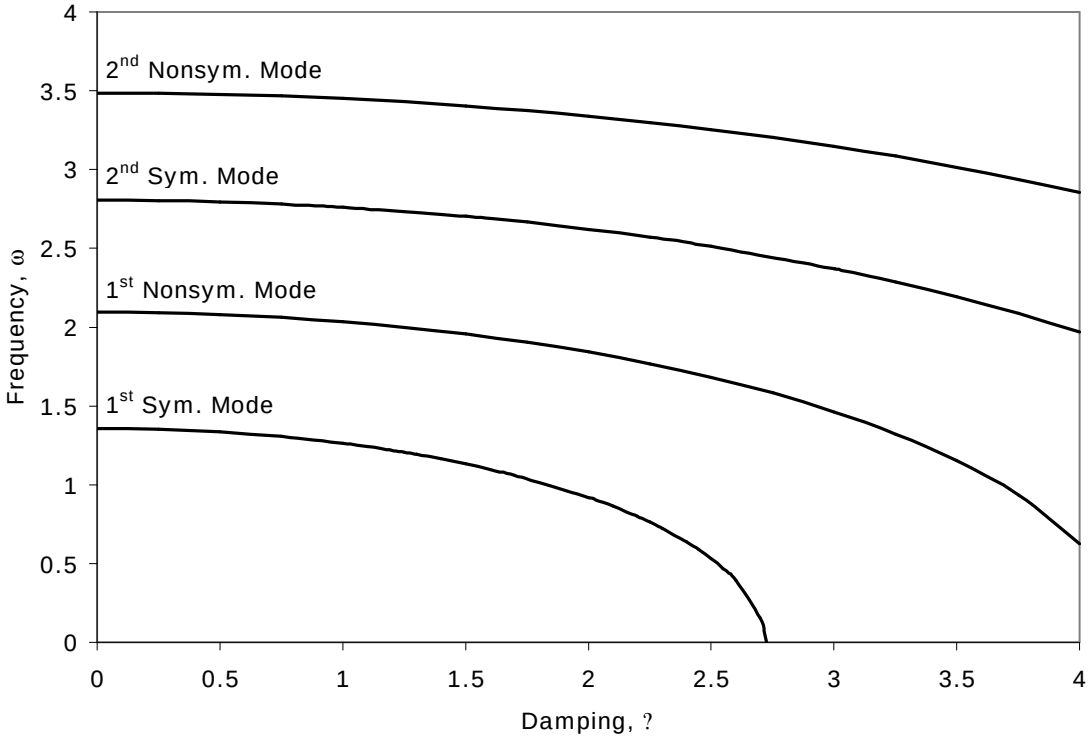

Figure 2.15 Frequency versus damping coefficient with h = 0.3 and no added mass

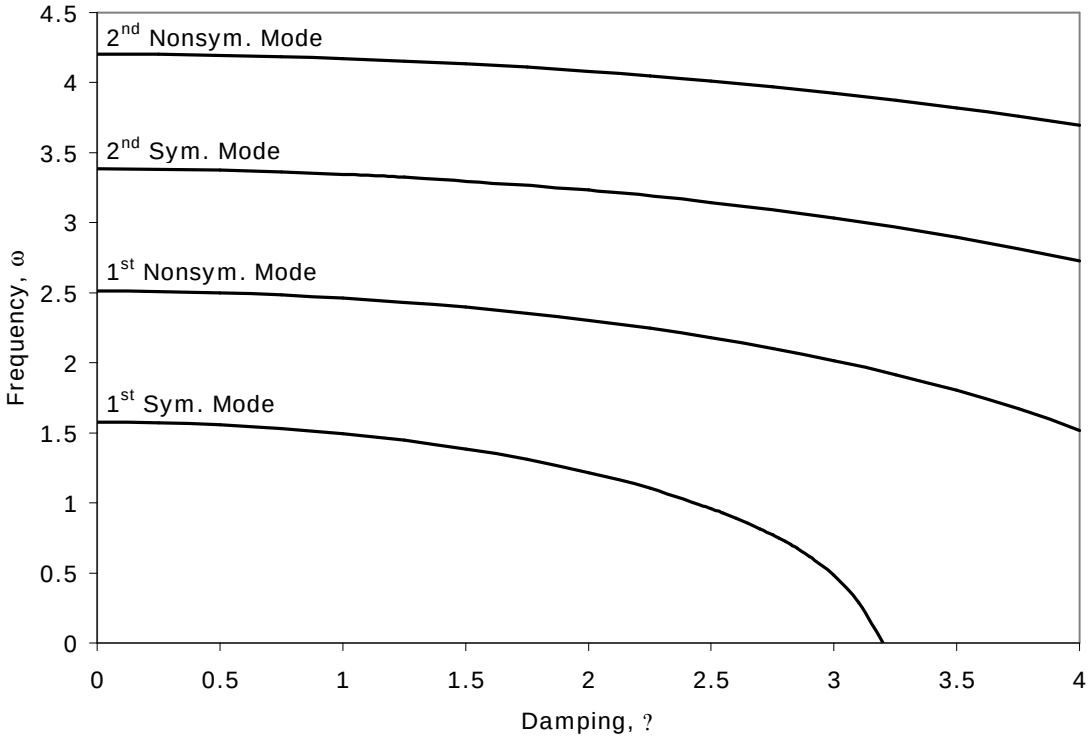

Figure 2.16 Frequency versus damping coefficient with h = 0.4 and no added mass

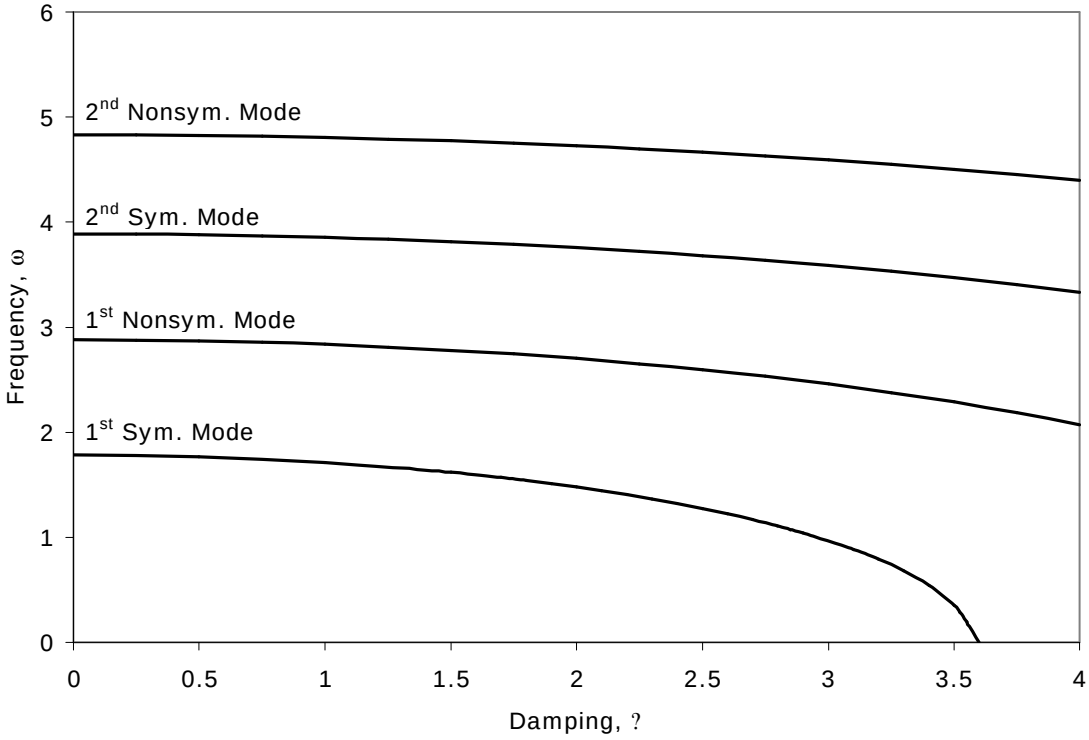

Figure 2.17 Frequency versus damping coefficient with h = 0.5 and no added mass

The tables below present different frequencies with set values for the damping coefficient ? and internal pressure head h. The motion is not harmonic, but decays with oscillation. These values correspond to the data plotted in Figures 2.14 through 2.17. These tables show a gentle decrease in frequency at first and then a tremendous drop in frequency when the frequency approaches zero and the mode becomes overdamped (i.e., when ? = 0 the motion decays without oscillation). Not all values of ? were calculated for all mode shapes. A dash signifies that a run was not executed for that specific ?.

	h			
b	0.2	0.3	0.4	0.5
0.0	1.160	1.359	1.577	1.786
0.5	1.133	1.336	1.557	1.768
1.0	1.047	1.263	1.495	1.714
1.5	0.885	1.133	1.387	1.620
2.0	0.588	0.920	1.219	1.479
2.5	0.000	0.533	0.961	1.275
2.6	-	0.395	0.892	1.224
2.7	-	0.155	0.814	1.169
2.725	-	0.000	-	-
2.8	-	-	0.725	1.108
2.9	-	-	0.619	1.042
3	-	-	0.485	-
3.1	-	-	0.288	0.886
3.2	-	-	0.000	0.793
3.3	-	-	-	0.682
3.4	-	-	-	0.546
3.5	-	-	-	0.354
3.6	-	-	-	0.000

(a) 1st symmetrical mode frequencies (?)

	h			
b	0.2	0.3	0.4	0.5
0.0	1.629	2.096	2.512	2.881
0.5	1.610	2.081	2.500	2.870
1.0	1.550	2.035	2.462	2.837
2.0	1.286	1.842	2.304	2.702
3.0	0.635	1.463	2.015	2.459
3.3	0.113	1.323	1.916	2.379
3.5	0.000	1.153	1.802	2.288
4.0	0.000	0.626	1.520	2.073

(b) 1st nonsymmetrical mode frequencies (?)

	h			
b	0.2	0.3	0.4	0.5
0.0	2.123	2.806	3.384	3.888
0.3	2.119	2.804	3.382	3.886
0.5	2.108	2.795	3.375	3.880
0.8	2.090	2.781	3.363	3.870
1.3	2.029	-	3.326	3.837
2.0	1.873	2.622	3.233	3.757
2.5	1.716	2.513	3.145	3.682
3.0	1.503	2.372	3.033	3.587
3.5	1.202	2.194	2.896	3.472
4.0	0.712	1.969	2.730	3.334

(c) 2nd symmetrical mode frequencies (?)

	h			
b	0.2	0.3	0.4	0.5
0.0	2.623	3.486	4.202	4.831
0.3	2.620	3.484	4.200	4.830
0.5	2.611	3.477	4.195	4.825
0.8	2.596	3.466	4.186	4.817
1.0	2.575	3.450	4.172	4.806
1.3	2.548	3.429	4.156	4.791
1.5	2.514	3.404	4.135	4.773
1.8	2.473	3.374	4.110	4.752
2.0	2.425	3.339	4.082	4.727
2.3	2.370	3.299	4.049	4.699
2.5	2.306	3.254	4.012	4.667
2.8	2.234	3.203	3.971	4.632
3.0	2.152	3.147	3.926	4.593
3.3	2.059	3.084	3.876	4.550
3.5	1.954	3.015	3.821	4.503
3.8	1.834	2.939	3.761	4.453
4.0	1.697	2.855	3.696	4.398

(d) 2nd symmetrical mode frequencies (?)

Table 2.3 Damping coefficient and modal frequencies

2.6.2 Added Mass Results

Figures 2.18 – 2.21 and Table 2.5 give the results using the added mass component. These results neglect damping. Notice that when increasing the internal mass per unit

length a decrease in the frequency is observed. Meaning that as the internal water's inertia is considered more of a factor the frequency decreases.

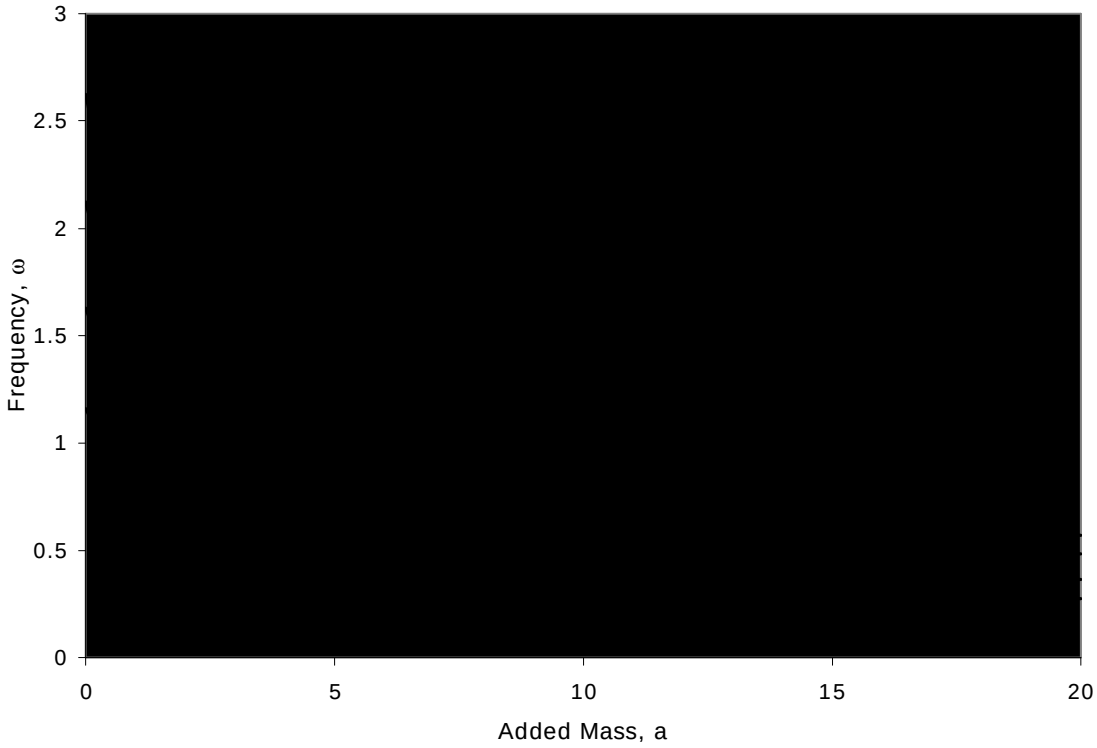

Figure 2.18 Frequency versus added mass with h = 0.2 and no damping

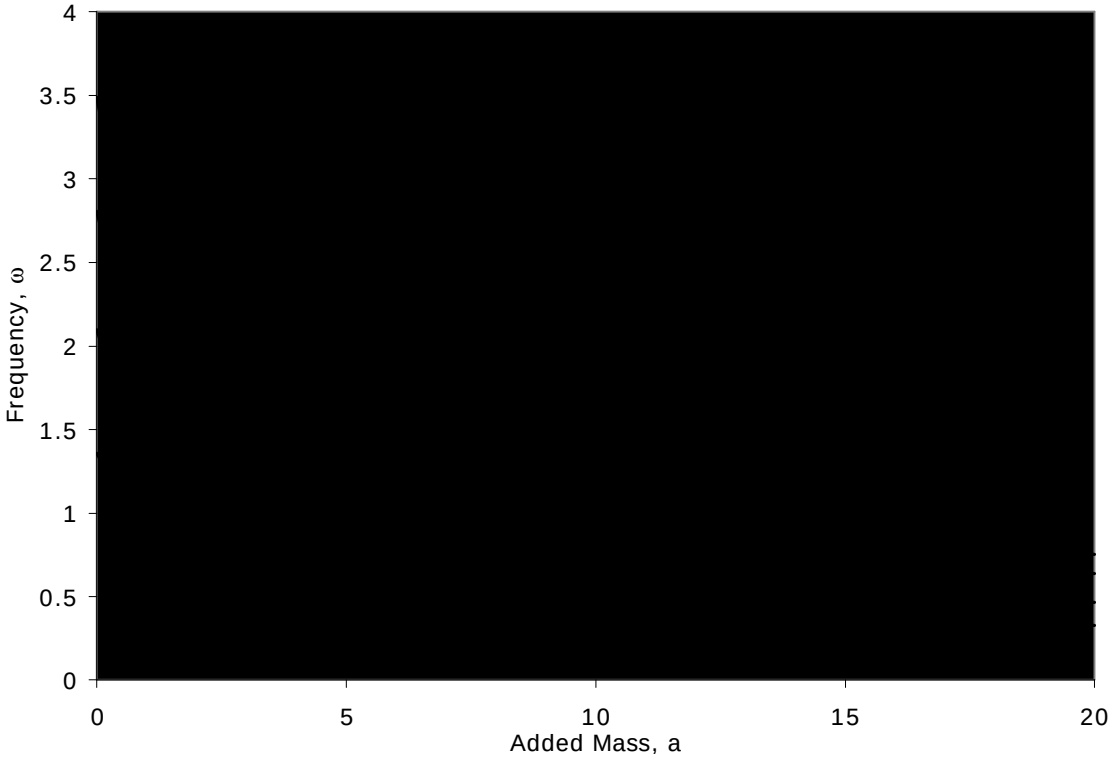

Figure 2.19 Frequency versus added mass with h = 0.3 and no damping

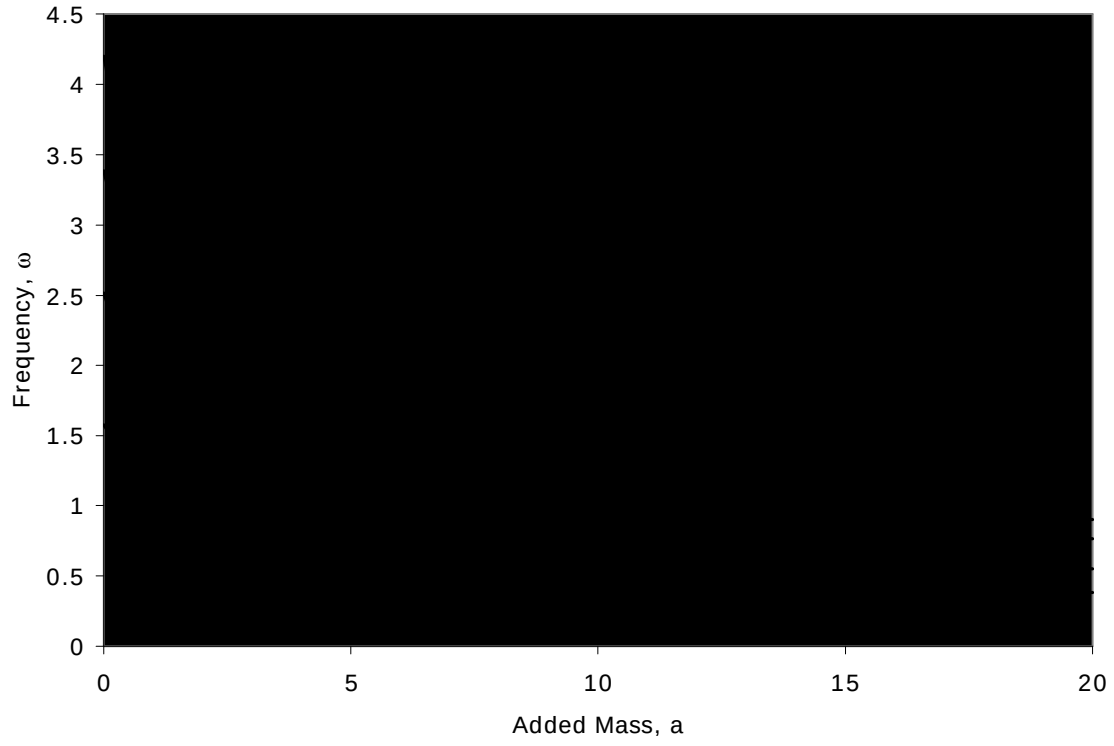

Figure 2.20 Frequency versus added mass with h = 0.4 and no damping

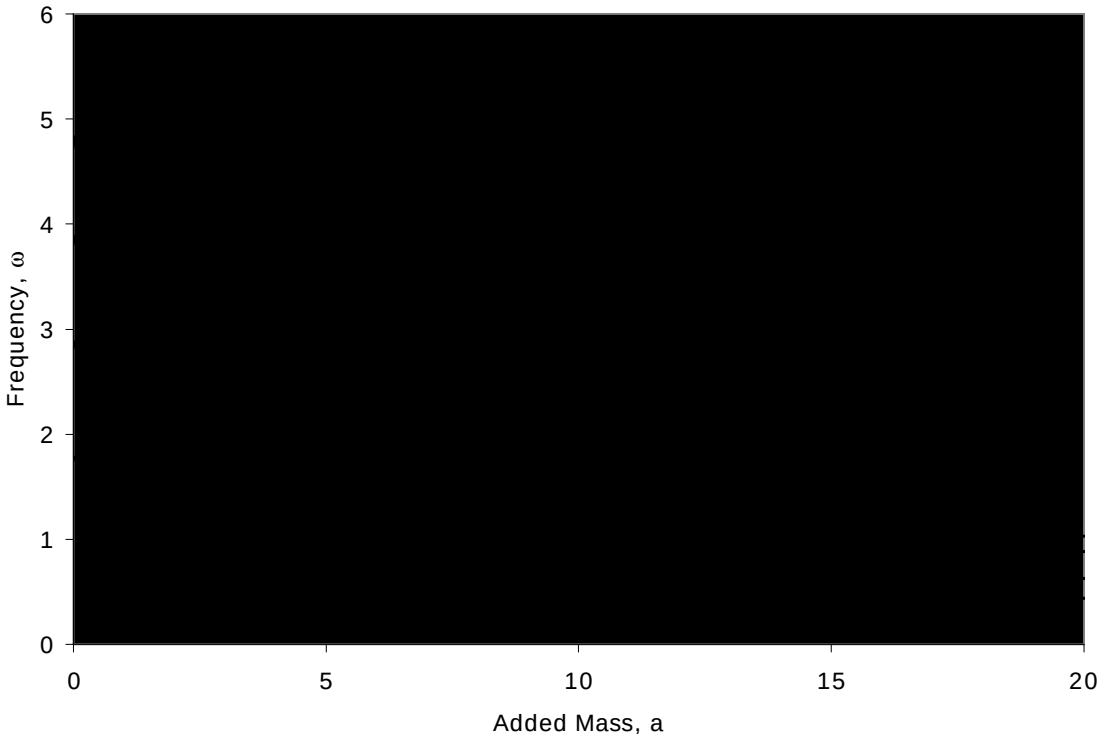

Figure 2.21 Frequency versus added mass with h = 0.5 and no damping

	h			
a	0.2	0.3	0.4	0.5
0.0	1.160	1.358	1.576	1.785
0.1	1.114	1.307	1.518	1.720
0.2	1.072	1.262	1.466	1.661
0.3	1.036	1.220	1.419	1.608
0.4	1.002	1.183	1.376	1.560
0.5	0.972	1.149	1.336	1.515
0.6	0.944	1.117	1.300	1.474
0.7	0.919	1.088	1.267	1.436
0.8	0.895	1.061	1.236	1.401
0.9	0.873	1.036	1.207	1.369
1.0	0.853	1.013	1.180	1.338
1.1	0.834	0.991	1.155	1.310
1.2	0.816	0.970	1.131	1.283
1.3	0.800	0.951	1.109	1.258
1.4	0.784	0.933	1.088	1.234
1.5	0.769	0.916	1.068	1.211
1.6	0.755	0.899	1.049	1.190
1.7	0.742	0.884	1.031	1.169
1.8	0.729	0.869	1.014	1.150
1.9	0.717	0.855	0.998	1.132
2.0	0.706	0.842	0.982	1.114
3.0	0.620	0.736	0.859	0.975
4.0	0.557	0.662	0.773	0.877
5.0	0.510	0.607	0.708	0.803
6.0	0.470	0.563	0.657	0.746
7.0	0.440	0.528	0.616	0.699
8.0	0.415	0.498	0.582	0.660
9.0	0.394	0.473	0.553	0.627
10.0	0.376	0.452	0.528	0.598
11.0	0.361	0.433	0.506	0.573
12.0	0.347	0.416	0.486	0.551
13.0	0.334	0.401	0.469	0.531
14.0	0.323	0.388	0.453	0.514
15.0	0.313	0.376	0.439	0.498
16.0	0.304	0.365	0.426	0.483
17.0	0.295	0.355	0.414	0.469
18.0	0.287	0.345	0.403	0.457
19.0	0.280	0.337	0.393	0.446
20.0	0.273	0.329	0.384	0.435

(a) 1st symmetrical mode frequencies (?)

	h			
a	0.2	0.3	0.4	0.5
0.0	1.629	2.096	2.512	2.881
0.1	1.560	2.009	2.409	2.764
0.2	1.499	1.932	2.318	2.659
0.3	1.445	1.863	2.235	2.565
0.4	1.396	1.801	2.161	2.480
0.5	1.352	1.744	2.093	2.402
0.6	1.311	1.693	2.031	2.331
0.7	1.274	1.645	1.974	2.266
0.8	1.240	1.601	1.922	2.205
0.9	1.209	1.560	1.873	2.149
1.0	1.179	1.523	1.828	2.097
1.1	1.152	1.487	1.785	2.048
1.2	1.126	1.454	1.745	2.003
1.3	1.103	1.423	1.708	1.960
1.4	1.080	1.394	1.673	1.919
1.5	1.059	1.367	1.640	1.881
1.6	1.039	1.341	1.609	1.845
1.7	1.020	1.316	1.579	1.811
1.8	1.002	1.293	1.551	1.779
1.9	0.985	1.271	1.524	1.748
2.0	0.969	1.249	1.498	1.718
3.0	0.840	1.082	1.297	1.486
4.0	0.752	0.967	1.157	1.325
5.0	0.686	0.881	1.054	1.206
6.0	0.635	0.815	0.974	1.114
7.0	0.594	0.761	0.909	1.039
8.0	0.559	0.716	0.855	0.977
9.0	0.530	0.679	0.810	0.925
10.0	0.505	0.647	0.771	0.881
11.0	0.484	0.618	0.737	0.842
12.0	0.464	0.594	0.707	0.807
13.0	0.447	0.572	0.681	0.777
14.0	0.432	0.552	0.657	0.750
15.0	0.418	0.534	0.635	0.725
16.0	0.406	0.518	0.616	0.703
17.0	0.394	0.503	0.598	0.682
18.0	0.383	0.489	0.582	0.664
19.0	0.374	0.476	0.567	0.646
20.0	0.365	0.465	0.553	0.630

(b) 1st nonsymmetrical mode frequencies (?)

	h			
a	0.2	0.3	0.4	0.5
0.0	2.123	2.806	3.384	3.891
0.1	2.033	2.687	3.244	3.727
0.2	1.953	2.582	3.118	3.583
0.3	1.881	2.489	3.005	3.453
0.4	1.817	2.405	2.904	3.337
0.5	1.760	2.329	2.812	3.231
0.6	1.707	2.259	2.728	3.135
0.7	1.659	2.195	2.651	3.047
0.8	1.614	2.136	2.581	2.965
0.9	1.573	2.082	2.515	2.890
1.0	1.535	2.032	2.454	2.820
1.1	1.499	1.985	2.397	2.755
1.2	1.466	1.941	2.345	2.694
1.3	1.435	1.900	2.295	2.637
1.4	1.406	1.862	2.248	2.583
1.5	1.379	1.825	2.204	2.533
1.6	1.353	1.791	2.163	2.485
1.7	1.329	1.758	2.124	2.440
1.8	1.305	1.728	2.086	2.397
1.9	1.283	1.698	2.051	2.357
2.0	1.262	1.671	2.018	2.318
3.0	1.100	1.451	1.751	2.012
4.0	0.985	1.300	1.568	1.802
5.0	0.901	1.188	1.433	1.646
6.0	0.835	1.101	1.327	1.525
7.0	0.781	1.030	1.242	1.427
8.0	0.737	0.972	1.171	1.346
9.0	0.700	0.922	1.111	1.277
10.0	0.667	0.879	1.060	1.217
11.0	0.639	0.842	1.015	1.166
12.0	0.614	0.809	0.975	1.120
13.0	0.592	0.780	0.940	1.079
14.0	0.570	0.753	0.908	1.043
15.0	0.554	0.729	0.879	1.010
16.0	0.537	0.708	0.853	0.979
17.0	0.522	0.688	0.829	0.952
18.0	0.508	0.670	0.807	0.926
19.0	0.494	0.653	0.786	0.903
20.0	0.484	0.637	0.767	0.881

(c) 2nd symmetrical mode frequencies (?)

	h			
a	0.2	0.3	0.4	0.5
0.0	2.624	3.487	4.202	4.835
0.1	2.509	3.336	4.026	4.626
0.2	2.408	3.203	3.865	4.441
0.3	2.319	3.083	3.722	4.276
0.4	2.238	2.976	3.593	4.129
0.5	2.166	2.880	3.476	3.995
0.6	2.099	2.792	3.372	3.873
0.7	2.041	2.711	3.274	3.761
0.8	1.983	2.637	3.185	3.657
0.9	1.931	2.569	3.102	3.562
1.0	1.884	2.505	3.025	3.474
1.1	1.839	2.445	2.953	3.392
1.2	1.798	2.390	2.886	3.315
1.3	1.759	2.339	2.824	3.242
1.4	1.722	2.290	2.765	3.175
1.5	1.688	2.244	2.709	3.110
1.6	1.656	2.201	2.657	3.050
1.7	1.625	2.160	2.607	2.993
1.8	1.596	2.120	2.560	2.939
1.9	1.568	2.084	2.515	2.889
2.0	1.542	2.049	2.473	2.839
3.0	1.334	1.771	2.134	2.451
4.0	1.192	1.580	1.903	2.185
5.0	1.086	1.439	1.732	1.988
6.0	1.004	1.329	1.599	1.835
7.0	0.938	1.241	1.491	1.711
8.0	0.883	1.167	1.403	1.608
9.0	0.837	1.105	1.327	1.522
10.0	0.797	1.051	1.263	1.448
11.0	0.762	1.005	1.207	1.383
12.0	0.731	0.964	1.157	1.326
13.0	0.704	0.928	1.113	1.276
14.0	0.680	0.895	1.074	1.232
15.0	0.657	0.865	1.039	1.191
16.0	0.637	0.837	1.007	1.154
17.0	0.619	0.813	0.977	1.120
18.0	0.602	0.792	0.950	1.089
19.0	0.586	0.771	0.925	1.059
20.0	0.572	0.752	0.902	1.032

(d) 2nd nonsymmetrical mode frequencies (?)

Table 2.4 Added mass and modal frequencies

2.7 Dimensional Example in SI Units

Given:

Consider a geosynthetic tube inflated with water that has a nondimensional internal pressure head of 0.30. The circumference L is equal to 1.50m and the thickness of the material is 0.52mm. The specific weight for water at ambient temperature (15.6 C) is $?_{int} ? 9.80 kN/m^3$ (Munson et al. 1998). From a sample of geotextile material, the density was measured to be $1175 kg/m^3$.

Required:

Find the following dimensional values: internal pressure head, membrane tension at the origin, and contact length. For a dynamic illustration, calculate the frequency if the tube were induced into the first mode of vibration, neglecting damping and added mass. Next, find the critical damping coefficient C_{CR} for the first mode. What is the lowest dimensional frequency for 15% of critical damping? Lastly, calculate the frequency that corresponds to an added mass value of 5.00.

Solution:

Using the given parameters, the dimensional equilibrium values for membrane tension, maximum height, and contact length are easily calculated from the nondimensional results.

The dimensional pressure head becomes

$$H ? hL ? 0.30 ? 1.50m ? \boxed{0.45m}$$

$$P_{bot} ? ?_{int} H ? 9.80 kN/m^3 ? 0.45m ? \boxed{4410 Pa}$$

In order to calculate the actual tube height, the value y_{max} will need to be determined either by Table 2.1 or Figure 2.3.

From Table 2.1, the value for y_{max} at h = 0.30 is roughly 0.22. Using this value and the circumferential length of 1.5m, the dimensional value for the tube height is found as

$$Y_{\max} ? y_{\max} L ? 0.22 ? 1.50m ? \boxed{0.33m}$$

$$P_{top} ? P_{bot} ? ?_{\text{int}} Y_{\max} ? 4410Pa ? 9800N/m^3 ? 0.33m ? \boxed{1176Pa}$$

According to some manufacturers, this means that roughly $75\%(0.33) ? 0.25m ? 0.82\,ft$ will be retained using this tube with an internal pressure head equal to 0.45m.

In choosing a membrane material to resist the required force for an internal pressure head of 0.45m, the membrane force versus internal pressure plot is employed. From Figure 2.4 or Table 2.1, the value for q_o at h = 0.30 is 0.021. This translates into

$$Q_o ? q_o ?_{\text{int}} L^2 ? 0.021 ? 9800N/m^3 ? (1.50m)^2 ? \boxed{463N/m}$$

Once knowing the membrane tension required to sustain an internal pressure head of 0.45m, the material is chosen. The next step is to see if the contact length between tube and surface is sufficient in counteracting roll and sliding behavior. After viewing Table 2.1 or Figure 2.5 the value for b at h = 0.30 is 0.23. The contact length in SI units is

$$B ? bL ? 0.23 ? 1.50m ? \boxed{0.35m}$$

The results for a nondimensional internal pressure head of h = 0.30 which is induced by a force that resolves the tube into the 1st symmetric mode (Figure 2.12 (a)) can be taken from Table 2.2 or drawn from Figure 2.11.

Using the frequency ? = 1.36, the dimensional frequency can be calculated as follows:

$$? g ? 1175\frac{kg}{m^3} ? 9.81\frac{N}{kg} ? 0.00052m ? 6.0\frac{N}{m^2}$$

$$? \; ? \; ? \sqrt{\frac{? _{\text{int}}}{?}} \; ? 1.359 \sqrt{\frac{9800 N/m^3 \; ? 9.81 m/s^2}{6.0 N/m^2}} \; ? \; \boxed{172.0 rad/s}$$

The nondimensional critical damping coefficient occurs where the frequency ? equals zero. From Figure 2.16, the corresponding ? value for a system in the 1st symmetric mode is found to be ? = 2.73. Using this value and Equation 2.28, the critical damping coefficient becomes

$$C_{CR} \; ? \; ? \sqrt{? _{\text{int}} ?} \; ? \; 2.73 \sqrt{9800 \frac{N}{m^3} ? 6 \frac{N}{m^2} ? \frac{1}{9.81} \frac{s^2}{m}} \; ? \; \boxed{211.4 Ngs/m^3}$$

15% of critical damping for the first symmetrical mode is $31.7 Ngs/m^3$. Next, the nondimensional damping coefficient must be calculated:

$$? \; ? \; \frac{C}{\sqrt{? _{\text{int}} ?}} ? \frac{31.7 Ngs/m^3}{\sqrt{9800 \frac{N}{m^3} ? 6 \frac{N}{m^2} ? \frac{1}{9.81} \frac{s^2}{m}}} ? \; \boxed{0.41}$$

From Figure 2.16, the nondimensional frequency that corresponds to this damping coefficient is ? = 1.34. This produces a frequency of

$$? \; ? \; ? \sqrt{\frac{? _{\text{int}}}{?}} \; ? 1.34 \sqrt{\frac{9800 N/m^3 \; ? 9.81 m/s^2}{6.0 N/m^2}} \; ? \; \boxed{169.6 rad/s}$$

Neglecting damping, and given a nondimensional added mass coefficient of 5.00, the related nondimensional frequency is ? = 1.44.

This yields a dimensional frequency of

$$? \quad ? \; ? \; \sqrt{\frac{?_{int}}{?}} \; ? \; 1.44\sqrt{\frac{9800N/m^3 \; ? \; 9.81m/s^2}{6.0N/m^2}} \; ? \; \boxed{182.3rad/s}$$

Chapter 3: Tube with internal air and rigid foundation

3.1 Introduction

Typically geosynthetic tubes are designed to carry a weighted fill material, such as water or slurry mix. Due to gravity, the weighted material produces a downward force which in turn counteracts (via friction) the tube's disposition to slide. However, there is one system that requires only air to function as a flood water protection device. NOAQ produces a distinctive design that uses an attached sheet of geotextile material to stabilize the device. This attached apron design uses the external water on site. The downward force produced by external water (i.e., floodwater itself) translates into a friction force between the geotextile material and the supporting surface. A minimal amount of personnel and equipment is used for the deployment of this tube system. Two workers and the use of an air compressor would satisfy the requirement for installation. FitzPatrick, Freeman, and Kim have conducted experimental and analytical studies involving this design with an apron, but with water inside the tube (FitzPatrick et al. 2001, Freeman 2002, and Kim 2003). However, no dynamic modeling has been conducted. Therefore, to study the dynamic effects of an air-filled system, a model of a freestanding geosynthetic tube supported by an undeformable foundation has been developed. (Chapter 4 will discuss the results of a deformable foundation, first with a Winkler soil model and then with a Pasternak soil model.) Without the need for weighted material, this device has the potential for a boarder possibility of use.

The following chapter presents the formulation and analysis results of an air-filled freestanding geosynthetic tube resting on a rigid foundation. The majority of previous studies have incorporated water or slurry filled tubes for their analysis subjects. Similar to the water-filled tube study in chapter 2, Mathematica 4.2 was used to solve the boundary value problems and obtain membrane behavior. Again, an accuracy goal of five or greater was used in all Mathematica coded calculations. Mathematica 4.2 solutions were then transferred to Microsoft Excel where property relationships, equilibrium shapes, and shapes of the vibrations about equilibrium were plotted.

AutoCAD 2002 was also used in presenting illustrations of free body diagrams and details of specific components to better explain the subject. All derivations within were performed by Dr. R. H. Plaut.

Section 3.2 presents the assumptions utilized in the formulation of the freestanding air-filled tube. Next, section 3.3 pictorially presents and discusses the method of deriving the equilibrium shape and membrane properties (contact length and membrane tension). Subsequently, these equilibrium results are discussed and presented in section 3.4. As in chapter 2, knowing the equilibrium parameters, the membrane vibration shapes and natural frequencies may be calculated. Formulation of vibrations about the equilibrium configuration is presented in section 3.5. To enhance the model, a damping component is introduced to mimic physical conditions. The damping feature is described and discussed in section 3.5.1. Section 3.6 covers the results of the dynamic model. In addition to the formulation of equilibrium and dynamic conditions, a dimensional example (in SI units) is presented and discussed in section 3.7. In section 3.8 the results from the dimensional example are compared to the water-filled example in chapter 2.

3.2 Assumptions

A freestanding geosynthetic tube filled with air and supported by an undeformable foundation is considered. Like the water-filled case, friction is neglected at the surface-tube interface (Plaut and Klusman 1998). The tube is assumed to be infinitely long and straight. Changes in cross-sectional area along the tube length are neglected. Therefore, the use of a two-dimensional model is justified. Since air is the fill material, the weight of the geotextile material was required to add mass and stabilize the system. In correlation, seven studies cover the vibrations of an inflatable dam filled with air. Firt's study covers small, two-dimensional vibrations about the circular static shape of an anchored inflatable dam (Firt 1983). Plaut and Fagan go further to include the weight of the membrane and discuss the difference when neglecting membrane weight (Plaut and Fagan 1988). Hsieh and Plaut take the anchored air-inflated dam on an extra step and consider external water (Hsieh and Plaut 1990). Wauer and Plaut investigate the effect of

membrane extensibility on the vibration frequencies and mode shapes (Wauer and Plaut 1991). Dakshina Moorthy and Reddy examine the dynamic effects of an inflatable dam anchored along two of its generators using a three-dimensional finite element model (Dakshina Moorthy and Reddy et al. 1994). Wu and Plaut study the effects of overflow of a dual anchored inflatable dam (Wu and Plaut 1996). Liapis et al. conduct three-dimensional models of air and water-filled single anchor dams with and without external water (Liapis et al. 1998). The geosynthetic material is assumed to act like an inextensible membrane and bending resistance is neglected. Because the tubes have no bending stiffness, it is assumed that they are able to conform to sharp corners. (An example of a tube with no bending stiffness is displayed in Figure 3.4. Notice the acute angles of the material contacting the rigid foundation.Equation Chapter 2 Section 2 Equation Chapter 2 Section 1)

3.3 Basic Equilibrium Formulation

Compared to the water-filled tube formulation, this approach is more simplistic. Either approach may be used. To begin the air-filled equilibrium formulation, consider Figure 3.1. This diagram illustrates the equilibrium geometry of the air-filled geosynthetic tube resting on a rigid foundation. The right contact point between the tube and the foundation (point O) represents the origin. Horizontal distance X and vertical distance Y represent the two-dimensional Cartesian coordinate system. The symbol ? signifies the angular measurement of a horizontal datum to the tube membrane. The measurement S corresponds to the arc length from the origin following along the membrane. X, Y, and ? are each a function of the arc length S. Y_{max} denotes the maximum height of the tube and W represents the complete width from left vertical tangent to right vertical tangent. The character B represents the contact length between the tube material and foundation, and L represents the circumferential length of the entire membrane.

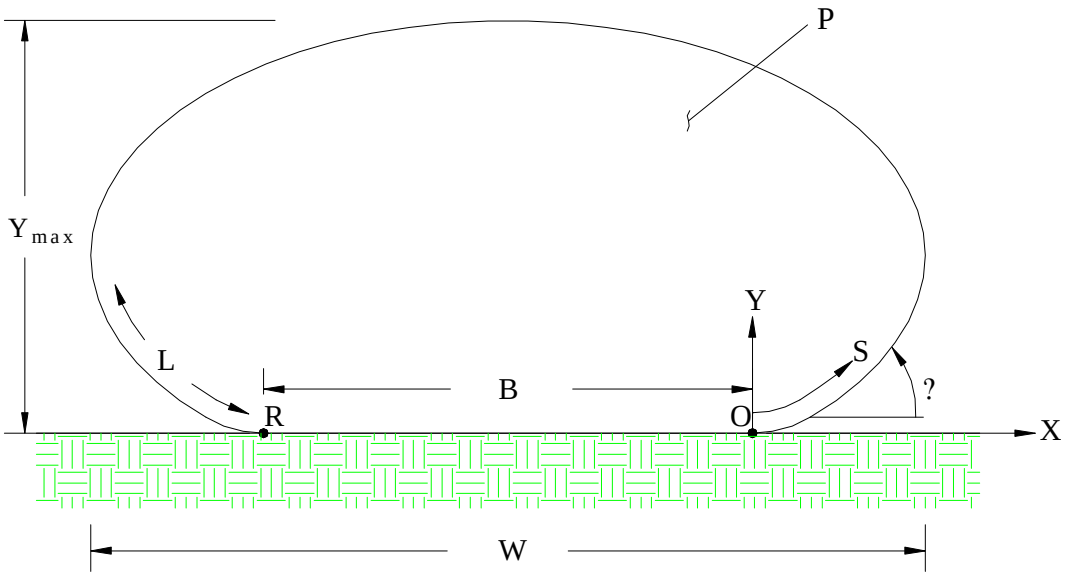

Figure 3.1 Equilibrium configuration

The internal pressure P is the set pressure within the tube that is applied to support the geosynthetic material and resist floodwater. Not pictured is the tension force Q_o in the membrane and the material mass per unit length ?.

The set values for this problem are the internal air pressure p and the material density ?? and the unknowns are the contact length, membrane tension, maximum tube height, and the equilibrium shape. From an element of the tube, presented in Figure 3.2, the following can be derived, where the subscript *e* denotes equilibrium values:

$$\frac{dX_e}{dS} ? \cos?_e, \qquad \frac{dY_e}{dS} ? \sin?_e \qquad (3.1, 3.2)$$

$$\frac{d?_e}{dS} ? \frac{P ? ? g\cos?_e}{Q_e}, \qquad \frac{dQ_e}{dS} ? ? g\sin?_e \qquad (3.3, 3.4)$$

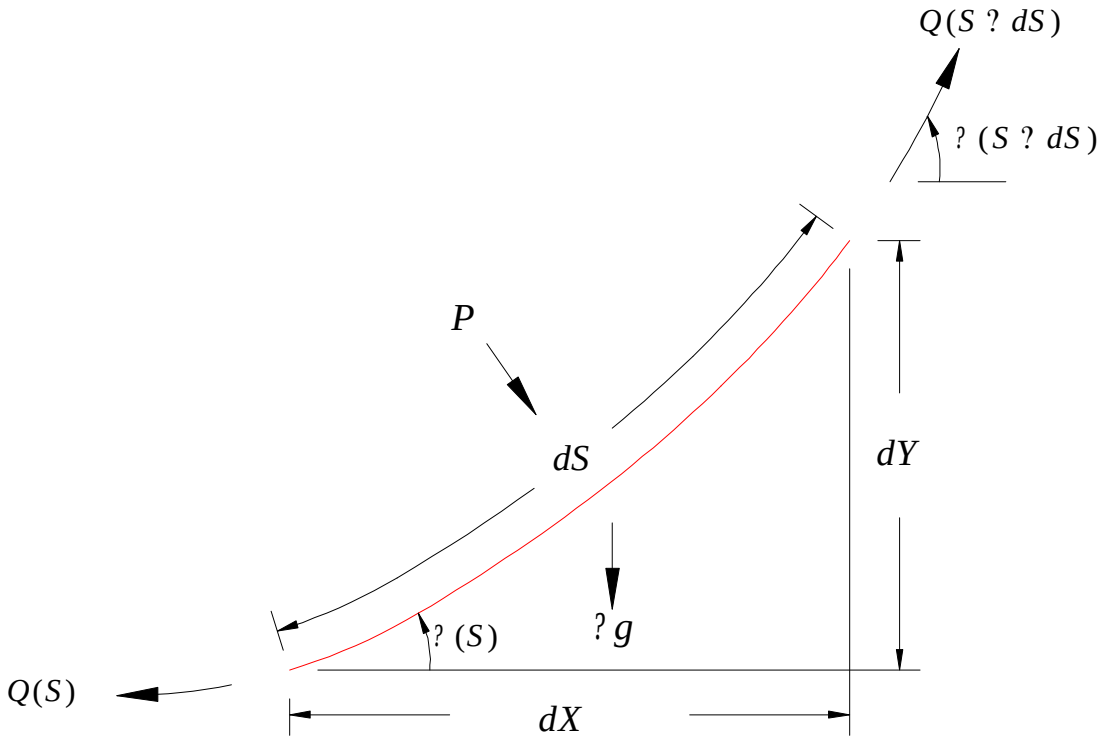

Figure 3.2 Tube element

To arrive at a series of expressions that would result in the unknown membrane properties, equilibrium is imposed on the system. The forces acting on the segment of membrane material in contact with the foundation are detailed in Figure 3.3. F is the reaction force per unit length to the downward action of both internal air pressure P and membrane weight ?g for the contact length B. Looking at the membrane segment, summing the forces in the y-direction, and setting that equal to zero gives

$$FB ? (P ? ? g)B \qquad \text{so that} \quad F ? P ? ? g \tag{3.5, 3.6}$$

Now take the entire tube and sum the forces in the y-direction. This results in

$$FB ? ? gL \tag{3.7}$$

Substituting Equation 3.6 in Equation 3.7 results in

$$(P ? ? g)B ? ? gL \tag{3.8}$$

For convenience and efficiency, the following nondimensional variables are defined:

$$x ? \frac{X}{L}, \qquad y ? \frac{Y}{L}, \qquad b ? \frac{B}{L}, \qquad s ? \frac{S}{L}, \qquad q_e ? \frac{Q_e}{? gL}, \qquad p ? \frac{P}{? g}$$

Using the nondimensional quantities and equilibrium above, the contact length becomes

$$b ? \frac{1}{p ? 1} \tag{3.9}$$

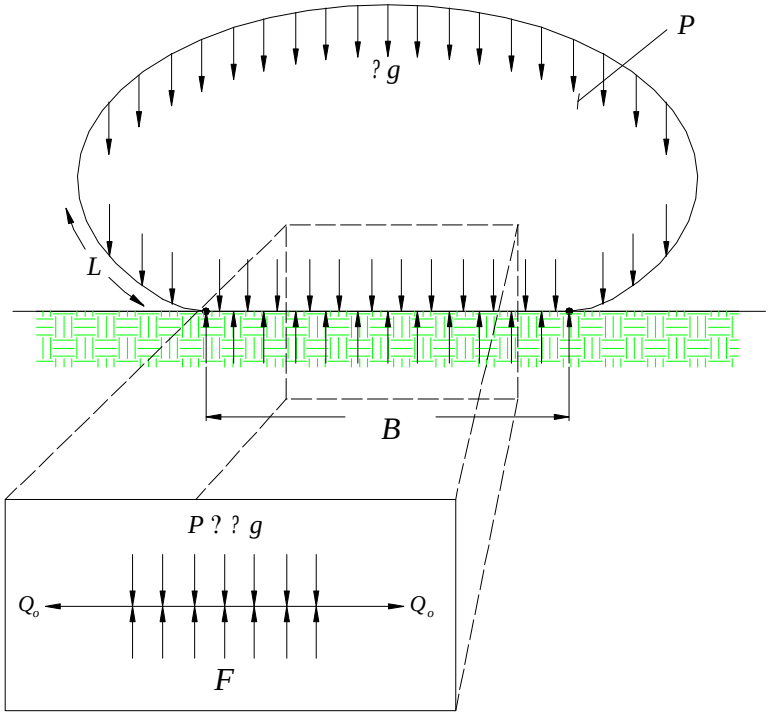

Figure 3.3 Equilibrium free body diagram

With the introduction of nondimensional quantities, the controlling equations become

$$\frac{dx_e}{ds} ? \cos?_e, \qquad \frac{dy_e}{ds} ? \sin?_e \tag{3.10, 3.11}$$

$$\frac{d?_e}{ds} ? \frac{p ? \cos?_e}{q_e}, \qquad \frac{dq_e}{ds} ? \sin?_e \tag{3.12, 3.13}$$

Based on Equations 3.11 and 3.13, $q_e(s) ? q_o ? y_e(s)$ where $q_o ? q_e(0)$. The shooting method was employed (discussed in greater detail in chapter 2) where equilibrium parameters can be calculated. A scaled arc length t was used which made it possible to

begin at $t ? 0$ (at the origin point O) and "shoot" to where $t ? 1$ (point R), making a complete revolution in $?_e$. Therefore, the following equations are derived:

$$t ? \frac{s}{(1 ? b)}, \qquad \frac{dx}{dt} ? (1 ? b)\cos[? (t)] \qquad (3.14, 3.15)$$

$$\frac{dy}{dt} ? (1 ? b)\sin[? (t)], \qquad \frac{d?}{dt} ? (1 ? b)\frac{(p ? \cos? (t))}{q_o ? y(t)}, \qquad (3.16, 3.17)$$

The two-point boundary conditions for a single air-filled freestanding tube resting on a rigid foundation are as follows:

For the range $0 ? t ? 1$

@ $t ? 0$ (point O): $x_e ? 0$, $y_e ? 0$, $?_e ? 0$

@ $t ? 1$ (point R): $x_e ? ?b$, $y_e ? 0$, $?_e ? 2?$

When using nondimensional terms, the maximum tension in the membrane is

$q_{\max} ? q_o ? y_{\max}$ where $y_{\max} ? y(t ? 0.5)$

With the use of Equations 3.14 through 3.17 and the boundary conditions above, a Mathematica file is coded to compute the equilibrium parameters. The Mathematica program is described and given in Appendix B.

3.4 Equilibrium Results

The following section discusses the equilibrium results of the above formulation. The process of analysis consisted of setting the internal air pressure, guessing values for the contact length b and membrane tension q_o at the origin, and shooting for two of the conditions at t = 1. Once the process converged to the correct contact length and membrane tension, the values were then written to multiple text files which included the equilibrium x and y coordinates, and equilibrium properties (contact length b, membrane tension q_o at the foundation, and maximum tube height y_{max}). These text files were opened in MS Excel in order to graph and tabularize the results. Table 3.1 displays the

results of the equilibrium calculations; these results are all dependent on the internal air pressure. Pressure values of p = 1.05, 2, 3, 4, and 5 were chosen.

Internal Pressure	Maximum Tube Height	Contact Length	Membrane Tension at Foundation	Maximum Membrane Tension
p	y_{max}	b	q_o	q_{max}
1.05	0.050	0.488	0.001	0.051
2.00	0.172	0.333	0.092	0.276
3.00	0.184	0.250	0.225	0.450
4.00	0.225	0.200	0.370	0.616
5.00	0.260	0.167	0.520	0.780

Table 3.1 Equilibrium results (nondimensional)

The lowest value for the internal pressure that has been calculated was p = 1.00085. This internal air pressure resulted in a near zero result for the membrane tension (q_o = 2.788×10^{-6}) and a large nondimensional contact length of b = 0.4998. Figure 3.4 illustrates the different equilibrium shapes produced by increasing the internal air pressure from p = 1.05 to 5.0. It was found that the value of p = 1.05 was the lowest pressure that could visibly be identified between the supporting ground and tube itself. Lower values were calculated, but did not show a difference between a tube laying flat on the surface and the surface itself. This characteristic is attributed to the need of having an initial pressure of p > 1 to raise the tube and induce form to it.

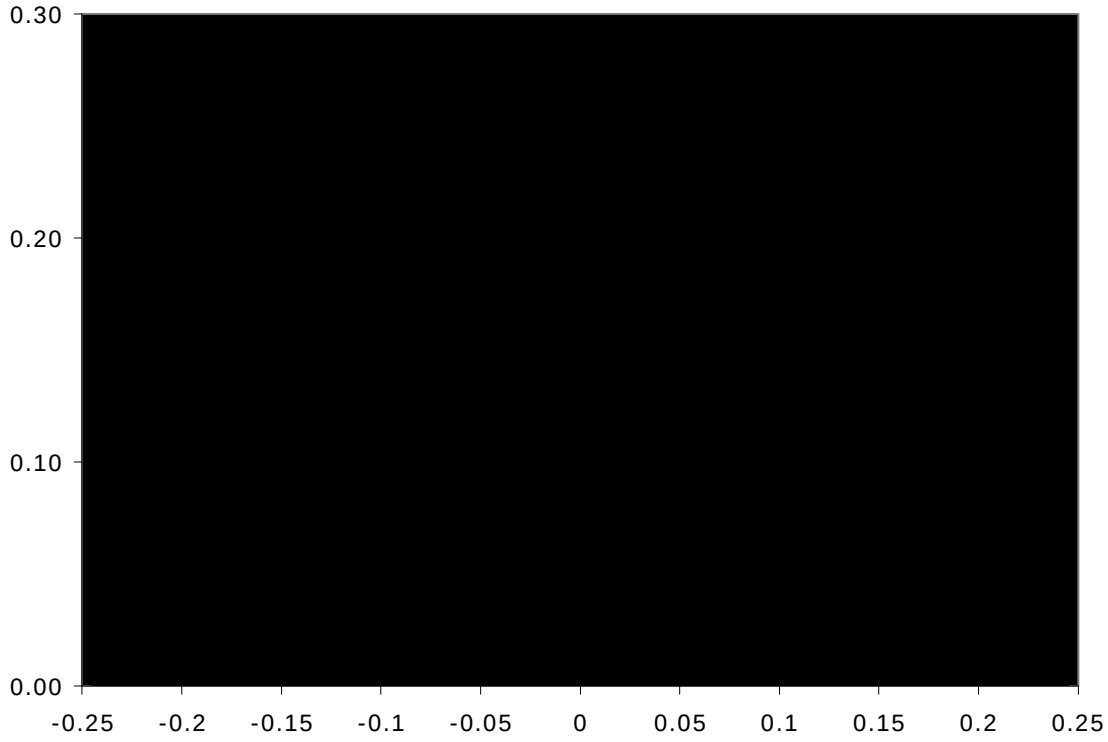

Figure 3.4 Equilibrium shapes

The following graphs illustrate the behavior of the parameters presented in Table 3.1. In Figure 3.5, the maximum height y_{max} of the tube is plotted versus the internal air pressure p. It is necessary to know the maximum sustained height for a given internal air pressure to defend against a charging flood depth. Figure 3.5 illustrates the nonlinearity of the solution, which converges to a maximum height and starts at an initial air pressure greater than one. Knowing the maximum height of the tube, a rough estimate of the retaining floodwater height may be calculated.

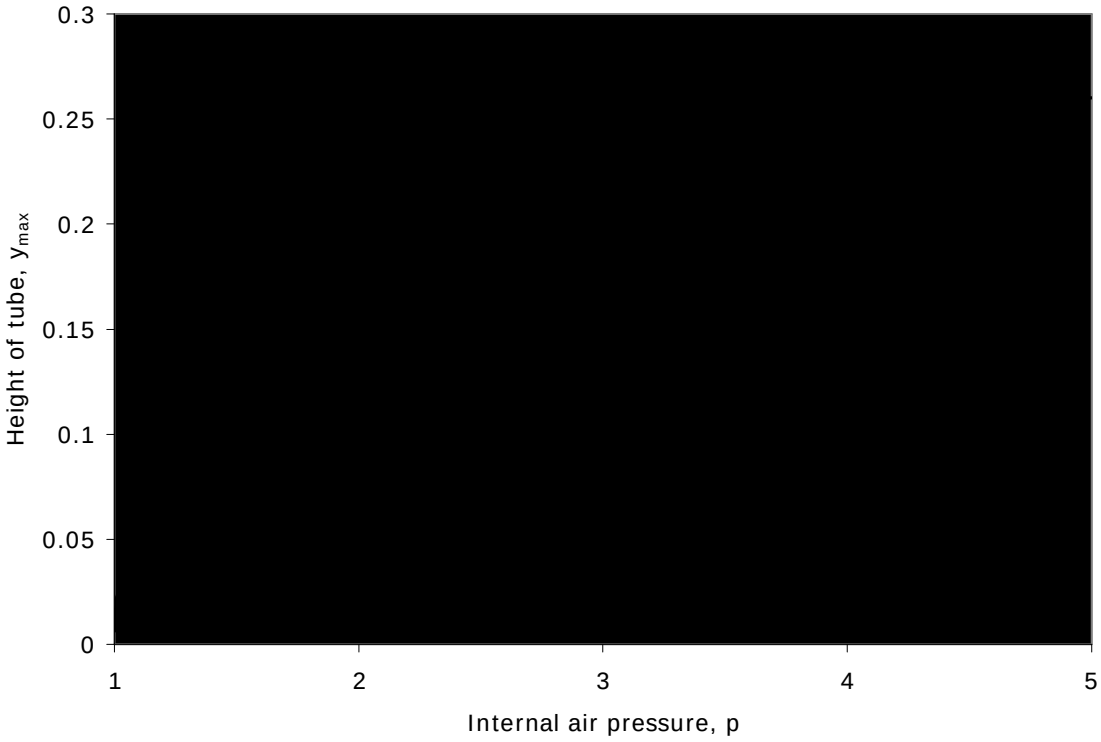

Figure 3.5 Maximum tube height versus internal air pressure

Figure 3.6 displays the increase in membrane tension at the origin as the internal air pressure is increased. Intuitively, this was assumed to occur; however, the relationship was unknown. Figure 3.7 presents the maximum membrane tension which the geotextile material should be able to withstand at a set internal air pressure. The maximum tension occurs at the top of the tube. For tube material selection, a given internal pressure relates to a certain maximum membrane tension. From this membrane tension value, the composition of the geosynthetic material may be selected based on the tension strength.

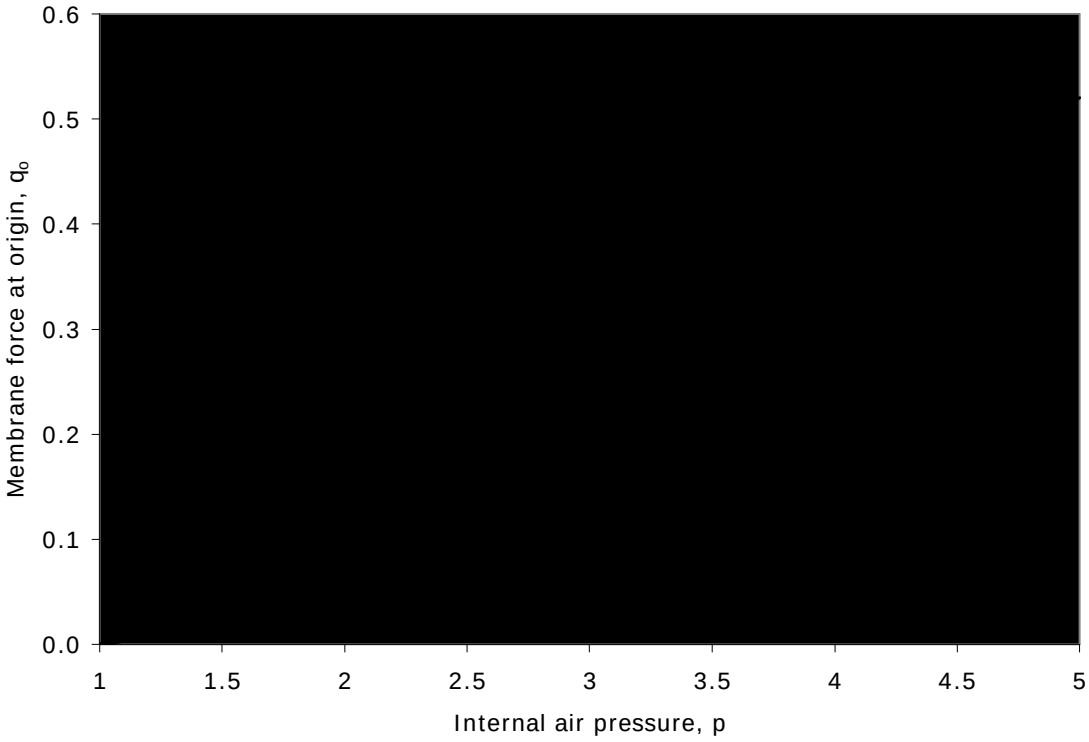

Figure 3.6 Membrane tension at origin versus internal air pressure

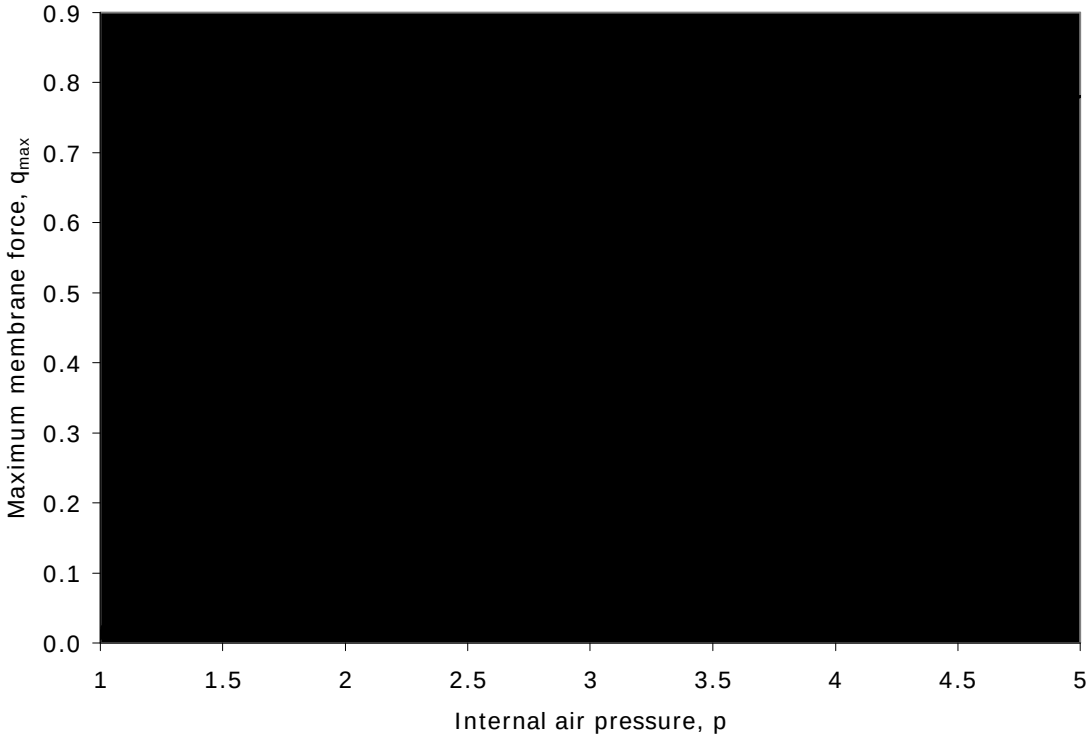

Figure 3.7 Maximum membrane tension versus internal air pressure

Figure 3.8 presents the relationship between contact length and internal air pressure. Again, this general trend of deceasing contact length while increasing the internal air pressure was predicted, however the curvature of the relationship was unknown. Figure 3.8 displays the serviceability characteristic of contact length. The contact length is important, because the friction force produced stabilizes the system from sliding. Another failure includes seepage, which is a function of the tube setup and support surface.

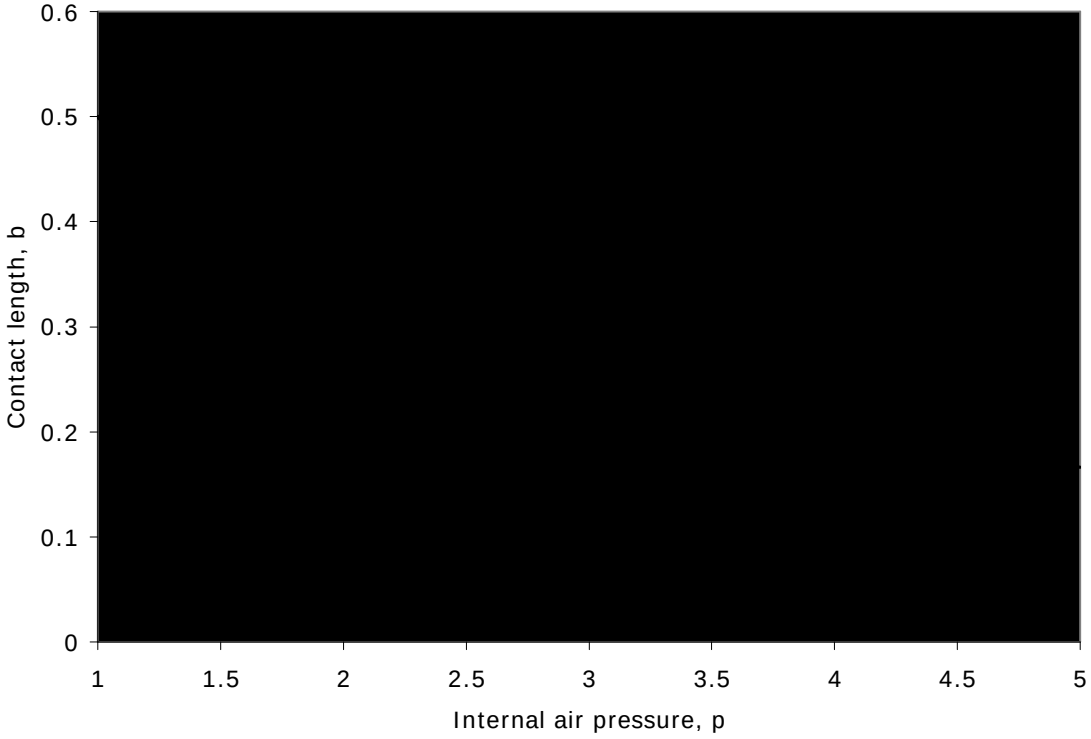

Figure 3.8 Contact length versus internal air pressure

3.5 Dynamic Formulation

Consider the free body diagram below in Figure 3.9. The D'Alembert Principle (explained in section 2.5) is employed and results in the kinetic equilibrium diagram illustrated in Figure 3.9. Initially, in this vibration study, damping of the air and material are neglected. Later an addition to the dynamic model will be viscous damping. The

notable difference in this air-filled kinetic equilibrium (Figure 3.9) and the water-filled kinetic equilibrium (Figure 2.7) is the consideration of the geosynthetic material weight (represented by ? *g*). In the water-filled dynamics the water made up the majority of the mass in the entire system and the membrane material could be neglected. However, with the air-filled tube, the air is assumed weightless and with out the weight of the tube there would be no form to the geosynthetic tube.

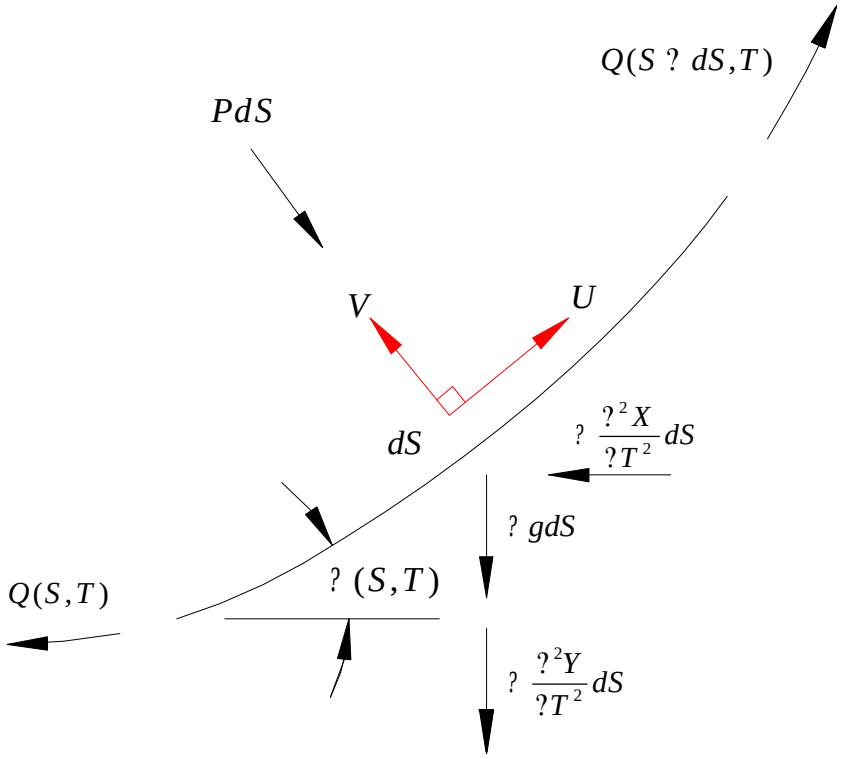

Figure 3.9 Kinetic equilibrium diagram

As in equilibrium, Q represents the membrane tension and ? is the angle of an element. All expressions are a function of the arc length S and the time T. The second derivatives of the horizontal and vertical displacements are the accelerations. Multiplying their accelerations by their respective mass gives a force acting in the opposite direction of this acceleration.

In order to analyze the vibrations about the equilibrium configuration of a single freestanding tube resting on a rigid foundation, consider the element shown in Figure 3.9. Using the geometry of the element, the two following formulas can be written:

$$\frac{?X}{?S} ? \cos? \ , \qquad \frac{?Y}{?S} ? \sin? \qquad (3.18, 3.19)$$

Now, take the kinetic equilibrium diagram (Figure 3.9) and sum the forces in the tangential and normal directions. This respectively produces

$$? \frac{?^2X}{?T^2}\cos? \ ? ? \frac{?^2Y}{?T^2}\sin? \ ? \frac{?Q}{?S} ? ? g\sin? \qquad (3.20)$$

$$? \frac{?^2Y}{?T^2}\cos? \ ? ? \frac{?^2X}{?T^2}\sin? \ ? Q\frac{??}{?S} ? P ? ? g\cos? \qquad (3.21)$$

Equations 3.18 through 3.21 describe the dynamics of a geosynthetic tube and are considered the equations of motion for this system.

At this point, it is appropriate to introduce $?$ as the dimensional frequency of the system. The following equations describe the total effect of motion on the equilibrium configuration, where the subscript d represents "dynamic":

$$X(S,T) ? X_e(S) ? X_d(S)\sin ? T, \qquad Y(S,T) ? Y_e(S) ? Y_d(S)\sin ? T \qquad (3.22, 3.23)$$

$$? (S,T) ? ?_e(S) ? ?_d(S)\sin ? T, \qquad Q(S,T) ? Q_e(S) ? Q_d(S)\sin ? T \qquad (3.24, 3.25)$$

In this study we assume infinitesimal vibrations. Therefore, nonlinear terms in the dynamic variables are neglected. For example, the products of two dynamic deflections are approximately zero ($u_d v_d ? 0$ and $v_d v_d ? 0$). Using small angle theory and trigonometry, the following can be derived:

$$\cos? \ ? \cos?_e \cos(?_d \sin ? T) ? \sin?_e \sin(?_d \sin ? T) ? \cos?_e ? (\sin?_e)?_d \sin ? T \qquad (3.26)$$

$$\sin? \ ? \sin?_e \cos(?_d \sin ? T) ? \cos?_e \sin(?_d \sin ? T) ? \sin?_e ? (\cos?_e)?_d \sin ? T \qquad (3.27)$$

Using Equations 3.18 through 3.21 with Equations 3.22 through 3.27, the following can be written:

$$\frac{dX_d}{dS} ? ??_d \sin?_e, \qquad \frac{dY_d}{dS} ? ?_d \cos?_e \qquad (3.28, 3.29)$$

$$??? \ ^2X_d \cos?_e ? ? ? \ ^2Y_d \sin?_e ? \frac{dQ_d}{dS} ? ? g?_d \cos?_e \qquad (3.30)$$

$$??? \,^2 Y_d \cos?_e ???\,^2 X_d \sin?_e ? Q_d \frac{d?_e}{dS} ? Q_e \frac{d?_d}{dS} ?? g?_d \sin?_e \qquad (3.31)$$

To eliminate $\frac{d?_e}{dS}$ in Equation 3.31, use Equation 3.3. This gives

$$\frac{d?_d}{dS} ? \frac{1}{Q_e}[?? \,^2 (X_d \sin?_e ? Y_d \cos?_e) ?? g?_d \sin?_e ? Q_d \frac{(P ?? g \cos?_e)}{Q_e}] \qquad (3.32)$$

and solving Equation 3.30 for $\frac{dQ_d}{dS}$ gives

$$\frac{dQ_d}{dS} ? ??? \,^2 (X_d \cos?_e ? Y_d \sin?_e) ?? g?_d \cos?_e \qquad (3.33)$$

For further derivation, it is convenient to nondimensionalize quantities as before, except for the time and frequency which are now nondimensionalized as

$$t ? T\sqrt{\frac{g}{L}}, \qquad ? ?? \sqrt{\frac{L}{g}}$$

Using nondimensional terms, the following dynamic expressions are produced:

$$\frac{dx_d}{ds} ? ??_d \sin?_e, \qquad \frac{dy_d}{ds} ?? _d \cos?_e \qquad (3.34, 3.35)$$

$$\frac{d?_d}{ds} ? \frac{1}{q_e}[? \,^2 (x_d \sin?_e ? y_d \cos?_e) ?? _d \sin?_e ? q_d \frac{(p ? \cos?_e)}{q_e}] \qquad (3.36)$$

$$\frac{dq_d}{ds} ? ??\,^2 (x_d \cos?_e ? y_d \sin?_e) ?? _d \cos?_e \qquad (3.37)$$

The two-point boundary conditions for an air-filled freestanding tube with material weight included are as follows:

For the range $0 ? s ? 1 ? b$

@ $s ? 0$: $\quad x_e ? y_e ?? _e ? 0, \quad x_d ? 0.001, \quad y_d ? 0, \quad ?_d ? 0$

@ $s ? 1 ? b$: $\quad y_d ? 0, \quad ?_d ? 0$

The amplitude of the vibration mode is determined by specifying a value for $x_d(0)$. Equations 3.34 through 3.37 along with 3.10 and 3.13 were written into a Mathematica program with the boundary conditions above, and the unknown parameters are $q_d(0)$ and ?. Convergent solutions were calculated and the results are presented in the next section. Separate versions of the program were used to obtain symmetric modes and nonsymmetric modes. The Mathematica code and the subject of symmetric and nonsymmetric modes are described in Appendix B and A, respectively.

3.5.1 Viscous Damping

Figure 3.10 incorporates two components for viscous damping; these are $C\frac{?X}{?T}$ and $C\frac{?Y}{?T}$. The way viscous damping works is to oppose the relative velocity of the vibrating system by a damping force F_C. This damping force F_C is proportional to the velocity. The coefficient C is the proportional constant. In this case the internal air molecules are colliding together and creating a friction within the system. This friction dampens the system via the damping force. This effect enhances the model of air within the geosynthetic tube and produces a more realistic representation of the system.

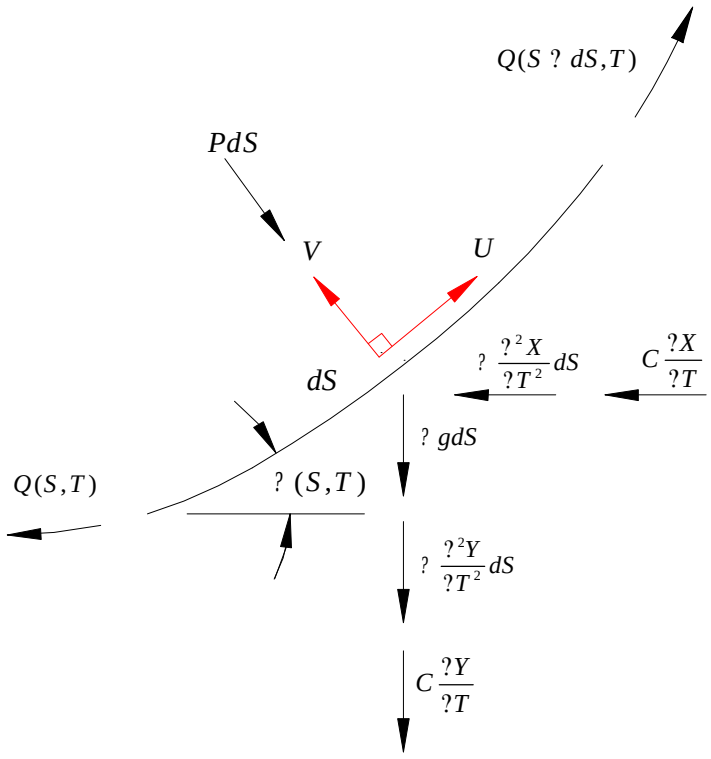

Figure 3.10 Kinetic equilibrium diagram with damping

To translate this into nondimensional terms, a viscous damping coefficient ? is introduced. The relationship between ? and *C* is given as

$$? \; ? \frac{C}{?} \sqrt{\frac{L}{g}} \tag{3.37}$$

By replacing the term $?^{2}$ in equations 3.36 and 3.37 with $?^{2} ? i? ?$, it is possible to incorporate viscous damping in the governing equations.

3.6 Dynamic Results

The following section displays and discusses the results of this vibration study. The plots and tables below represent the lowest four mode shapes for the air-filled case. The lowest mode shapes were taken, because it takes the least amount of energy to excite the tube into these shapes. Table 3.2 represents the calculated frequencies for the given internal air pressures p.

p	1st Sym. Mode	1st Nonsym. Mode	2nd Sym. Mode	2nd Nonsym. Mode
1.05	1.561	2.674	3.782	4.911
1.10	1.897	3.256	4.607	5.979
1.25	2.502	4.312	6.001	7.829
1.50	3.118	5.377	7.525	9.564
1.75	3.624	6.111	8.486	10.724
2.00	3.970	6.690	9.241	11.631
3.00	5.023	8.370	11.439	14.290
4.00	5.816	9.630	13.100	16.315
5.00	6.488	10.700	14.511	18.031

Table 3.2 Frequencies (?) for tube with internal pressure and rigid foundation

The results of Table 3.2 are plotted in Figure 3.11. As the height of the tube increases, the frequencies rise nonlinearly. This is attributed to the nonlinearity of the system of equations used to produce these results.

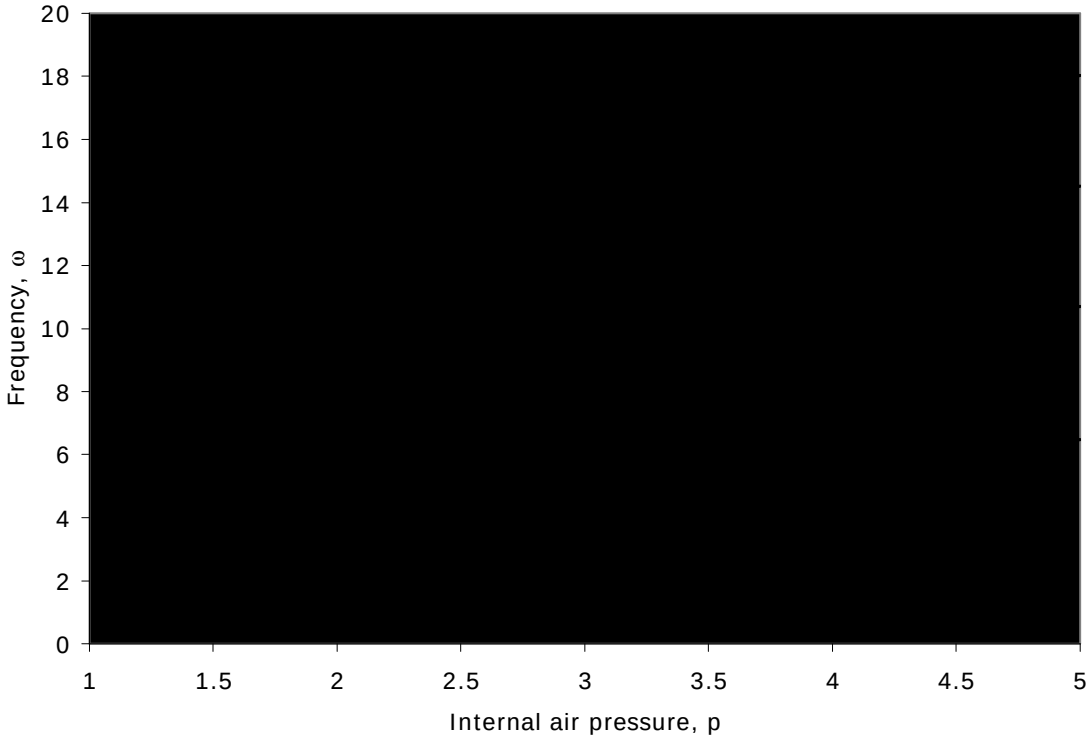

Figure 3.11 Frequency versus internal pressure

The four mode shapes fall into two categories: symmetric and nonsymmetric. Symmetric and nonsymmetric refer to the dynamic shape of the tube being symmetrical

or nonsymmetrical about the centerline of the equilibrium configuration. This concept is illustrated in Figures 3.12 through 3.16. Figures 3.12 – 3.16 show the mode shapes (in black) transcribed over the equilibrium configuration (in red). Damping is neglected and a coefficient, c, was used in order to obtain an amplitude of the vibration mode which would provide an appropriate separation between the equilibrium shape and the dynamic shape. The number of nodes corresponds to the level of frequency. For instance, in Figure 3.13 (a) there are two points of intersection (nodes) between the equilibrium configuration and the dynamic shape. In the dynamic results for anchored dams, the first mode shape contained a single node. This may happen because the inflatable dam has at least one anchored point or line. However, due to the nature of a freestanding tube, the first mode shape was not a sidesway oscillation, since it would not have a restoring force.

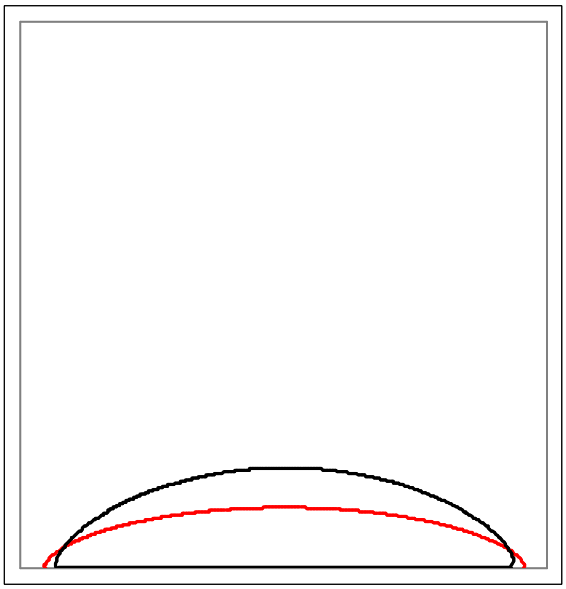

1st symmetrical mode

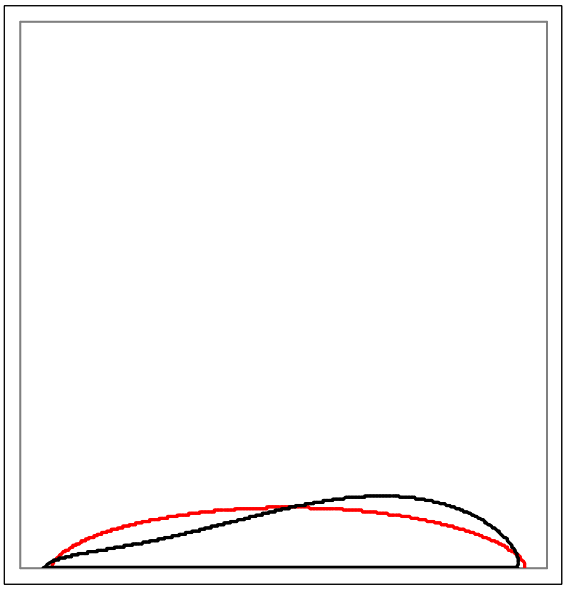

(b) 1st nonsymmetrical mode

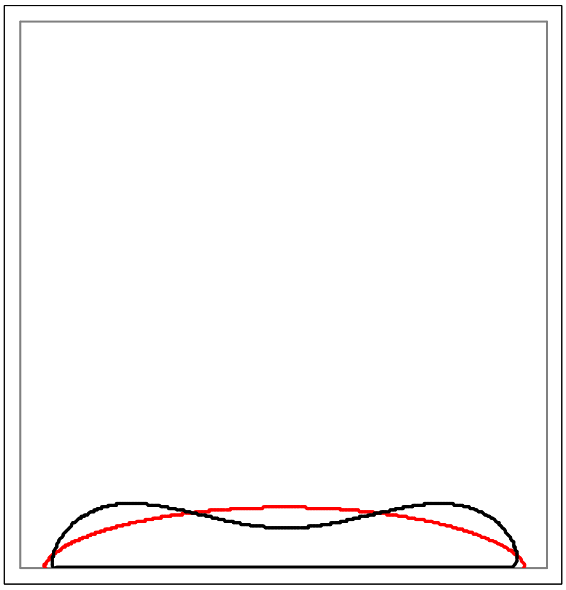

(c) 2nd symmetrical mode

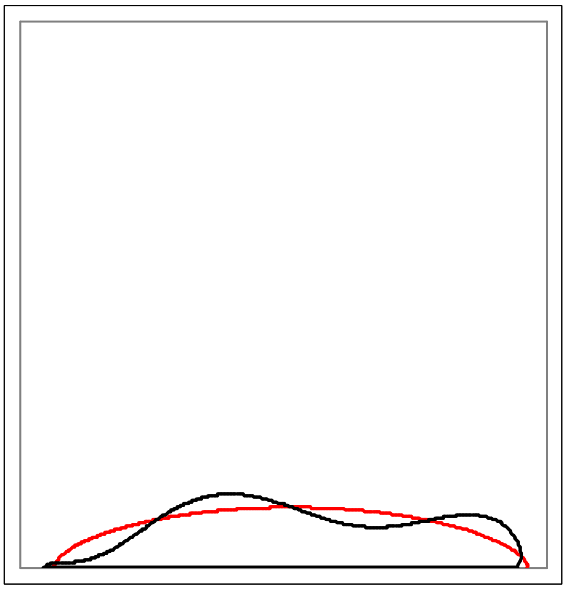

(d) 2nd nonsymmetrical mode

Figure 3.12 Mode shapes for p = 1.05

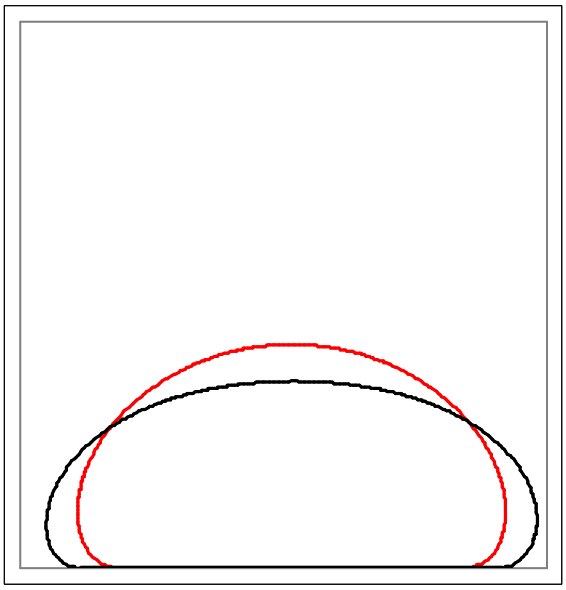

(a) 1st symmetrical mode

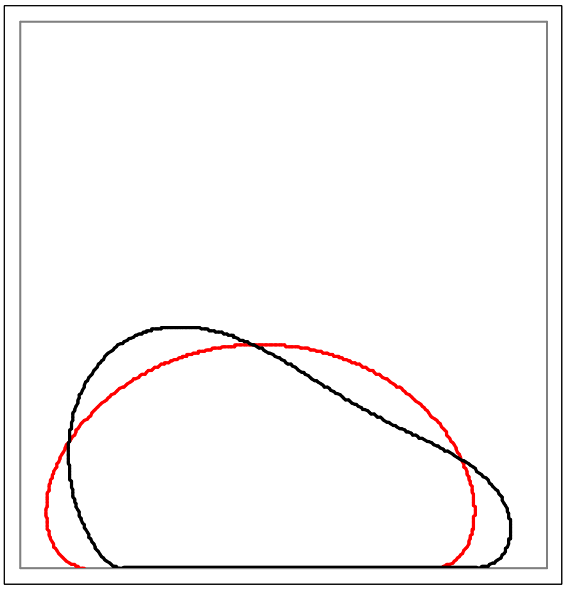

(b) 1st nonsymmetrical mode

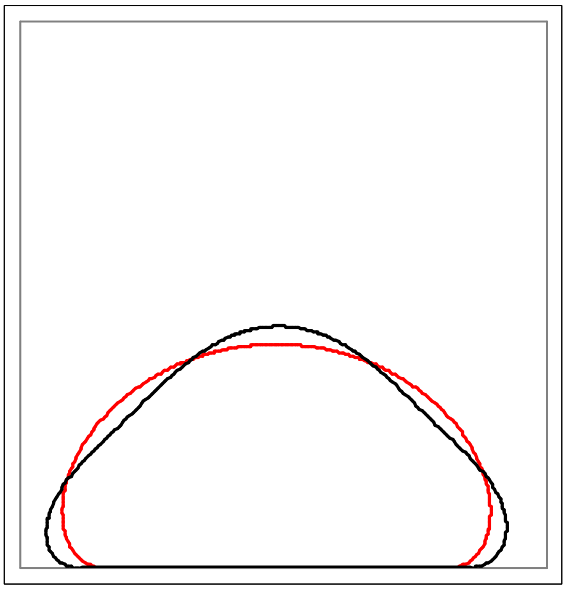

(c) 2nd symmetrical mode

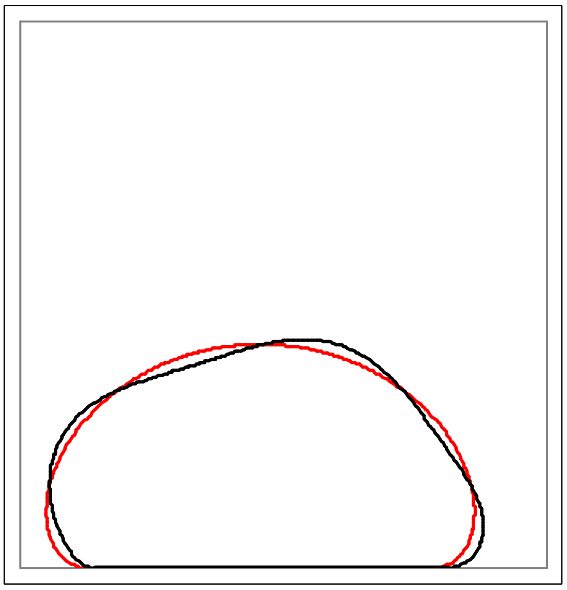

(d) 2nd nonsymmetrical mode

Figure 3.13 Mode shapes for p = 2

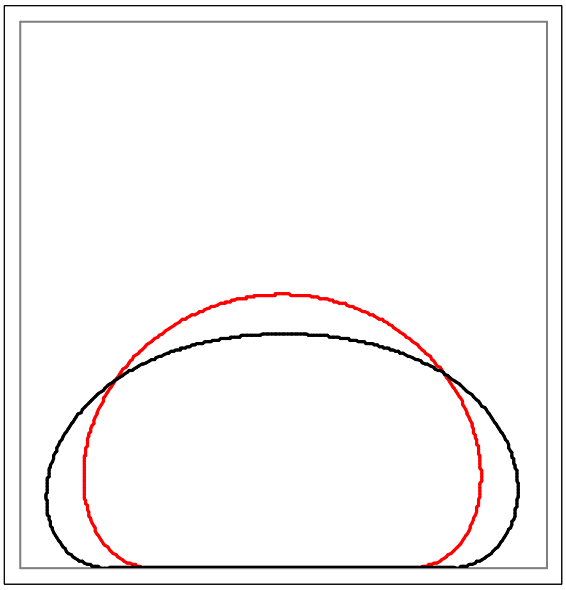

(a) 1st symmetrical mode

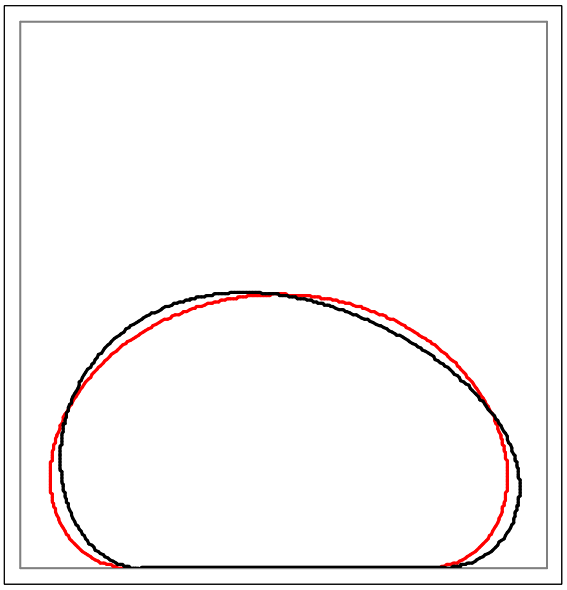

(b) 1st nonsymmetrical mode

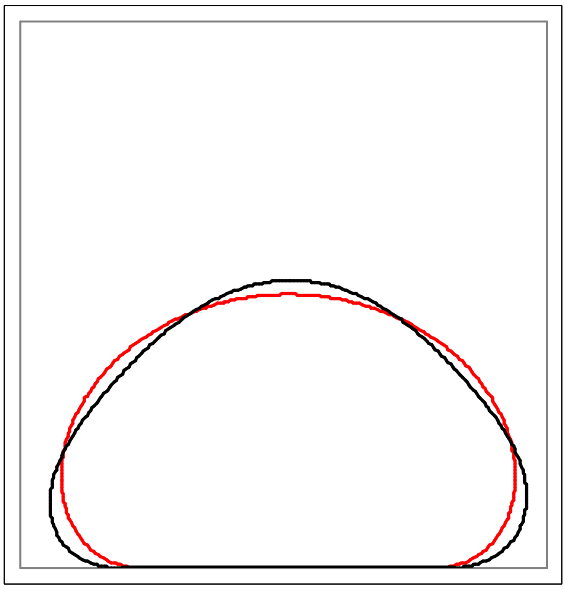

(c) 2nd symmetrical mode

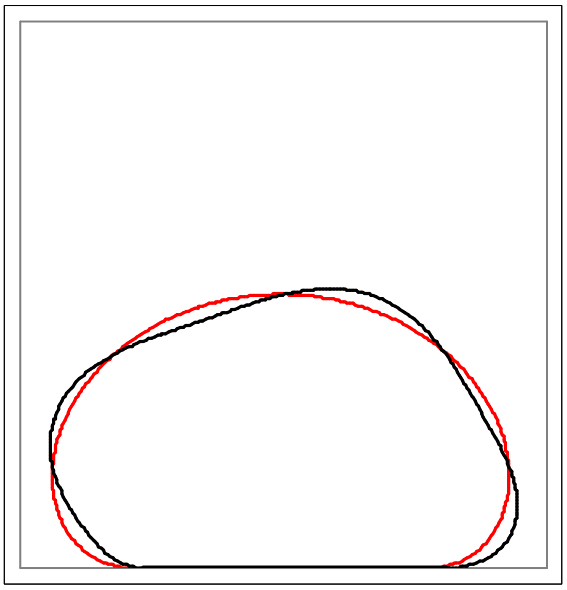

(d) 2nd nonsymmetrical mode

Figure 3.14 Mode shapes for p = 3

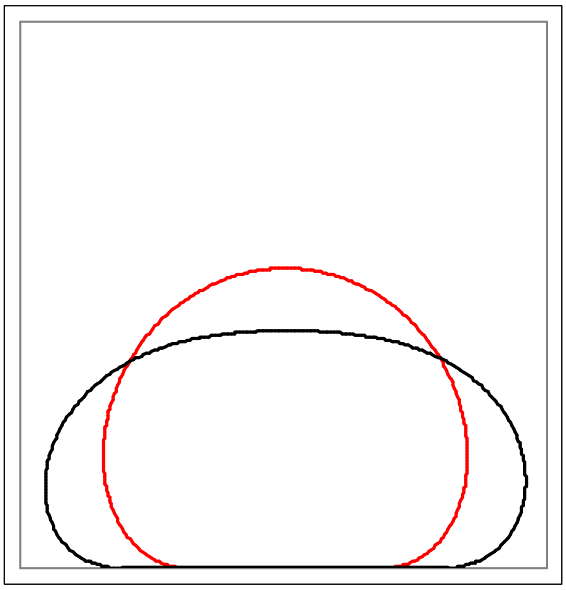

(a) 1st symmetrical mode

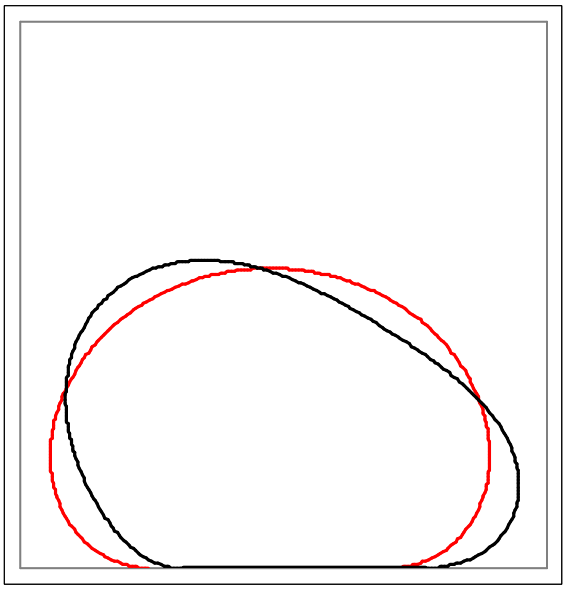

(b) 1st nonsymmetrical mode

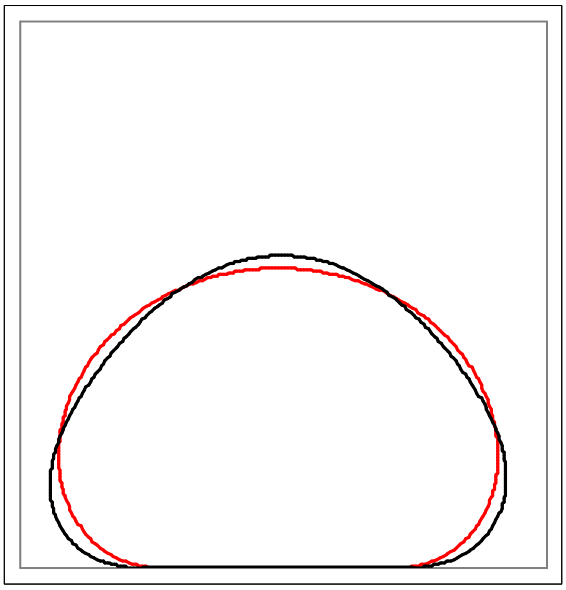

(c) 2nd symmetrical mode

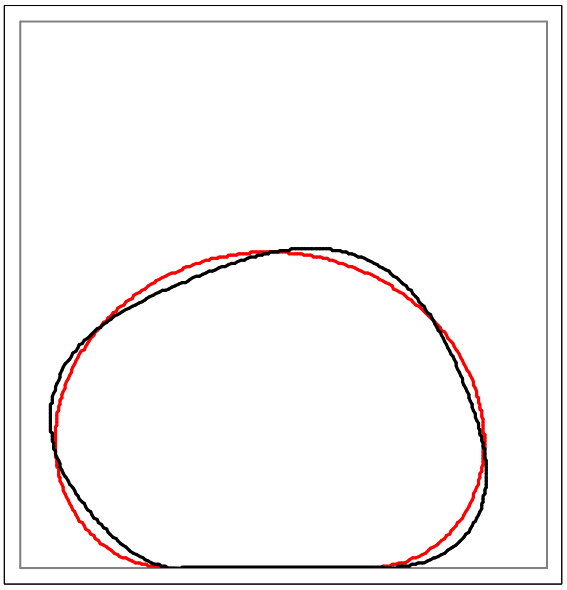

(d) 2nd nonsymmetrical mode

Figure 3.15 Mode shapes for p = 4

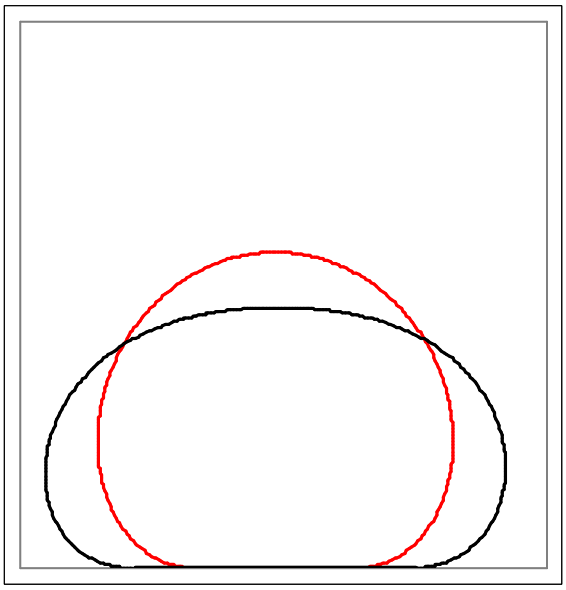

(a) 1st symmetrical mode

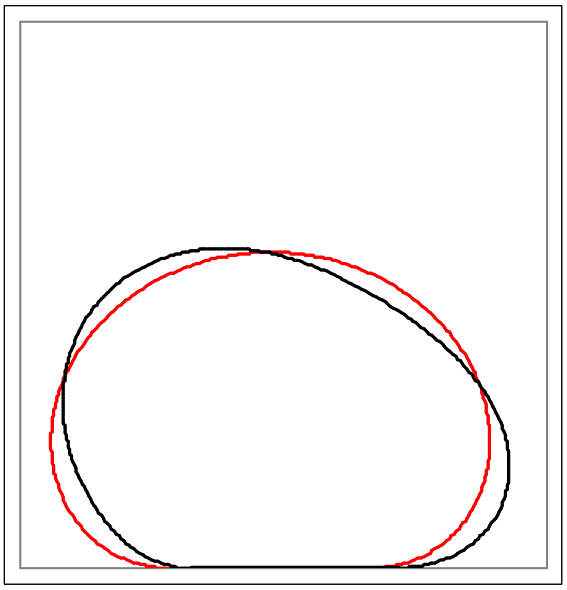

(b) 1st nonsymmetrical mode

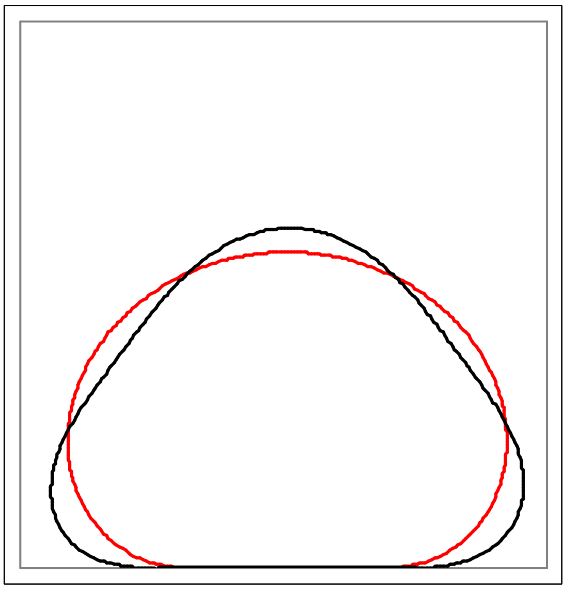

(c) 2nd symmetrical mode

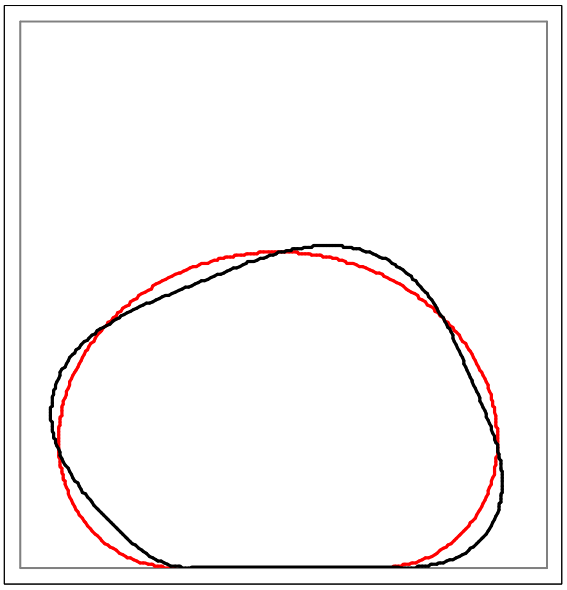

(d) 2nd nonsymmetrical mode

Figure 3.16 Mode shapes for p = 5

3.6.1 Damping Results

Figure 3.17 through 3.21 display the results of damping the freestanding system. For an internal air pressure of 1.05 the frequencies of all four mode shapes "die-out" with a nondimensional damping coefficient of less than ten. Notice that there is a dramatic jump in frequency going from an internal air pressure value of 1.05 to 2.

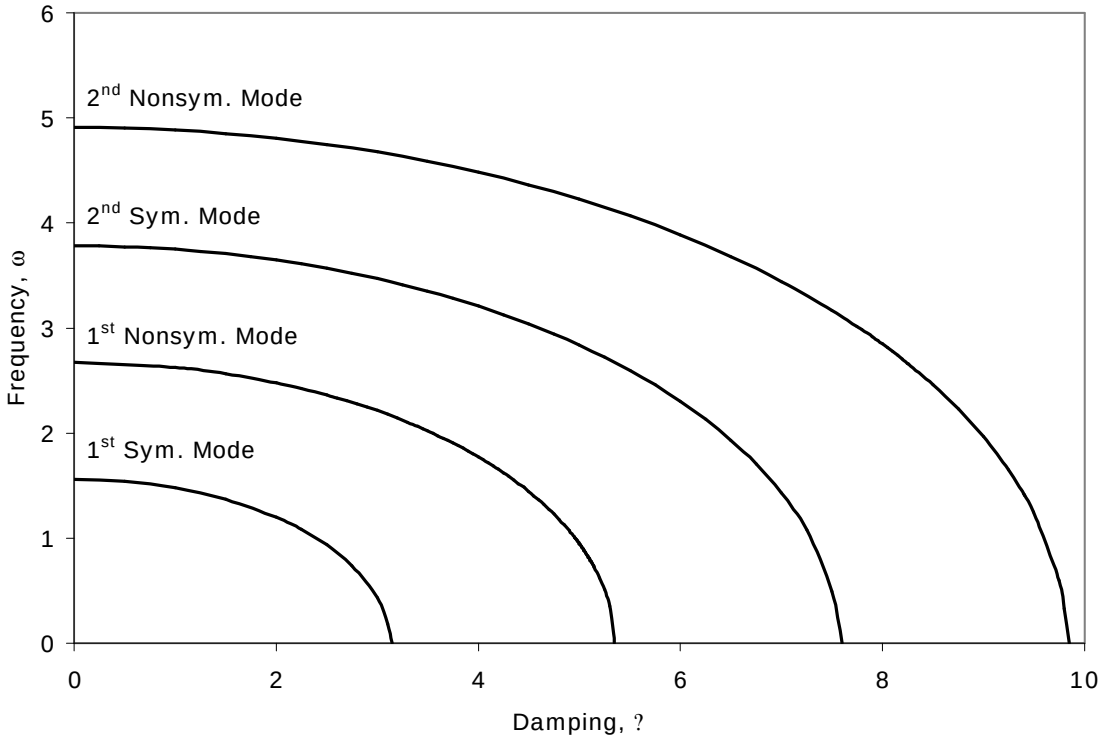

Figure 3.17 Frequency versus damping coefficient with p = 1.05

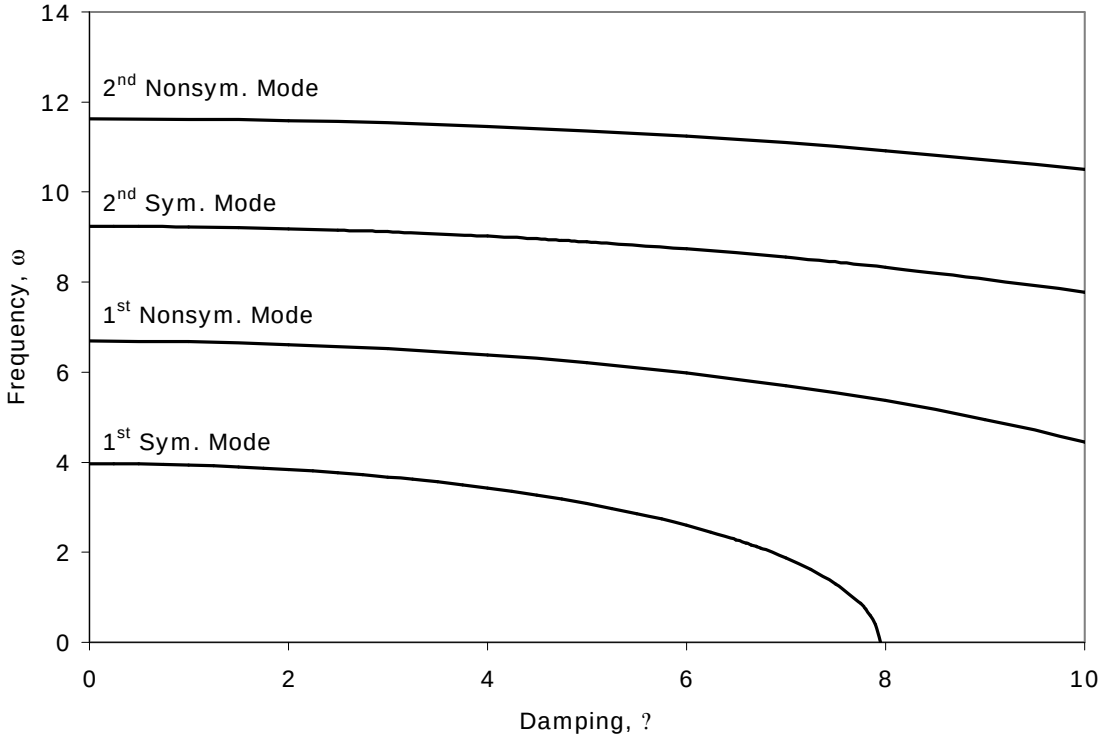

Figure 3.18 Frequency versus damping coefficient with p = 2

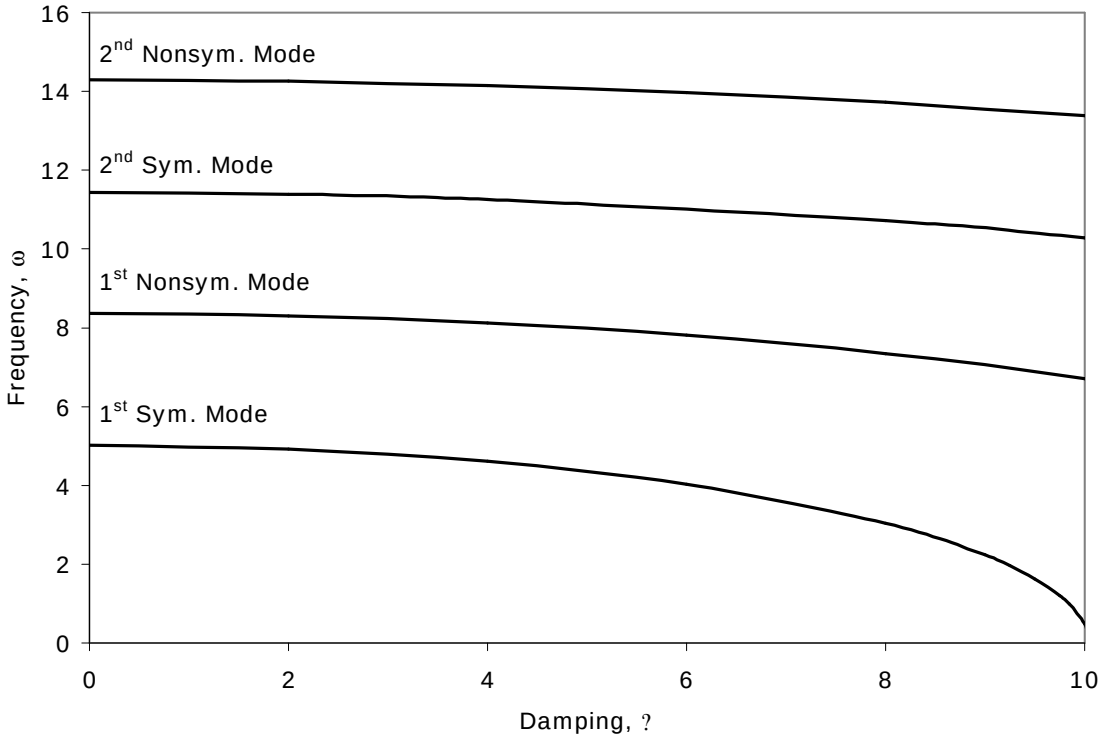

Figure 3.19 Frequency versus damping coefficient with p = 3

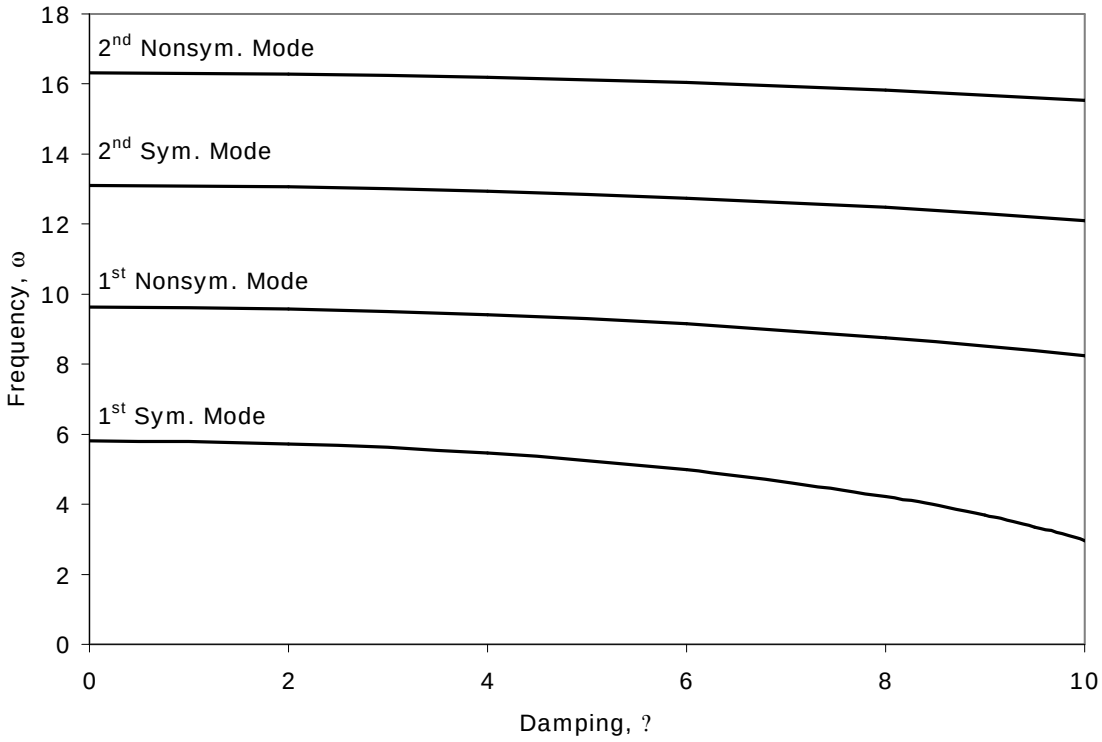

Figure 3.20 Frequency versus damping coefficient with p = 4

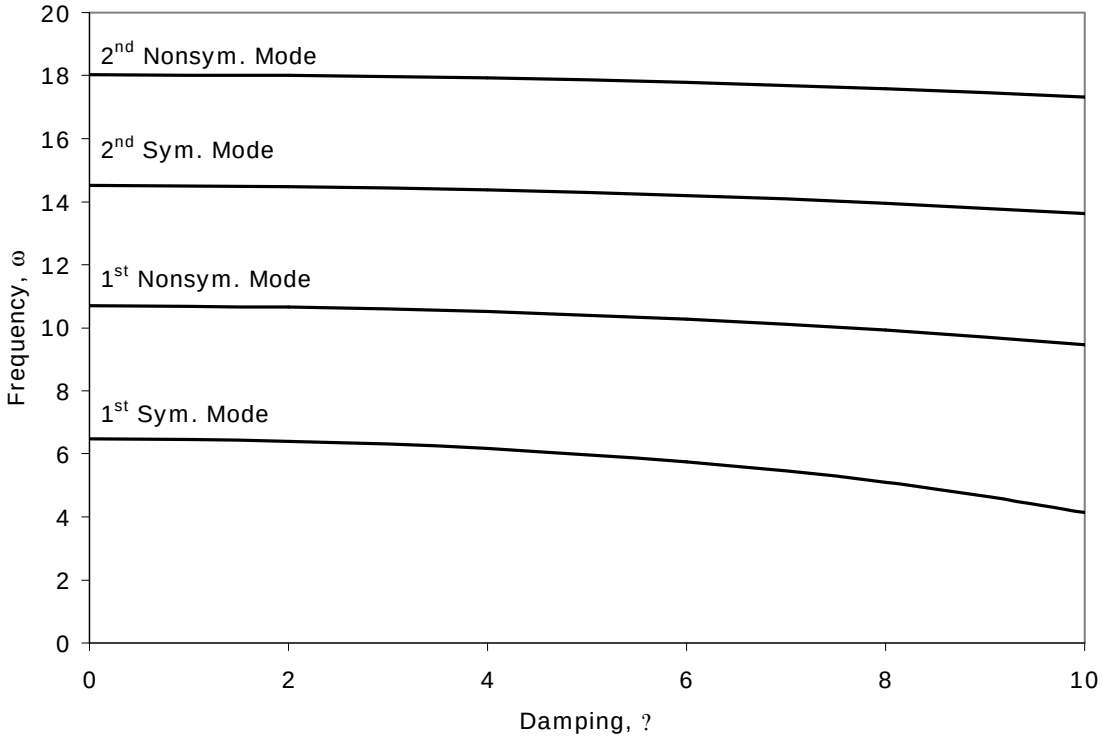

Figure 3.21 Frequency versus damping coefficient with p = 5

The tables below present different frequencies with set values for the damping coefficient ? and internal pressure p. The motion is not harmonic, but decays with oscillation. These values correspond to the data plotted in Figures 3.17 through 3.21. These tables show a gentle decrease in frequency at first and then a tremendous drop when the frequency approaches zero and the mode becomes overdamped (i.e., when ? = 0 the motion decays without oscillation). A dash represents values of the damping coefficient which were not calculated for the respected internal air pressure. Once the frequency dropped to zero, it was not necessary to compute further, because the value of critical damping has been reached.

	p				
?	1.05	2	3	4	5
0.00	1.561	3.970	5.023	5.816	6.488
2.00	1.199	3.842	4.923	5.730	6.410
3.15	0.000	-	-	-	-
4.00	-	3.430	4.608	5.461	6.172
6.00	-	2.600	4.029	4.983	5.753
7.95	-	0.000	-	-	-
8.00	-	-	3.038	4.222	5.108
10.00	-	-	0.482	2.971	4.134

(a) 1st symmetrical mode frequencies

	p				
?	1.05	2	3	4	5
0.00	2.674	6.690	8.370	9.630	10.700
2.00	2.480	6.615	8.310	9.578	10.653
4.00	1.775	6.385	8.128	9.420	10.512
5.35	0.000	-	-	-	-
6.00	-	5.980	7.814	9.151	10.271
8.00	-	5.363	7.352	8.760	9.924
10.00	-	4.445	6.712	8.230	9.460

(b) 1st nonsymmetrical mode frequencies

	p				
?	1.05	2	3	4	5
0.00	3.782	9.241	11.439	13.100	14.511
2.00	3.648	9.187	11.395	13.062	14.477
4.00	3.210	9.022	11.263	12.946	14.373
6.00	2.303	8.740	-	12.752	14.198
7.60	0.000	-	-	-	-
8.00	-	8.330	10.717	12.474	13.949
10.00	-	7.771	10.288	12.108	13.622

(c) 2nd symmetrical mode frequencies

	p				
?	1.05	2	3	4	5
0.00	4.911	11.631	14.290	16.315	18.031
2.00	4.808	11.588	14.255	16.284	18.004
4.00	4.485	11.458	14.149	16.192	17.920
6.00	3.888	11.238	13.971	16.037	17.780
8.00	2.849	10.922	13.718	15.817	17.582
9.85	0.000	-	-	-	-
10.00	-	10.502	13.386	15.530	17.324

(d) 2nd nonsymmetrical mode frequencies

Table 3.3 Modal frequencies for damped system

3.7 Dimensional Example in SI Units

The following section presents a dimensional example of converting values from the nondimensional charts to information with physical meaning. This example is similar to the one presented in section 2.7 of chapter 2. The next section will cover a comparison between the air-filled and water-filled results.

Given:

Consider a geosynthetic tube with a nondimensional internal air pressure of 2.85. The circumference L is equal to 1.50 m with a thickness of 0.52 mm. A sample of the geosynthetic material was measured and the density was found to be 1175kg/m^3.

Required:

Find the dimensional values of internal air pressure, membrane tension, and contact length. For a dynamic illustration, calculate the frequency if the tube if induced into the first mode of vibration, where damping and added mass are neglected. Next, find the critical damping coefficient C_{CR} for the first mode. Lastly, what is the lowest dimensional frequency for 15% of critical damping?

Solution:

Using the given parameters, the dimensional equilibrium values for membrane tension, maximum height, and contact length are easily calculated from the nondimensional results. The dimensional pressure becomes

$$P = p \cdot g = 2.85 \cdot 1175 kg/m^3 \cdot 0.00052 m \cdot 9.81 N/kg) = \boxed{17.08 Pa} = \boxed{0.0025 psi}$$

In order to calculate the actual tube height, the value y_{max} will need to be determined by Figure 3.5. From Figure 3.5, the value for y_{max} at p = 2.85 is roughly 0.22. Using this value and the circumferential length of 1.5m, the dimensional value for the tube height is found as

$$Y_{max} = y_{max} L = 0.22 \cdot 1.50 m = \boxed{0.33 m}$$

That means that roughly $75\%(0.33m) ? 0.25m$ will be retained using this tube with an internal air pressure equal to 17.08Pa, according to some manufacturers.

In choosing a membrane material to resist the required force for an internal air pressure of 17.08Pa, both the initial tension and maximum membrane force versus internal pressure plot are employed. From Figure 3.6 and 3.7, the value for q_o at p = 2.85 is 0.204 and q_{max} is 0.425. This translates into

$$Q_o ? q_o ? gL ? 0.204 ? 1175kg/m^3 ? 9.81N/kg ? 1.50m ? 0.00052m ? \boxed{1.83N/m}$$

$$Q_{\max} ? q_{\max} ? gL ? 0.425 ? 1175kg/m^3 ? 9.81N/kg ? 1.50m ? 0.00052m ? \boxed{3.82N/m}$$

Once knowing the membrane tension required to sustain an internal pressure of 17.08Pa, the material is chosen. The next step is to see if the contact length between tube and surface is sufficient in counteracting sliding behavior. After viewing Figure 3.8, the value for b at p = 2.85 is 0.26. The contact length in SI units is

$$B ? bL ? 0.26 ? 1.50 ? \boxed{0.39m}$$

The results for a nondimensional internal pressure of p = 2.85, which is induced by a force that resolves the tube into the 1st symmetric mode (Figure 3.14 (a)) can be taken from Figure 3.11. Using the frequency of 4.23, the dimensional frequency can be calculated as follows:

$$? ? ? \sqrt{\frac{g}{L}} ? 4.23\sqrt{\frac{9.81m/s^2}{1.5m}} ? \boxed{10.82rad/s}$$

The critical nondimensional damping coefficient is where the frequency ? equals zero. After running the Mathematica vibration program with an internal air pressure of 2.85, the resulting ? corresponding to an ? of zero is 9.80. Using this value and Equation 3.37, the critical damping coefficient becomes

$$C_{CR} ? ? ? \sqrt{\frac{L}{g}} ? 9.80 ? 1175kg/m^3 ? 0.00052m\sqrt{\frac{1.5m}{9.81m/s^2}} ? \boxed{2.34\frac{kg\,g\,s}{m^2}}$$

15% of critical damping for the first symmetrical mode is $0.35\frac{kg\,gs}{m^2}$. Next, the nondimensional damping coefficient must be calculated:

$$? \; ? \; \frac{C}{?}\sqrt{\frac{L}{g}} \; ? \; \frac{?}{?}\frac{0.35kg\,gs^2/m^2}{1175kg/m^3 \; ? \; 0.00052m}\frac{?}{?}\sqrt{\frac{1.5m}{9.81m/s^2}} \; ? \; \boxed{0.22}$$

From the vibration program run with an internal pressure of 2.85, the nondimensional frequency that corresponds to a damping coefficient of 0.98 is 4.36.
This produces a frequency of

$$? \; ? \; ? \; \sqrt{\frac{g}{L}} \; ? \; 4.36\sqrt{\frac{9.81m/s^2}{1.5m}} \; ? \; \boxed{11.15rad/s}$$

3.8 Internal Air Pressure and Internal Water Head Comparison

The internal air pressure of 2.85 was chosen, because it shares the same aspect ratio AR (ratio of tube width to tube height) with the internal pressure head 0.3. The concept is: if the two different values for air pressure and pressure head produce a similar shape, then the values for equilibrium properties and dynamic properties can be compared. Shown in Figure 3.22 is the relationship of the internal pressure head and internal air pressure versus the aspect ratio AR.

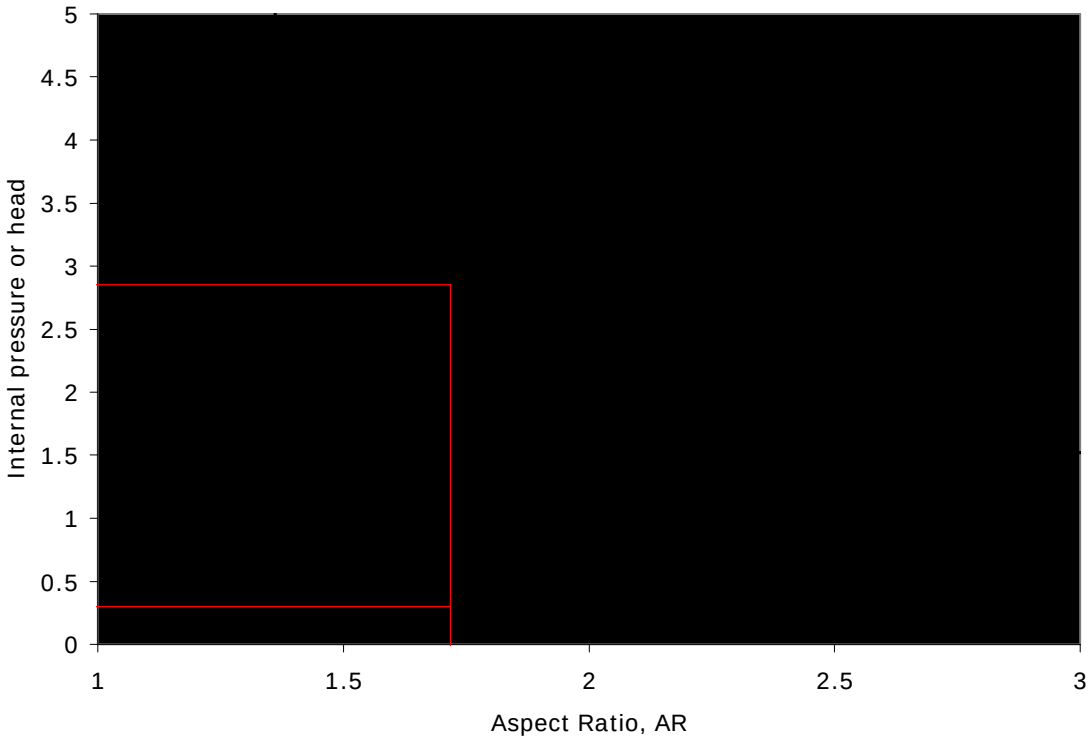

Figure 3.22 Internal air pressure versus aspect ratio

Figure 3.23 displays the two equilibrium shapes of the internal pressure head h = 0.3 (red line) and the internal air pressure p = 2.85 (black line). The aspect ratio was taken as $AR ? \frac{b ? 2x_{\max}}{y_{\max}}$ and was equal to 1.73.

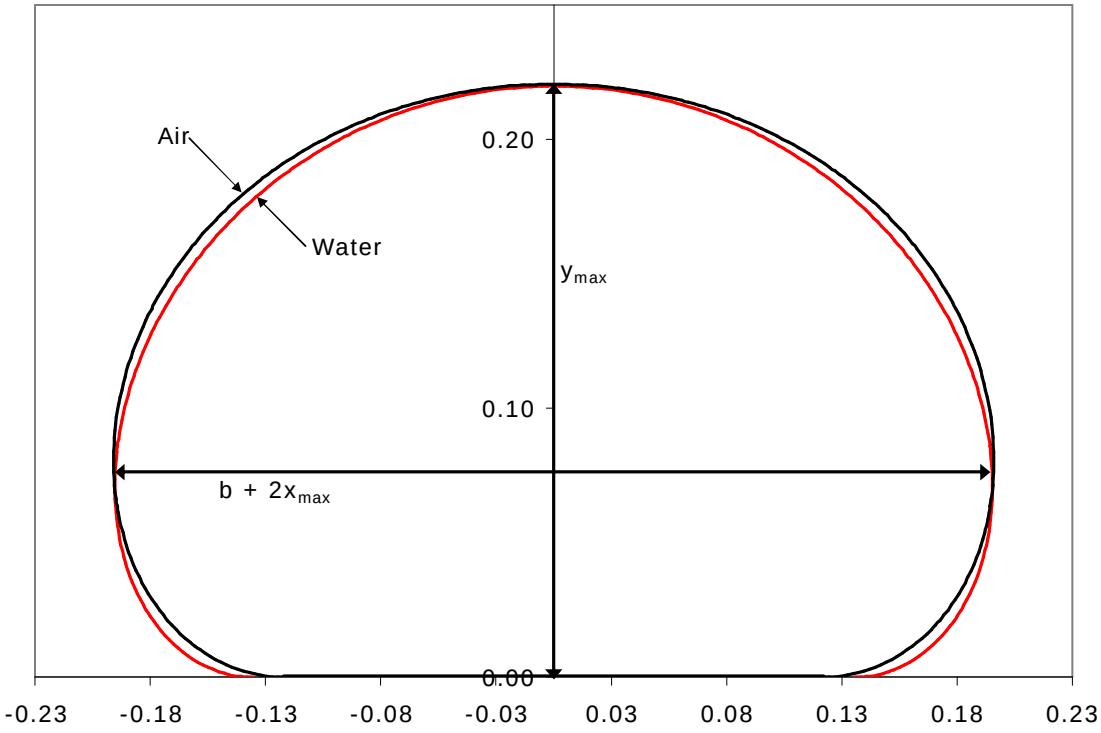

Figure 3.23 Equilibrium shape comparison of h = 0.3 and p = 2.85

Table 3.4 displays a summary of the results from the internal water and air examples. For the pressure column, the internal water pressure value was calculated for the bottom of the tube and for the air case the pressure remains constant throughout the tube. The results display a dramatic change when using internal air pressure versus an internal water head. An explanation of this drastic contrast in pressure, initial tension, and maximum tension could be the exclusion of extensibility. The air-filled tube needs only the air pressure to lift the weight of the tube to a certain height. The measured density of the geotextile material used in the examples was 1175kg/m^3. With a common thickness of 0.52mm, this is an incredibly light weight material which needs very little air pressure to expand the single tube to a desired shape. On the other hand, it takes much more water pressure to raise the tube. In order for the water-filled tube to achieve the same resulting height as the air-filled tube an internal pressure head greater than the actual height of the tube is required. Viewing Equation 2.12, we see that the curvature is inversely proportional to the membrane tension. Given the identical curvature, the membrane

tension would increase as the internal pressure increases. Notice the curvature at the origin for both the air and water-filled tube are roughly the same. However, at the crown of the tube the curvatures are largely different; meaning that these models are two separate problems all together and no change to the derivation would change the outcome of the results.

		Pressure, Pa (psi)	Ymax, m (ft)	Q_o, N/m (plf)	Q_{max}, N/m (plf)	B, m (ft)	C_{CR}
Water	h = 0.3	4410.00 (0.6400)	0.33 (1.08)	463.00 (31.72)	4410.00 (0.64)	0.35 (1.15)	211.4
Air	p = 2.85	17.08 (0.0025)	0.33 (1.08)	1.83 (0.13)	3.82 (0.26)	0.39 (1.28)	2.3

Table 3.4 Internal water and air comparison

Table 3.5 presents a comparison of the internal water and air frequencies neglecting damping and added mass. Consider Table 3.5. When comparing the frequencies of the internal water and air cases, notice the large difference between each mode. This difference is a direct function of neglecting the weight of the tube within the water-filled case.

		? ?(rad/s?			
		1st Sym. Mode	1st Nonsym. Mode	2nd Sym. Mode	2nd Nonsym. Mode
Water	h = 0.3	172.00	265.26	355.23	441.24
Air	p = 2.85	10.83	20.86	28.54	35.69

Table 3.5 Internal water and air frequency comparison

Chapter 4: Tube with internal water and deformable foundation

4.1 Introduction

The majority of geosynthetic tubes rely on the fill material to maintain the barrier's stability. Designed for the primary purpose of segregating dry land from wet land, these tubular structures are considered gravity dams. The weight of the material within offsets the tube's tendency to roll or slide given an external load. Water on site is the most obvious and abundant material that possesses both weight for stability and fluidity for pumping. Nevertheless, with this added weight of water the tube will tend to settle below the ideal horizontal surface of a soft foundation. Hence, the water-filled model presented in chapter 2 will need to accommodate this change in the tube's elevation. Resting on a deformable foundation, the equilibrium and dynamic response of a geosynthetic tube with internal water behaves quite differently than an air-filled tube (which is presented in the next chapter). Within this chapter the investigation of a water-filled tube resting on two deformable foundation models will be examined.

Four analytical studies of the geotextile tube's equilibrium response have been performed. Two of these studies employed the use of FLAC while the other two used Mathematica software for a two-dimensional analysis. Huong (2001) selected FLAC to explore the effects of varying the soil characteristics of soft clays. His results included the amount of settlement, tube height, and membrane tension. Kim (2003) also used FLAC to investigate the apron, baffle, sleeved, and stacked tube designs with a Mohr Coulomb soil model. Her results consisted of finding the critical external water levels, membrane tension, deformations (when loaded externally), and pore pressures. Plaut and Suherman (1997) used Mathematica to develop equilibrium models that considered the effects of submergence, deformable foundation, and impounding water. Specific to this chapter, Plaut and Suherman considered a tensionless Winkler foundation with the tension below the supporting surface not to be constant. Their process in computing equilibrium properties matches the shooting procedure used in section 4.3. With the aid of Mathematica, Plaut and Klusman investigated a single tube, two stacked tubes, and a

three tube pyramid formation with rigid and modified Winkler foundations (Klusman 1998, Plaut and Klusman 1999). Klusman modified Suherman's Winkler model by assuming a normal foundation force and allowing the tension to be constant along the tube's entire perimeter. The results from the Suherman, Klusman, and Plaut studies along with the current investigation are compared in section 4.4.

This chapter presents the formulation and analysis results of a water-filled freestanding geosynthetic tube resting on both a Winkler and Pasternak foundation. Similar to the water-filled tube study in chapter 2, Mathematica 4.2 is used to solve boundary value problems and compute membrane properties. An accuracy goal of five or greater was used in all Mathematica coded calculations. Mathematica 4.2 solutions were then transferred to Microsoft Excel where property relationships, equilibrium shapes, and shapes of the vibrations about equilibrium were plotted. AutoCAD 2002 was also used in presenting illustrations of free body diagrams and details of specific formulation components to better clarify the subject. All derivations within were performed by Dr. R. H. Plaut.

Section 4.2 presents the assumptions utilized in the formulation of the freestanding water-filled tube resting upon a Winkler foundation. Next, section 4.3 pictorially introduces and discusses the method of deriving the equilibrium shape and membrane properties. Subsequently, these equilibrium results are discussed and presented in section 4.4. As in chapters 2 and 3, knowing the equilibrium parameters, the membrane mode shapes and natural frequencies may be calculated. Formulation of vibrations about the equilibrium configuration with a Winkler foundation is presented in section 4.5 followed by the dynamic results in section 4.6. Introduced in section 4.7 is the Pasternak foundation. Details for the equilibrium formulation of a water-filled barrier resting on a Pasternak foundation are presented in section 4.7 followed by the calculated membrane properties presented in section 4.8. The dynamic derivation of a water-filled tube resting a Pasternak foundation is found in section 4.9 followed by the results presented in section 4.10.

4.2 Winkler Foundation Model

A freestanding geosynthetic tube filled with water and supported by a Winkler foundation is considered. The tube is assumed to be infinitely long and straight catering to a two-dimensional model. Typical assumptions discussed in chapters two and three hold. These assumptions include: longitudinal changes in cross-sectional area are negligible, geosynthetic material is inextensible, and bending resistance is neglected. Originally proposed by Winkler in 1867, this is the most fundamental foundation model used in many initial analyses. The Winkler foundation model assumes that the downward deflection of the soil at a point is directly proportional to the stress applied at that point and independent of the surrounding soil behavior (Selvadurai 1979). The deflection occurs directly under the load applied. To model this behavior, numerous independent vertical springs are integrated into foundation. The Winkler model has been investigated with problems associated with floating structures (floating bridges and ice sheets), cemented lap joints, and the state of stress at the tip of a crack in an elastic continuum (Selvadurai 1979). When the tube is in contact with the Winkler foundation, tension is not assumed constant. However, above the surface of the Winkler foundation the membrane tension is constant. The internal water is hydrostatically modeled.

4.3 Winkler Foundation Equilibrium Derivation

Figure 4.1 presents the equilibrium geometry of a geosynthetic tube resting on a Winkler foundation. The origin is located at the tube's subsurface centerline (point O). The points A and C signify the right and left tube-surface contact regions. Horizontal distance X and vertical distance Y represent the two-dimensional coordinate system. The symbol ? signifies the angular measurement from a horizontal datum to the tube membrane. The measurement S corresponds to the arc length from the origin following along the membrane. X, Y, and ? are each a function of the arc length S. Y_{max} denotes the maximum height of the tube. L represents the circumferential length of the entire membrane. The internal pressure head H is a virtual measurement of a column of fluid with specific weight $?_{int}$ that is required to give a specified pressure. P_{bot} and P_{top} are the

pressures at the bottom and top of the tube, respectively. P represents the pressure at any level in the tube. The tension force in the membrane per unit length (into the page) is represented by the character Q. K is the stiffness of the supporting soil which is representative of the vertical Winkler springs. Scott (1981) gives dimensional values for K in MN per meter cubed which include: 6-8 for loose sand, 18-90 for medium dense sand, 90-300 for dense sand, and 15-30 for stiff clay, 30-60 for very stiff clay, over 60 for hard clay, and "very small" for soft to medium-stiff, normally-consolidated clays. The tube settlement H_f is the maximum distance of the tube below the surface of the supporting foundation.

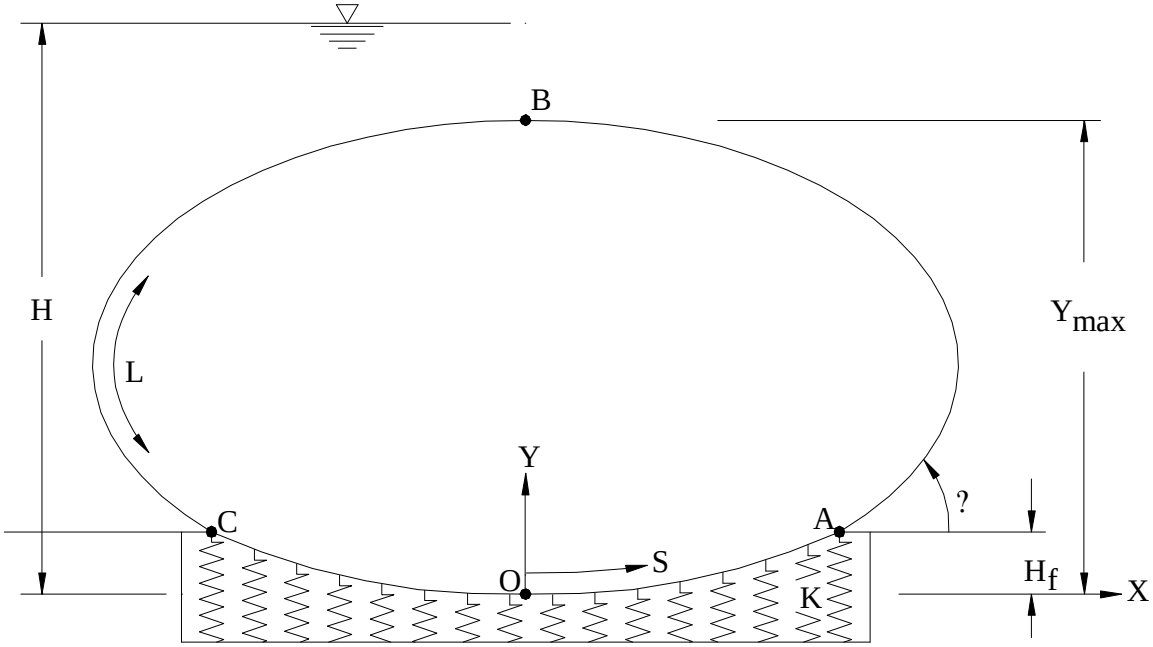

Figure 4.1 Winkler foundation model

Equations 2.1 and 2.2 describe the dimensional pressure at any point and hold true for the tube resting on a deformable foundation:

$$P ? P_{bot} ? ?_{\text{int}} Y, \qquad \text{where} \quad P_{bot} ? ?_{\text{int}} H \tag{2.1, 2.2}$$

To simplify the derivation, the following nondimensional terms are used in the equilibrium formulation:

$$x ? \frac{X}{L}, \qquad y ? \frac{Y}{L}, \qquad s ? \frac{S}{L}, \qquad k ? \frac{K}{? _{\text{int}}}$$

$$h ? \frac{H}{L}, \qquad q_e ? \frac{Q_e}{? _{\text{int}} L^2}, \qquad p ? \frac{P}{? _{\text{int}} L}, \qquad h_f ? \frac{H_f}{L}$$

Figure 4.2 exhibits a segment of the geosynthetic membrane below the surface of the Winkler foundation. The resultant force of a vertical Winkler spring is proportional to the deflection in the opposite direction multiplied by the soil stiffness coefficient k.

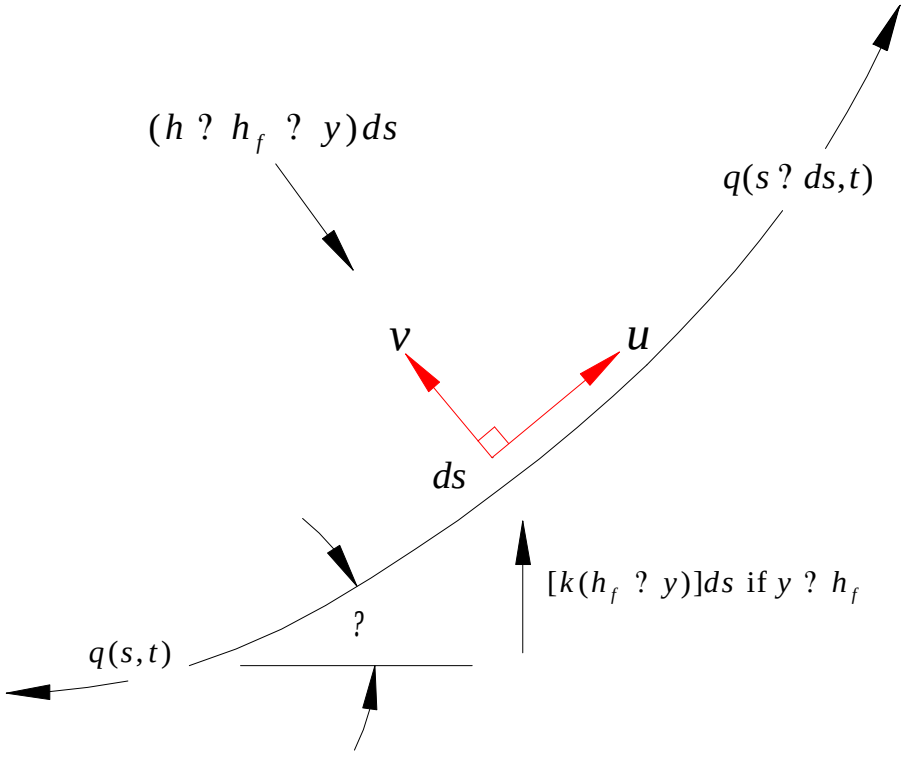

Figure 4.2 Tube segment below Winkler foundation

Since the general geometry of the tube has not been altered, Equations 2.6 and 2.7 maintain in describing the equilibrium configuration:

$$\frac{dx_e}{ds} ? \cos ? _e, \qquad \frac{dy_e}{ds} ? \sin ? _e \qquad (2.6, 2.7)$$

However, with the incorporation of a Winkler foundation, two equations are needed to describe both the change in angle measurement $?_e$ and change in membrane tension q_e

with respect to the arc length s. Using Figure 4.2, sum the forces in the tangential and normal directions with respect to the membrane segment. When the segment of the tube is below the surface of the foundation, the change in angle and change in membrane tension become

$$\frac{d\theta_e}{ds} = \left(\frac{1}{q_e}\right)\left(h - h_f - y_e\right) - k\left(h_f - y_e\right)\cos\theta_e, \qquad \frac{dq_e}{ds} = -k\left(h_f - y_e\right)\sin\theta_e \quad \text{(4.1a, 4.1b)}$$

When the tube lies above points A and C, Equations 4.1a and b simplify to

$$\frac{d\theta_e}{ds} = \left(\frac{1}{q_e}\right)\left(h - h_f - y_e\right), \qquad \frac{dq_e}{ds} = 0 \quad \text{(4.2a, 4.2b)}$$

The two-point boundary conditions for a single freestanding tube resting on a Winkler foundation are as follows:

For the range $0 \le s \le 0.5$

@ $s = 0$ (point O): $x_e = 0$, $y_e = 0$, $\theta_e = 0$

@ $s = 0.5$ (point R): $x_e = 0$, $\theta_e = ?$

When using nondimensional terms, the maximum tension in the membrane is

$q_{\max} = q_o = y_{\max}$ where $y_{\max} = y(t = 0.5)$ and $q_o = q(t = 0)$

An "if then" command is used to decipher between above foundation and below foundation computations. If the vertical tangent points of the tube ever fall below the surface of the Winkler foundation, the calculated values are not admissible. This means that the Winkler springs must be in contact with the tube only below its vertical tangents. The Mathematica equilibrium program for the Winkler foundation is presented and discussed in Appendix C.

4.4 Winkler Foundation Equilibrium Results

Presented within this section are the Mathematica produced equilibrium results of a water-filled tube resting upon a Winkler foundation. As in Chapter 2, four values of internal pressure head, h = 0.2, 0.3, 0.4, 0.5, were designated. Three values for the soil stiffness coefficient, k = 5, 100, and 200, were chosen to view the tube's behavior if placed on an extremely deformable foundation (e.g., water), an intermediate foundation (such as soft soil), and an approximately rigid foundation (hard soil). Once the internal pressure head h and soil stiffness k were designated, the unknown quantities of tube settlement, height of tube above surface, membrane tension at the origin, and maximum tension were determined.

The equilibrium properties for the nondimensional internal pressure head equal to 0.25 were computed with the described Mathematica program in Appendix C. A comparison of the results from Klusman and Suherman, and the current study, are presented in Tables 4.1 and 4.2. Values produced from this study are approximately, if not identically, equal to the results from the Winkler foundation model of Klusman and Suherman.

Membrane Tension Below Foundation Surface at Maximum Depth		
h = 0.25		
k	Suherman	present
10	0.020	0.020
25	0.017	0.017

Table 4.1 Nondimensional comparison of membrane tension below a Winkler foundation

h = 0.25	Membrane Tension Above Foundation		
k	Suherman	Klusman	present
10	0.017	0.017	0.017
25	0.016	0.016	0.016
	0.015	0.015	0.015

Table 4.2 Nondimensional comparison of membrane tension above a Winkler foundation

Figure 4.3 exhibits the changes in equilibrium shapes when the internal pressure head increases and the soil stiffness is held at 5. Physically, the shapes placed on a soil with

stiffness coefficient of 5 approaches the formations of a tube placed upon an extremely yielding foundation. Szyszkowski and Glockner (1987) discuss the application of thin-walled membrane structures transporting or storing environmentally safe liquids such as fresh water over salt water. Published in this paper is a reduction of required stiffness and material strength if a membrane structure is to perform as a transporting device. In maintaining the integrity of the equilibrium (and later the dynamic) derivation, this unique application suggests that low stiffness values for the supporting foundation should be employed for tubes resting on water.

Figure 4.3 Equilibrium configurations for set internal pressure heads when k = 5

Figure 4.4 demonstrates the effect on equilibrium configurations when varying the foundation stiffness (5, 30, and 200) when the set internal pressure head is equal to 0.2.

Figure 4.4 Equilibrium configurations varying soil stiffness coefficients when h = 0.2

Both the height of the tube above the supporting Winkler foundation and the tube settlement below the foundation are presented in Figure 4.5. The lowest foundation stiffness allowed by the vertical tangent criterion is 5. A soil stiffness of 200 is near rigid and would be an appropriate value for the majority of hard soils.

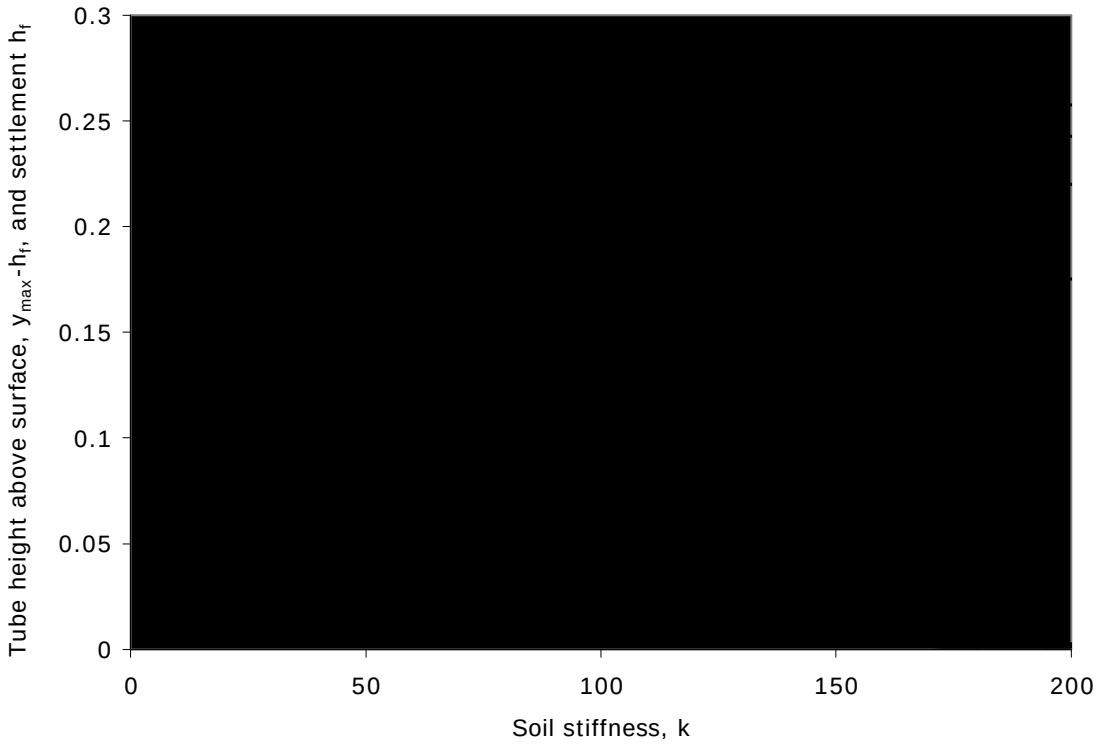

Figure 4.5 Tube height above surface and tube settlement versus soil stiffness

Figure 4.6 presents the relationship of maximum membrane tension versus internal pressure head. A close to linear increase is viewed when the maximum membrane tension is related to the internal pressure head. The maximum membrane tension occurs at the bottom of the tube. Figure 4.7 displays the tension along the membrane. The constant membrane tension represents the values computed above the Winkler supporting surface. Figure 4.7 exhibits a significant decrease in membrane tension when the soil stiffness of the deformable foundation is increased.

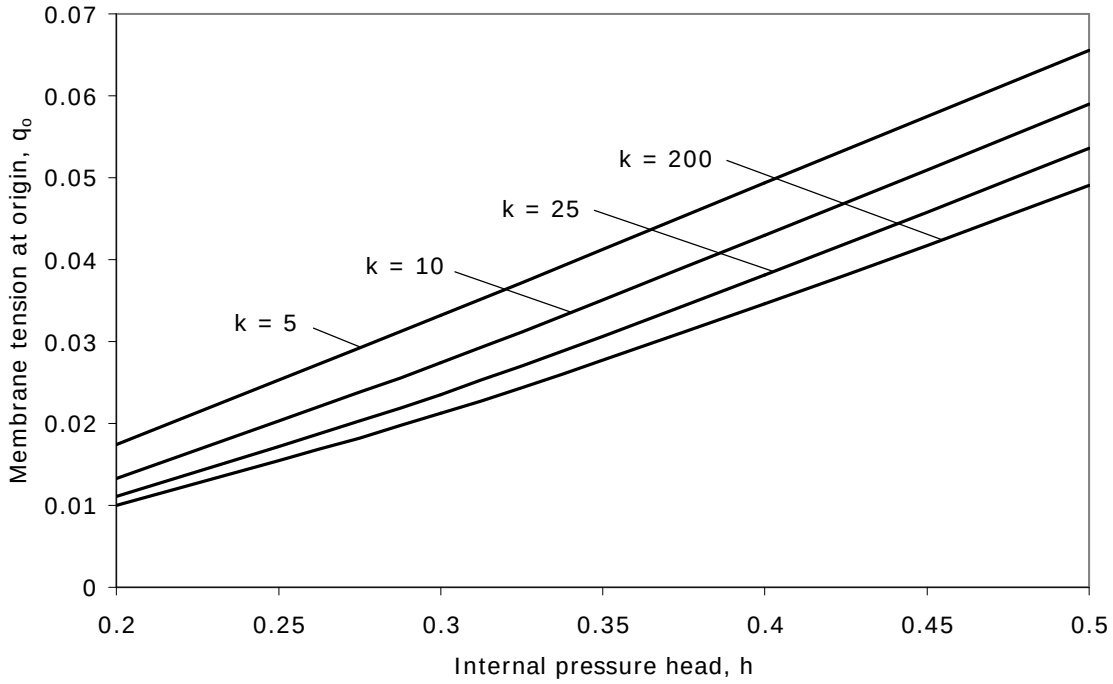

Figure 4.6 Membrane tension at origin versus internal pressure head

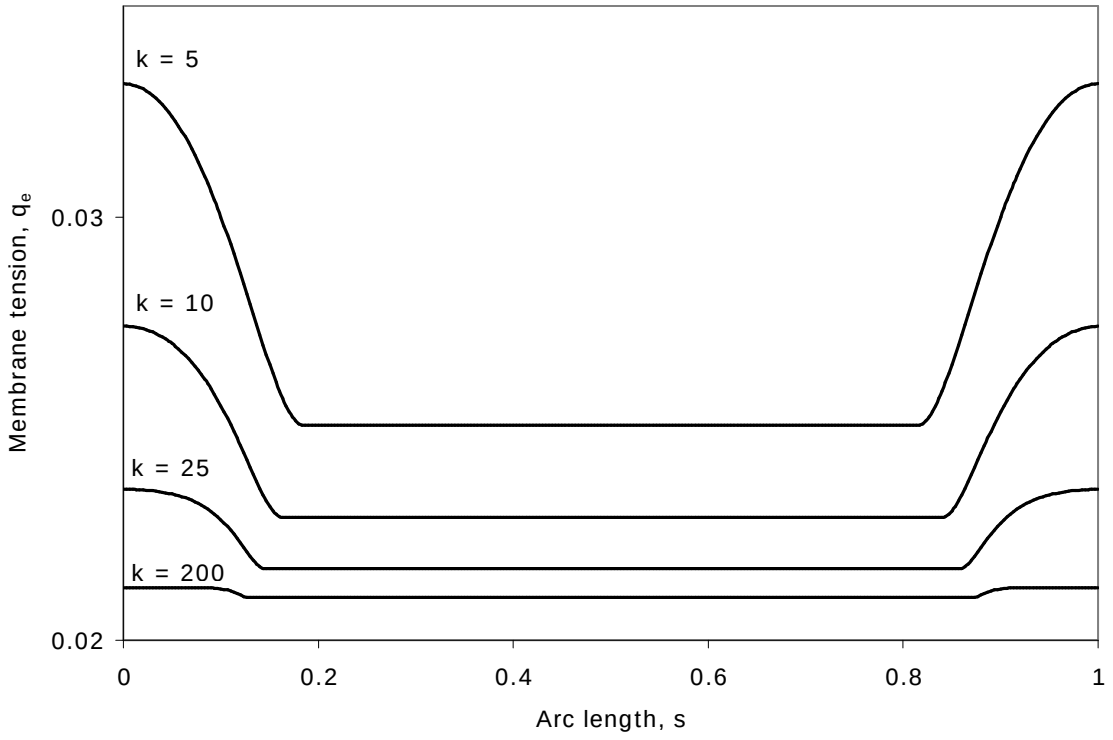

Figure 4.7 Tension along the membrane versus arc length when h = 0.3

Consider Figure 4.8. Little change is noticed past the soil stiffness value of 25

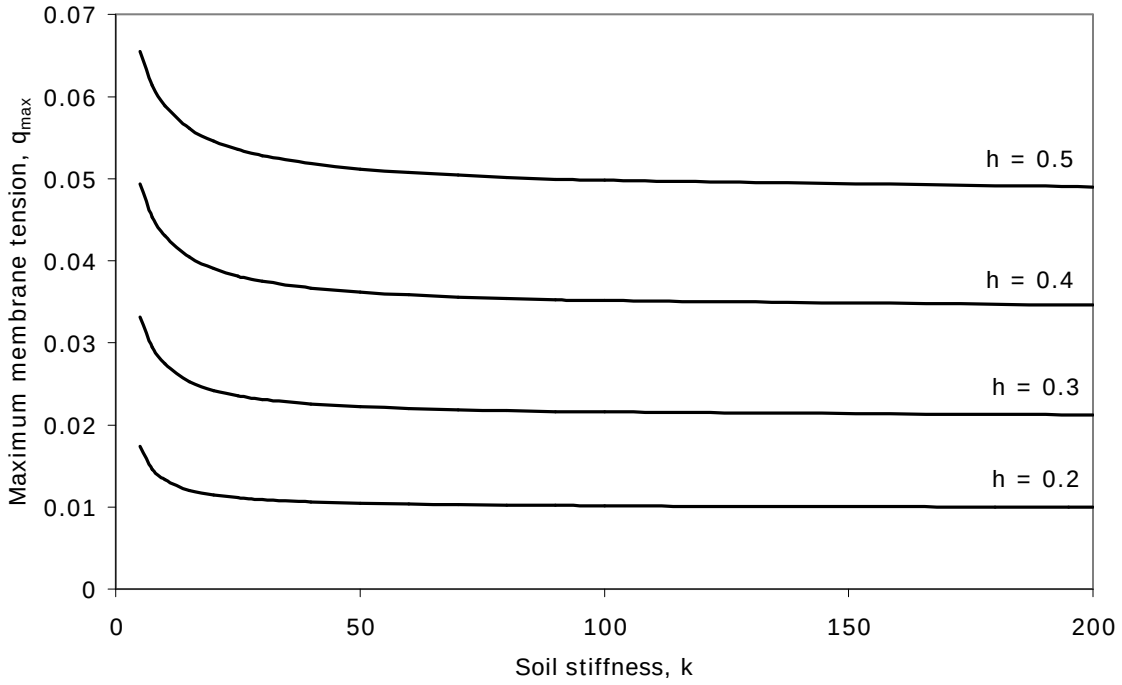

Figure 4.8 Maximum membrane tension versus soil stiffness

4.5 Winkler Foundation Dynamic Derivation

Now the equilibrium configuration is permitted to move with small vibrations. Consider the kinetic equilibrium diagram presented in Figure 4.9. In maintaining consistent tube geometry, nondimensional versions of Equations 3.18 and 3.19 are used:

$$\frac{?x}{?s} ? \cos? \qquad \frac{?y}{?s} ? \sin? \qquad (4.3, 4.4)$$

The D'Alembert Principle (covered in section 2.5) is employed and equilibrium is induced upon the system. Summing the forces in the tangential (u) and normal (v) directions (with respect to the membrane element) results in

$$\frac{??}{?s} ? \frac{1}{q}[(h ? h_f ? y) ? k(h_f ? y)\cos? ? \frac{?^2 x}{?t^2}\sin? ? \frac{?^2 y}{?t^2}\cos?] \quad (4.5)$$

$$\frac{?q}{?s} ? ?k(h_f ? y)\sin? ? \frac{?^2 x}{?t^2}\cos? ? \frac{?^2 y}{?t^2}\sin? \quad (4.6)$$

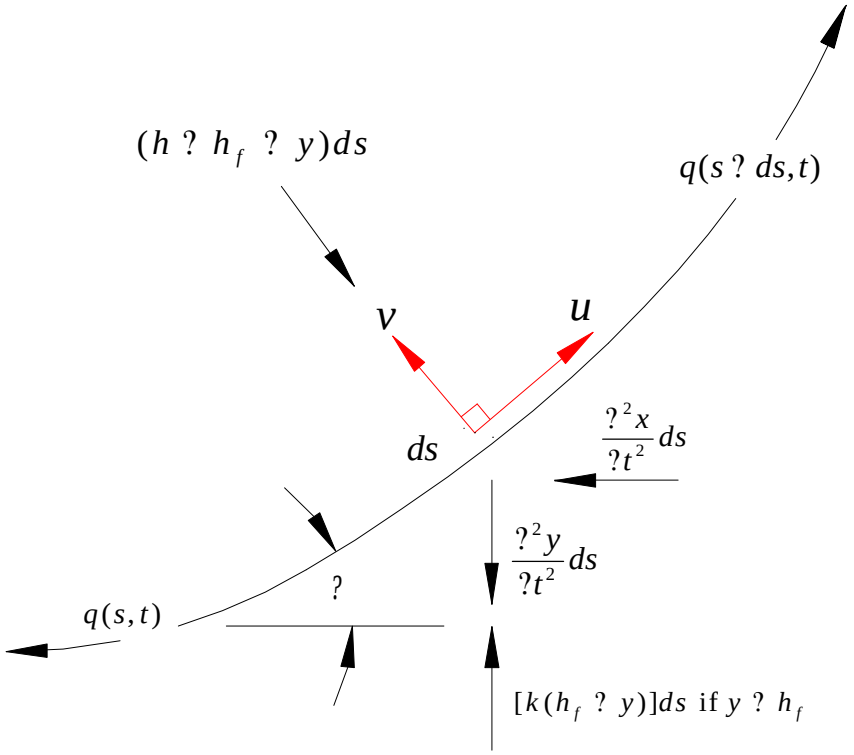

Figure 4.9 Winkler foundation kinetic equilibrium diagram

Equations 4.3 through 4.6 describe the dynamics of a geosynthetic tube supported by a Winkler foundation when y is less than h_f. These equations are considered the equations of motion for this system. As defined in chapter 2, ? is the nondimensional frequency of the system and t is time. Using an identical setup as in Section 3.5, nondimensional versions of Equations 3.22 through 3.26 will be utilized and are presented below. These nondimensional equations describe the total effect of motion on the equilibrium configuration, where the subscript d represents "dynamic":

$$x(s,t) ? x_e(s) ? x_d(s)\sin? t, \qquad y(s,t) ? y_e(s) ? y_d(s)\sin? t \quad (4.7, 4.8)$$

$$? (s,t) ? ?_e(s) ? ?_d(s)\sin? t, \qquad q(s,t) ? q_e(s) ? q_d(s)\sin? t \quad (4.9, 4.10)$$

Infinitesimal vibrations are assumed; therefore nonlinear terms in the dynamic variables are neglected. For example, the products of two dynamic deflections are approximately zero ($x_d y_d ? 0$ and $x_d x_d ? 0$). Observing small angle theory by using the nondimensional approximations of *sin?* and *cos?* similar to those presented in Equations 3.26 and 3.27 and dividing all terms by sin(? t), Equations 4.3 through 4.6 resolve into

$$\frac{dx_d}{ds} ? ??_d \sin?_e, \qquad \frac{dy_d}{ds} ? ?_d \cos?_e \qquad (4.11, 4.12)$$

$$\frac{d?_d}{ds} ? \frac{1}{q_e}\left(\frac{q_d}{q_e}(h ? h_f ? y_e) ? k(y_e ? h_f)\cos?_e ? y_d\right) \qquad (4.13a)$$

$$\frac{dq_d}{ds} ? ??^2(x_d \cos?_e ? y_d \sin?_e) ? k(y_e ? h_f)?_d \cos?_e ? ky_d \sin?_e \qquad (4.13b)$$

Equations 4.13a and 4.13b apply when $y ? h_f$. If membrane properties lie above the surface of the foundation, then the soil stiffness terms drop out:

$$\frac{d?_d}{ds} ? \frac{1}{q_e}??^2(x_d \sin?_e ? y_d \cos?_e) ? y_d ? q_d \frac{(h ? h_f ? y)}{q_e} \qquad (4.14a)$$

$$\frac{dq_d}{ds} ? ??^2(x_d \cos?_e ? y_d \sin?_e) \qquad (4.14b)$$

The two-point boundary conditions for symmetrical vibrations about the equilibrium of a water-filled freestanding tube resting on a Winkler foundation are as follows:

For the range $0 ? s ? 0.5$

@ $s ? 0$: $x_e ? y_e ??_e ? 0$, $x_d ? 0$, $y_d ? 0.0001$, $?_d ? 0$

@ $s ? 0.5$: $x_e ? 0$, $?_e ??$, $x_d ? 0$, $?_d ? 0$

Two changes are made when dealing with nonsymmetrical vibrations: at $s = 0.5$, $x_d = 0$ *and* $y_d = 0$. The concept of symmetrical and nonsymmetrical vibrations is further examined in Appendix A.

The conditional "if-then" command was used, within the Mathematica program, in order to calculate x_d, y_d, $?_d$, and q_d above and below the surface of the foundation. Also, a condition where the vertical tangent of the tube is to always be above the surface of the foundation is enforced for all solutions. Physically, the tube can only be supported by springs that are under it. With the use of Equations 4.11, 4.12, 4.13a and b, 4.14a and b and the boundary conditions above, a Mathematica file was coded to compute the dynamic parameters. The Mathematica program is described and given in Appendix C.

4.6 Winkler Foundation Dynamic Results

Figures 4.10 through 4.13 show the relationship of frequency versus soil stiffness when a certain internal pressure head is designated. As the soil stiffness increases, the frequencies tend to increase. There is no considerable change in frequency when the soil stiffness is above 25, meaning the stiffer the soil, the less effect it has on the frequency.

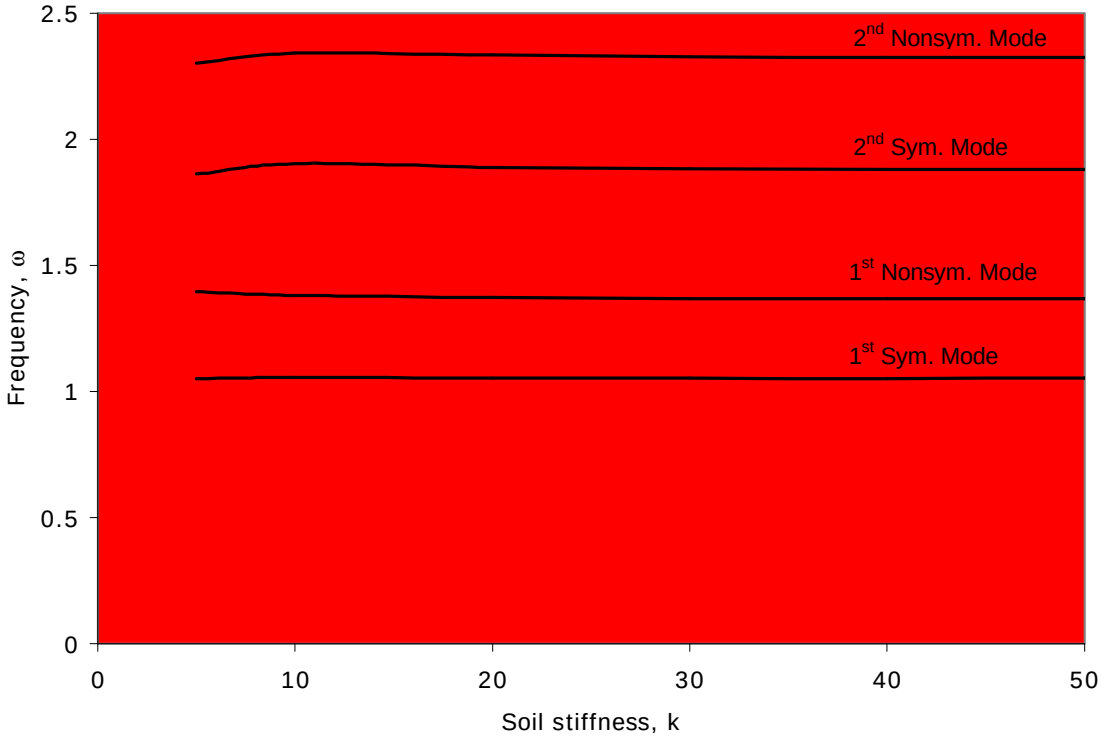

Figure 4.10 Frequency versus soil stiffness when h = 0.2

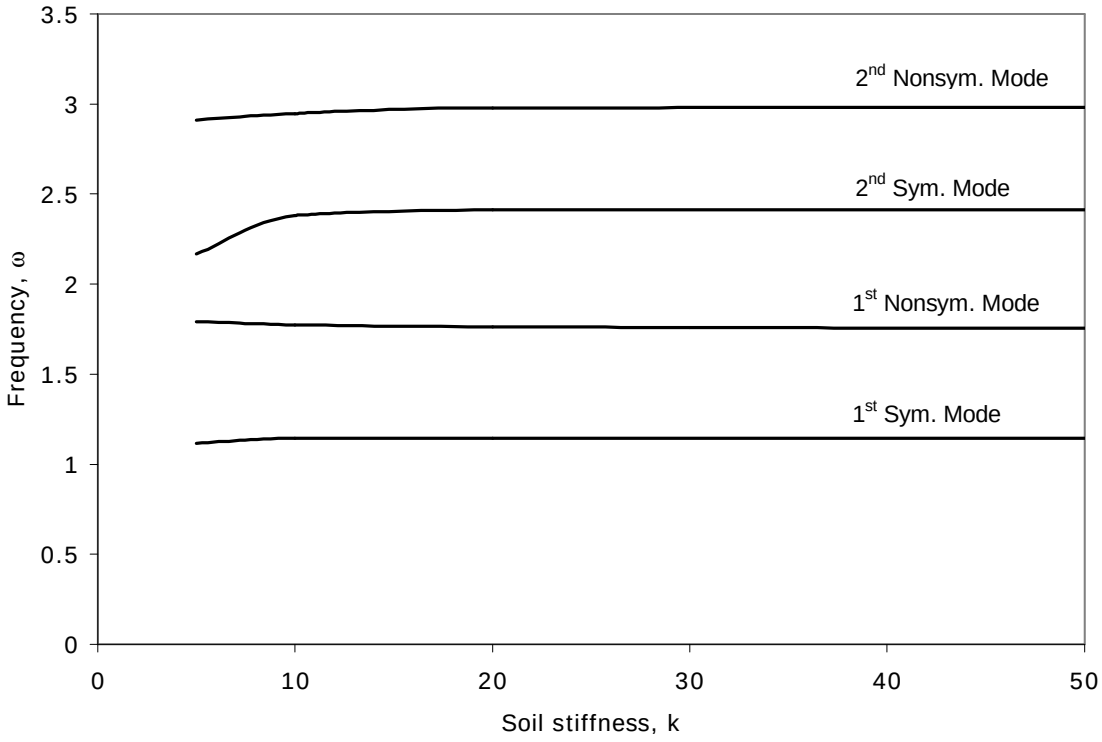

Figure 4.11 Frequency versus soil stiffness when h = 0.3

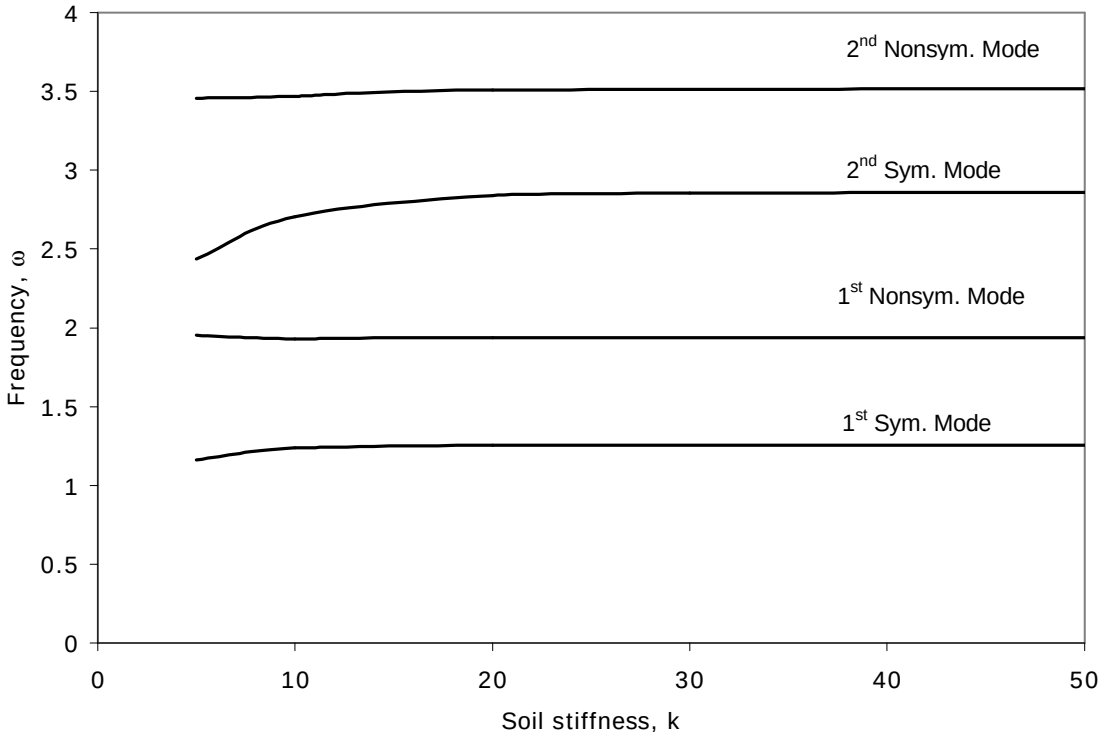

Figure 4.12 Frequency versus soil stiffness when h = 0.4

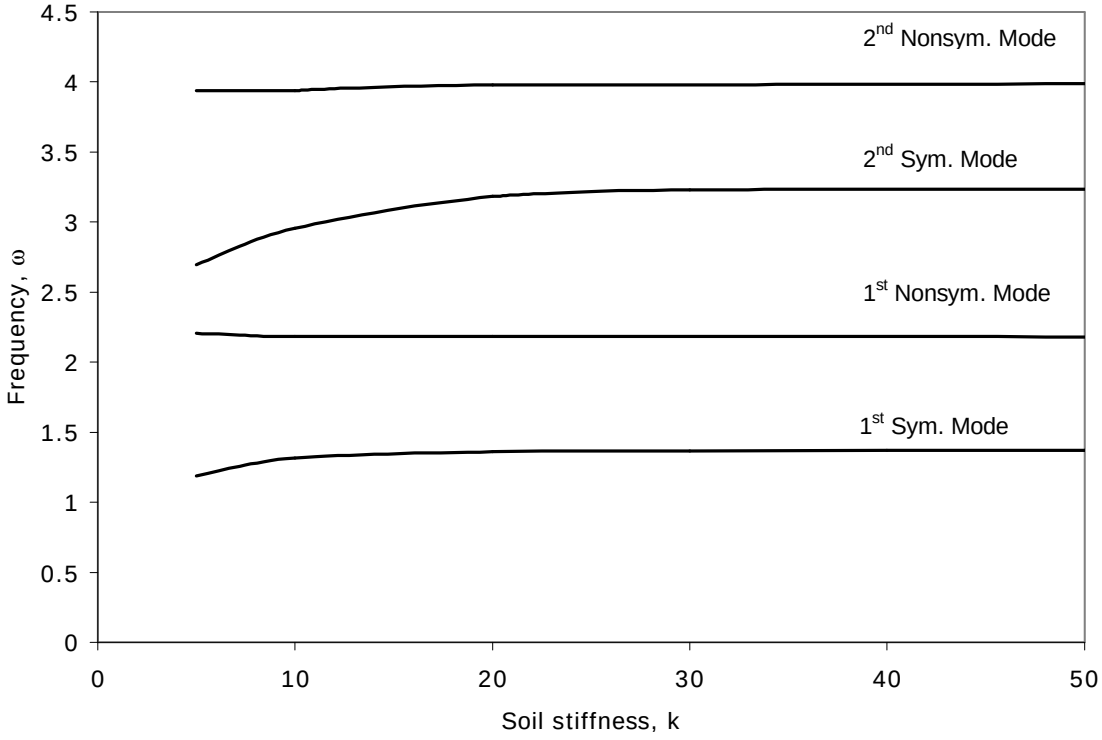

Figure 4.13 Frequency versus soil stiffness when h = 0.5

4.7 Pasternak Foundation Model

A long freestanding geosynthetic tube filled with water and supported by a Pasternak foundation is considered. The general traits of the geosynthetic tube remain the same as before. This includes the assumptions of a long straight tube, neglecting longitudinal changes in cross-sectional area, geosynthetic material being inextensible, neglecting bending resistance, and weight of the geotextile material is not included. Proposed by Pasternak in 1954, this model extends the Winkler model by adding a shear layer to the vertical springs. The primary difference between the Winkler and Pasternak foundation models is the presence of the shear interaction layer between the Winkler spring elements. This shear layer is composed of incompressible vertical elements which deform in the transverse shear direction only (Selvadurai 1979). The results from this model should more closely approach what actually occurs in a real world application.

4.8 Pasternak Foundation Equilibrium Formulation

Consider the freestanding water-filled tube resting on a Pasternak foundation in Figure 4.14. The descriptions of the geosynthetic properties are identical to the Winkler definitions with the exception of an added shear modulus G_P. The shear modulus G_P represents the incompressible shear layer as described in Selvadurai's definition of a Pasternak soil model.

To begin the formulation, consider the Pasternak foundation equilibrium element in Figure 4.15. The internal air pressure, soil stiffness coefficient, and shear modulus are the prescribed values, and the calculated unknown quantities include the membrane tension, maximum tube height, ground deflection, and the equilibrium shape. The nondimensional quantities presented in chapter 3 are used, along with k and g_p:

$$x ? \frac{X}{L}, \quad y ? \frac{Y}{L}, \quad s ? \frac{S}{L}, \quad q_e ? \frac{Q_e}{?_{int} L^2}, \quad p ? \frac{P}{?_{int} L}, \quad k ? \frac{K}{?_{int}}, \quad g_P ? \frac{G_P}{?_{int} L^2}$$

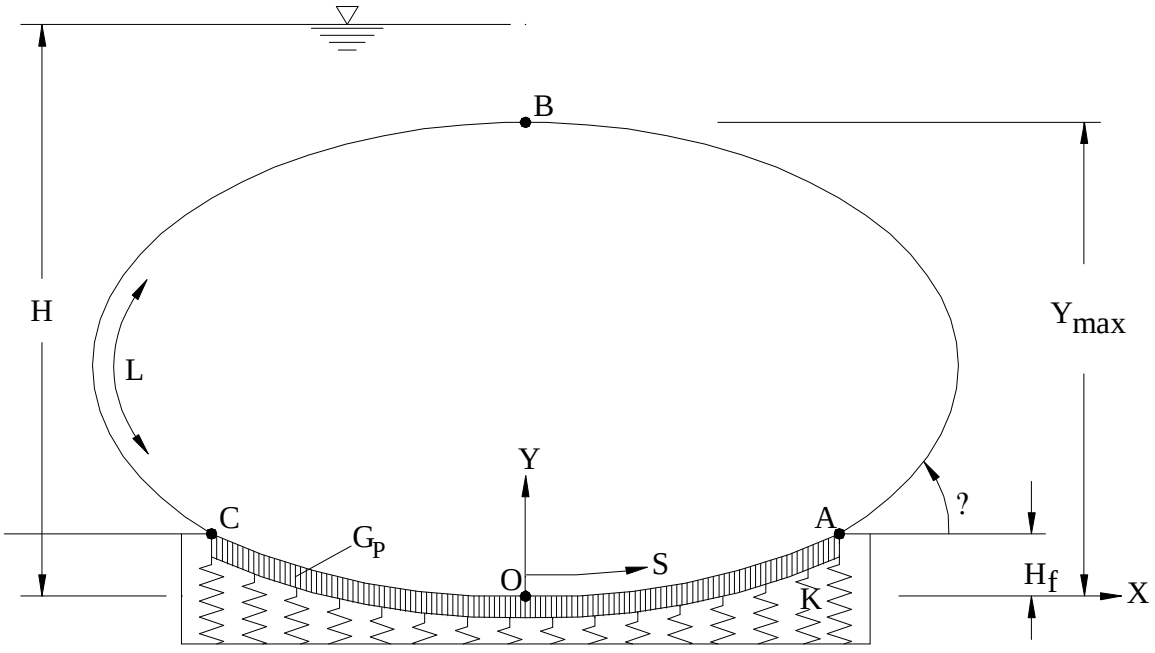

Figure 4.14 Pasternak foundation model

The same coordinate system of the Winkler model is adopted for the Pasternak foundation case, therefore the horizontal and vertical coordinates x_e and y_e remain the same and Equations 3.10 and 3.11 are once again employed:

$$\frac{dx_e}{ds} = \cos\theta_e, \qquad \frac{dy_e}{ds} = \sin\theta_e \tag{3.10, 3.11}$$

From the tube element, presented in Figure 4.15, the following can be derived, where the subscript e denotes equilibrium values. If y_e is less than h_f, the following equations are derived by summing the forces in the tangential direction and the normal direction of the membrane, respectively:

$$\frac{d\theta_e}{ds} = \frac{1}{q_e}\left[h - h_f - y_e - k(y_e - h_f)\cos\theta_e - g_P\frac{d^2y}{ds^2}\right] \tag{4.17a}$$

$$\frac{dq_e}{ds} = k(y_e - h_f) - g_P\frac{d^2y_e}{ds^2}\sin\theta_e \tag{4.17b}$$

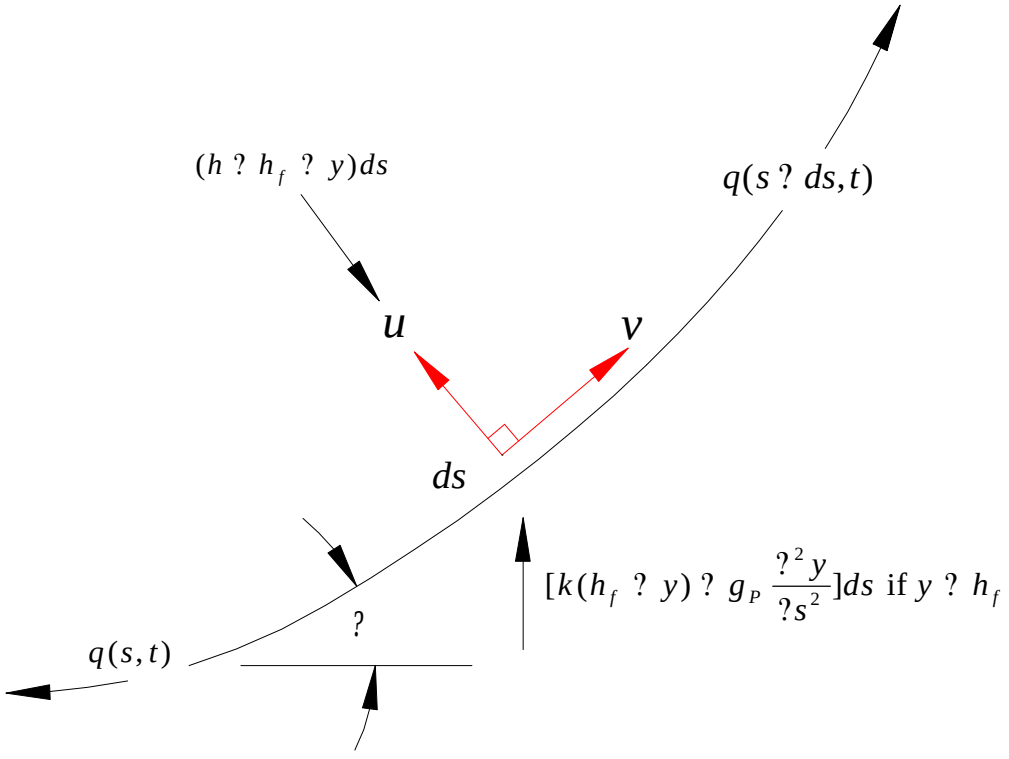

Figure 4.15 Pasternak foundation equilibrium element

Knowing Equation 3.11, Equations 4.17a and b can be simplified by using calculus and substituting $\frac{d^2 y_e}{ds^2} = \frac{d\theta_e}{ds}\cos\theta_e$. This produces the following:

$$\frac{d\theta_e}{ds} = \left\{\frac{h - h_f - y_e - k(y_e - h_f)\cos\theta_e}{q_e - g_P\cos^2\theta_e}\right\} \tag{4.18a}$$

$$\frac{dq_e}{ds} = k\left(y_e - h_f\right)\sin\theta_e - \left\{\frac{g_P\sin\theta_e\cos\theta_e\left(h - h_f - y_e - k(y_e - h_f)\cos\theta_e\right)}{q_e - g_P\cos^2\theta_e}\right\} \tag{4.18b}$$

When the vertical coordinate y_e is greater than h_f, the soil stiffness and shear modulus are not considered, therefore Equations 4.18a and b resort back to Equations 4.2a and 4.2b:

$$\frac{d\theta_e}{ds} = \frac{1}{q_e}[h - h_f - y_e], \qquad \frac{dq_e}{ds} = 0 \tag{4.2a, 4.2b}$$

The two-point boundary conditions for equilibrium of a single water-filled freestanding tube resting on a Pasternak foundation are as follows:

For the range $0 \le s \le 0.5$

@ $s = 0$ (point O): $x_e = 0$, $y_e = 0$, $\theta_e = 0$

@ $s = 0.5$ (point B): $x_e = 0$, $\theta_e = ?$

Again, an "if-then" command is used, within the Mathematica program, in order to calculate x_e, y_e, θ_e, and q_e above and below the surface of the foundation. A condition where the vertical tangent of the tube is to always be above the surface of the foundation is enforced for all solutions. The Mathematica program is described and given in Appendix D.

4.9 Pasternak Foundation Equilibrium Results

Presented in Figures 4.16 and 4.17 is the relationship of membrane tension at the origin versus the shear modulus of the Pasternak model. When the soil stiffness parameter is increased to 200 the shear modulus has little effect, if any, on the initial tension.

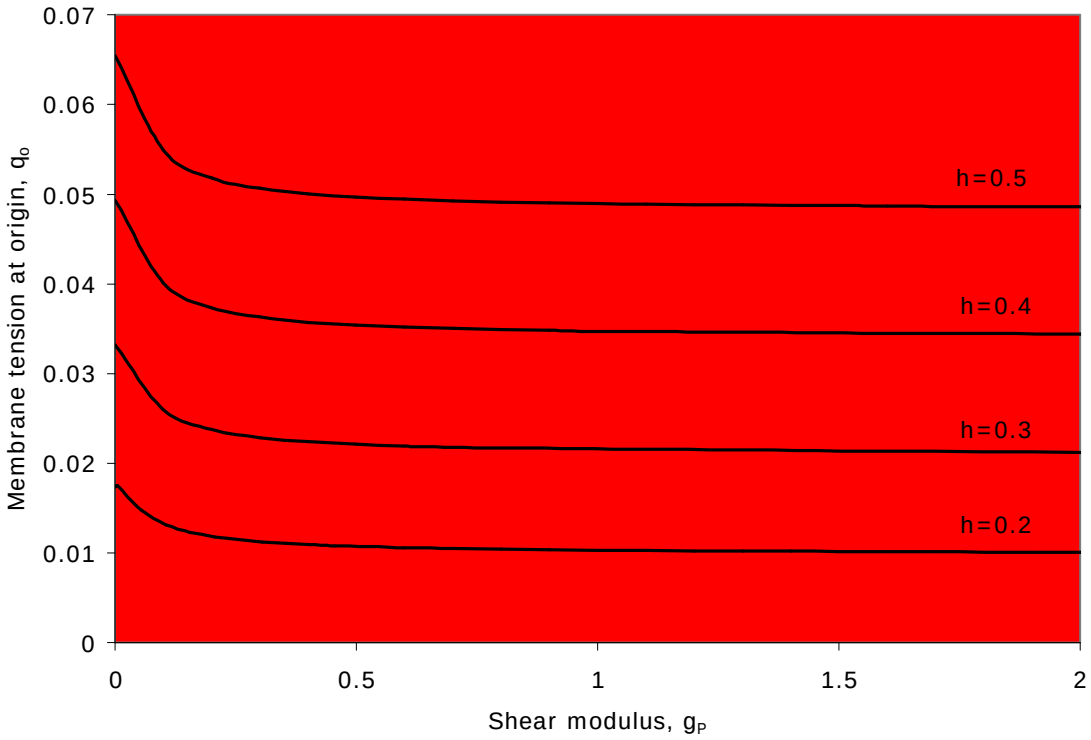

Figure 4.16 Membrane tension at origin versus shear modulus when k = 5

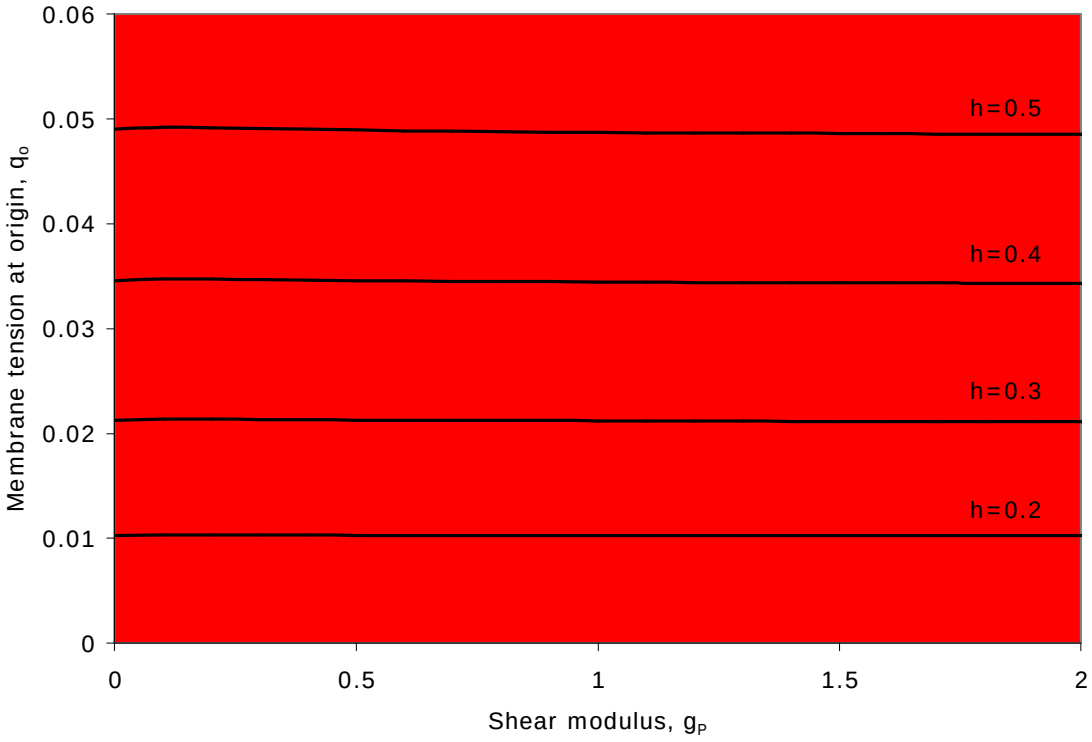

Figure 4.17 Membrane tension at origin versus shear modulus when k = 200

Figure 4.18 reveals the relationship of maximum tube settlement to the change in shear modulus when the soil stiffness is 200. As the shear modulus is increased, tube settlement decreases. This situation is expected. When the soil on a supporting surface has the ability to rely on the surrounding soil for a broader stress distribution, then the tube settlement should decrease appropriately. Consider Figure 4.19. Tube height above the Pasternak foundation surface does not change significantly as a function of the soil's shear modulus.

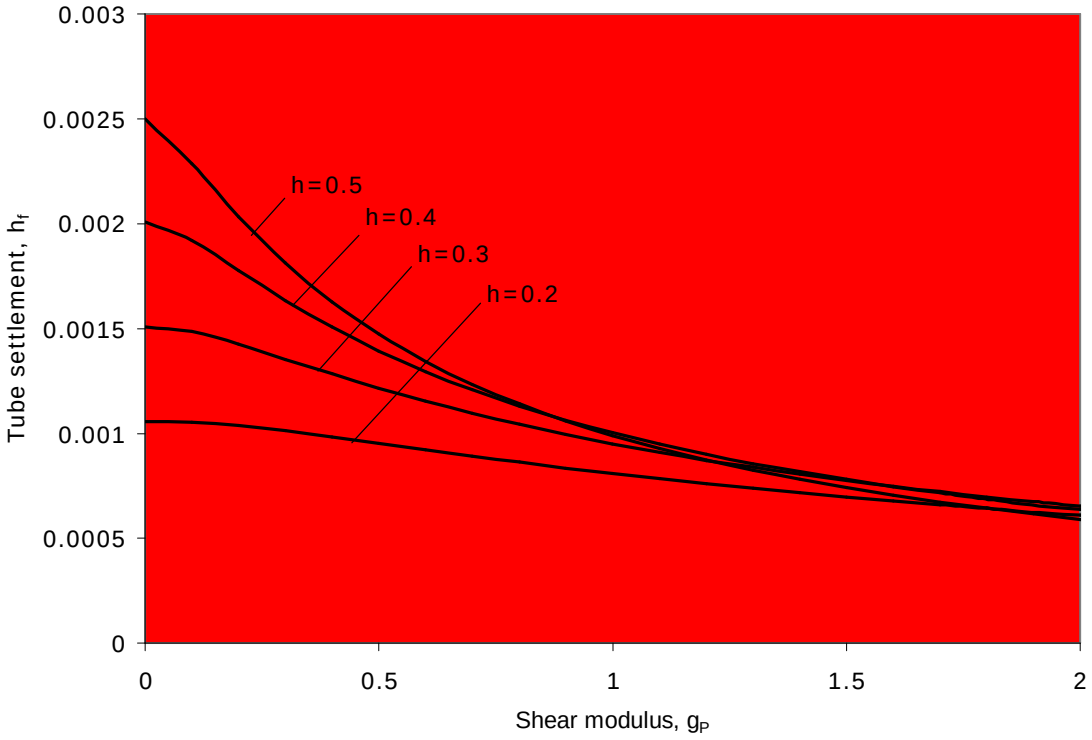

Figure 4.18 Tube depth below surface versus shear modulus when k = 200

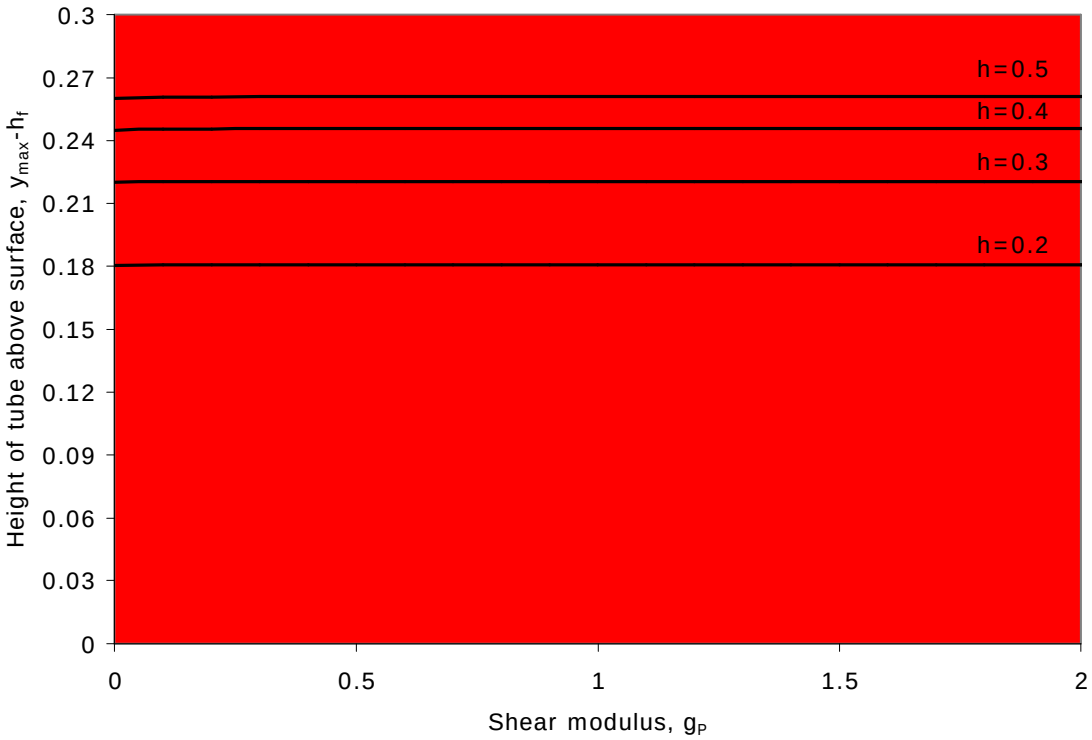

Figure 4.19 Tube height above surface versus shear modulus when k = 200

4.10 Pasternak Foundation Dynamic Derivation

The dynamic derivation of a freestanding geosynthetic tube resting on a Pasternak foundation is presented within this section. Figure 4.20 displays the kinetic equilibrium of the system undergoing infinitesimal vibrations about its initial equilibrium configuration. The set-up geometry is identical to the Winkler foundation model (presented in section 4.5). Therefore, Equations 4.3 and 4.4 hold true:

$$\frac{?x}{?s} ? \cos? \qquad \frac{?y}{?s} ? \sin? \qquad (4.3, 4.4)$$

Pictured in Figure 4.20, the D'Alembert Principle is used and equilibrium is induced upon an element. Summing the forces in the tangential and normal directions (with respect to the membrane element) results in

$$q\frac{??}{?s} ? \frac{?^2 y}{?t^2}\cos? ? \frac{?^2 x}{?t^2}\sin? ? h ? h_f ? y ? k(h_f ? y)\cos? ? g_P \frac{?^2 y}{?s^2}\cos? \qquad (4.21a)$$

$$\frac{?q}{?s} ? \frac{?^2 x}{?t^2}\cos? ? \frac{?^2 y}{?t^2}\sin? ? k(h_f ? y)\sin? ? g_P \frac{?^2 y}{?s^2}\sin? \qquad (4.21b)$$

The geometric Equations 5.3 and 5.4, plus the force Equations 5.21 and 5.22, express the dynamics of a geosynthetic tube supported by a Pasternak foundation. These equations are considered the equations of motion for this system when $y_e < h_f$. Introduced in chapter 2, ? is the nondimensional frequency of the system. Nondimensional forms of Equations 3.22 through 3.25 are used to relate equilibrium and dynamic terms:

$$x(s,t) ? x_e(s) ? x_d(s)\sin? t, \qquad y(s,t) ? y_e(s) ? y_d(s)\sin? t \qquad (3.22, 3.23)$$

$$? (s,t) ? ?_e(s) ? ?_d(s)\sin? t, \qquad q(s,t) ? q_e(s) ? q_d(s)\sin? t \qquad (3.24, 3.25)$$

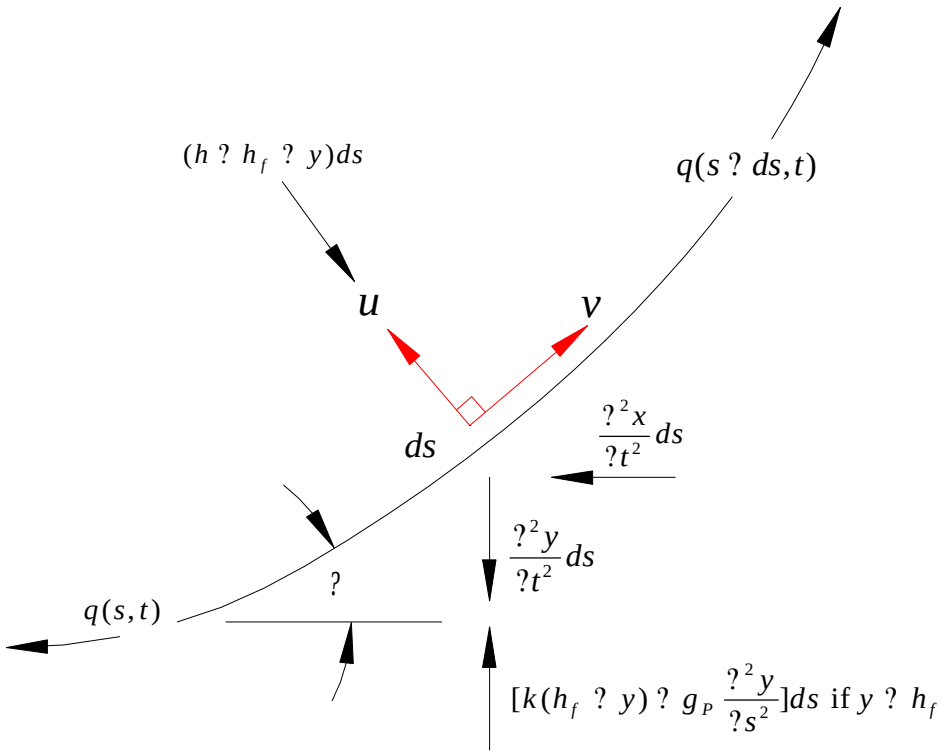

Figure 4.20 Pasternak foundation kinetic equilibrium element

Equations 3.22 to 3.25 are substituted into the two summation of forces equations (Equations 4.21a and b), and nonlinear terms in the dynamic variables are neglected. Using the consistent geometry of a single freestanding tube, Equations 3.10 and 3.11 are substituted into the resulting expressions and the term sin(?t) drops out once divided through. This produces the following governing equations:

$$\frac{dx_d}{ds} ? ?? _d \sin ?_e , \qquad \frac{dy_d}{ds} ? ?_d \cos ?_e \qquad (3.10, 3.11)$$

$$\frac{d?_d}{ds} ? \frac{1}{q_e ? g_P \cos^2 ?_e}[? ^2 ?x_d \sin ?_e ? y_d \cos ?_e ?? y_d ? ky_d \cos ?_e ?$$
$$k(h_f ? y_e)?_d \sin ?_e ? q_d \frac{k(y_e ? h_f)\cos ?_e ? h ? h_f ? y_e}{q_e ? g_P \cos^2 ?_e} \qquad (4.22a)$$

$$\frac{dq_d}{ds} ? ?? ^2 ?x_d \cos ?_e ? y_d \sin ?_e ?? k(h_f ? y_e)?_d \cos ?_e ? ky_d \sin ?_e$$
$$? g_P \frac{d^2 y_e}{ds^2} ?_d \cos ?_e ? g_P \frac{d^2 y_d}{ds^2} \sin ?_e \qquad (4.22b)$$

where $\frac{d^2 y_e}{ds^2} = \frac{d\theta_e}{ds}\cos\theta_e$, $\frac{d^2 y_d}{ds^2} = \frac{d\theta_d}{ds}\cos\theta_e - \theta_d \frac{d\theta_e}{ds}\sin\theta_e$

$\frac{d\theta_d}{ds}$ is given by Equation 4.22a and $\frac{d\theta_e}{ds}$ is given by Equation 4.18a.

When membrane properties being calculated are above the surface of the foundation, any term with a soil coefficient or shear modulus falls out. Therefore, the two Equations 4.22a and b result in:

$$\frac{d\theta_d}{ds} = \frac{1}{q_e}\left(y_d - \theta_d^2 y_d \cos\theta_e - x_d \sin\theta_e - q_d \left(\frac{h - h_f - y}{q_e}\right)\right) \tag{4.23a}$$

$$\frac{dq_d}{ds} = -\theta_d^2 x_d \cos\theta_e - y_d \sin\theta_e \tag{4.23b}$$

The two-point boundary conditions for symmetrical vibrations about equilibrium of an air-filled freestanding tube resting on a Pasternak foundation are as follows:

For the range $0 \le s \le 0.5$

@ $s = 0$: $x_e = y_e = \theta_e = 0$, $x_d = \theta_d = 0$, $y_d = 0.001$

@ $s = 0.5$: $x_e = 0$, $\theta_e = \pi$, $x_d = 0$, $\theta_d = 0$

For nonsymmetrical vibrations, $y_d = 0$ instead of $\theta_d = 0$ at $s = 0.5$.

The "if-then" command was used, within the Mathematica program, in order to calculate x_d, y_d, θ_d, and q_d above and below the surface of the foundation. A condition where the vertical tangent of the tube is to always be above the surface of the foundation is enforced for all solutions. The Mathematica program is described and given in Appendix D.

4.11 Pasternak Foundation Dynamic Results

Presented in this section are the results from the dynamic derivation of a freestanding geosynthetic tube resting on a Pasternak foundation. If the soil stiffness coefficient is held at 200, then the Pasternak foundation mode shapes are identical to the Winkler

foundation mode shapes, with the exception of varying with the shear modulus. For given internal pressure heads h = 0.2, 0.3, 0.4, and 0.5, the lowest four natural frequencies conform to the curves displayed in the following frequency to shear modulus graphs. A decrease in frequency occurs when the shear modulus g_P is increased. Physically, the number of times the mode shapes pass through the equilibrium configuration for a given range of time decreases slightly.

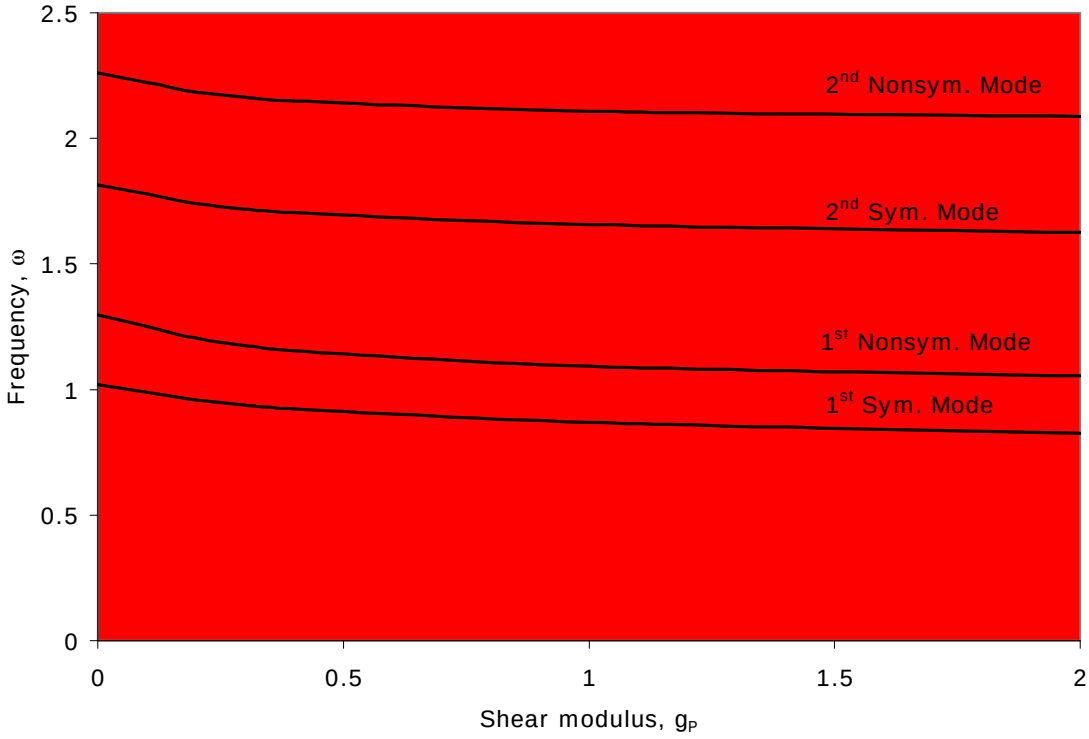

Figure 4.21 Frequency versus shear modulus when h = 0.2 and k = 200

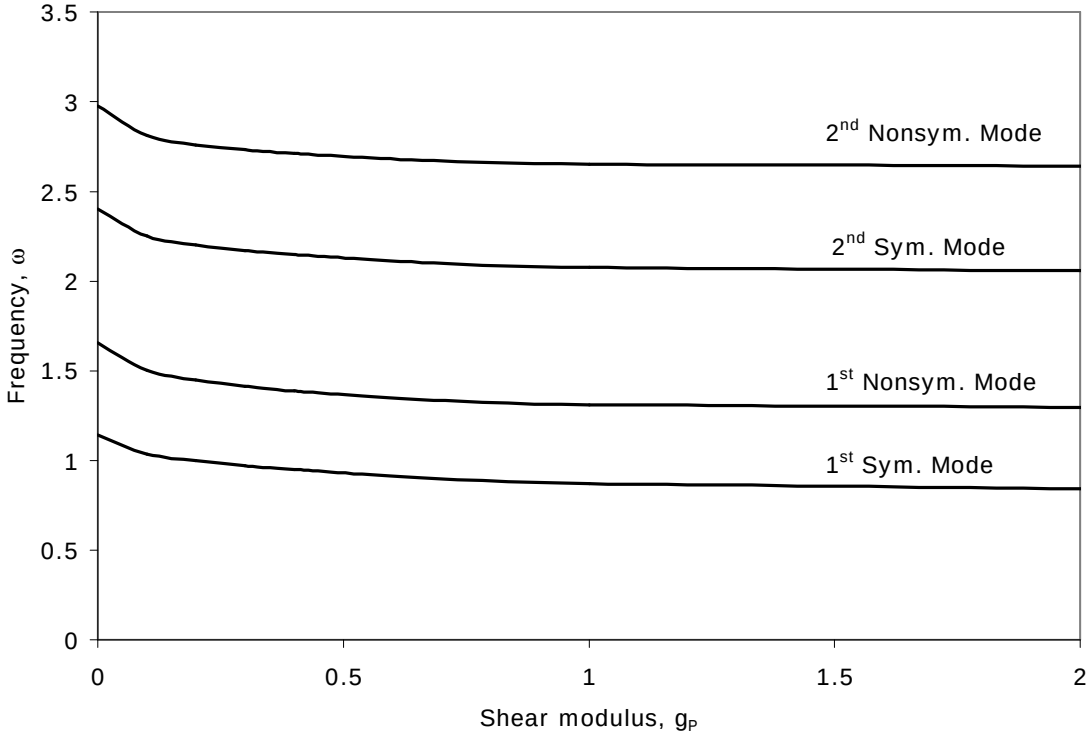

Figure 4.22 Frequency versus shear modulus when h = 0.3 and k = 200

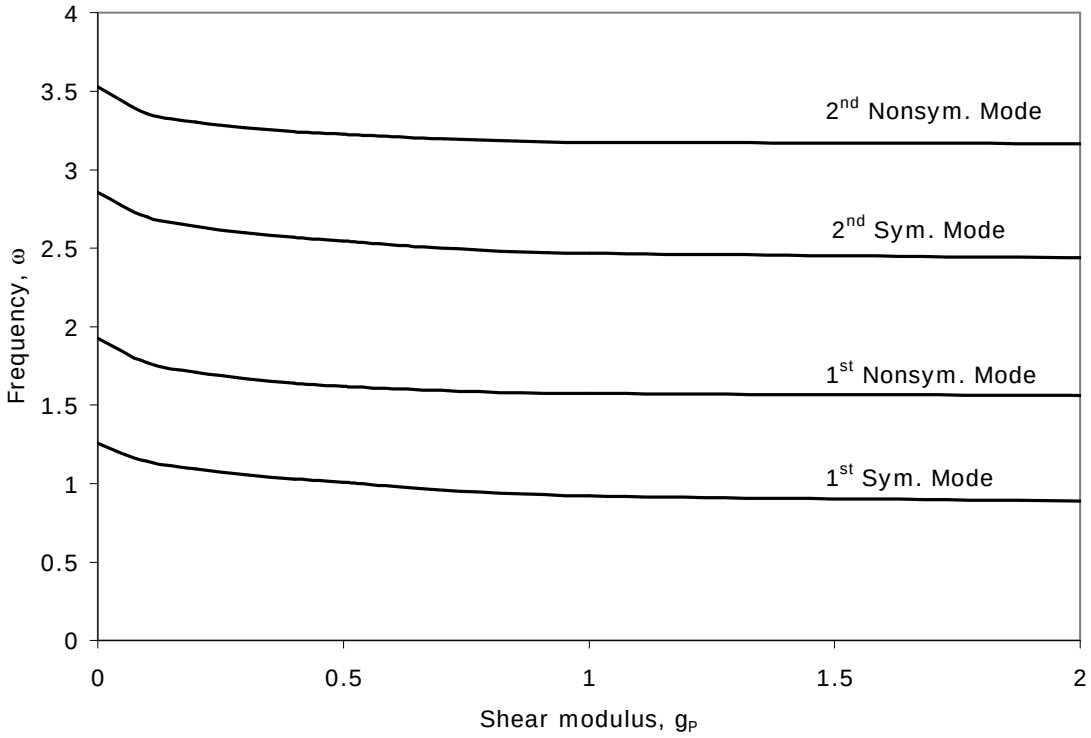

Figure 4.23 Frequency versus shear modulus when h = 0.4 and k = 200

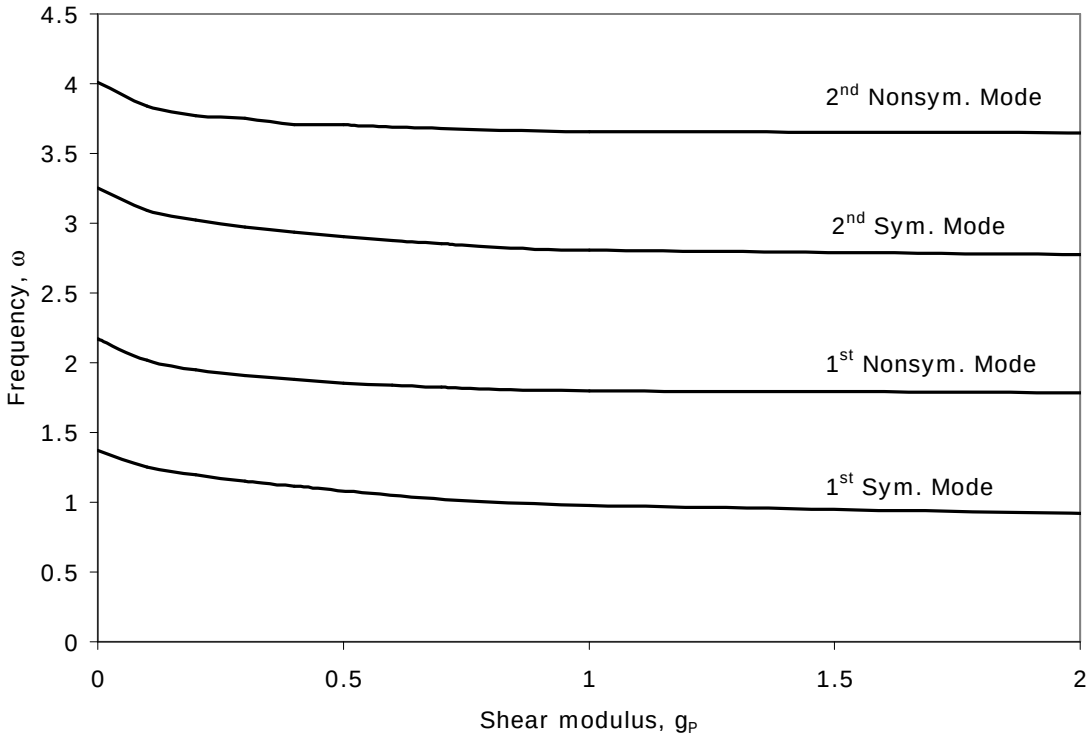

Figure 4.24 Frequency versus shear modulus when h = 0.5 and k = 200

Chapter 5: Tube with internal air and deformable foundation

5.1 Introduction

The majority of applications and testimonies of the flood-fighting geosynthetic tubes, presented in the literature review, occur on soft soil, muddy riverbanks, or grass-covered ground. In order to understand the behavior of the geosynthetic tubes in these environments, it is necessary to investigate the tube's response to variable terrain. The membrane shape, circumferential tension, and overall system height are a function of what type of media the tubes are placed upon. Chapter 3 considered the air-filled geosynthetic tube resting on a rigid foundation (i.e., concrete, rock, etc.). Therefore, a more enhanced model of chapter 3 is presented within. In this chapter the geosynthetic tube is filled with air and supported by a deformable foundation, which is a closer representation of the physical behavior that occurs in previously discussed applications.

Five studies have covered the investigation of geosynthetic tubes and their response when supported by a deformable foundation. Klusman, Plaut, and Suherman have modeled a slurry-filled (modeled as a hydrostatic pressure) geotextile tube supported by a Winkler foundation (Klusman 1998, Plaut and Klusman 1999, and Plaut and Suherman 1997). The results of these three studies were produced by Mathematica software, and include the tube height, ground deflection, membrane tension, and various tube shapes. Suherman and Plaut studied a single tube resting on a Winkler foundation with and without impounding external water. Plaut and Klusman (1999) analyzed single, two stacked, and 2-1 tube configurations resting on a modified Winkler foundation where the foundation pressure acted normal to the tube (so that friction between the tube and the foundation was neglected and the membrane tension was constant). Huong (2001) and Kim (2003) used the finite difference software of FLAC to model water-filled tubes supported by a Mohr-Coulomb soil foundation. Huong investigated a single geosynthetic tube with a wedged stabilizing block, and computed the membrane tension, tube height, tube settlement, and deformation of the tube with impounding external water (Huong 2001 and Huong et. al. 2001). Kim studied four tube configurations which included the

attached apron tube, single baffle tube, sleeved tubes, and a 2-1 stacked barrier (Kim 2003). The results from Kim's FLAC study included critical external water levels, pore pressure, membrane tension, and deformations of the tube with impounding external water.

Contained in section 5.2 is a discussion of the Winkler foundation model and the assumptions applied. Next, section 5.3 is devoted to the Winkler derivation and is followed by the equilibrium results produced by the analysis in section 5.4. Once the values from the Winkler equilibrium model are known, these values are used for the dynamic problem presented in section 5.5 followed by the results presented in section 5.6. Section 5.7 introduces the Pasternak foundation model with a discussion of the assumptions and components involved. The Pasternak foundation equilibrium formulation (section 5.8) and equilibrium results (section 5.9) follow section 5.7. The Pasternak dynamic case follows the equilibrium results in section 5.10 with the results in section 5.11. In closing, section 5.12 presents a comparison of the results from the rigid, Winkler, and Pasternak foundation models.

Mathematica 4.2 was used to solve the boundary value problems and obtain membrane properties. An accuracy goal of five or greater was used in all Mathematica coded calculations. The typical Mathematica to MS Excel transference was executed, which related key properties and displayed equilibrium and dynamic shapes. AutoCAD 2002 was also used in presenting illustrations of free body diagrams and details of specific components to better explain the subject. All derivations within were performed by Dr. R. H. Plaut.

5.2 Winkler Foundation Model

A long freestanding geosynthetic tube filled with air and supported by a Winkler foundation is considered. The tube is assumed to be infinitely long and straight as in previous chapters. Therefore, changes in cross-sectional area along the tube length are neglected. This justifies the use of a two-dimensional analysis. Since air is the fill

material, the weight of the geotextile material was required to add mass and stabilize the system. Originally proposed by Winkler in 1867, this is the most fundamental foundation model used in many initial analyses. The Winkler foundation model assumes that the downward deflection of the soil at a point is directly proportional to the stress applied at that point and independent of the surrounding soil behavior (Selvadurai 1979). The deflection occurs directly under the load applied. To model this behavior, numerous independent vertical springs are integrated into foundation. The geosynthetic material was assumed to act like an inextensible membrane and bending resistance is neglected. Because the tubes have no bending stiffness, it is assumed that they are able to conform to sharp corners.

5.3 Winkler Foundation Equilibrium Derivation

Consider the freestanding air-filled tube resting on a Winkler foundation in Figure 5.1. The center of the tube at the lowest point of the membrane (point O) is considered the origin. The right and left contact points of the soil surface and tube membrane are designated as A and C, respectively. Both horizontal distance X and vertical distance Y make up the Cartesian coordinate system, which begins at zero from point O. The symbol ? signifies the angular measurement of a horizontal datum to the tube membrane. Point B denotes the location where ? equals ? (this is the location of the end boundary condition). The measurement S corresponds to the arc length from the origin following along the membrane. X, Y, and ? are each a function of the arc length S. Y_{max} denotes the maximum height of the tube above the origin. L represents the circumferential length of the entire membrane.

The internal pressure P is a designated constant pressure within the tube that is needed to expand the geosynthetic material and resist flood-water. H_f is the displacement of the tube below the surface of the foundation. The soil stiffness coefficient (which is the stiffness of the springs within the Winkler foundation model) is designated K. Not pictured is the tension force Q_e in the membrane (Q_o is the values of $Q_e(s)$ at $s = 0$), and the material mass per unit length ?.

Set values for this problem include the internal air pressure and the soil stiffness coefficient. The calculated unknowns are the membrane tension, maximum tube height, ground deflection, and the equilibrium shape. The nondimensional quantities used here are

$$x ? \frac{X}{L}, \qquad y ? \frac{Y}{L}, \qquad b ? \frac{B}{L}, \qquad s ? \frac{S}{L}, \qquad q_e ? \frac{Q_e}{? gL}, \qquad p ? \frac{P}{? g}, \qquad k ? \frac{KL}{? g}$$

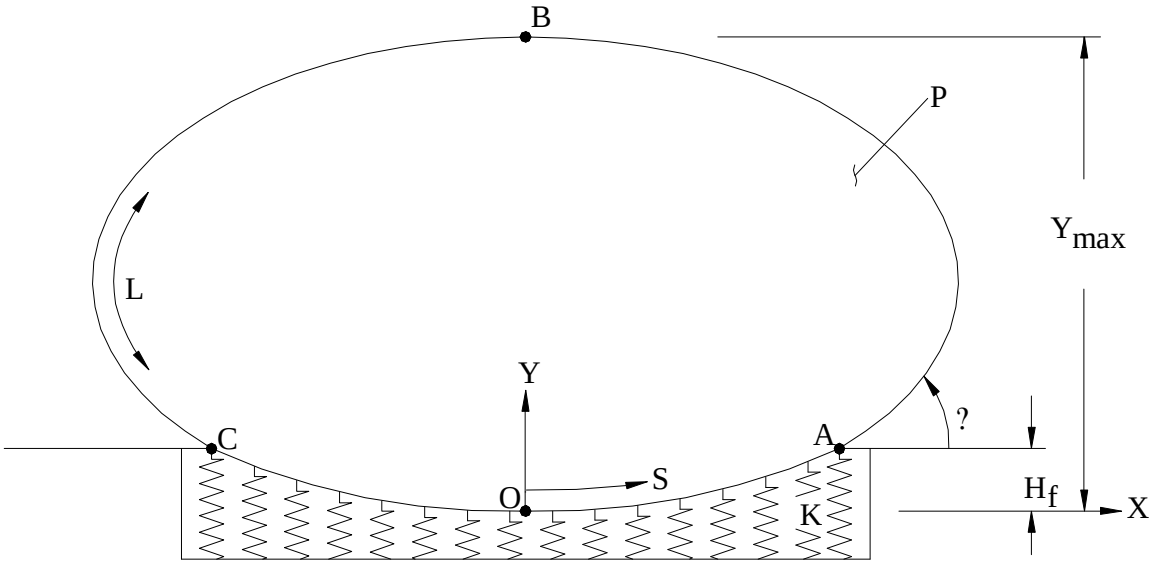

Figure 5.1 Winkler foundation model

The horizontal and vertical coordinates x_e and y_e remain the same; therefore, Equations 3.10 and 3.11 will be employed:

$$\frac{dx_e}{ds} ? \cos?_e, \qquad \frac{dy_e}{ds} ? \sin?_e \qquad (3.10, 3.11)$$

From the tube element, presented in Figure 5.2, the following can be derived, where the subscript *e* denotes equilibrium values. A unit load is produced by the tube weight per length in nondimensional ($\frac{? g}{? g} ? 1$) terms. If the vertical coordinate y_e is less than h_f, the

following equations are derived by summing the forces in the tangential direction and the normal direction of the membrane, respectively:

$$\frac{d?_e}{ds} ? \frac{1}{q_e}[k(y_e ? h_f)\cos?_e ? p ? \cos?_e], \qquad \frac{dq_e}{ds} ? k(y_e ? h_f)\sin?_e ? \sin?_e \qquad (5.1a, 5.1b)$$

When the vertical coordinate y_e is greater than h_f, the soil stiffness is not involved, therefore Equations 5.1a and 5.1b simplify to

$$\frac{d?_e}{ds} ? \frac{1}{q_e}[p ? \cos?_e], \qquad \frac{dq_e}{ds} ? \sin?_e \qquad (5.2a, 5.2b)$$

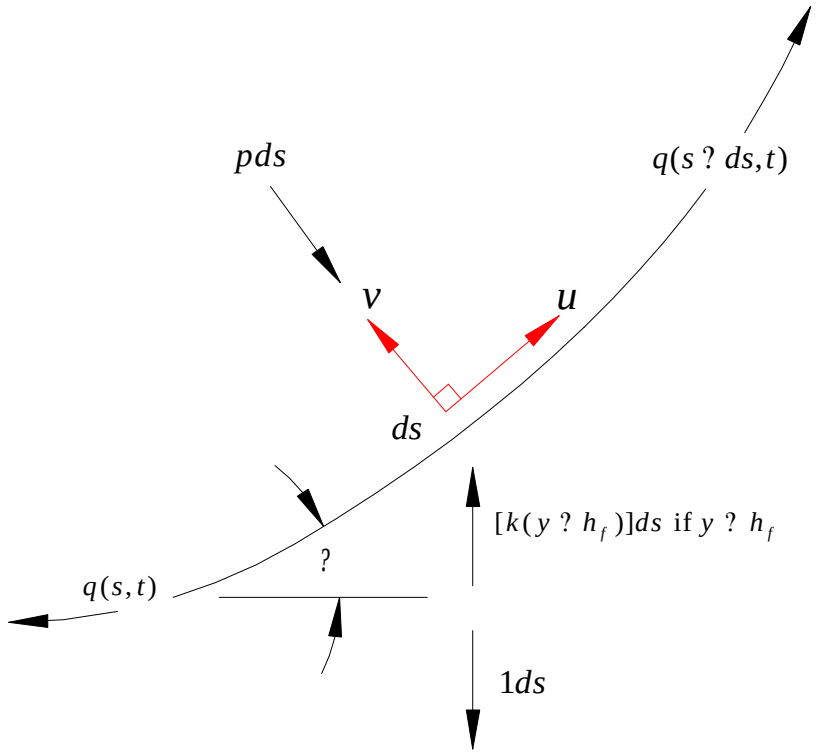

Figure 5.2 Winkler foundation equilibrium diagram

The two-point boundary conditions for a single air-filled freestanding tube resting on a Winkler foundation are as follows:

For the range $0 ? s ? 0.5$

@ $s ? 0$ (point O): $x_e ? 0$, $y_e ? 0$, $?_e ? 0$

@ $s ? 0.5$ (point B): $x_e ? 0$, $?_e ? ?$

An "if-then" command was used, within the Mathematica program, in order to calculate x_e, y_e, ?$_e$, and q_e above and below the surface of the foundation. A condition where the vertical tangent of the tube is to always be above the surface of the foundation is enforced for all solutions. With the use of Equations 3.10, 3.11, 5.1a and b, 5.2a and b, and the boundary conditions above, a Mathematica file was coded to compute the equilibrium parameters. The Mathematica program is described and given in Appendix E.

5.4 Winkler Foundation Equilibrium Results

The following results were produced by the Mathematica file of the internal air equilibrium plus Winkler foundation presented in Appendix E. Results for a value of internal air pressure equal to 1.05 could not be calculated. A reason for this is that not enough air pressure was available to counteract the pushing of the Winkler springs. Therefore, p = 2.0, 3.0, 4.0, and 5.0 are the remaining values of internal air pressure used in chapter 3 and were set along with variable values of soil stiffness coefficients ranging from 40 to 200. Values lower than k = 40 were disregarded, because the shapes produced did not satisfy the condition where the vertical tangent is to reside at or above the foundation surface. Table 5.1 presents the values used to graph Figures 5.4 through 5.10.

p = 2				
k	h_f	q_o	y_{max}	q_{max}
40	0.071	0.158	0.215	0.230
60	0.049	0.139	0.206	0.188
80	0.037	0.128	0.201	0.165
100	0.030	0.121	0.198	0.151
120	0.025	0.116	0.196	0.141
140	0.021	0.113	0.194	0.134
160	0.019	0.110	0.193	0.129
180	0.017	0.108	0.192	0.125
200	0.015	0.107	0.191	0.122

(a) p = 2

p = 3				
k	h_f	q_o	y_{max}	q_{max}
40	0.082	0.322	0.255	0.404
60	0.059	0.300	0.249	0.358
80	0.046	0.286	0.244	0.332
100	0.037	0.276	0.241	0.314
120	0.032	0.269	0.239	0.301
140	0.027	0.264	0.238	0.291
160	0.024	0.260	0.236	0.284
180	0.022	0.256	0.235	0.278
200	0.020	0.253	0.233	0.273

(b) p = 3

p = 4				
k	h_f	q_o	y_{max}	q_{max}
40	0.087	0.486	0.273	0.573
60	0.064	0.463	0.268	0.527
80	0.050	0.449	0.265	0.499
100	0.042	0.438	0.263	0.480
120	0.036	0.430	0.261	0.466
140	0.032	0.424	0.260	0.456
160	0.028	0.419	0.258	0.447
180	0.025	0.415	0.257	0.440
200	0.023	0.411	0.267	0.434

(c) p = 4

p = 5				
k	h_f	q_o	y_{max}	q_{max}
40	0.090	0.648	0.283	0.739
60	0.067	0.626	0.280	0.693
80	0.053	0.611	0.277	0.665
100	0.045	0.601	0.275	0.645
120	0.039	0.592	0.274	0.631
140	0.034	0.586	0.273	0.620
160	0.031	0.581	0.272	0.611
180	0.028	0.576	0.271	0.604
200	0.025	0.572	0.282	0.598

(d) p = 5

Table 5.1 Winkler foundation equilibrium results (nondimensional)

Figure 5.3 displays the equilibrium configurations for the four values of internal air pressure used in chapter 3 where the soil stiffness coefficient equals 200. If the soil stiffness coefficient used was less than 200, a much more noticeable settlement of the tube would occur.

Figure 5.3 Equilibrium configurations of set internal pressures when k = 200

Figure 5.4 displays the maximum height of the tube above the foundation with the settlement of the tube within the foundation versus the specified internal air pressure. Three different values of the soil stiffness, k = 40, 100, and 200, are presented. For a weak soil (e.g., k = 40) the geosynthetic tube is able to bear into the foundation more. This graph gives an indication of what to expect from a tube in a particular soil.

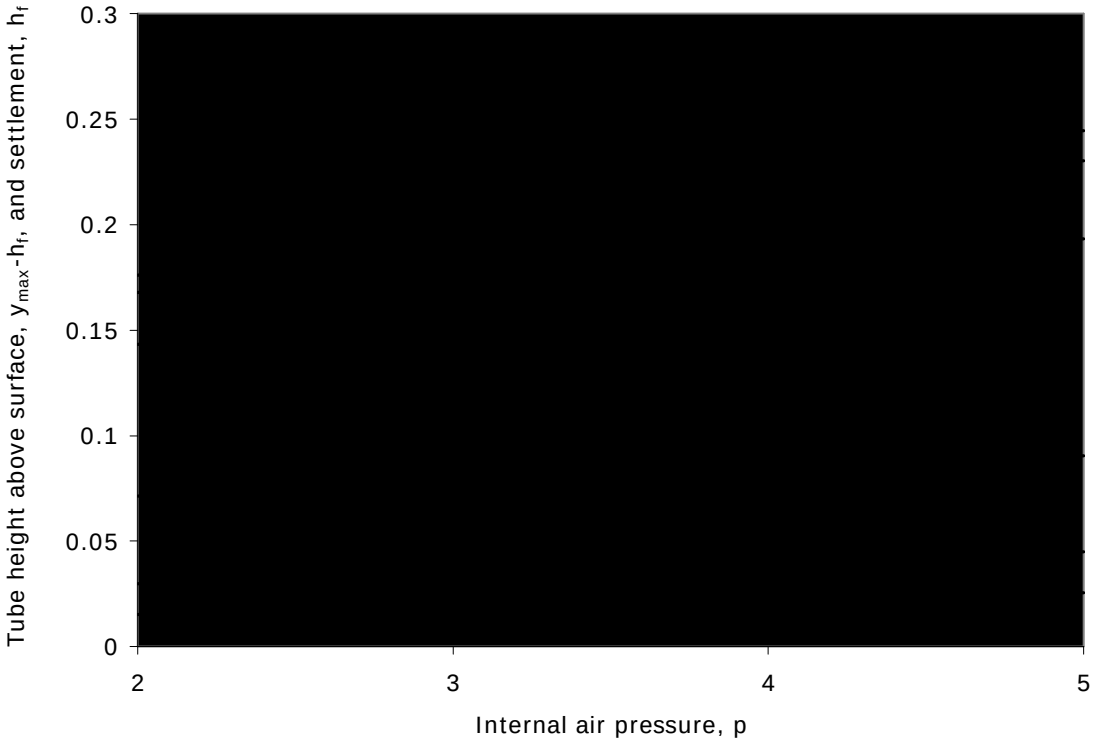

Figure 5.4 Maximum tube height above surface and tube settlement versus internal air pressure

Figures 5.5 displays a linear rise in maximum membrane tension q_{max} (located at the base of the tube) as the internal air pressure increases. Large differences in soil stiffness k produce small changes in membrane tension q_{max}.

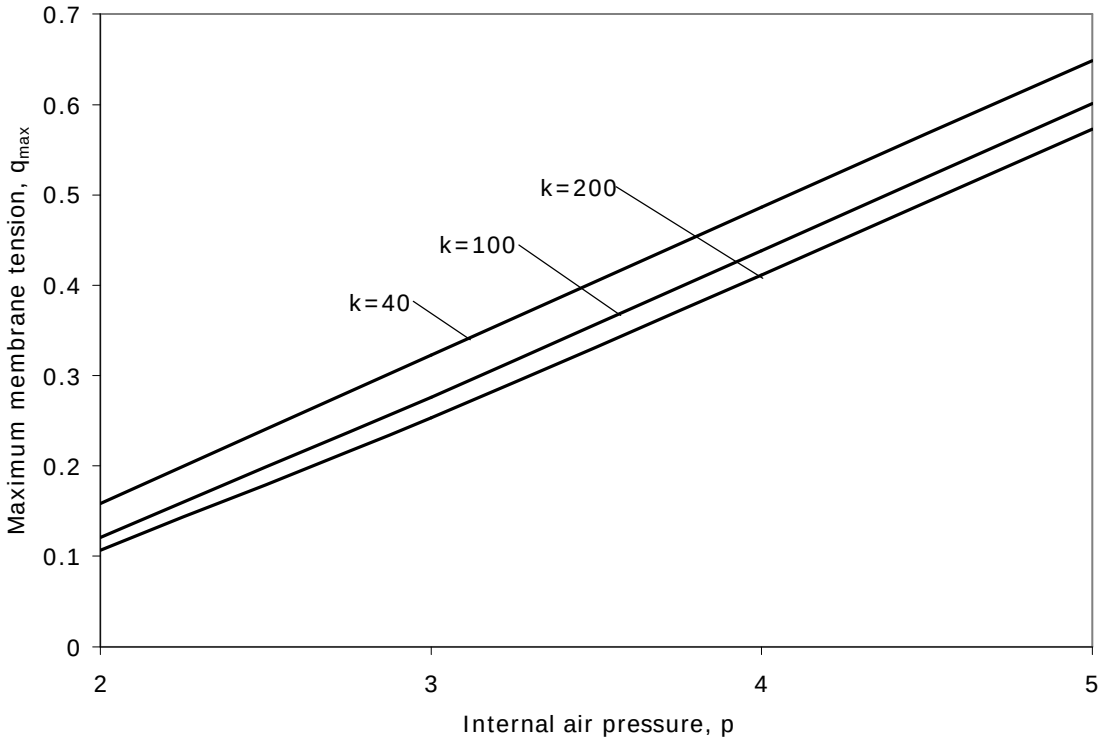

Figure 5.5 Maximum membrane tension versus internal air pressure

Figure 5.7 displays the maximum membrane tension versus soil stiffness. The results show that as the soil stiffness of the foundation increases as the maximum membrane tension decrease. If the soil is of a soft saturated nature (e.g., riverbed), a low value for the soil stiffness would be utilized. On the contrary, if the geosynthetic tube happens to be used in Canada (a very cold climate) or placed upon a concrete base, it is safe to assume the values from the rigid case will be justified. Therefore, a larger soil stiffness would be employed.

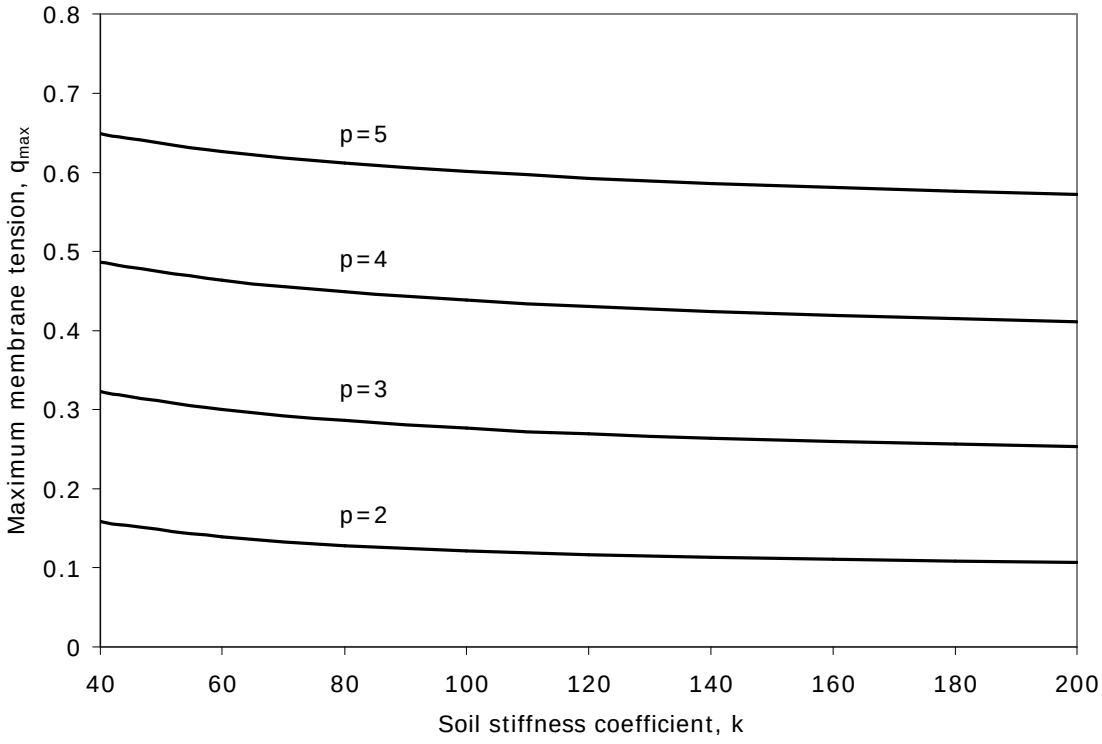

Figure 5.6 Maximum membrane tension versus soil stiffness

Figure 5.7 presents the maximum tube settlement h_f as a function of soil stiffness. After viewing Figure 5.7, much more ground deflection is observed in a less stiff soil.

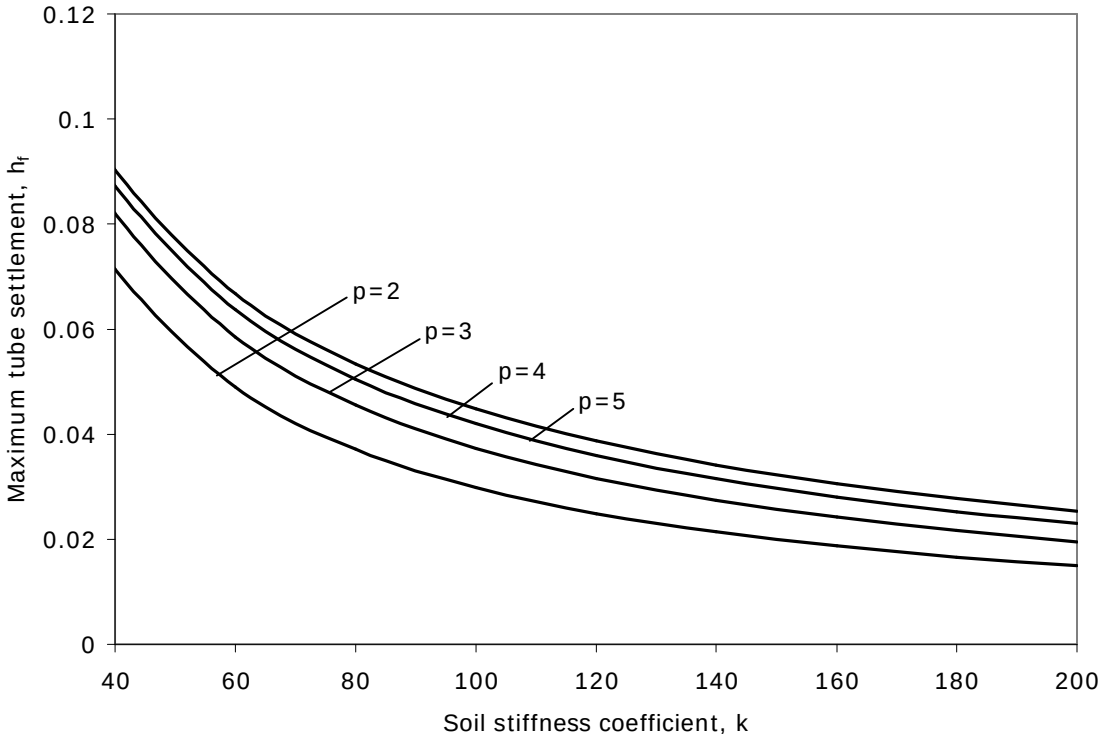

Figure 5.7 Maximum tube settlement versus soil stiffness

As the soil stiffness approaches infinity, the values for the Winkler foundation model should approach the membrane properties of the rigid foundation case presented in chapter 3. A comparison between rigid, Winkler, and Pasternak foundation results are displayed in Tables 5.2 through 5.7 and Figures 5.28 through 5.33.

5.5 Dynamic Derivation with Winkler Foundation

This section covers the equilibrium configuration with the addition of small vibrations. Consider the kinetic equilibrium diagram presented in Figure 5.8. From geometry, the following can be deduced:

$$\frac{?x}{?s} ? \cos? \qquad \frac{?y}{?s} ? \sin? \qquad (5.3, 5.4)$$

Once again the D'Alembert Principle (explained in section 2.5) is employed and equilibrium is induced upon the system. Summing the forces in the tangential and normal directions (with respect to the membrane element) results in

$$\frac{??}{?s} ? \frac{?}{?}\frac{1}{q}\frac{??}{??}p ? \cos? ? k(h_f ? y)\cos? ? \frac{?^2 x}{?t^2}\sin? ? \frac{?^2 y}{?t^2}\cos? \frac{?}{?} \quad (5.5)$$

$$\frac{?q}{?s} ? \sin? ? k(h_f ? y)\sin? ? \frac{?^2 x}{?t^2}\cos? ? \frac{?^2 y}{?t^2}\sin? \quad (5.6)$$

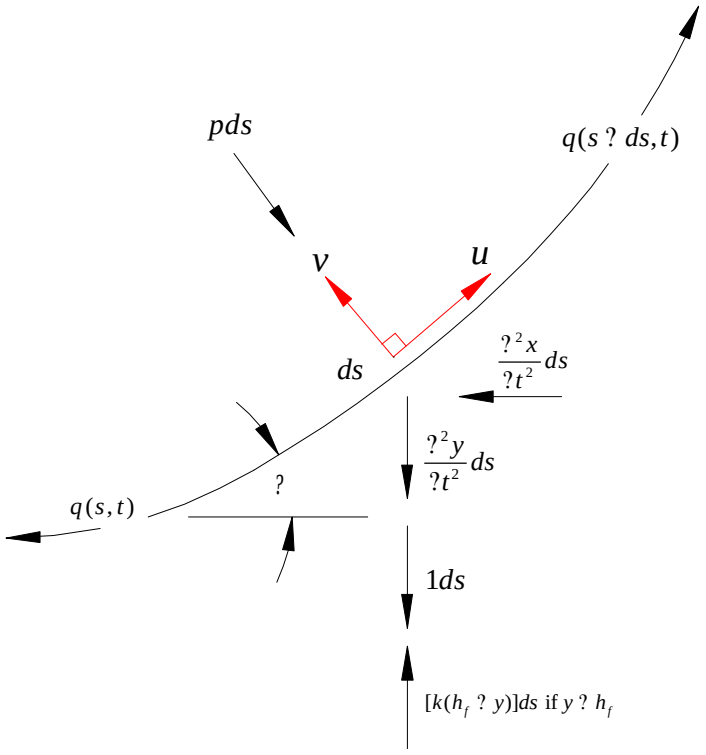

Figure 5.8 Winkler foundation kinetic equilibrium diagram

Equations 5.3 through 5.6 describe the dynamics of a geosynthetic tube supported by a Winkler foundation when y_e is less than h_f, and are considered the equations of motion for this system. As defined in chapter 3, ? is the nondimensional frequency of the system and t is time. Given a similar tube layout as in Chapter 4, Equations 4.7 to 4.10 are used. These nondimensional equations describe the total effect of motion on the equilibrium configuration, where the subscript *d* represents "dynamic":

$$x(s,t) ? x_e(s) ? x_d(s)\sin? t, \qquad y(s,t) ? y_e(s) ? y_d(s)\sin? t \quad (4.7, 4.8)$$

$$? (s,t) ? ? _e(s) ? ? _d(s)\sin? t, \qquad q(s,t) ? q_e(s) ? q_d(s)\sin? t \quad (4.9, 4.10)$$

Infinitesimal vibrations are assumed; therefore nonlinear terms in the dynamic variables are neglected. For example, the products of two dynamic deflections are approximately zero ($x_d y_d ? 0$ and $x_d x_d ? 0$). Using the nondimensional approximations of sin? and cos? presented in Section 3.5 and dividing all terms by sin(? t), Equations 5.3 through 5.6 resolve into

$$\frac{dx_d}{ds} ? ??_d \sin?_e, \qquad \frac{dy_d}{ds} ? ?_d \cos?_e \qquad (5.11, 5.12)$$

$$\frac{d?_d}{ds} ? \frac{1}{q_e}[? ^2(x_d \sin?_e ? y_d \cos?_e) ? ?_d \sin?_e ? q_d \frac{(p ? \cos?_e)}{q_e} \\ ?ky_d \cos?_e ? k(y_e ? h_f)?_d \sin?_e ? (\frac{q_d}{q_e})k(y_e ? h_f)\cos?_e] \qquad (5.13a)$$

$$\frac{dq_d}{ds} ? ??^2(x_d \cos?_e ? y_d \sin?_e) ? ?_d \cos?_e ? k(y_e ? h_f)?_d \cos?_e ? ky_d \sin?_e \qquad (5.13b)$$

Equations 5.13a and 5.13b apply when $y ? h_f$. The governing dynamic equations above the surface of the foundation ($y_e > h_f$) are as follows:

$$\frac{d?_d}{ds} ? \frac{1}{q_e}[? ^2(x_d \sin?_e ? y_d \cos?_e) ? ?_d \sin?_e ? q_d \frac{(p ? \cos?_e)}{q_e}] \qquad (5.14a)$$

$$\frac{dq_d}{ds} ? ??^2(x_d \cos?_e ? y_d \sin?_e) ? ?_d \cos?_e \qquad (5.14b)$$

The two-point boundary conditions for nonsymmetrical vibrations about the equilibrium of an air-filled freestanding tube resting on a Winkler foundation are as follows:
For the range $0 ? s ? 0.5$

@ $s ? 0$: $x_e ? y_e ? ?_e ? 0$, $x_d ? y_d ? 0$, $?_d ? 0.001$

@ $s ? 0.5$: $x_d ? 0$, $y_d ? 0$

Two changes are made when dealing with symmetrical vibrations: y_d equals 0.0001 and $?_d$ equals zero.

The conditional "if-then" command was used, within the Mathematica program, in order to calculate x_d, y_d, $?_d$, and q_d above and below the surface of the foundation. Also, a condition where the vertical tangent of the tube is to always be above the surface of the foundation is enforced for all solutions. Physically, the tube can only be supported by as many springs are under it. If the vertical tangents fall below the surface of the foundation, illogical springs will be supporting nothing. With the use of Equations 5.11, 5.12, 5.13a and b, 5.14a and b and the boundary conditions above, a Mathematica file was coded to compute the dynamic parameters. The Mathematica program is described and given in Appendix E.

5.6 Winkler Foundation Dynamic Results

In this section the results from the dynamic analysis of the Winkler foundation model are displayed. Figures 5.9 through 5.12 present a graphical depiction of these dynamic results related to their respected internal air pressure. The general trend follows that as the soil stiffness increases the frequency increases. Physically, this means that a tube placed upon tundra will tend to oscillate more than a tube placed on a soft soil. Figure 5.13 presents a representative group of resulting dynamic shapes where the internal air pressure equals 2 and k = 200. The red line represents the equilibrium shape and the black line depicts the vibrating shape. These shapes appear identical to the tube shapes presented in the rigid foundation results (Chapter 3), with one exception: tube settlement below the surface.

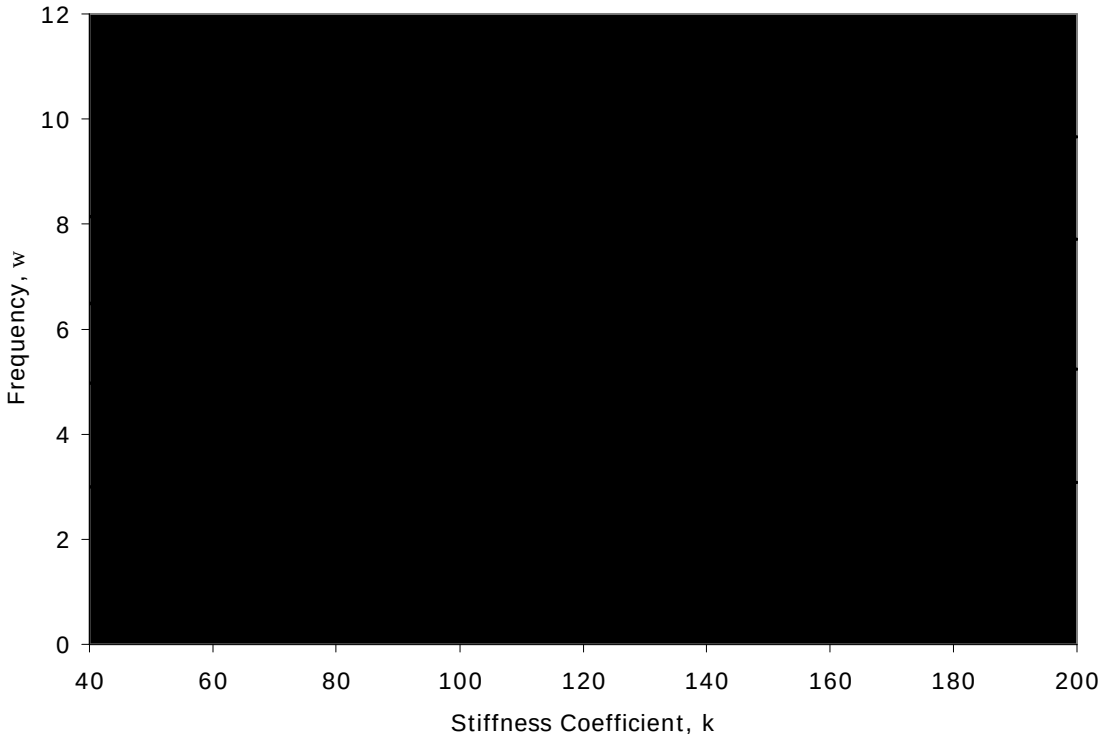

Figure 5.9 Frequency versus soil stiffness when p = 2

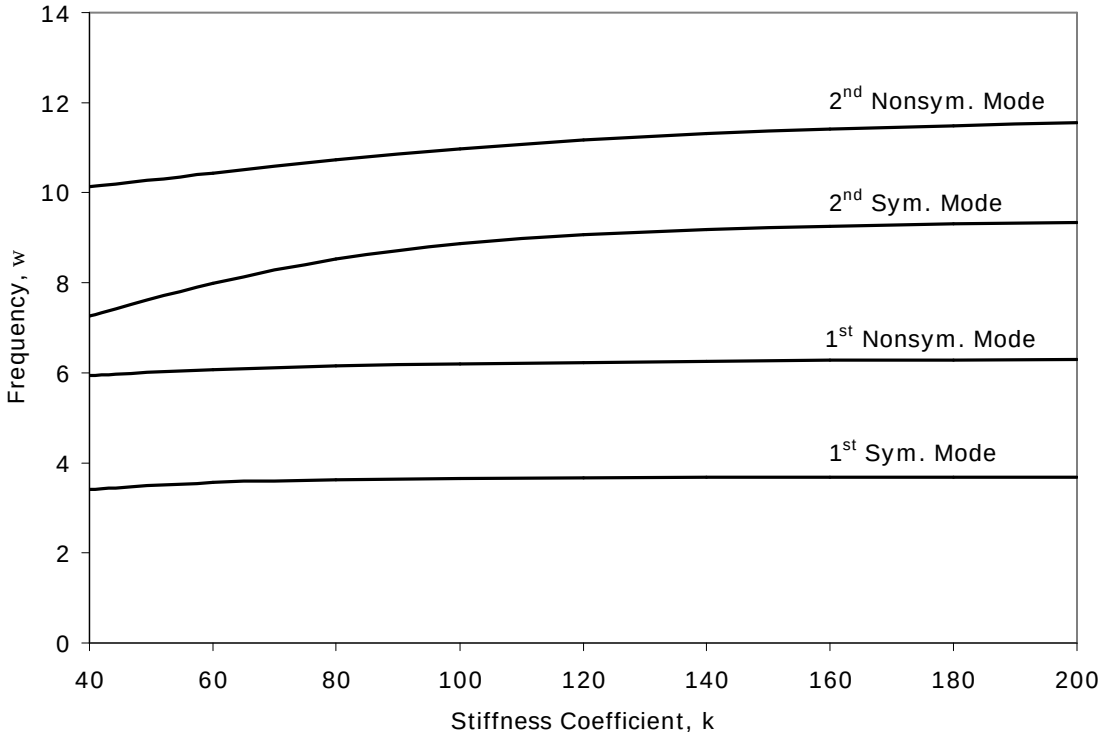

Figure 5.10 Frequency versus soil stiffness when p = 3

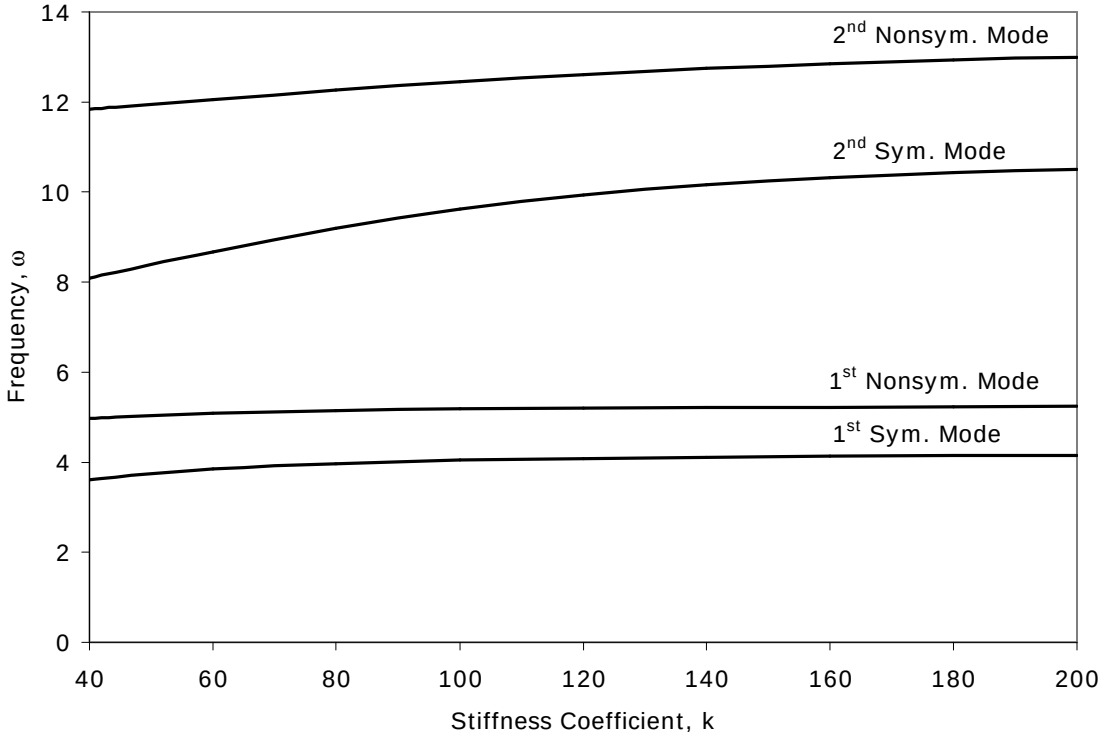

Figure 5.11 Frequency versus soil stiffness when p = 4

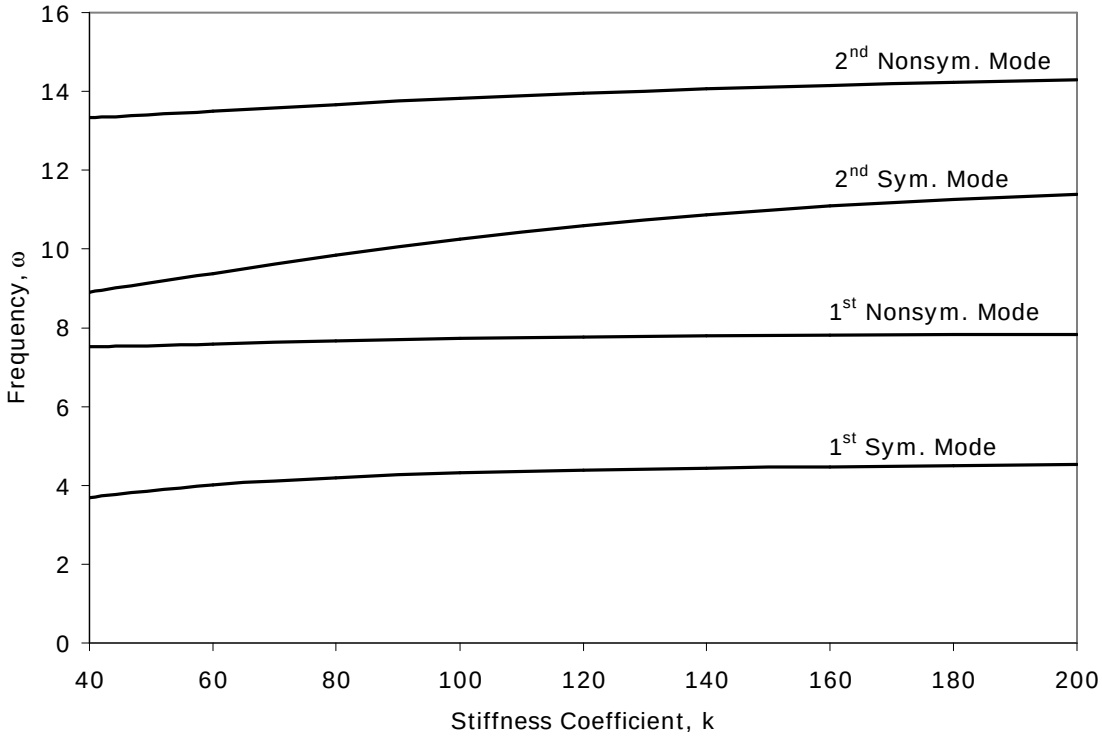

Figure 5.12 Frequency versus soil stiffness when p = 5

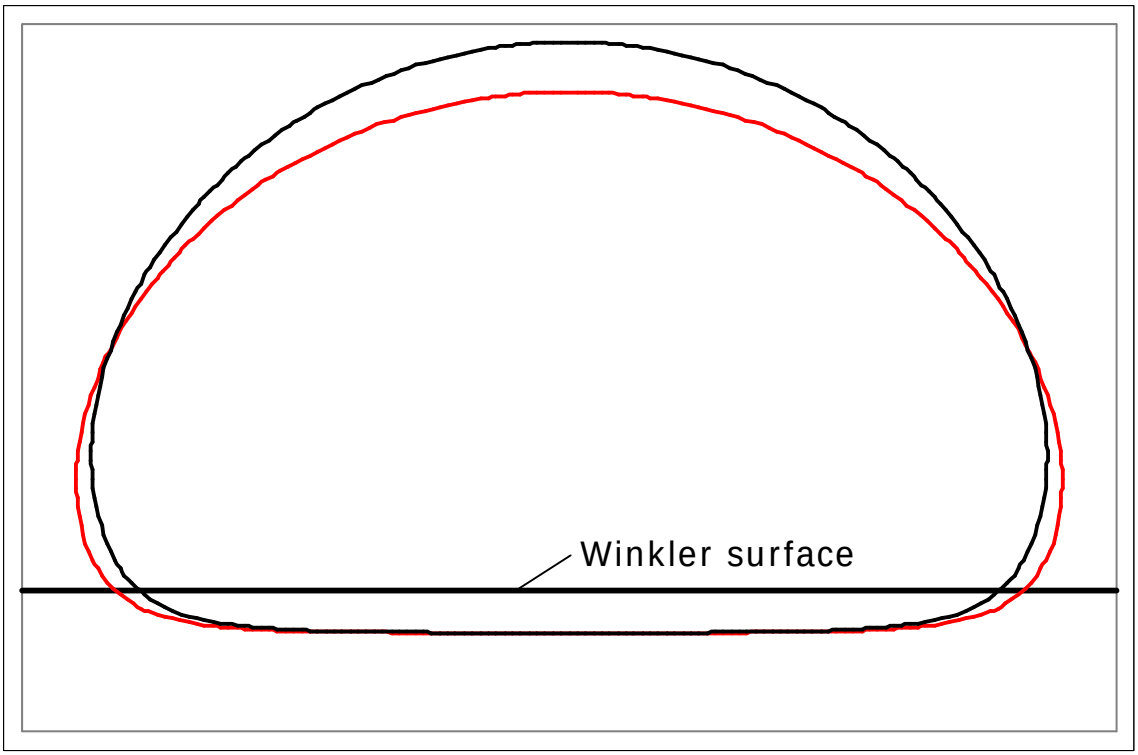

(a) 1st symmetrical mode

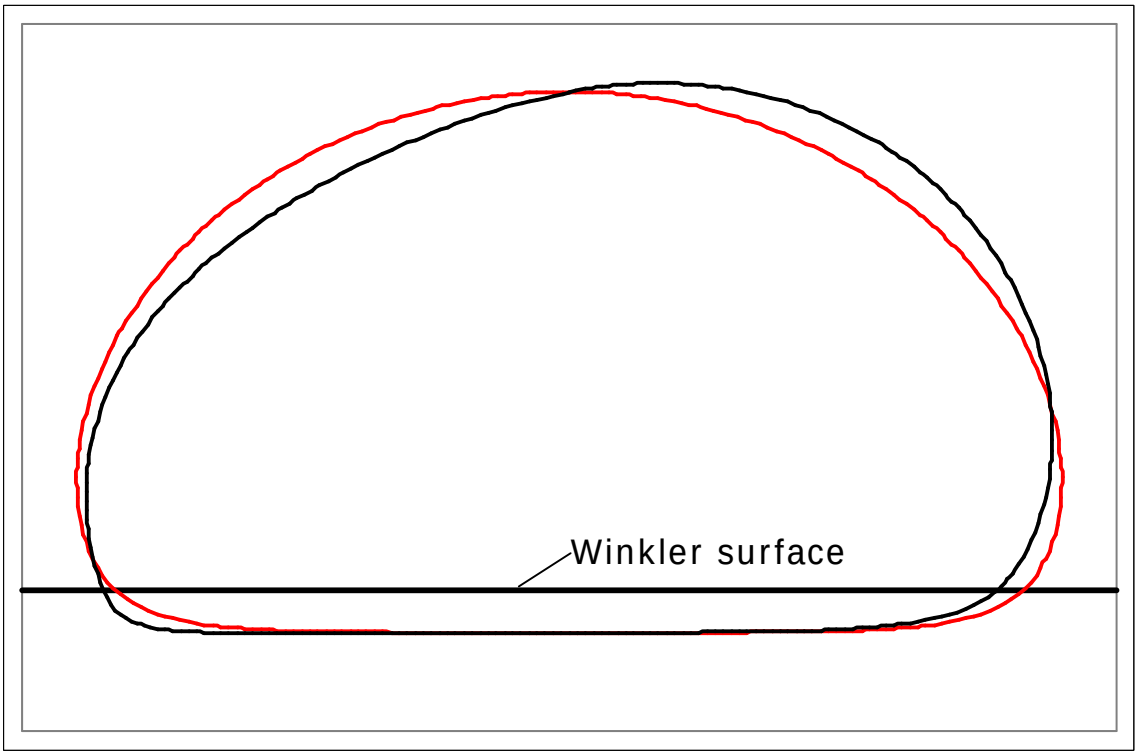

(b) 1st nonsymmetrical mode

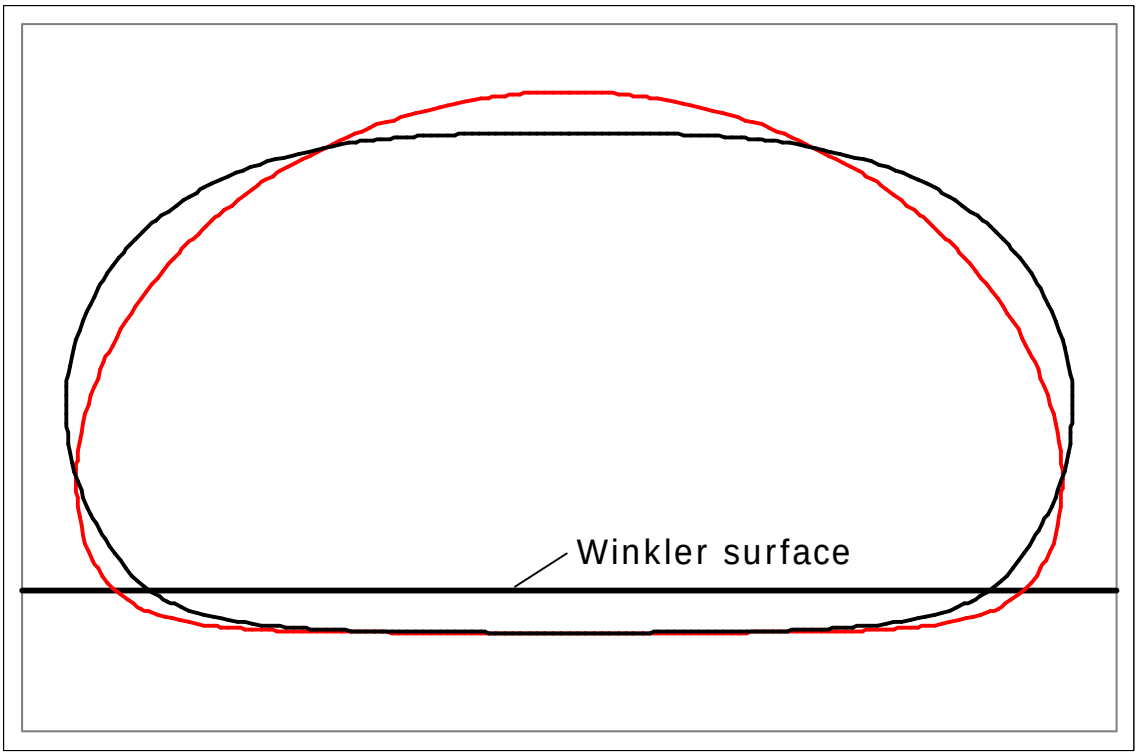

(c) 2nd symmetrical mode

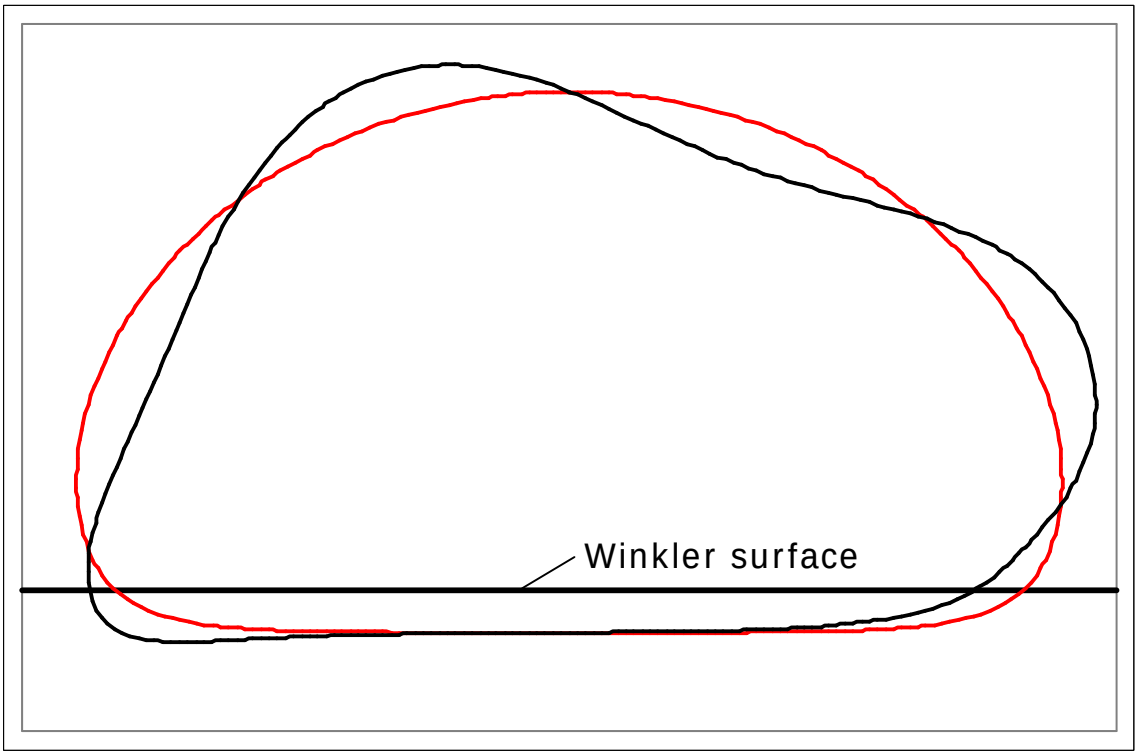

(d) 2nd nonsymmetrical mode

Figure 5.13 Mode shapes for p = 2 and k = 200

5.7 Pasternak Model

A long freestanding geosynthetic tube filled with air and supported by a Pasternak foundation is considered. The general traits of the geosynthetic tube remain the same as before. This includes the assumptions of a long straight tube, neglecting changes in cross-sectional area, geosynthetic material being inextensible, neglecting bending resistance, and weight of the geotextile material is included. Proposed by Pasternak in 1954, this model extends the Winkler model by adding a shear layer to the vertical springs. The primary difference between the Winkler and Pasternak foundation models is the presence of a shear interaction layer between the Winkler spring elements. This shear layer is composed of incompressible vertical elements which deform in the transverse shear direction only (Selvadurai 1979).

5.8 Pasternak Foundation Formulation

Consider the freestanding air-filled tube resting on a Pasternak foundation in Figure 5.14. The descriptions of the geosynthetic properties are identical to the Winkler definitions with the exception of an added shear modulus G_P. The shear modulus G_P represents the incompressible shear layer as described in Selvadurai's definition of a Pasternak soil model.

To begin the formulation, consider the Pasternak foundation equilibrium element in Figure 5.15. The internal air pressure, soil stiffness coefficient, and the shear modulus are the prescribed values, and the calculated unknown quantities include the membrane tension, maximum tube height, ground deflection, and the equilibrium shape. The nondimensional quantities presented in chapter 3 are used, along with k and g_p:

$$x ? \frac{X}{L}, \quad y ? \frac{Y}{L}, \quad b ? \frac{B}{L}, \quad s ? \frac{S}{L}, \quad q_e ? \frac{Q_e}{? gL}, \quad p ? \frac{P}{? g}, \quad k ? \frac{KL}{? g}, \quad g_P ? \frac{G_P}{? gL}$$

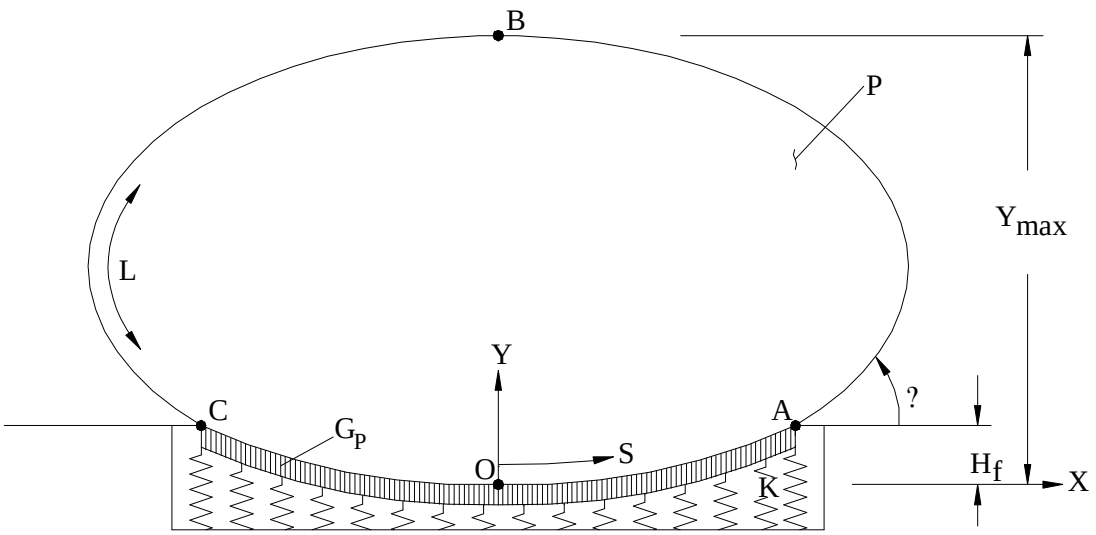

Figure 5.14 Pasternak foundation model

The same coordinate system is adopted for the Pasternak foundation case, therefore the horizontal and vertical coordinates x_e and y_e remain the same and Equations 3.10 and 3.11 are once again employed:

$$\frac{dx_e}{ds} ? \cos?_e, \qquad \frac{dy_e}{ds} ? \sin?_e \qquad (3.10, 3.11)$$

From the tube element, presented in Figure 5.15, the following can be derived, where the subscript *e* denotes equilibrium values. Again, a unit load produced by normalizing the weight ($\frac{? g}{? g} ? 1$) is represented by 1. If the vertical coordinate y_e is less than h_f, the following equations are derived by summing the forces in the tangential direction and the normal direction of the membrane, respectively:

$$\frac{d?_e}{ds} ? \frac{1}{q_e}[k(y_e ? h_f)\cos?_e ? g_P \frac{d^2 y_e}{ds^2}\cos?_e ? p ? \cos?_e] \qquad (5.17a)$$

$$\frac{dq_e}{ds} ? [k(y_e ? h_f) ? g_P \frac{d^2 y_e}{ds^2} ? 1]\sin ?_e \qquad (5.17b)$$

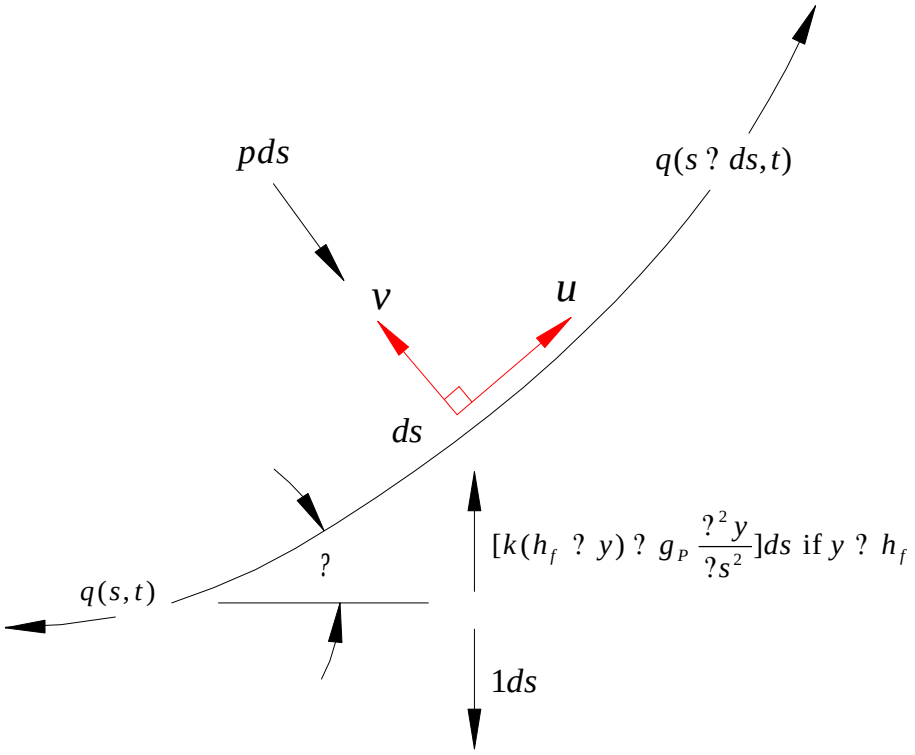

Figure 5.15 Pasternak foundation equilibrium element

Knowing Equation 3.11, Equations 5.17 and 5.18 can be simplified by using calculus and substituting $\frac{d^2 y_e}{ds^2} ? \frac{d?_e}{ds}\cos ?_e$. This produces the following:

$$\frac{d?_e}{ds} ? \frac{1}{q_e ? g_P \cos^2 ?_e}[k(y_e ? h_f)\cos ?_e ? p ? \cos ?_e] \qquad (5.18a)$$

$$\frac{dq_e}{ds} ? [k(y_e ? h_f) ? 1]\sin ?_e ? [\frac{g_P \sin ?_e \cos ?_e (p ? \cos ?_e ? k(y_e ? h_f)\cos ?_e)}{q_e ? g_P \cos^2 ?_e}] \qquad (5.18b)$$

When the vertical coordinate y_e is greater than h_f, the soil stiffness and shear modulus are not considered, therefore Equations 5.18 a and b resort back to Equations 5.1a and 5.1b:

$$\frac{d?_e}{ds} ? \frac{1}{q_e}[p ? \cos ?_e], \qquad \frac{dq_e}{ds} ? \sin ?_e \qquad (5.1a, 5.1b)$$

The two-point boundary conditions for equilibrium of a single air-filled freestanding tube resting on a Pasternak foundation are as follows:

For the range $0 ? s ? 0.5$

@ $s ? 0$ (point O): $x_e ? 0,$ $y_e ? 0,$ $? _e ? 0$

@ $s ? 0.5$ (point B): $x_e ? 0,$ $? _e ? ?$

Again, an "if-then" command is used, within the Mathematica program, in order to calculate x_e, y_e, $? _e$, and q_e above and below the surface of the foundation. A condition where the vertical tangent of the tube is to always be above the surface of the foundation is enforced for all solutions. With the use of Equations 3.9, 3.10, 5.1a, 5.1b, and 5.18a and b and the boundary conditions above, a Mathematica file was coded to compute the equilibrium parameters. The Mathematica program is described and given in Appendix F.

5.9 Pasternak Foundation Equilibrium Results

Presented in Figures 5.16 – 5.26 are the results from the Pasternak foundation equilibrium model. In general, the results follow an expected trend of decreasing membrane tension and ground deflection as the shear modulus increases. However, consider Figure 5.18. There is an unexplainable rise and fall in the maximum membrane tension as the shear modulus increases. This phenomenon converges as the internal air pressure is greater. Physically, this quick rise in membrane tension could be attributed to the adjustment of the tube to the different soil media (i.e., changes in the shear modulus). An explicit example of this change in initial membrane tension may be viewed in Figures 5.17a, 5.17b, 5.18a, and 5.18b. Figure 5.18b shows that when $g_P = 0.5$ the maximum membrane tension is less than when $g_P = 2$. Notice that this slight hump in maximum membrane tension becomes shallower as the internal air pressure increases.

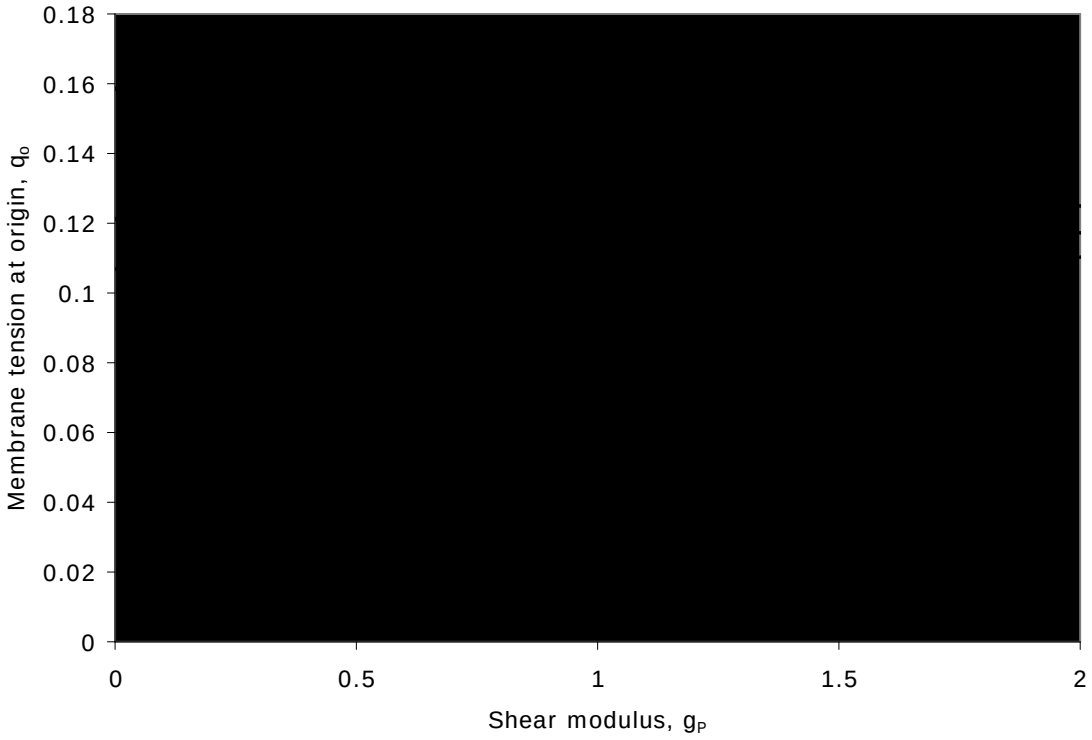

Figure 5.16 Membrane tension at origin versus shear modulus when p = 2

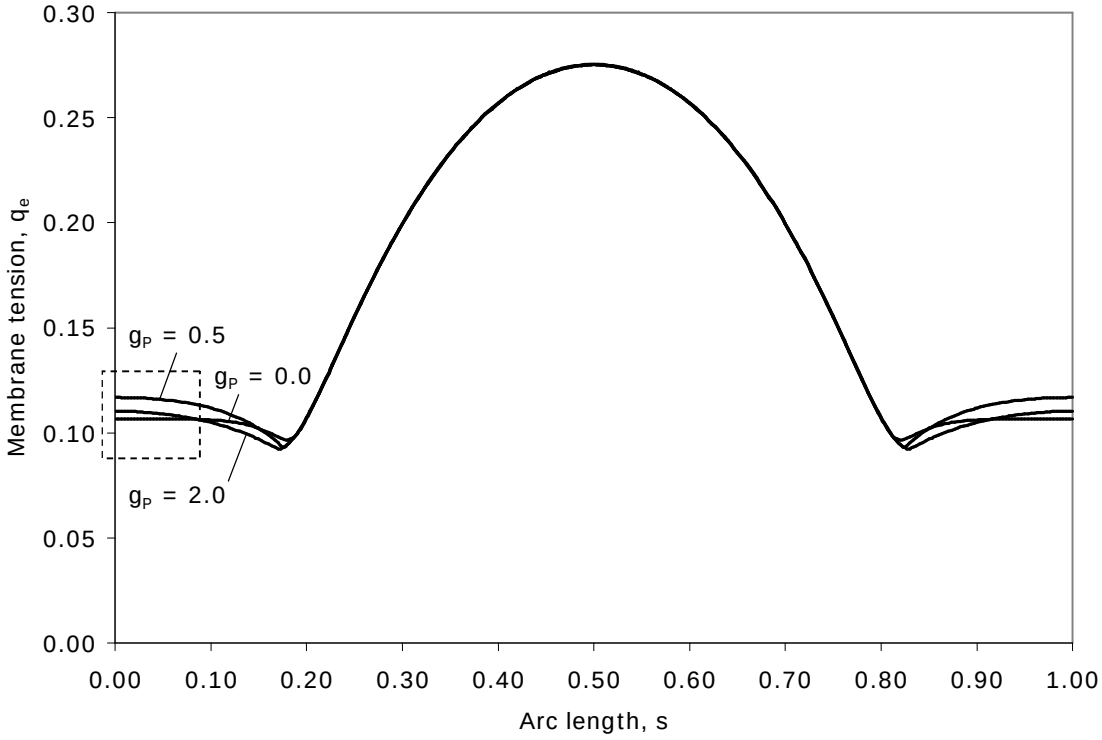

Figure 5.17a Membrane tension versus arc length when p = 2 and k = 200

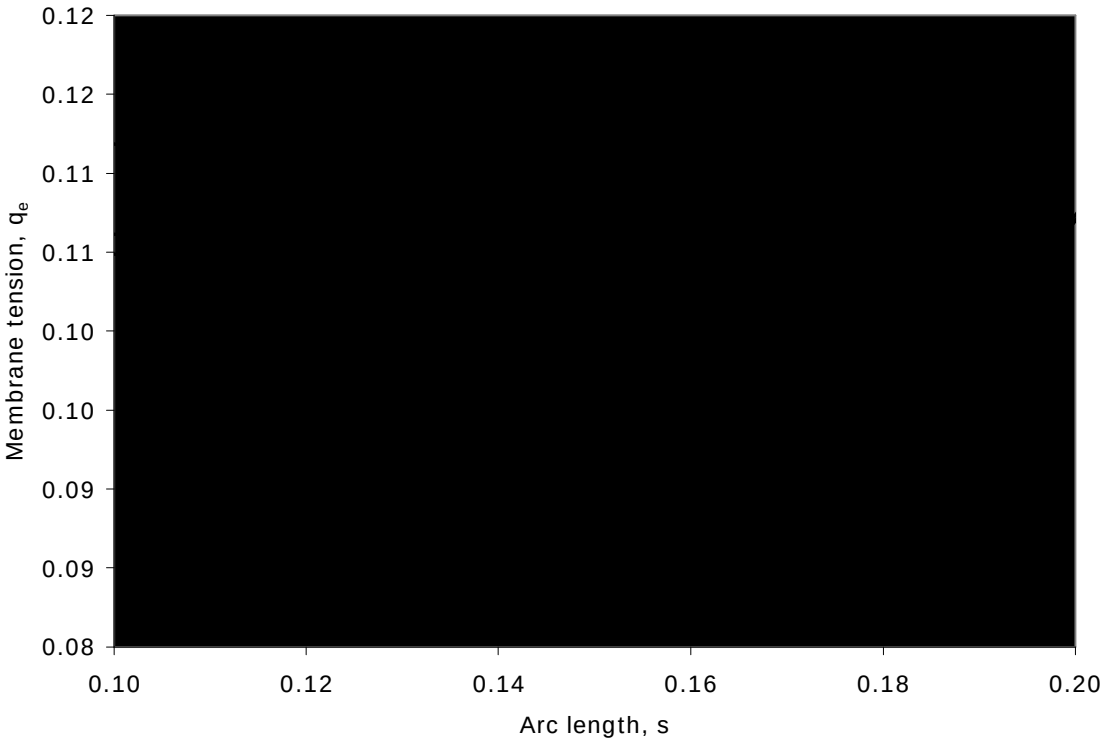

Figure 5.17b Zoom of membrane tension versus arc length when p = 2 and k = 200

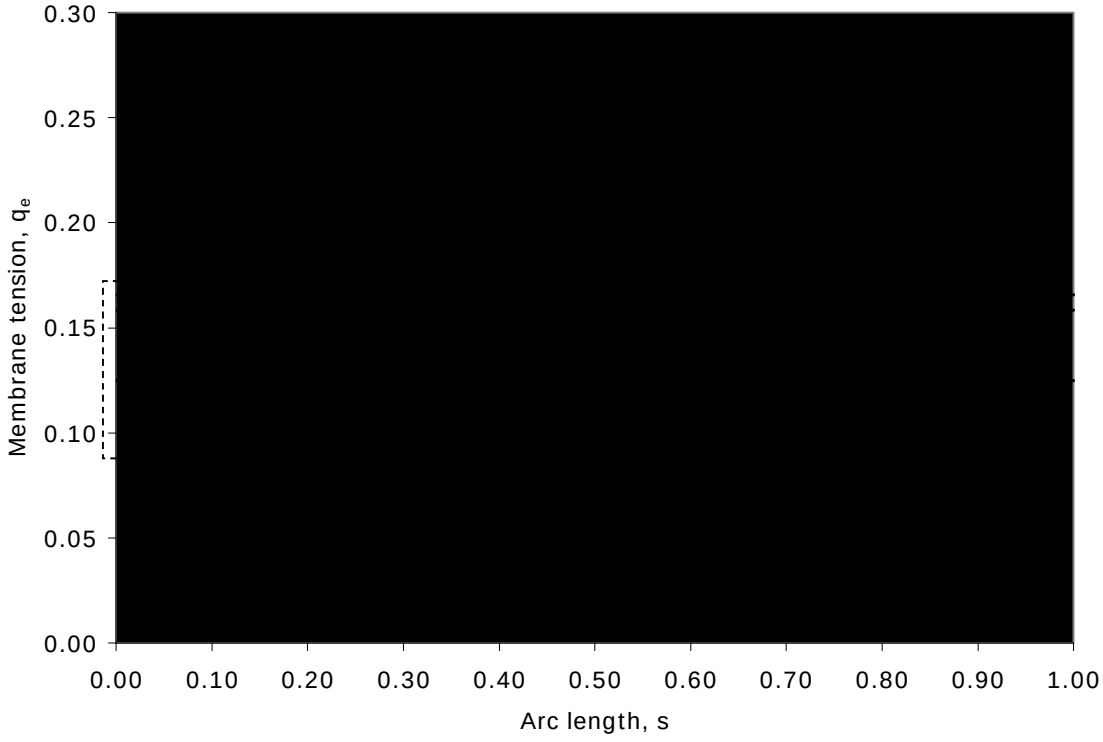

Figure 5.18a Membrane tension versus arc length when p = 2 and k = 40

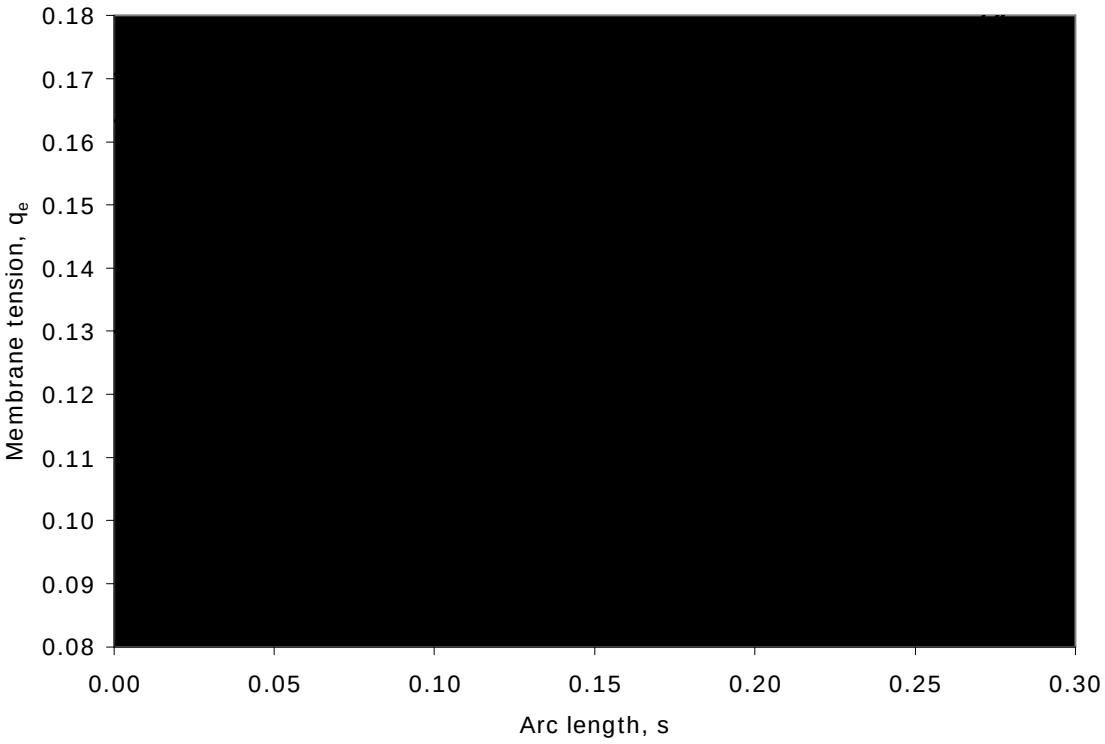

Figure 5.18b Zoom of membrane tension versus arc length when p = 2 and k = 40

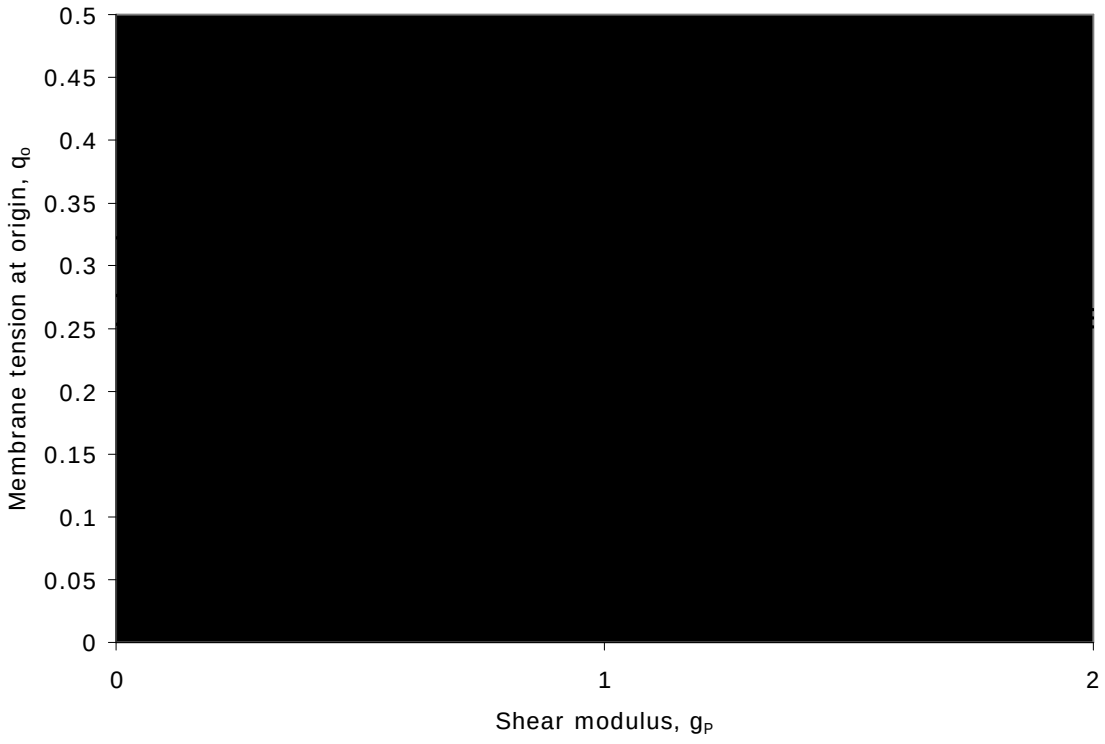

Figure 5.19 Membrane tension at origin versus shear modulus when p = 3

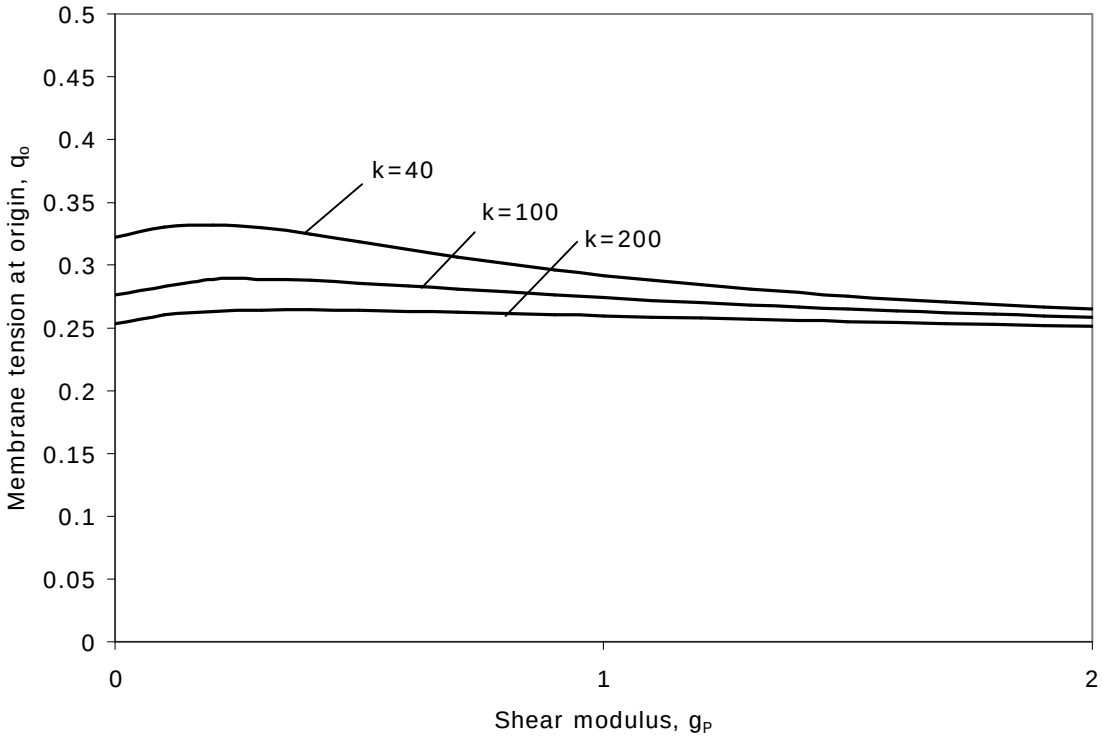

Figure 5.20 Membrane tension at origin versus shear modulus when p = 4

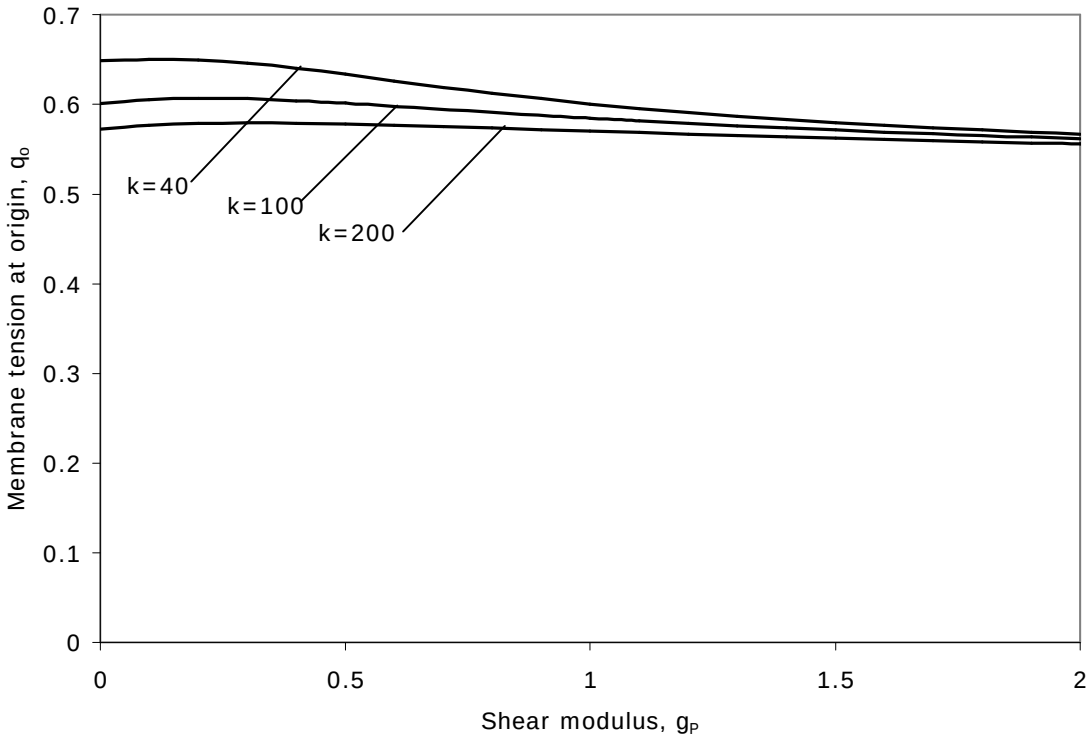

Figure 5.21 Membrane tension at origin versus shear modulus when p = 5

Figures 5.22 through 5.25 reveal the relationship of maximum tube settlement to the change in shear modulus. The added shear layer (adjoining vertical springs) has a much greater effect on the behavior of the model than does the change in soil stiffness.

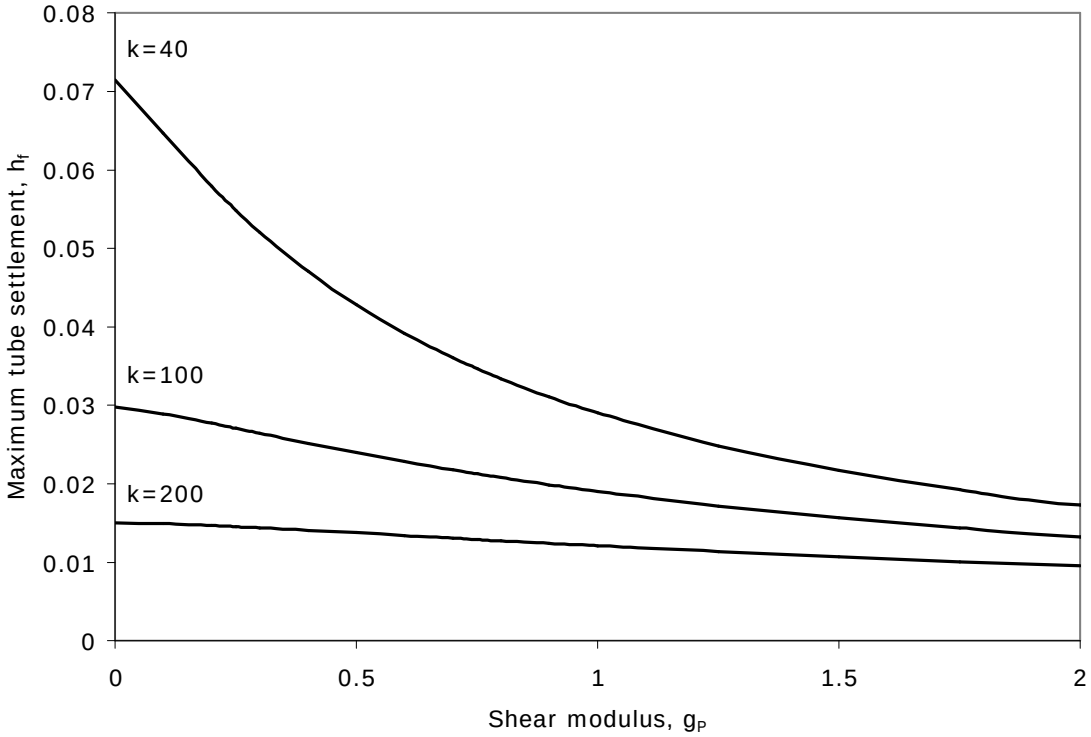

Figure 5.22 Tube depth below surface versus shear modulus when p = 2

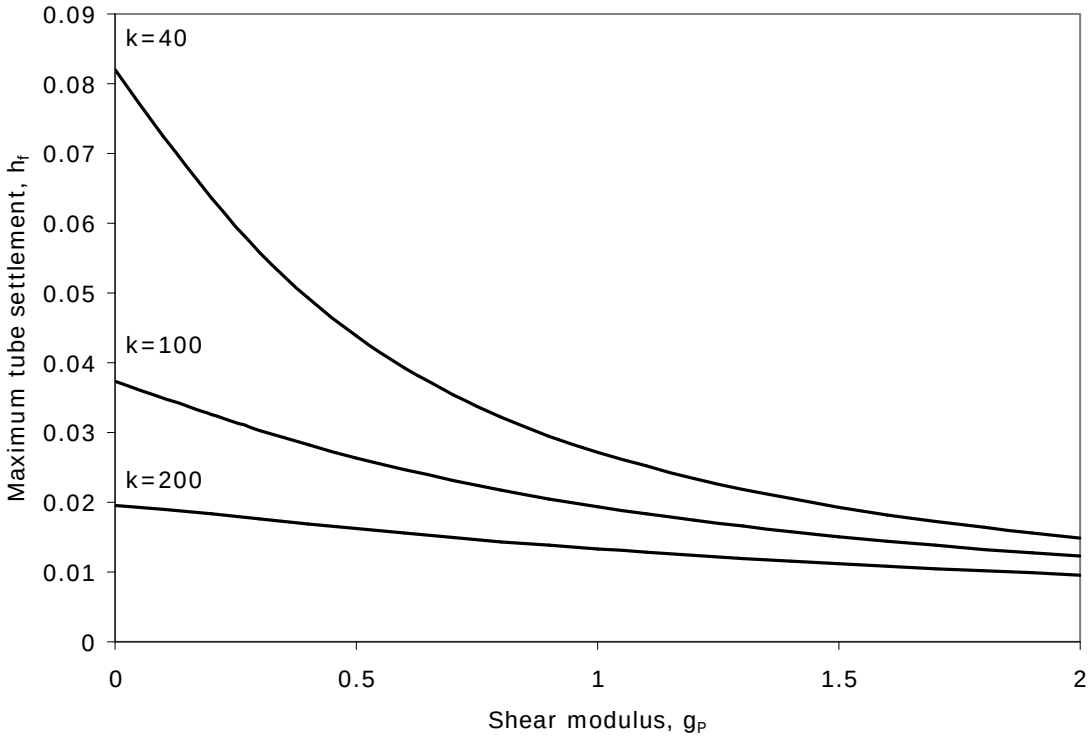

Figure 5.23 Tube depth below surface versus shear modulus when p = 3

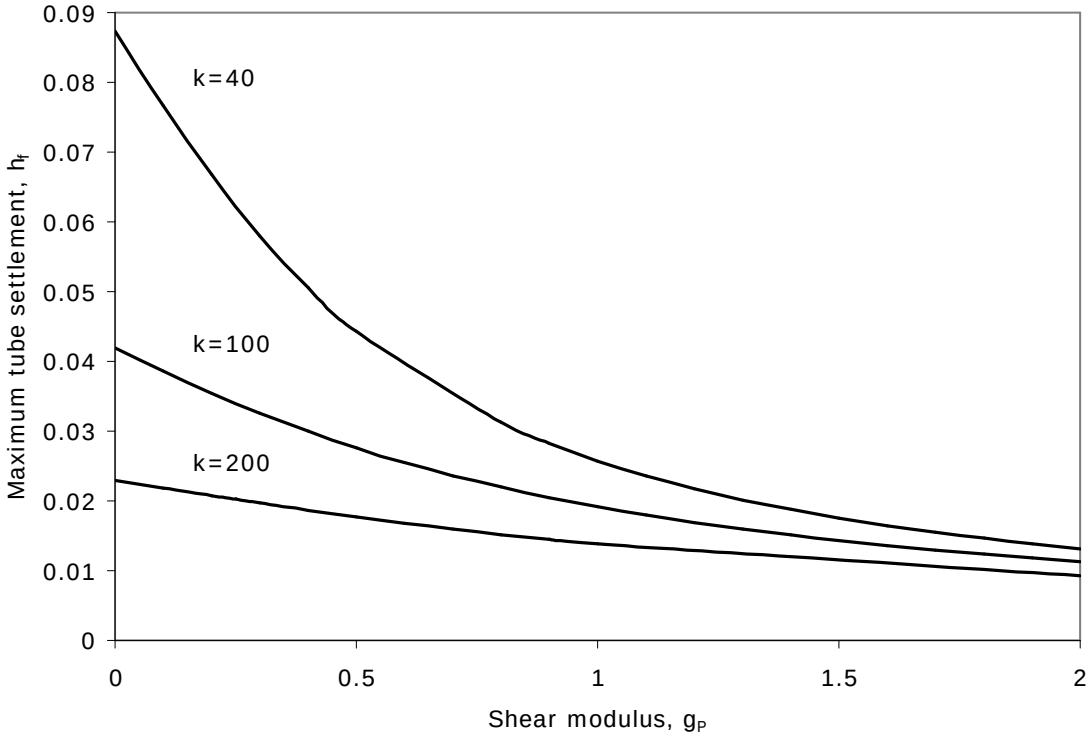

Figure 5.24 Tube depth below surface versus shear modulus when p = 4

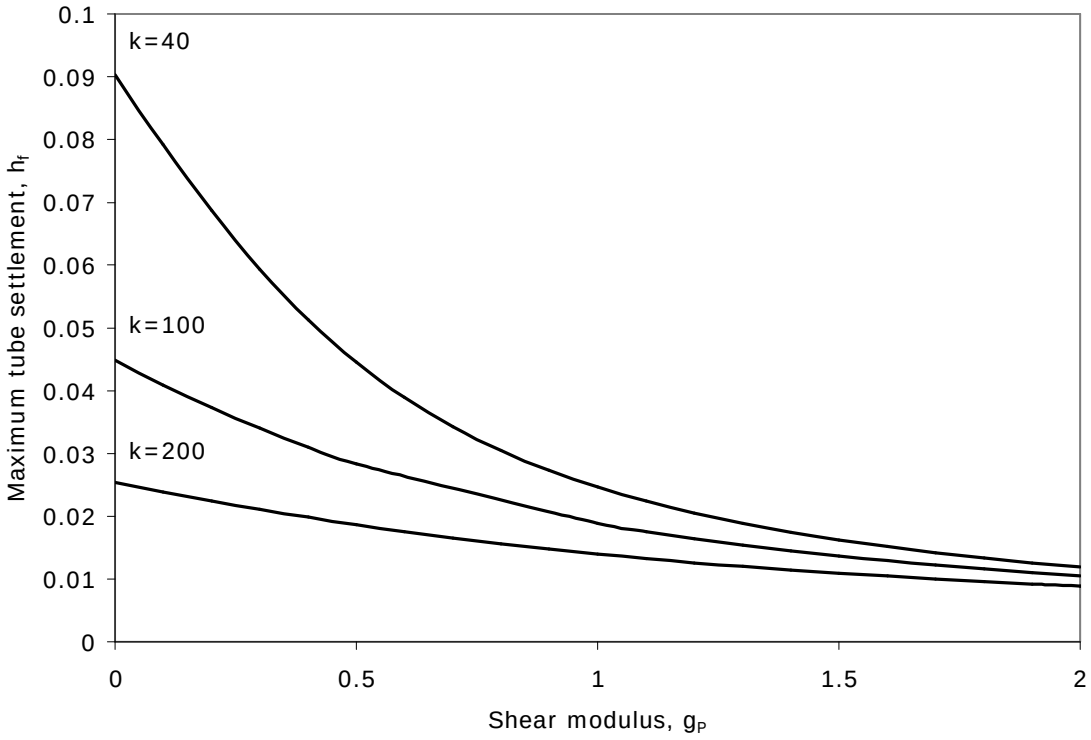

Figure 5.25 Tube depth below surface versus shear modulus when p = 5

Figure 5.26 exhibits the equilibrium shape of a geosynthetic tube resting on a Pasternak foundation. Values of the shear modulus g_P = 0.0, 0.5, and 30 were used to depict a notable change in shape. When g_P = 30 the tube base is most near the rigid foundation scenario.

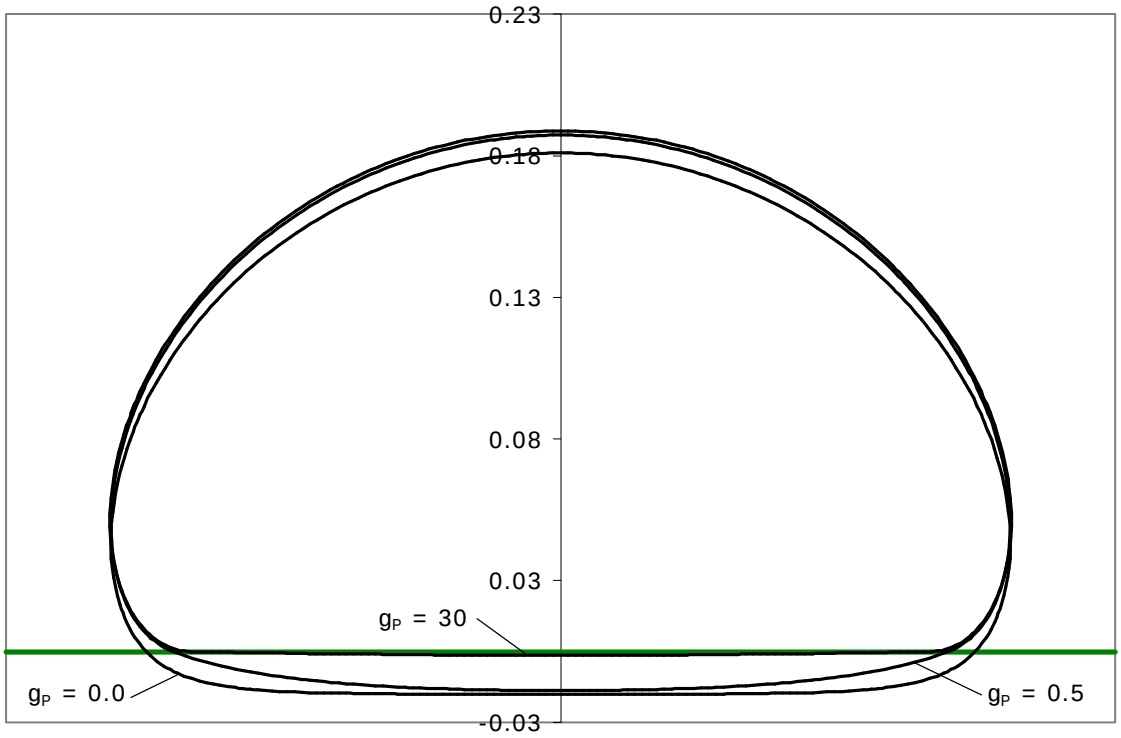

Figure 5.26 Pasternak foundation equilibrium shapes when p = 2 and k = 200

5.10 Pasternak Foundation Dynamic Derivation

Within this section the dynamic derivation of a freestanding geosynthetic tube resting on a Pasternak foundation is presented. Figure 5.27 displays the kinetic equilibrium of the system undergoing vibration about its initial equilibrium configuration. The set-up geometry is identical to the Winkler foundation model (presented in section 5.5). Therefore, Equations 5.3 and 5.4 hold true:

$$\frac{?x}{?s} ? \cos? \qquad \frac{?y}{?s} ? \sin? \qquad (5.3, 5.4)$$

The D'Alembert Principle (explained in section 2.5) is used and equilibrium is induced upon an element, pictured in Figure 5.27. Summing the forces in the tangential and normal directions (with respect to the membrane element) results in

$$q\frac{??}{?s} ? \frac{?^2 y}{?t^2}\cos? ? \frac{?^2 x}{?t^2}\sin? ? p ? \cos? ? k(h_f ? y)\cos? ? g_P \frac{?^2 y}{?s^2}\cos? \qquad (5.21)$$

$$\frac{?q}{?s} ? \frac{?^2 x}{?t^2}\cos? ? \frac{?^2 y}{?t^2}\sin? ? \sin? ? k(h_f ? y)\sin? ? g_P \frac{?^2 y}{?s^2}\sin? \qquad (5.22)$$

Equations 5.3, 5.4, 5.21, and 5.22 describe the dynamics of a geosynthetic tube supported by a Pasternak foundation and are considered the equations of motion for this system when $y_e < h_f$. As defined in Section 3.5, ? is the nondimensional frequency of the system. To relate equilibrium and dynamic terms, Equations 5.7 through 5.10 are employed:

$$x(s,t) ? x_e(s) ? x_d(s)\sin? t, \qquad y(s,t) ? y_e(s) ? y_d(s)\sin? t \qquad (5.7, 5.8)$$

$$? (s,t) ? ?_e(s) ? ?_d(s)\sin? t, \qquad q(s,t) ? q_e(s) ? q_d(s)\sin? t \qquad (5.9, 5.10)$$

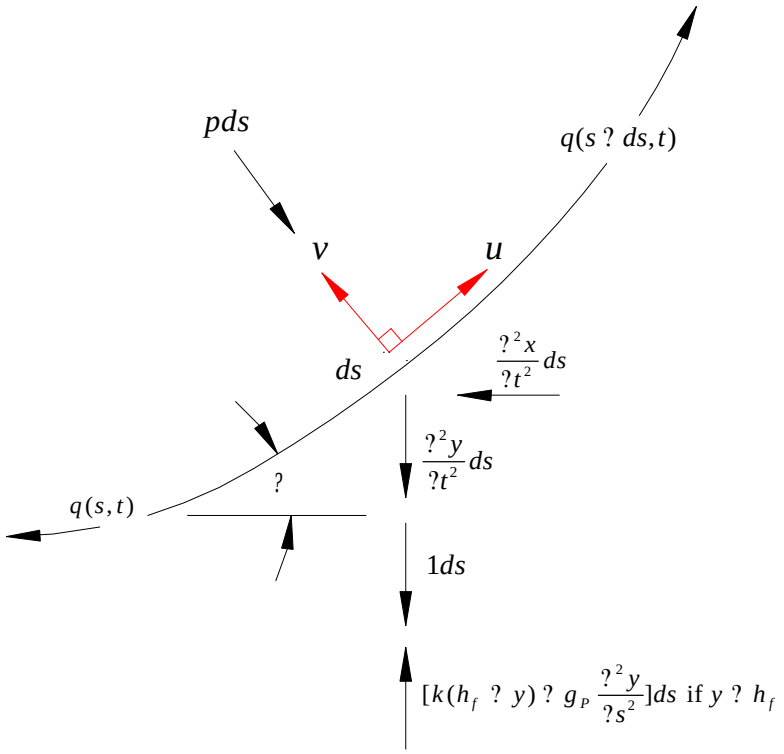

Figure 5.27 Pasternak foundation kinetic equilibrium element

Equations 5.7 to 5.10 are substituted into the two summations of forces equations (Equations 5.21 and 5.22), infinitesimal vibrations are assumed, meaning nonlinear terms in the dynamic variables are neglected. For example, the products of two dynamic deflections are approximately zero ($x_d y_d ? 0$ and $x_d x_d ? 0$). Using consistent geometry,

Equations 5.11 and 5.12 are substituted into the resulting expressions and the term sin(? t) drops out once divided through. This produces the following governing equations:

$$\frac{dx_d}{ds} ? ??_d \sin?_e, \qquad \frac{dy_d}{ds} ? ?_d \cos?_e \tag{5.11, 5.12}$$

$$\frac{d?_d}{ds} ? \frac{1}{(q_e ? g_P \cos^2?_e)}\{?? ^2 y_d \cos?_e ? ? ^2 x_d \sin?_e ? ?_d \sin?_e ? ky_d \cos?_e ? k(h_f ? y_e)?_d \sin?_e ? (2g_P?_d \sin?_e \cos?_e ? q_d)[\frac{k(y_e ? h_f)\cos?_e ? p ? \cos?_e}{(q_e ? g_P \cos^2?_e)}]\} \tag{5.23a}$$

$$\frac{dq_d}{ds} ? ?? ^2 x_d \cos?_e ? ? ^2 y_d \sin?_e ? ?_d \cos?_e ? k(h_f ? y_e)?_d \cos?_e ? ky_d \sin?_e ? g_P \frac{d^2 y_e}{ds^2}?_d \cos?_e ? g_P \frac{d^2 y_d}{ds^2}\sin?_e \tag{5.23b}$$

where $\frac{d^2 y_e}{ds^2} ? \frac{d?_e}{ds}\cos?_e$, $\frac{d^2 y_d}{ds^2} ? \frac{d?_d}{ds}\cos?_e ? ?_d \frac{d?_e}{ds}\sin?_e$

$\frac{d?_d}{ds}$ is given by Equation 5.23a and $\frac{d?_e}{ds}$ is given by Equation 5.19.

If the membrane properties being calculated are above the surface of the foundation, any term with a soil coefficient or shear modulus fall out. Therefore, the two Equations 5.23a and b result:

$$\frac{d?_d}{ds} ? \frac{1}{q_e}[?? ^2 y_d \cos?_e ? ? ^2 x_d \sin?_e ? ?_d \sin?_e ? q_d(\frac{p ? \cos?_e}{q_e})] \tag{5.24a}$$

$$\frac{dq_d}{ds} ? ?? ^2 x_d \cos?_e ? ? ^2 y_d \sin?_e ? ?_d \cos?_e \tag{5.24b}$$

The two-point boundary conditions for vibrations about equilibrium of an air-filled freestanding tube resting on a Pasternak foundation are as follows:

For the range $0 ? s ? 0.5$

@ $s ? 0$: $x_e ? y_e ? ?_e ? 0$, $x_d ? ?_d ? 0$, $y_d ? 0.001$

@ $s ? 0.5$: $x_d ? 0$, $?_d ? 0$

The "if-then" command was used, within the Mathematica program, in order to calculate x_d, y_d, $?_d$, and q_d above and below the surface of the foundation. A condition where the vertical tangent of the tube is to always be above the surface of the foundation is enforced for all solutions. With the use of Equations 5.11, 5.12, 5.23a and b, 5.24a and b, and the boundary conditions above, a Mathematica file was coded to solve the equilibrium parameters. The Mathematica program is described and given in Appendix F.

5.11 Pasternak Foundation Dynamic Results

Presented in this section are the results from the dynamic derivation of a freestanding geosynthetic tube resting on a Pasternak foundation. If the soil stiffness coefficient is held at 200, then the Pasternak foundation mode shapes are identical to the Winkler foundation mode shapes, with the exception of varying with the shear modulus. For given internal air pressures p = 2, 3, 4, and 5, the lowest four natural frequencies conform to the curves displayed in Figures 5.28 through 5.31. A decrease in frequency occurs when the shear modulus g_P is increased.

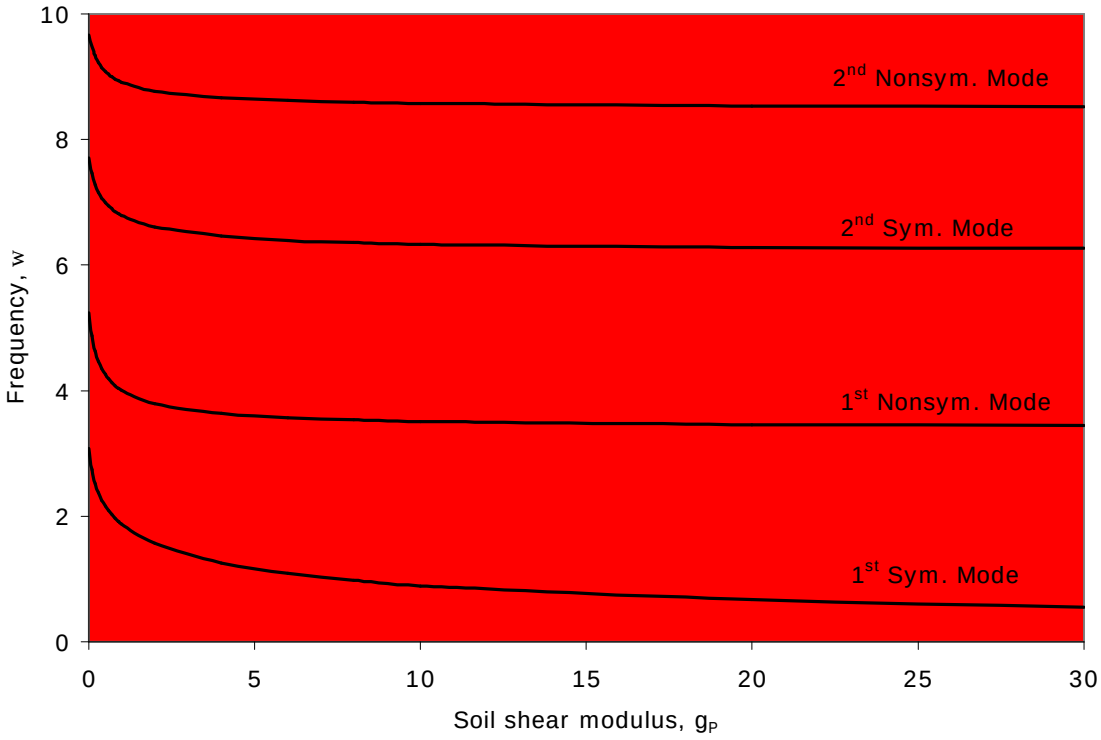

Figure 5.28 Frequency versus shear modulus when p = 2 and k = 200

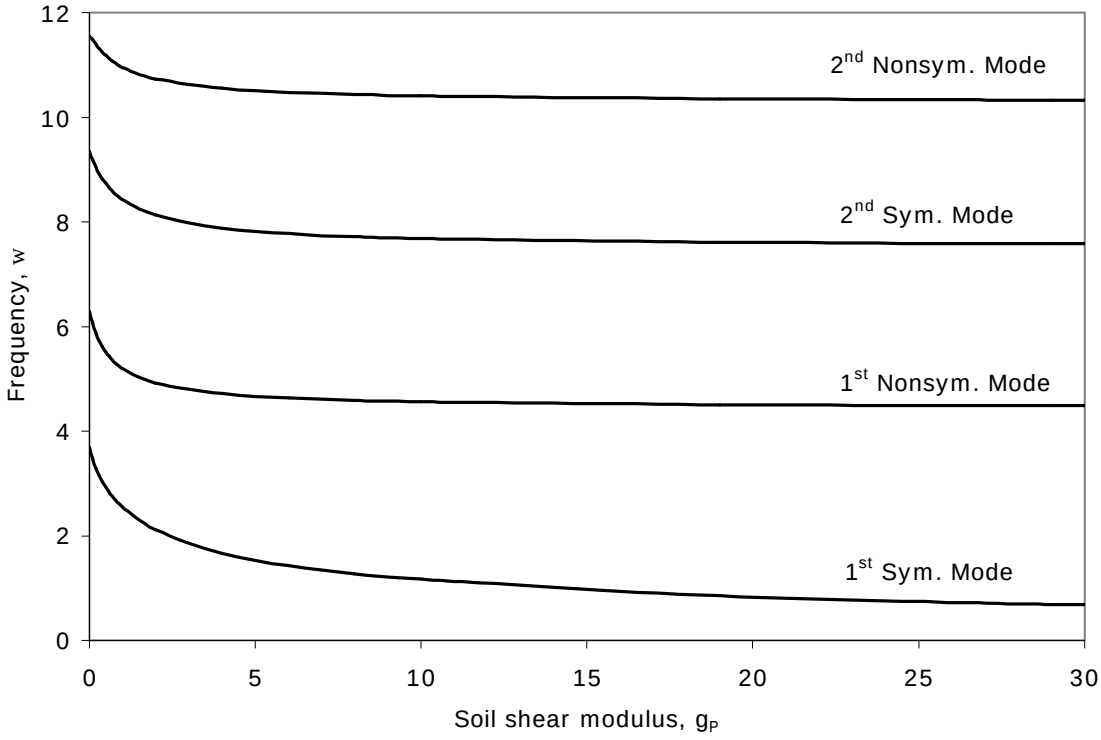

Figure 5.29 Frequency versus shear modulus when p = 3 and k = 200

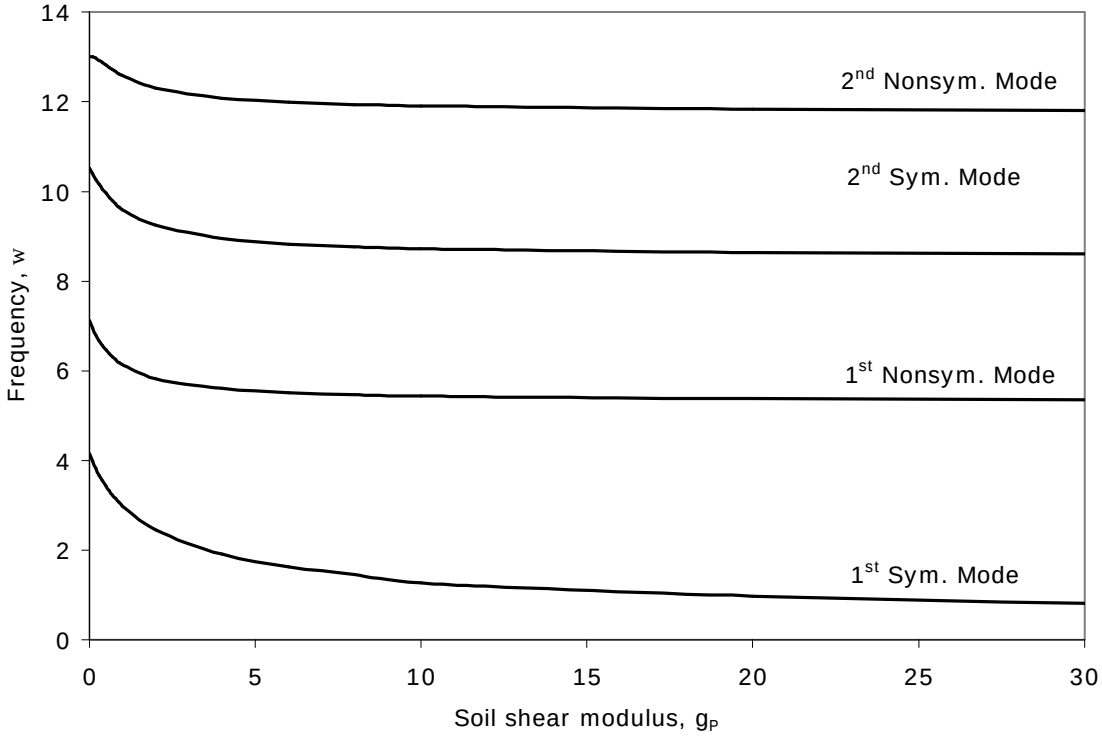

Figure 5.30 Frequency versus shear modulus when p = 4 and k = 200

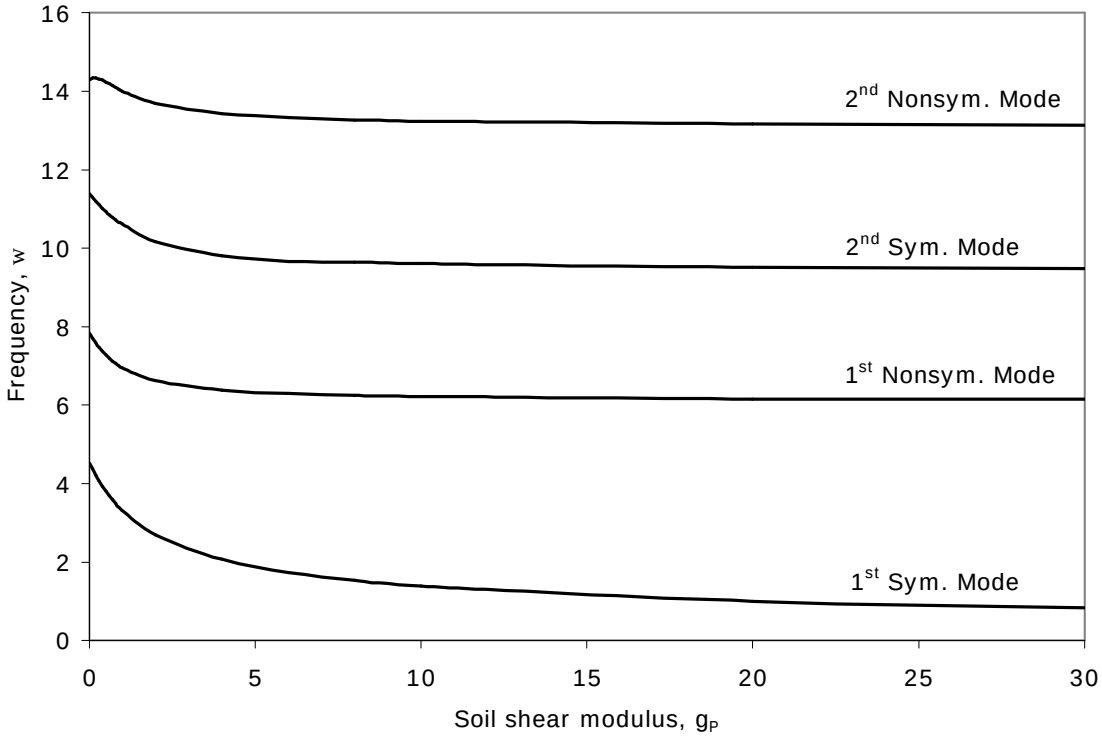

Figure 5.31 Frequency versus shear modulus when p = 5 and k = 200

5.12 Rigid, Winkler, and Pasternak Foundation Comparison

In this section, the results of the three types of foundations used to model an air-filled geosynthetic tube will be compared and discussed. Table 5.2 and Figure 5.32 display the results of the membrane tension at the origin, and Table 5.3 with Figure 5.33 present the results of the three types of foundations and their maximum membrane tension produced. Rigid and Pasternak foundation models display good agreement in both the membrane tension at the origin and the maximum tension.

For the Winkler foundation, a much larger soil stiffness coefficient would be needed to obtain equilibrium values close to both the rigid and Pasternak results. The dual parameter (k and g_P) foundation model of Pasternak develops equilibrium values close to those of the rigid foundation case when k = 200 and g_P = 30.

Internal Pressure	Membrane Tension at Origin, q_o		
p	Rigid	Winkler (k=200)	Pasternak (k=200, g_P=30)
2	0.092	0.107	0.094
3	0.225	0.253	0.228
4	0.370	0.411	0.373
5	0.520	0.572	0.523

Table 5.2 Membrane tension at origin comparison

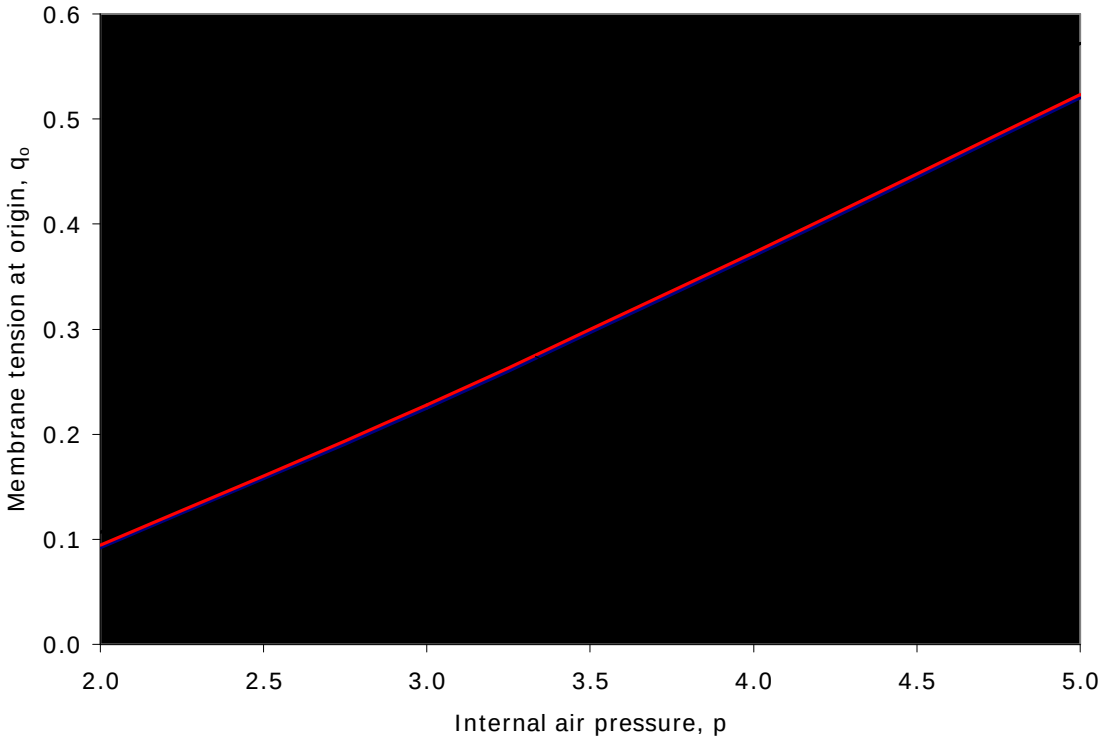

Figure 5.32 Membrane tension at origin comparison

Internal Pressure	Maximum Membrane Tension, q_{max}		
p	Rigid	Winkler (k=200)	Pasternak (k=200, g_P=30)
2	0.276	0.122	0.280
3	0.450	0.273	0.454
4	0.616	0.434	0.621
5	0.780	0.598	0.784

Table 5.3 Maximum membrane tension comparison

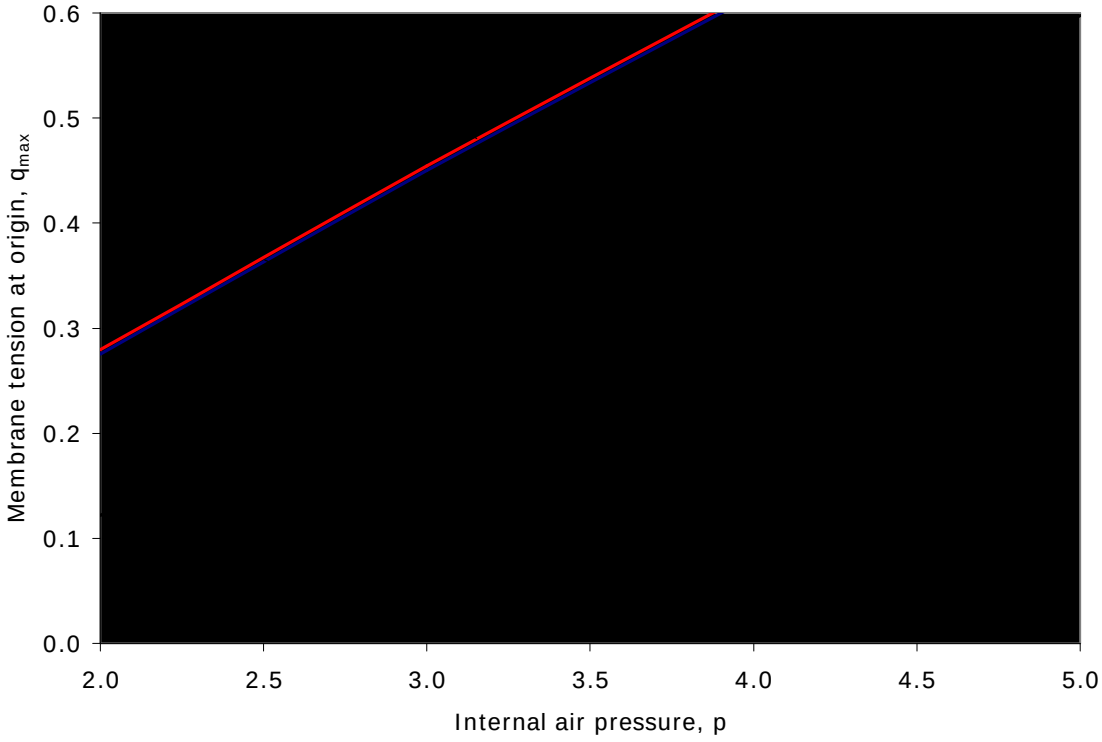

Figure 5.33 Maximum membrane tension comparison

Tables 5.4 through 5.7, along with Figures 5.34 to 5.37, present the frequencies of the three types of foundation models used. The fact that the rigid foundation results in a much higher set of frequencies than both the Winkler and Pasternak foundation models ensures that for a rigid case the tube oscillates more. In the physical world, the Pasternak foundation would be the model of choice when conducting analysis of a geosynthetic tube resting on a variable soil medium. This conclusion is a function of the surface on which the geotextile tube is placed.

	1st Symmetrical Mode		
Internal pressure, p	Rigid	Winkler (k=200)	Pasternak (k=200, g_P=30)
2	3.970	3.076	0.554
3	5.023	3.692	0.691
4	5.816	4.157	0.816
5	6.488	4.527	0.825

Table 5.4 1st Symmetric mode frequency comparison

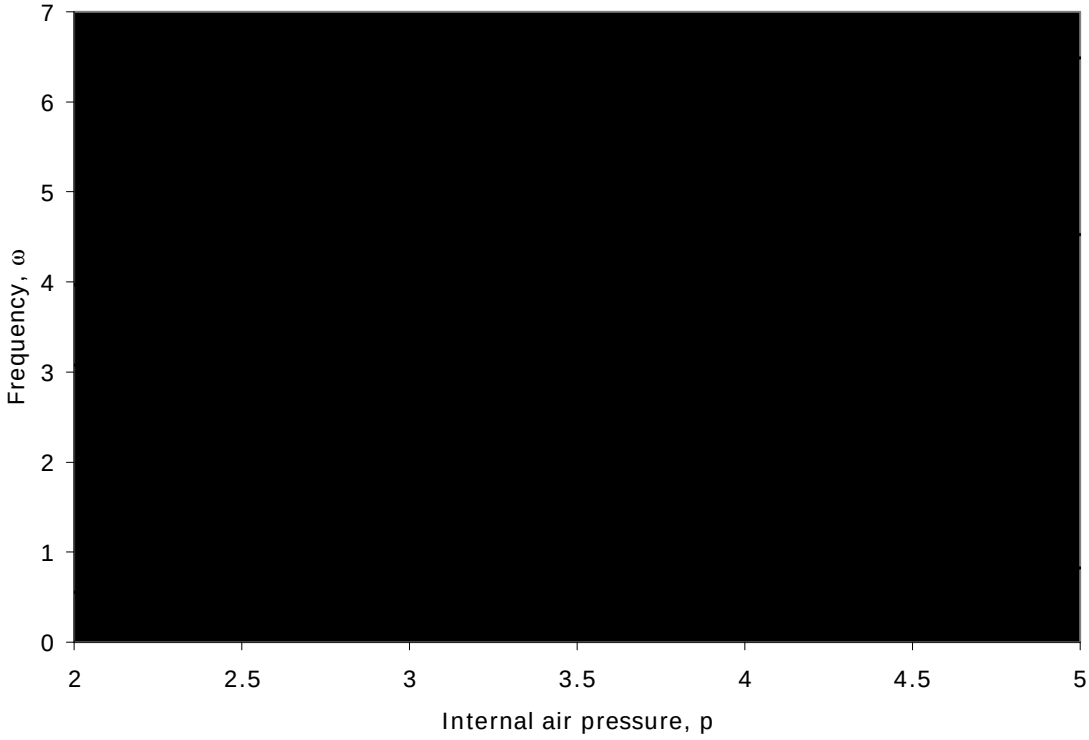

Figure 5.34 1st Symmetrical mode foundation comparison

	1st Nonsymmetrical Mode		
Internal pressure, p	Rigid	Winkler (k=200)	Pasternak (k=200, g_P=30)
2	6.690	5.238	3.445
3	8.370	6.297	4.483
4	9.630	7.119	5.358
5	10.700	7.827	6.143

Table 5.5 1st Nonsymmetric mode frequency summary

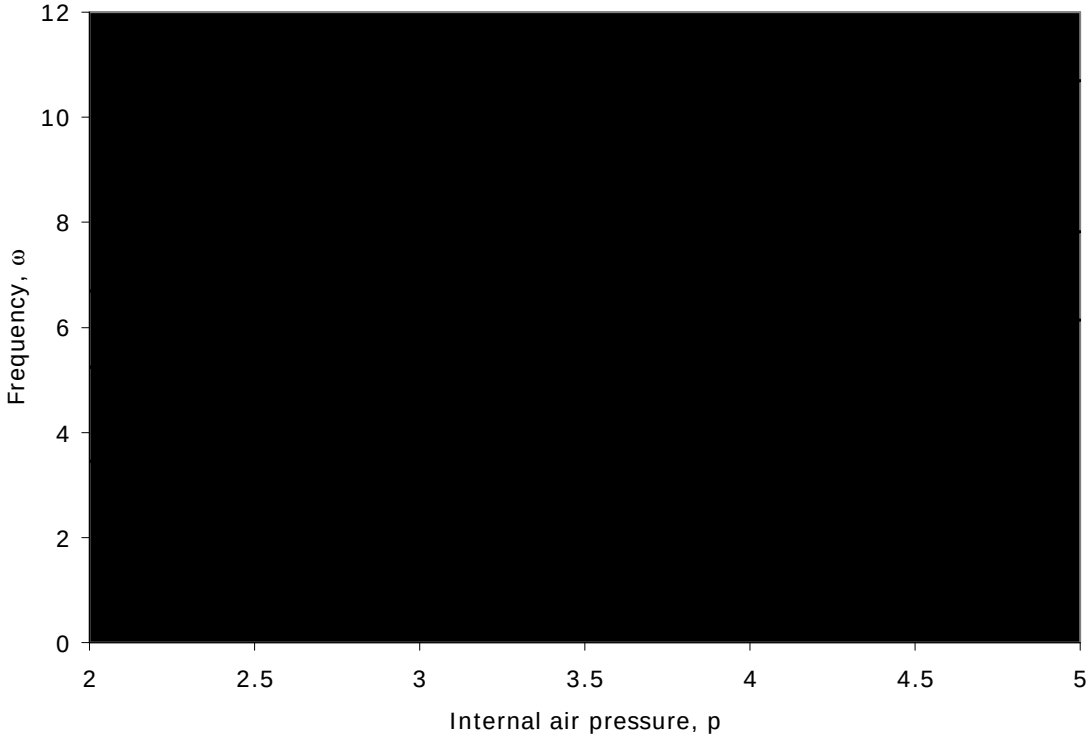

Figure 5.35 1st Nonsymmetrical mode foundation comparison

	2nd Symmetrical mode		
Internal pressure, p	Rigid	Winkler (k=200)	Pasternak (k=200, g_P=30)
2	9.241	7.708	6.265
3	11.439	9.344	7.580
4	13.100	10.511	8.607
5	14.511	11.387	9.477

Table 5.6 2nd Symmetric mode frequency summary

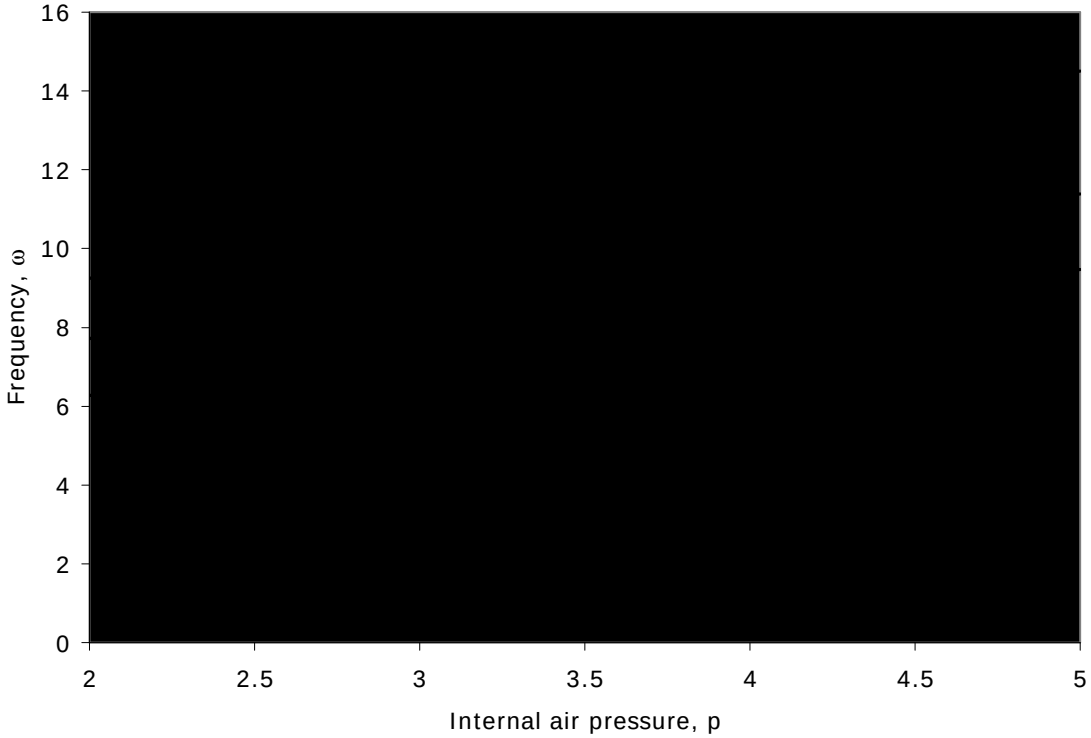

Figure 5.36 2nd Symmetrical mode foundation comparison

	2nd Nonsymmetrical mode		
Internal pressure, p	Rigid	Winkler (k=200)	Pasternak (k=200, g_P=30)
2	11.631	9.661	8.523
3	14.290	11.551	10.335
4	16.315	13.001	11.812
5	18.031	14.288	13.132

Table 5.7 2nd Nonsymmetric mode foundation frequency comparison

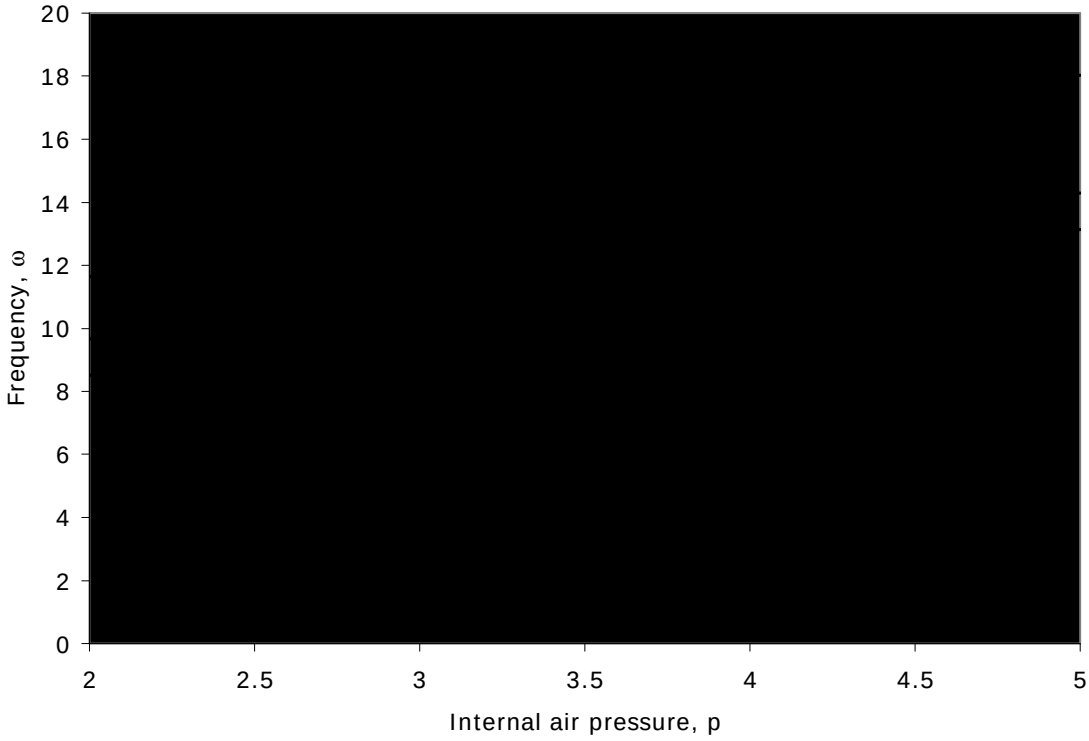

Figure 5.37 2nd Nonsymmetrical mode foundation comparison

Chapter 6: Summary and conclusions

Using Mathematica 4.2, two-dimensional freestanding models of both air and water-filled geosynthetic tubes were analyzed. In conjunction with these two internal materials, three supporting foundations were investigated: rigid, Winkler, and Pasternak. The primary difference between the Winkler and Pasternak foundation model is that the Pasternak model employs a shear resistance layer in order to distribute a load to surrounding vertical springs. General assumptions regarding the geotextile membrane include: modeling the membrane as an inextensible material along with neglecting both bending resistance and changes in cross-sectional area longitudinally. The internal water is modeled as a hydrostatic pressure. The internal air pressure is assumed to be constant within the tube's cross-sectional area. To facilitate the use of a two-dimensional analysis, the tube was assumed to be extremely long and straight.

Due to the structure's ease to form vibrating shapes with lower frequencies, the lowest four frequencies and corresponding mode shapes were computed. These four mode shapes are denoted First symmetrical, First nonsymmetrical, Second symmetrical, and Second nonsymmetrical. The primary goal of vibration analysis is to be able to predict the response, or motion, of a vibrating system (Inman 2001).

6.1 Summary of Rigid Foundation Procedure

Once the equilibrium program was executed (with respect to the designated internal pressure head or internal air pressure) and the results of contact length and initial membrane tension were calculated, vibrations about the equilibrium configuration may be introduced. Set values for the dynamic computations for both the internal water and air cases include: the internal pressure head or air pressure, contact length of tube/surface interface, and membrane tension at the origin. These equilibrium properties were used to solve for unknown parameters (for example, the dynamic tension parameter q_d as in the air-filled tube resting on a rigid foundation presented in Appendix B), the natural frequencies, and the mode shapes.

6.2 Summary of Winkler and Pasternak Foundation Procedure

The two deformable foundation scenarios for both air and water-filled tubes follow much the same procedure as in the rigid foundation case. The designated values for the Winkler foundation equilibrium are the internal pressure head or air pressure and the soil stiffness coefficient. The only additional parameter for the Pasternak foundation from the Winkler foundation equilibrium is the shear modulus. Equilibrium membrane properties are computed via the Mathematica files presented in Appendices E through H. Once known, these equilibrium values are incorporated in the dynamic program. The results of this dynamic program are the unknown parameters, the natural frequencies, and the mode shapes.

6.3 Conclusions

Consider the equilibrium results presented in Section 2.4. The largest value of tension occurs primarily at the highest internal pressure head. This translates into needing a more durable material that has enough tension capacity to withstand the expanding of the membrane that an increase in pressure head would cause. Though the water and air results are not directly comparable, this trend of increasing membrane tension as the internal pressure rises is maintained within each of the six cases considered: internal air and water tubes resting on rigid, Winkler, and Pasternak foundations.

The four frequencies and corresponding mode shapes are classified by the number of intersection points or nodes that are present between the equilibrium configuration and dynamic shape. Thus, the First symmetrical mode possesses two nodes, next the First nonsymmetrical mode has three nodes, the Second symmetrical mode has four nodes, and lastly, the Second symmetrical mode has five nodes. The frequencies will decrease or increase by adjusting the internal pressure head or internal air pressure, damping coefficient, added mass multiplier (where applicable), soil stiffness coefficient, and the shear modulus. Focusing on the deformable foundation models, the frequency tends to

increase as the soil stiffness increases, but decreases as the shear modulus increases. It stands to reason that a tube on a vertically stiffened soil (without the presence of transverse soil interaction) will tend to vibrate faster than on the same soil with the presence of transverse soil interaction (i.e., shear modulus).

Though the dimensional comparison of rigid foundation equilibrium and dynamic results of water and air did not correlate well regarding tension, tube settlement, and tube height above the supporting surface, the difference can be reasoned. Since the geosynthetic material is assumed to be inextensible, the demand for internal air pressure is only that of raising the weight of the tube material. In contrast, the water-filled case needs water to expand in all directions in order to fill the tube's cross-section in its entirety with water, and has relatively large downward components of pressure near the bottom of the tube. The problem also lies with the combination of neglecting the weight of the material in the water-filled case and assuming that the material is inextensible. Therefore, the air and water-filled results are incompatible and are two independent models.

With the addition of damping, the dynamic results for both the rigid foundation with air and with water shared the general trend of a curved downward transition to where the oscillation died out. Overall the general shapes for the four modes computed share both the number of nodes (intersection points with the equilibrium configuration) and dynamic shape, considering the tube settlement involved with the deformable foundations.

6.4 Suggestions for Further Research

This section recommends areas for further research in the field of geosynthetic dynamics. One aspect for further study would be to see an applied external load such as floodwater or debris, and how the dynamic response is affected. Regarding a simulation, it would be good to see a total model incorporating various foundation theories and combined mode shapes. A dimensional solution should be computed for comparison to physical experiments that would investigate equilibrium properties (membrane tension and geometry), dynamic response (geometry), and various soil parameters (soil stiffness and

shear modulus). A three-dimensional analysis, possibly using the finite element method, could produce useful results.

References

Aqua-Barriers (2002). Hydro-Solutions. Houston, TX. Web site: www.hydrologicalsolutions.com

Aqua Dam™ (2002). Water Structures Unlimited. Web site: www.waterstructures.com

Austin, T. (1995). "A second life for dredged material." *Civil Engineering*, ASCE, Vol. 65, No. 11, pp. 60-63

Bedford, A, and Fowler, W. (1999). Engineering Mechanics: Dynamics, 2nd ed. Addison-Wesley, Berkeley, CA.

Biggar, K., and Masala, S. (1998). Alternatives to Sandbags for Temporary Flood Protection, Alberta Transportation and Utilities, Disaster Services Branch and Emergency Preparedness Canada, Edmonton, Alberta.

Bogossian, F., Smith, R. T., Vertematti, J. C., and Yazbek, O. (1982). "Continuous retaining dikes by means of geotextiles." *Proceedings, 2nd International Conference on Geotextiles*, Las Vegas, NV, Vol. I, pp. 211-216.

de Bruin, P. , and Loos, C. (1995). "The use of Geotubes as an essential part of an 8.8 m high North Sea dike and embankment, Leybucht, Germany." *Geosynthetics World*, Vol. 5, No. 3, pp. 7-10.

Erchinger, H.F. (1993). "Geotextile tubes filled with sand for beach erosion control, North Sea Coast, Germany." *Geosynthetics Case Histories*, G. P. Raymond and J.-P. Giroud, eds., BiTech Publishers, Richmond, BC, Canada, 102-103.

Filz, G. M., Freeman, M., Moler, M., and Plaut, R. H. (2001). Pilot-Scale Tests of Stacked Three-Tube Configuration of Water-Filled Tubes for Resisting Floodwaters, Technical Report, Department of Civil and Environmental Engineering, Virginia Tech, Blacksburg, VA.

Firt, V. (1983). Statics, Formfinding and Dynamics of Air-Supported Membrane Structures, Martinus Nijhoff, The Hague.

FitzPatrick, B. T., Nevius, D. B., Filz, G. M., and Plaut, R. H. (2001). Pilot-Scale Tests of Water-Filled Tubes Resisting Floodwaters, Technical Report, Department of Civil and Environmental Engineering, Virginia Tech, Blacksburg, VA.

Freeman, M. (2002). Experiments and Analysis of Water-filled Tubes Used as

Temporary Flood Barriers, M. S. Thesis, Virginia Tech, Blacksburg, VA.

Gadd, P. E. (1988). "Sand bag slope protection: design, construction, and performance." *Arctic Coastal Processes and Slope Protection Design*, A.T. Chen and C. B. Leidersdorf, eds., ASCE, New York, pp. 145-165.

Geosynthetic Materials Association (2002) "Handbook of Geosynthetics." Web site: www.gmanow.com/pdf/GMAHandbook_v002.pdf

Glockner, P. G., and Szyszkowski, W. (1987). "On the statics of large-scale cylindrical floating membrane containers." *International Journal of Non-Linear Mechanics,* Vol. 22, pp. 275-282.

Gutman, A. L. (1979). "Low-cost shoreline protection in Massachusetts." *Coastal Structures '79*, Vol. 1, ASCE, New York, pp. 373-387.

Hsieh, J.-C., and Plaut, R. H. (1990). "Free vibrations of inflatable dams," *Acta Mechanica*, Vol. 85, pp. 207-220.

Hsieh, J.-C., Plaut, R. H., and Yucel. O. (1989). "Vibrations of an inextensible cylindrical membrane inflated with liquid," *Journal of Fluids and Structures*, Vol. 3, pp. 151-163.

Huong, T. C. (2001). Two-Dimensional Analysis of Water-Filled Geomembrane Tubes Used As Temporary Flood-Fighting Devices, M. S. Thesis, Virginia Tech, Blacksburg, VA.

Huong, T. C., Plaut, R. H., and Filz, G. M., (2001). "Wedged geomembrane tubes as temporary flood-fighting devices," *Thin-Walled Structures*, Vol. 40, pp. 913-923.

Inman, D. J. (2001). Engineering Vibration, 2nd ed. Prentice Hall, Englewood Cliffs, New Jersey.

Itasca Consulting Group (1998). Fast Lagrangian Analysis of Continua (FLAC), Minneapolis, MN. Web site: www.itascacg.com

Klusman, C. R. (1998). Two-Dimensional Analysis of Stacked Geosynthetic Tubes, M. S. Thesis, Virginia Tech, Blacksburg, VA.

Kim, M. (2003). Two-Dimensional Analysis of Different Types of Water-filled Geomembrane Tubes as Temporary Flood-Fighting Devices, Ph. D. Dissertation, Virginia Tech, Blacksburg, VA.

Koerner, R. M., and Welsh, J. P. (1980). "Fabric forms conform to any shape." *Concrete*

Construction, Vol. 25, pp. 401-409.

Landis, K. (2000). " Control floods with geotextile cofferdams," *Geotechnical Fabrics Report*, Vol. 18, No. 3, pp. 24-29.

Dakshina Moorthy, C. M., Reddy, J. N., and Plaut, R. H. (1995). "Three-dimensional vibrations of inflatable dams," *Thin-Walled Structures*, Vol. 21, pp. 291-306.

Munson, B. R., Okiishi, T. H., and Young, D. F. (1998) Fundamentals of Fluid Mechanics, 3rd ed. Wiley, New York.

Mysore, G. V., Liapis, S. I., and Plaut, R. H. (1997). "Vibration analysis of single-anchor inflatable dams," *Proceedings of the Fourth International Symposium on Fluid-Structure Interactions, Aeroelasticity, Flow-Induced Vibration and Noise*, ASME, New York, Vol. 2, pp. 119-124.

Mysore, G. V., Liapis, S. I., and Plaut, R. H. (1998). "Dynamic analysis of single-anchor inflatable dams," *Journal of Sound and Vibration*, Vol. 215, pp. 251-272.

NOAQ Flood Fighting System (2002). NOAQ Flood Protection AB. Näsviken, Sweden. Web site: www.noaq.com

Pilarczyk, K. W. (1995). " Geotextile systems for coastal protection – an overview." *Proceedings, 4th International Conference on Coastal and Port Engineering in Developing Countries*, Rio de Janeiro, Brazil.

Plaut, R. H., and Fagan, T. D. (1988). "Vibration of an inextensible, air-inflated, cylindrical membrane," *Journal of Applied Mechanics*, Vol. 55, pp. 672-675.

Plaut, R. H., and Klusman, C. R. (1999). "Two-dimensional analysis of stacked geosynthetic tubes on deformable foundations," *Thin-Walled Structures*, Vol. 34, pp. 179-194.

Plaut, R. H., Liapis, S. I., and Telionis, D. P. (1998). "When the levee inflates." *Civil Engineering*, ASCE, Vol. 68, No. 1, pp. 62-64.

Plaut, R. H., and Suherman, S. (1998). "Two-dimensional analysis of geosynthetic tubes," *Acta Mechanica*, Vol. 129, pp. 207-218.

Pramila, A. (1987). "Natural frequencies of a submerged axially moving band." *Journal of Sound and Vibration*, Vol. 113, pp. 198-203.

Scott, R. F. (1981). Foundation Analysis. Prentice-Hall, Englewood Cliffs, NJ.

Seay, P. A., and Plaut, R. H. (1998). "Three-dimensional behavior of geosynthetic

tubes." *Thin-Walled Structures*, Vol. 32, pp. 263-274.

Selvadurai, A.P.S. (1979). Elastic Analysis of Soil-Foundation Interaction. Elsevier, New York.

Superior Dams (2002). Superior Dam, LLC. Carlotta, CA. Web site: www.superiordam.com

Terzaghi, K., and LaCroix, Y. (1964). "Mission Dam: an Earth Dam on a Highly Compressible Foundation." *Geotechnique*. Vol. 14, pp. 14-50.

U.S. Flood Control Corporation (2001). *Flood Fighter Corp*. Floodfighter, Calgary, Alberta, Canada, 1-4. Web site: www.usfloodcontrol.com

van Santvoort, G. P. T. M. (1995). *Geosynthetics in Civil Engineering*. A. A. Balkema, Rotterdam.

Wauer, J., and Plaut, R. H. (1991). "Vibrations of an extensible, air-inflated, cylindrical membrane," *Zeitschrift für angewandte Mathematik und Mechanik*, Vol. 71, pp. 191-192.

Wolfram, S. (1996). The Mathematica Book, 3rd ed., Cambridge University Press, Cambridge, UK.

Wu, P.-H., and Plaut, R. H. (1996). "Analysis of the vibrations of inflatable dams under overflow conditions," *Thin-Walled Structures*, Vol. 26, pp. 241-259.

Appendix A:

A.1 Water-filled tube equilibrium resting on a rigid foundation

Mathematica code

```
(*Variables defined:
    h=internal pressure head
  b=contact length of tube supporting surface
   qe=initial membrane tension at origin
    xe=horizontal coordinate
     ye=vertical coordinate
      =intial angle measured from rigid surface to membrane*)

(*Clearing variables for solving a set of new cells*)
Clear[h, b, gb, qe, gqe, pi, y, y1, y2, y3];
(*where y1=xe, y2=ye, y3==e*)
h = 0.25;
(*guess values for contact length and membrane tension, respectively*)
gb = 0.2250435284842482;
gqe = 0.015187081041433357;
pi = N[];
(*Naming text of equilibrium properties*)
SAVE = "eFS.txt";
(*Naming the text file of xe and ye coordinates
   h = water equilibrium rigid foundation = coordinate*)
X = "0.2WERFXe.txt";
Y = "0.2WERFYe.txt";

(*Defining terms which were derived in Chapter 2 Section 2.3*)
de[b_, qe_] := {y1'[t] = 1 b Cos[y3[t]], y2'[t] = 1 b Sin[y3[t]],
  y3'[t] = 1 b (h y2[t])} qe

(*Defining initial boundary conditions*)
leftBC := {y1[0] = 0, y2[0] = 0, y3[0] = 0}

soln := NDSolve[Flatten[Append[de[b, qe], leftBC]], {y1, y2, y3}, {t, 0, 1},
  MaxSteps = 5000]

endpt[b_, qe_] :=
  {y1[t], y2[t], y3[t]} /.
    First[NDSolve[Flatten[Append[de[b, qe], leftBC]], {y1[t], y2[t], y3[t]},
      {t, 0, 1}, MaxSteps = 3000]] /. t = 1;

endpt[gb, gqe];

Clear[b, qe]
```

```
(*Define end point boundary conditions*)
rts := FindRoot[{endpt[b, qe][[2]] == 0, endpt[b, qe][[3]] == 2 pi},
  {b, {gb, 0.95 gb}}, {qe, {gqe, 0.95 gqe}}, AccuracyGoal -> 7, MaxIterations -> 70000]

endpt[b] /. rts, qe /. rts

$Aborted

(*Displaying results*)
b = b /. rts
qe = qe /. rts

0.225044

0.0151871

(*Solving out other variables in order to plot*)
{yy1[t_], yy2[t_], yy3[t_], yy4[t_]} = {y1[t], y2[t], y3[t], y4[t]} /. First[soln];

(*Maximum tube height*)
ymax = Evaluate[yy2[0.5]]

0.208153

J = Table[Evaluate[{yy1[t]} /. soln /. rts], {t, 0, 1, 1/300}];
K = Table[Evaluate[{yy2[t]} /. soln /. rts], {t, 0, 1, 1/300}];

(*Location of left and right vertical tangent*)
xmin = Min[J]
xmax = Max[J]

-0.365352

0.0645962

(*Calculating aspect ratio for air and water comparison*)
AR = (b - 2 xmax) / y

0.354236
-------
   y

(*Plotting xe and ye coordinates*)
G = ParametricPlot[Evaluate[{yy1[t], yy2[t]}] /. soln /. rts, {t, 0, 1},
   PlotRange -> All, AspectRatio -> Automatic, PlotPoints -> 100];
```

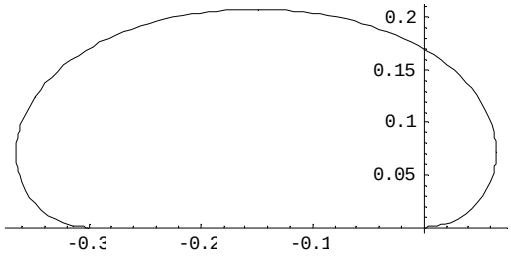

```
?Writing coordinate xe to a text file in order to plot more clearly
  in MS Excel?
xe = Table[Evaluate[{yy1[t]}] /. soln /. rts], {t, 0, 1, 1/300}];
tempt = OpenAppend[X, PageWidth = 30]
Write[tempt, xe, ffffffffffffffffffffffffffff ]
Close[tempt]
```

```
OutputStream[0.2WERFXe.txt, 15]
```

```
0.2WERFXe.txt
```

```
?Writing coordinate ye to a text file in order to plot more clearly
  in MS Excel?
ye = Table[Evaluate[{yy2[t]}] /. soln /. rts], {t, 0, 1, 1/300}];
tempt = OpenAppend[Y, PageWidth = 30]
Write[tempt, ye, ffffffffffffffffffffffffffff ]
Close[tempt]
```

```
OutputStream[0.2WERFYe.txt, 16]
```

```
0.2WERFYe.txt
```

```
?Writing to a text file to graph equilibrium properties?
PutAppend[h, b, qe, y, ash, ur, ui, a, beta, SAVE]
```

A.2 Symmetrical and nonsymmetrical vibration mode concept

Figures A.1 and A.2 represent the two different shifts of horizontal displacement when symmetrical and nonsymmetrical vibrations are considered. The equilibrium configuration is distinguished by a red line, and the black line represents the dynamic shape; u is the horizontal displacement, and b is the contact length of the geosynthetic tube with the supporting surface. Symmetrical modes are considered to expand outward at the foundation. This results in a scaled arc length of $t ? \frac{s}{1 ? b ? 2u}$. In the Mathematica files presented within, the derivative of the scaled arc length is used. This yields

$$\frac{d}{dt} ? (1 ? b ? 2u)\frac{d}{ds} \qquad \text{(A.1)}$$

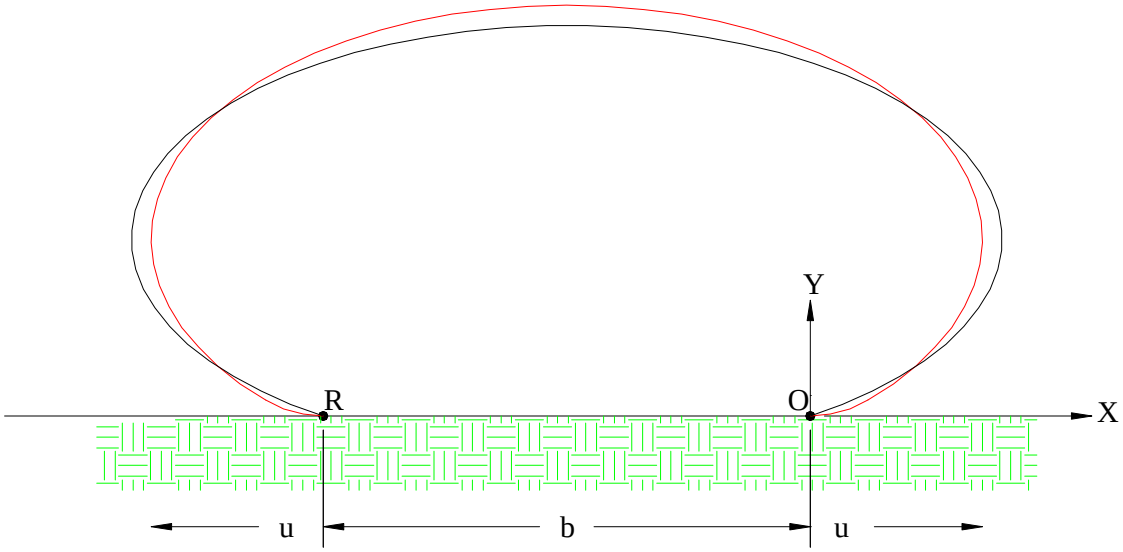

Symmetrical Mode

Figure A.1 Symmetrical mode example

The horizontal displacement of a nonsymmetrical mode is considered to shift to the right at O. This results in a scaled arc length of $t ? \frac{s}{1 ? b}$ and in the Mathematica files below differentiates into

$$\frac{d}{dt} ? (1 ? b)\frac{d}{ds} \tag{A.2}$$

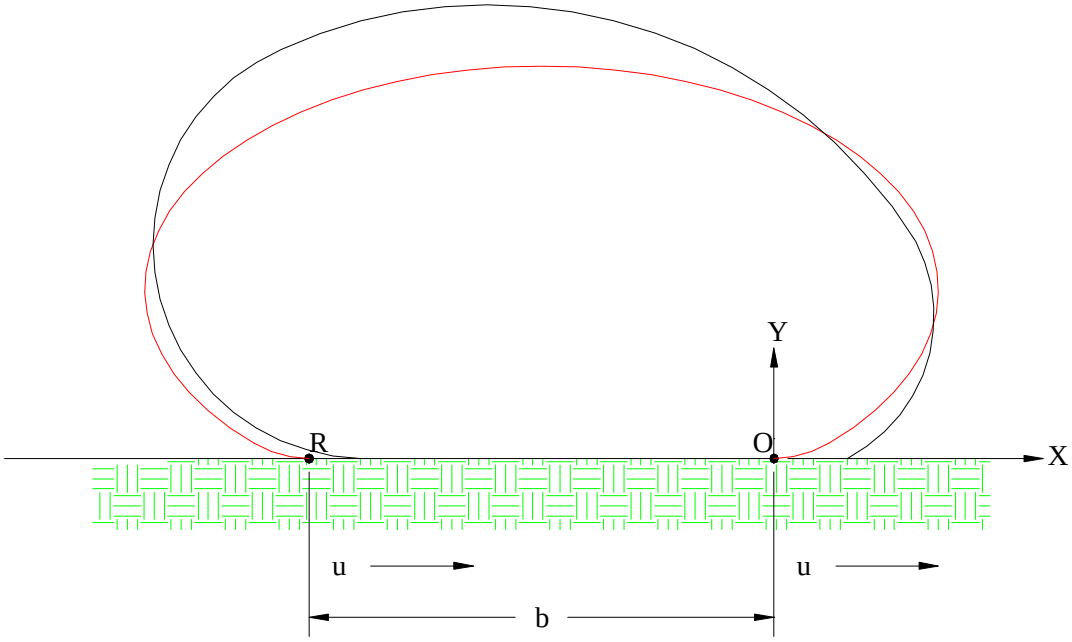

Figure A.2 Nonsymmetrical mode example

A.3 Symmetrical vibrations about equilibrium of a water-filled tube resting on a rigid foundation with damping and added mass

Mathematica code

```
}?Defining Variable:
    h?internal pressure head
   b?contact length between tube membrane and supporting surface
    qe?initial membrane tension at origin
     w?frequency of vibrations about equilibrium shape
       u?tangential displacement
        v?normal displacement
         a?added mass coefficient
          beta???damping coefficient
            i?imaginery number
             c?multiplier to visually vary the dynamic shape about the
              equilibrium shape
              t?scaled arc length?}
```

```
(*Clearing variables for solving a set of new cells*)
Clear[c, h, b, qe, gw, gu, y1, y2, y3, y4, y5, y6, y7, yy1, yy2, yy3, yy4, yy5,
  yy6, yy7, t, u, w];
(*where y1=ud, y2=vd, y3=d, y4=qd, y5=ye, y6=e*)
(*Defining the constant pi*)
pi = N[Pi];
(*Specifying internal pressure head*)
h = 0.4;
(*Equilibrium values (b and qe) obtained from WaterEquilibrium.nb*)
b = 0.185436;
qe = 0.0340458;
(*Guessing frequency and tangential displacement*)
gw = 0.724966002;
gu = 0.00004659377919036581;
(*Setting added mass coefficient*)
a = 0;
(*Setting damping coefficient*)
beta = 3;
(*Defining imaginery number*)
i = (1)^0.5;
(*Setting arbitrary amplitude multiplier*)
c = 500;
(*Naming output text file*)
SAVE = "FSvib(h=0.4,a=0,beta=vary)2.txt";

(*Defining terms with equations taken from the derivation described in
  Chapter 2 Section 2.5*)
de[y1_, y2_, y3_, y4_, y5_, y6_, w_, u_] :=
 {y1'[t] == ((h - y5[t]) - y2[t]) qe - (1 - b - 2 u),
  y2'[t] == y3[t] - (h - y5[t]) - y1[t]) qe - (1 - b - 2 u),
  y3'[t] ==
   (1 - qe - (y4[t] - (h - y5[t])) qe - (1 - a) w^2 - i beta w) - y2[t] -
     y1[t] Sin[y6[t]] - y2[t] Cos[y6[t]]) - (1 - b - 2 u),
  y4'[t] == (w^2 - i beta w) - y1[t]) - (1 - b - 2 u), y5'[t] == Sin[y6[t]]) - (1 - b),
  y6'[t] == ((h - y5[t])) qe - (1 - b), y7'[t] == Cos[y6[t]]) - (1 - b)}

(*Defining initial boundary conditions*)
leftBC[u_] := {y1[0] == u, y2[0] == 0, y3[0] == 0, y4[0] == 0.00001, y5[0] == 0,
  y6[0] == 0, y7[0] == 0}

(*Numerically solving the defined derivatives above*)
soln := NDSolve[Flatten[Append[de[y1, y2, y3, y4, y5, y6, w, u], leftBC[u]]],
  {y1, y2, y3, y4, y5, y6, y7}, {t, 0, 1}, MaxSteps == 20000]

(*Applying the end point boundary conditions*)
endpt[w_, u_] :=
  {y1[t], y2[t], y3[t], y4[t], y5[t], y6[t], y7[t]} /.
    First[NDSolve[Flatten[Append[de[y1, y2, y3, y4, y5, y6, w, u], leftBC[u]]],
      {y1[t], y2[t], y3[t], y4[t], y5[t], y6[t], y7[t]}, {t, 0, 1}, MaxSteps == 3000]] /.
   t == 1;
```

```
(*Displaying end point values solved above before iterations*)
endpt[gw, gu]
```

```
{0.000708549 0.000118187, 0.000994457 0.000196171, 0.0120609 0.00838289,
 0.000255178 0.0000102011, 1.96252 10^6, 6.2832, 0.185434}
```

```
Clear[w, u]
```

```
(*Defining end point boundary conditions: {{5}}*y5 condition,
 setting the percent to change guess values in order to iterate,
 setting the accuracy goal of 7, setting number of iterations*)
rts := FindRoot[{endpt[w, u][[2]] == 0, endpt[w, u][[3]] == 0}, {w, {gw, 0.95 gw}},
  {u, {gu, 0.95 gu}}, AccuracyGoal -> 7, MaxIterations -> 70000]
```

```
(*Displaying end point values solved above after iterations*)
endpt[w /. rts, u /. rts]
```

```
{0.0000466171 7.78468 10^-10,
 1.14451 10^-10 4.98715 10^-10, 2.34103 10^-9 1.01694 10^-8,
 0.0000100054 2.91748 10^-10, 1.96252 10^6, 6.2832, 0.185434}
```

```
(*Displaying results of above shooting method*)
w = w /. rts
u = u /. rts
```

```
0.485349 1.5
```

```
0.0000465919 5.87345 10^-12
```

```
(*Separating real from imaginery values*)
wr = Re[w];
wi = Im[w];
ur = Re[u];
ui = Im[u];
```

```
(*Solving terms in order to plot*)
{yy1[t_], yy2[t_], yy5[t_], yy6[t_], yy7[t_]} =
  {y1[t], y2[t], y5[t], y6[t], y7[t]} /. First[soln];
F = ParametricPlot[Evaluate[{Re[yy7[t]], Re[yy5[t]]} /. soln /. rts], {t, 0, 1},
   PlotRange -> All, AspectRatio -> Automatic, PlotPoints -> 1000];
G = ParametricPlot[
   Evaluate[
    {Re[yy7[t]] + c (yy1[t] Cos[yy6[t]] + yy2[t] Sin[yy6[t]]),
     Re[yy5[t]] + c (yy1[t] Sin[yy6[t]] + yy2[t] Cos[yy6[t]])} /. soln /. rts],
   {t, 0, 1}, PlotRange -> All, AspectRatio -> Automatic, PlotPoints -> 1000];
(*Plotting both equilibrium shape H and dynamic shape G*)
H = Show[F, G];
```

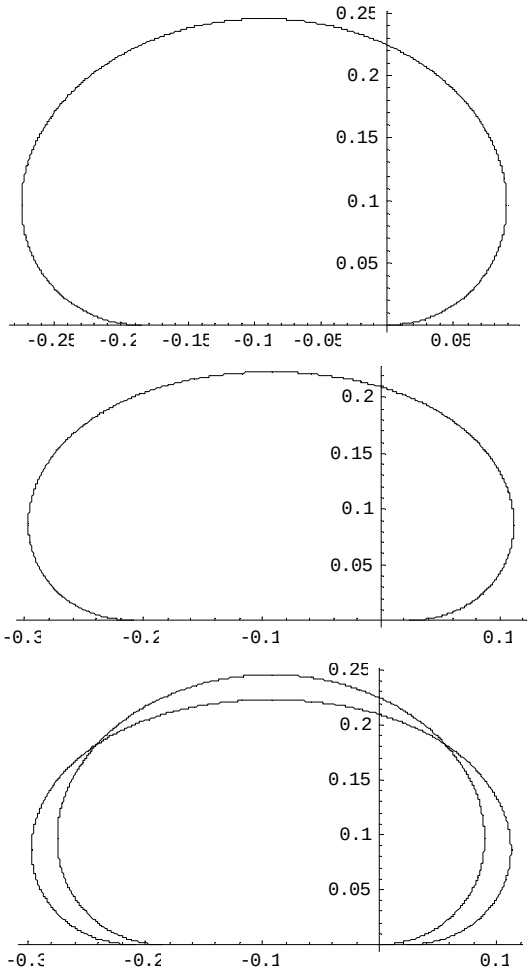


```
{?writing to a text file in order to graph relationships?}
PutAppend{h, b, qe, wr, wi, ur, ui, a, beta, SAVE}
```

A.4 Nonsymmetrical vibrations about equilibrium of a water-filled tube resting on a rigid foundation with damping and added mass

Mathematica code

```
(*Defining nondimensional variables:
    h=internal pressure head
   b=contact length between tube membrane and supporting surface
    qe=initial equilibrium membrane tension at origin
    w=frequency of vibrations about equilibrium shape
       u=tangential displacement
        v=normal displacement
         a=added mass coefficient
          beta===damping coefficient
            i=imagery number
             qd=initial dynamic membrane tension at origin
              c=multiplier to visually vary the dynamic shape about the equilibrium
               shape
               t=scaled arc length=*)

(*Clearing variables for solving a set of new cells=*)
Clear[c, h, b, qe, gw, gu, y1, y2, y3, y4, y5, y6, y7, yy1, yy2, yy3, yy4, yy5, yy6, yy7, t, u, w];
(*where y1=ud, y2=vd, y3==d, y4=qd, y5=ye, y6==e=*)
(*Defining the constant ==*)
pi = N[=];
(*Specifying internal pressure head=*)
h = 0.2;
(*Equilibrium values [b and qe] obtained from WaterEquilibrium.nb=*)
b = 0.30571680499906023;
qe = 0.009857747508667608;
(*Guessing frequency and tangential displacement=*)
gw = 0.981539381298068;
gu = 0.00007898061514531715;
(*Setting added mass coefficient=*)
a = 0;
(*Setting damping coefficient=*)
beta = 3.25775;
(*Defining imagery number=*)
i = (=1)^0.5;
(*Setting arbitrary amplitude multiplier=*)
c = 250;
(*Naming output text file=*)
SAVE = "FSvib[h=0.2,a=0,beta=vary]3.txt";

(*Defining terms with equations taken from the derivation described in Chapter 2,
 Section 2.5=*)
de[y1_, y2_, y3_, y4_, y5_, y6_, w_, u_] :=
 {y1'[t] == ((h - y5[t]) - y2[t])/qe - 1 - b, y2'[t] == y3[t] - (h - y5[t]) - y1[t])/qe - 1 - b,
  y3'[t] ==
   (1/qe - (y4[t] - (h - y5[t]))/qe - 1 - a) - w^2 - i - beta - w - y2[t] - y1[t] - Sin[y6[t]] -
     y2[t] - Cos[y6[t]])/(1 - b), y4'[t] == -w^2 - i - beta - w - y1[t] - 1 - b - 2 - u,
  y5'[t] == Sin[y6[t]]/(1 - b), y6'[t] == ((h - y5[t])/qe - 1 - b), y7'[t] == Cos[y6[t]]/(1 - b)}

(*Defining initial boundary conditions=*)
leftBC[u_] := {y1[0] == u, y2[0] == 0, y3[0] == 0, y4[0] == 0.00001, y5[0] == 0, y6[0] == 0, y7[0] == 0}
```

```
(*Numerically solving the defined derivatives above*)
soln := NDSolve[Flatten[Append[de[y1, y2, y3, y4, y5, y6, w, u], leftBC[u]]],
  {y1, y2, y3, y4, y5, y6, y7}, {t, 0, 1}, MaxSteps → 20000]

(*Applying the end point boundary conditions*)
endpt[w_, u_] :=
  {y1[t], y2[t], y3[t], y4[t], y5[t], y6[t], y7[t]} /.
    First[NDSolve[Flatten[Append[de[y1, y2, y3, y4, y5, y6, w, u], leftBC[u]]],
      {y1[t], y2[t], y3[t], y4[t], y5[t], y6[t], y7[t]}, {t, 0, 1}, MaxSteps → 3000]] /. t → 1;

(*Displaying end point values solved above before iterations*)
endpt[gw, gu]
```

```
{0.0168156 - 0.0428224 I, 0.0152877 - 0.0310114 I, -0.847767 - 0.492654 I,
 0.0139857 - 0.000481806 I, -4.61801 * 10^-7, 6.28322, -0.305713}
```

```
Clear[w, u]

(*Defining end point boundary conditions: {{5}} y5 condition,
 setting the percent to change guess values in order to iterate,
 setting the accuracy goal of 7, setting number of iterations*)
rts := FindRoot[{endpt[w, u][[2]] == 0, endpt[w, u][[3]] == 0}, {w, {gw, 0.95 gw}},
  {u, {gu, 0.95 gu}}, AccuracyGoal → 7, MaxIterations → 7000]

(*Displaying end point values solved above after iterations*)
endpt[w /. rts, u /. rts]
```

```
{0.0000791377 - 1.00488 * 10^-9 I,
 -9.11579 * 10^-11 - 4.89263 * 10^-10 I, -4.70809 * 10^-9 - 2.52779 * 10^-8 I,
 -0.0000100205 - 2.59426 * 10^-10 I, -2.6747 * 10^-6, 6.28318, -0.305717}
```

```
(*Displaying results of above shooting method*)
w → w /. rts
u → u /. rts
```

```
0.013625 - 1.62884 I
```

```
0.000078991 - 8.18876 * 10^-15 I
```

```
(*Separating real from imagery values*)
wr → Re[w];
wi → Im[w];
ur → Re[u];
ui → Im[u];
```

```
(*Solving terms in order to plot*)
{{yy1[t_], yy2[t_], yy5[t_], yy6[t_], yy7[t_]} =
  {y1[t], y2[t], y5[t], y6[t], y7[t]} /. First[soln];
F = ParametricPlot[Evaluate[{Re[yy7[t]], Re[yy5[t]]} /. soln /. rts], {t, 0, 1},
   PlotRange -> All, AspectRatio -> Automatic, PlotPoints -> 1000];
G =
  ParametricPlot[
   Evaluate[
    {Re[yy7[t] * c * {yy1[t] * Cos[yy6[t]] * yy2[t] * Sin[yy6[t]]]],
     Re[yy5[t] * c * {yy1[t] * Sin[yy6[t]] * yy2[t] * Cos[yy6[t]]}]} /. soln /. rts],
   {t, 0, 1}, PlotRange -> All, AspectRatio -> Automatic, PlotPoints -> 1000];
(*Plotting both equilibrium shape H and dynamic shape G*)
H = Show[F, G];
```

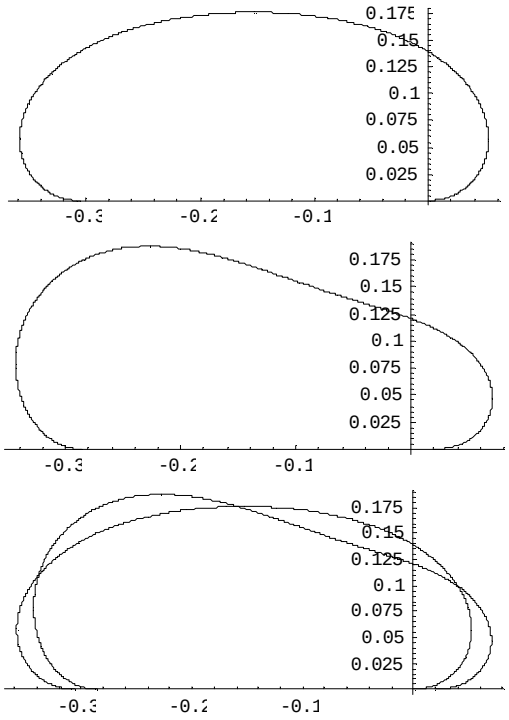


```
(*writing to a text file in order to graph relationships*)
PutAppend[h, b, qe, wr, wi, ur, ui, a, beta, SAVE]
```

Appendix B:

B.1 Equilibrium of an air-filled tube resting on a rigid foundation

Mathematica code

```
(*Variables defined:
    p=internal air pressure
   b=contact length of tube supporting surface
    qo=initial equilibrium membrane tension (located at origin)
     xe=horizontal coordinate
      ye=vertical coordinate
       theta_e=initial equilibrium angle measured from rigid surface to
          membrane
          t=scaled arc length*)

(*Clearing variables for solving a set of new cells*)
Clear[p, b, gb, qo, gqo, pi, y, y1, y2, y3];
(*where y1=xe, y2=ye, y3=e*)
(*Defining the constant *)
pi = N[];
(*Specifying internal air pressure*)
p = 2;
(*Guessing tube surface contact length and initial equilibrium membrane tension*)
gb = 1 / (1 + p);
gqo = 0.0918887197743147;
(*Naming output text file to contain dynamic properties*)
SAVE = "AirEq.txt";

(*Defining terms with equations taken from the derivation described in Chapter 3,
 Section 3.3*)
de[y2_, y3_, b_, qo_] := {y1'[t] == (1 + b) Cos[y3[t]], y2'[t] == (1 + b) Sin[y3[t]],
  y3'[t] == (1 + b) (p Cos[y3[t]] - y2[t] + qo)}

(*Defining initial boundary conditions*)
leftBC := {y1[0] == 0, y2[0] == 0, y3[0] == 0}

(*Numerically solving the defined derivatives above*)
soln := NDSolve[Flatten[Append[de[y2, y3, b, qo], leftBC]], {y1, y2, y3}, {t, 0, 1},
  MaxSteps -> 5000]

(*Applying the end point boundary conditions*)
endpt[b_, qo_] :=
  {y1[t], y2[t], y3[t]} /.
    First[NDSolve[Flatten[Append[de[y2, y3, b, qo], leftBC]], {y1[t], y2[t], y3[t]},
      {t, 0, 1}, MaxSteps -> 4000]] /. t -> 1;
```

```
{?end point values solved above before interations?}
endpt[gb, gqo];

Clear[b, qo]

{?Defining end point boundary conditions: {{3}}?y3 condition,
 setting the percent to change guess values in order to interate,
 setting the accuracy goal of 7, setting number of iterations?}
rts :? FindRoot[{endpt[b, qo][[1]] ? ?b, endpt[b, qo][[3]] ? 2? pi}, {b, {gb, 0.95? gb}},
  {qo, {gqo, 0.95? gqo}}, AccuracyGoal ? 7, MaxIterations ? 3000]

{?Displaying end point values solved above after interations?}
endpt[b]. rts, qo]. rts]

{?0.333331, 1.36019? 10^-6, 6.28319}

{?Displaying results of above shooting method?}
b? b]. rts
qo? qo]. rts

0.333331

0.0918887

{?Solving terms in order to plot?}
{{yy1[t_], yy2[t_], yy3[t_], yy4[t_]} ? {y1[t], y2[t], y3[t], y4[t]}}. First[soln];

{?Maximum tube height measured from origin?}
y? Evaluate[yy2[0.5]]

0.183777

{?Plotting equilibrium shape?}
G? ParametricPlot[Evaluate[{yy1[t], yy2[t]}]. soln]. rts], {t, 0, 1},
   PlotRange ? All, AspectRatio ? Automatic, PlotPoints ? 100];
```

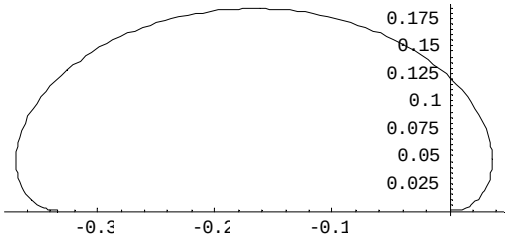


```
{?Writing new results to the SAVE text file to open later in MS Excel in order
  to graph relationships?}
PutAppend[p, b, qo, y, x, 0, 0, 0, 0, SAVE]
```

B.2 Symmetrical vibrations about equilibrium of an air-filled tube resting on a rigid foundation with damping

Mathematica code

```
{?Variables defined:
    p?internal air pressure
   b?contact length of tube supporting surface
    qo?initial equilibrium membrane tension {located at origin}
     xe?horizontal coordinate
      ye?vertical coordinate
       theta_e??e?intial equilibrium angle measured from rigid surface to membrane
         theta_d??d?initial dynamic angle measured form the rigid surface
            to membrane
           qd?initial dynamic membrane tension {located at origin}
             w?frequency of vibrations about equilibrium shape
              u?tangential displacement
               beta???damping coefficient
                 c?multiplier to visually vary the dynamic shape about the
                  equilibrium shape
                  t?scaled arc length?}

{?Clearing variables for solving a set of new cells?}
Clear{c, h, b, qe, qd, gw, gqd, y1, y2, y3, y4, y5, y6, y7, yy1, yy2, yy3, yy4,
  yy5, yy6, yy7, t, u, w};
```

```
(*where y1=xe, y2=ye, y3=theta_e, y4=xd, y5=yd, y6=theta_d, y7=qd*)
(*Defining the constant pi*)
pi = N[Pi];
(*Setting the tangential displacement*)
u = 0.0001;
(*Specifying internal air pressure*)
p = 2.85;
(*Equilibrium values {b and qo} obtained from AirEquilibrium.nb*)
b = 1}}p = 1};
qo = 0.204100534959496;
(*Guessing frequency and initial dynamic membrane tension*)
gw = 4.86229777606933;
gqd = 0.0005;
(*Setting damping coefficient*)
beta = 1;
(*Defining imaginery number*)
i = (-1)^0.5;
(*Setting arbitrary amplitude multiplier*)
c = 500;
(*Naming output text file to contain dynamic properties*)
SAVE = "2.85AirVibDampNonsym2.txt";
(*Naming output directory*)
DIR = "2.85AirVibDampNonsym2";
(*Naming output text files to contain coordinate information*)
COORx = "x.txt";
COORy = "y.txt";
COORxd = "xd.txt";
COORyd = "yd.txt";

(*Resetting the directory in order to start at the top of the driectory chain*)
ResetDirectory[];
(*Creating the directory DIR*)
CreateDirectory[DIR];
(*Setting the directory to DIR where files will finally be placed*)
SetDirectory[DIR];

(*Defining terms with equations taken from the derivation described in Chapter 3,
  Section 3.5*)
de[y2_, y3_, y4_, y5_, y6_, y7_, w_] :=
 {y1'[t] == (1 - b) Cos[y3[t]], y2'[t] == (1 - b) Sin[y3[t]],
  y3'[t] == (1 - b) (p Cos[y3[t]]) - y2[t] qo,
  y4'[t] == -(1 - b - 2 u) y6[t] Sin[y3[t]], y5'[t] == (1 - b - 2 u) y6[t] Cos[y3[t]],
  y6'[t] ==
   (1 - b - 2 u) (
    y7[t] (p Cos[y3[t]] - y2[t] qo) - y6[t] Sin[y3[t]] -
     w^2 (y4[t] Sin[y3[t]] - y5[t] Cos[y3[t]] - y2[t] qo),
  y7'[t] ==
   (1 - b - 2 u) (y6[t] Cos[y3[t]] - w^2 (y4[t] Cos[y3[t]] - y5[t] Sin[y3[t]]))}
```

```
(*Defining initial boundary conditions*)
leftBC[qd_] := {y1[0] == 0, y2[0] == 0, y3[0] == 0, y4[0] == u, y5[0] == 0, y6[0] == 0,
  y7[0] == qd}

(*Numerically solving the defined derivatives above*)
soln := NDSolve[Flatten[Append[de[y2, y3, y4, y5, y6, y7, w], leftBC[qd]]],
  {y1, y2, y3, y4, y5, y6, y7}, {t, 0, 1}, MaxSteps == 20000]

(*Applying the end point boundary conditions*)
endpt[w_, qd_] :=
  {y1[t], y2[t], y3[t], y4[t], y5[t], y6[t], y7[t]} /.
    First[NDSolve[Flatten[Append[de[y2, y3, y4, y5, y6, y7, w], leftBC[qd]]],
      {y1[t], y2[t], y3[t], y4[t], y5[t], y6[t], y7[t]}, {t, 0, 1}, MaxSteps == 4000]] /.
   t == 1;

(*Displaying end point values solved above before iterations*)
endpt[gw, gqd]

{0.333333, 1.3602 10^-6, 6.28311,
 -0.000333902, -1.97852 10^-6, -0.000229732, 0.000109439}

Clear[w, qd]

(*Defining end point boundary conditions: [[5]]==y5 condition,
 setting the percent to change guess values in order to iterate,
 setting the accuracy goal of 6, setting number of iterations*)
rts := FindRoot[{endpt[w, qd][[5]] == 0, endpt[w, qd][[6]] == 0}, {w, {gw, 0.98 gw}},
  {qd, {gqd, 0.98 gqd}}, AccuracyGoal == 6, MaxIterations == 7000]

(*Displaying end point values solved above after iterations*)
endpt[w /. rts, qd /. rts]

{0.333333, 1.3602 10^-6, 6.28311,
 -0.000326993, 3.53504 10^-8, 4.88026 10^-7, 0.0000990316}

(*Displaying results of above shooting method*)
w == w /. rts
qd == qd /. rts

3.96469

0.0000990226

(*Separating real from imaginery values*)
wr == Re[w];
wi == Im[w];
qdr == Re[u];
qdi == Im[u];
```

```
(*Solving terms in order to plot*)
{yy1[t_], yy2[t_], yy3[t_], yy4[t_], yy5[t_], yy6[t_], yy7[t_]} =
  {y1[t], y2[t], y3[t], y4[t], y5[t], y6[t], y7[t]} /. First[soln];
F = ParametricPlot[Evaluate[{yy1[t], yy2[t]} /. soln /. rts], {t, 0, 1},
   PlotRange -> All, AspectRatio -> Automatic, PlotPoints -> 1000];
G = ParametricPlot[Evaluate[{yy1[t] + c * yy4[t], yy2[t] + c * yy5[t]} /. soln /. rts],
   {t, 0, 1}, PlotRange -> All, AspectRatio -> Automatic, PlotPoints -> 1000];
(*Plotting both equilibrium shape F and dynamic shape G*)
H = Show[F, G];
```

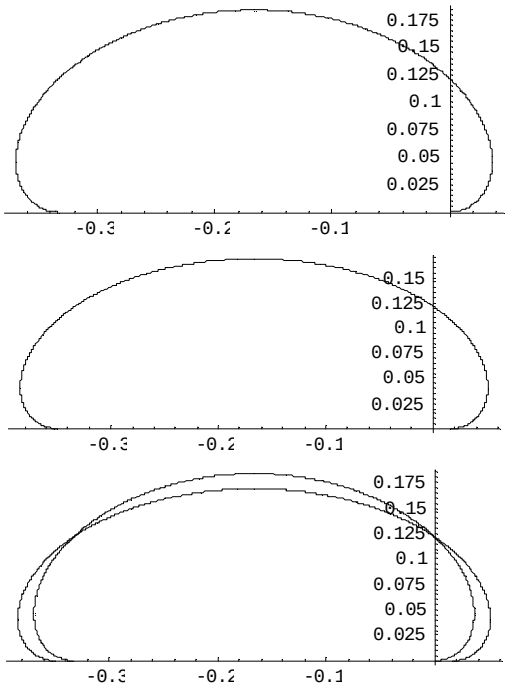

```
?Tabulating equilibrium x coordinate values in order to display shapes in Excel?
xe ? Table[Evaluate[{Re[yy1[t]]} /. soln /. rts], {t, 0, 1, 1/300}];
?Tabulating equilibrium y coordinate values in order to display shapes in Excel?
ye ? Table[Evaluate[{Re[yy2[t]]} /. soln /. rts], {t, 0, 1, 1/300}];
?Tabulating dynamic x coordinate values in order to display shapes in Excel?
xd ? Table[Evaluate[{Re[yy1[t]] ? c ? Re[yy4[t]]} /. soln /. rts], {t, 0, 1, 1/300}];
?Tabulating dynamic y coordinate values in order to display shapes in Excel?
yd ? Table[Evaluate[{Re[yy2[t]] ? c ? Re[yy5[t]]} /. soln /. rts], {t, 0, 1, 1/300}];
?Creating and opening COORx text file, Writing to COORx text file,
 Closing COORx text file?
tempt ? OpenAppend[COORx, PageWidth ? 30]
Write[tempt, xe, ffffffffffffffffffffffffffff ]
Close[tempt]
tempt ? OpenAppend[COORy, PageWidth ? 30]
Write[tempt, ye, ffffffffffffffffffffffffffff ]
Close[tempt]
tempt ? OpenAppend[COORxd, PageWidth ? 30]
Write[tempt, xd, ffffffffffffffffffffffffffff ]
Close[tempt]
tempt ? OpenAppend[COORyd, PageWidth ? 30]
Write[tempt, yd, ffffffffffffffffffffffffffff ]
Close[tempt]

?Writing new results to the SAVE text file to open later in MS Excel
  in order to graph relationships?
PutAppend[p, b, qo, wr, wi, qdr, qdi, beta, c, SAVE]
```

B.3 Nonsymmetrical vibrations about equilibrium of an air-filled tube resting on a rigid foundation with damping

Mathematica code

```
(*Variables defined:
    p=internal air pressure
   b=contact length of tube supporting surface
    qo=initial equilibrium membrane tension (*located at origin*)
     xe=horizontal coordinate
      ye=vertical coordinate
       theta_e=e=intial equilibrium angle measured from rigid surface to membrane
         theta_d=d=initial dynamic angle measured form the rigid surface
            to membrane
          qd=initial dynamic membrane tension (*located at origin*)
            w=frequency of vibrations about equilibrium shape
             u=tangential displacement
              beta=damping coefficient
                c=multiplier to visually vary the dynamic shape about the
                 equilibrium shape
                 t=scaled arc length=*)

(*Clearing variables for solving a set of new cells=*)
Clear[c, h, b, qe, qd, gw, gqd, y1, y2, y3, y4, y5, y6, y7, yy1, yy2, yy3, yy4,
  yy5, yy6, yy7, t, u, w];

(*where y1=xe, y2=ye, y3=theta_e, y4=xd, y5=yd, y6=theta_d, y7=qd=*)
(*Defining the constant =*)
pi = N[=]=;
(*Setting the tangential displacement=*)
u = 0.0001;
(*Specifying internal air pressure=*)
p = 2.85;
(*Equilibrium values (*b and qo*) obtained from AirEquilibrium.nb=*)
b = 1[[p = 1]];
qo = 0.204100534959496;
(*Guessing frequency and initial dynamic membrane tension=*)
gw = 8.13994962931331;
gqd = 0.0005;
(*Setting damping coefficient=*)
beta = 1;
(*Defining imaginery number=*)
i = (*=1[=]^0.5;
(*Setting arbitrary amplitude multiplier=*)
c = 500;
(*Naming output text file to contain dynamic properties=*)
SAVE = "2.85AirVibDampNonsym3.txt";
(*Naming output directory=*)
DIR = "2.85AirVibDampNonsym3";
(*Naming output text files to contain coordinate information=*)
COORx = "x.txt";
COORy = "y.txt";
COORxd = "xd.txt";
COORyd = "yd.txt";
```

```
(*Resetting the directory in order to start at the top of the driectory chain*)
ResetDirectory[];
(*Creating the directory DIR*)
CreateDirectory[DIR];
(*Setting the directory to DIR where files will finally be placed*)
SetDirectory[DIR];

(*Defining terms with equations taken from the derivation described in Chapter 3,
 Section 3.5*)
de[y2_, y3_, y4_, y5_, y6_, y7_, w_] :=
 {y1'[t] == 1 - b Cos[y3[t]], y2'[t] == 1 - b Sin[y3[t]],
  y3'[t] == 1 - b - p Cos[y3[t]] y2[t] - qo, y4'[t] == -1 - b y6[t] Sin[y3[t]],
  y5'[t] == 1 - b y6[t] Cos[y3[t]],
  y6'[t] ==
   1 - b
    (y7[t] - p Cos[y3[t]] y2[t] - qo) y6[t] Sin[y3[t]] +
     (w^2 - i beta w) y4[t] Sin[y3[t]] y5[t] Cos[y3[t]] y2[t] - qo),
  y7'[t] ==
   1 - b
    (y6[t] Cos[y3[t]] (w^2 - i beta w) y4[t] Cos[y3[t]] y5[t] Sin[y3[t]])}

(*Defining initial boundary conditions*)
leftBC[qd_] := {y1[0] == 0, y2[0] == 0, y3[0] == 0, y4[0] == u, y5[0] == 0, y6[0] == 0,
  y7[0] == qd}

(*Numerically solving the defined derivatives above*)
soln = NDSolve[Flatten[Append[de[y2, y3, y4, y5, y6, y7, w], leftBC[qd]]],
  {y1, y2, y3, y4, y5, y6, y7}, {t, 0, 1}, MaxSteps -> 20000]

(*Applying the end point boundary conditions*)
endpt[w_, qd_] :=
  {y1[t], y2[t], y3[t], y4[t], y5[t], y6[t], y7[t]} /.
    First[NDSolve[Flatten[Append[de[y2, y3, y4, y5, y6, y7, w], leftBC[qd]]],
      {y1[t], y2[t], y3[t], y4[t], y5[t], y6[t], y7[t]}, {t, 0, 1}, MaxSteps -> 4000]] /.
   t -> 1;

(*Displaying end point values solved above before iterations*)
endpt[gw, gqd]

{-0.25974, 1.72056 10^-6, 6.28319, -0.00108086, 0.000434498,
 -0.000885326, 0.000254524, -0.0315593, 0.0111179, 0.00685741, 0.00208677}

Clear[w, qd]

(*Defining end point boundary conditions: [[5]]y5 condition,
 setting the percent to change guess values in order to iterate,
 setting the accuracy goal of 6, setting number of iterations*)
rts = FindRoot[endpt[w, qd][[5]] == 0, endpt[w, qd][[6]] == 0, {w, gw, 0.98 gw},
  {qd, gqd, 0.98 gqd}, AccuracyGoal -> 6, MaxIterations -> 7000]

(*Displaying end point values solved above after iterations*)
endpt[w] /. rts, qd /. rts
```

```
{0.25974, 1.7203 10^-6, 6.28319,
 0.000100038 + 8.03009 10^-9 I, 1.93667 10^-9 - 5.01715 10^-9 I,
 -3.87937 10^-8 + 2.28357 10^-7 I, 0.000368098 + 5.36198 10^-8 I}

{Displaying results of above shooting method}
w = w /. rts
qd = qd /. rts

8.13965 + 0.499985 I

0.000368026 + 6.04071 10^-10 I

{Separating real from imaginery values}
wr = Re[w];
wi = Im[w];
qdr = Re[u];
qdi = Im[u];

{Solving terms in order to plot}
{yy1[t_], yy2[t_], yy3[t_], yy4[t_], yy5[t_], yy6[t_], yy7[t_]} =
  {y1[t], y2[t], y3[t], y4[t], y5[t], y6[t], y7[t]} /. First[soln];
F = ParametricPlot[Evaluate[{Re[yy1[t]], Re[yy2[t]]} /. soln /. rts], {t, 0, 1},
   PlotRange -> All, AspectRatio -> Automatic, PlotPoints -> 1000];
G =
  ParametricPlot[
   Evaluate[{Re[yy1[t]] + c Re[yy4[t]], Re[yy2[t]] + c Re[yy5[t]]} /. soln /. rts],
   {t, 0, 1}, PlotRange -> All, AspectRatio -> Automatic, PlotPoints -> 1000];
{Plotting both equilibrium shape F and dynamic shape G}
H = Show[F, G];
```

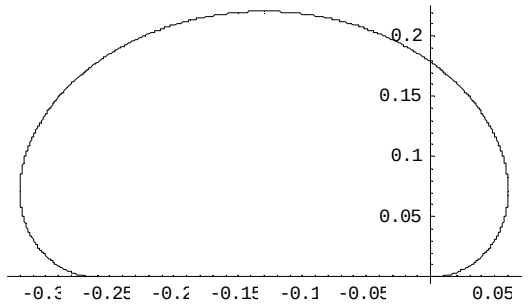

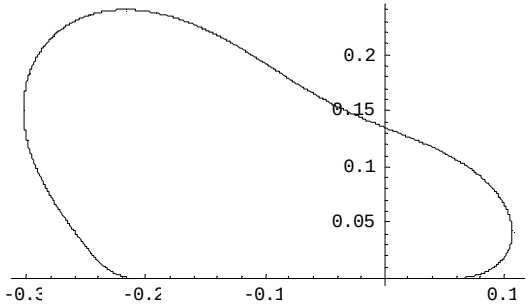

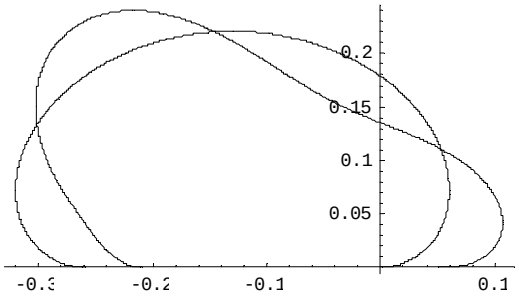


```
?Tabulating equilibrium x coordinate values in order to display shapes in Excel?
xe ? Table Evaluate Re yy1 t . soln . rts , t, 0, 1, 1 300 ;
?Tabulating equilibrium y coordinate values in order to display shapes in Excel?
ye ? Table Evaluate Re yy2 t . soln . rts , t, 0, 1, 1 300 ;
?Tabulating dynamic x coordinate values in order to display shapes in Excel?
xd ? Table Evaluate Re yy1 t ? c ? Re yy4 t . soln . rts , t, 0, 1, 1 300 ;
?Tabulating dynamic y coordinate values in order to display shapes in Excel?
yd ? Table Evaluate Re yy2 t ? c ? Re yy5 t . soln . rts , t, 0, 1, 1 300 ;
?Creating and opening COORx text file, Writing to COORx text file,
 Closing COORx text file?
tempt ? OpenAppend COORx, PageWidth ? 30
Write tempt, xe, fffffffffffffffffffffffffff
Close tempt
tempt ? OpenAppend COORy, PageWidth ? 30
Write tempt, ye, fffffffffffffffffffffffffff
Close tempt
tempt ? OpenAppend COORxd, PageWidth ? 30
Write tempt, xd, fffffffffffffffffffffffffff
Close tempt
tempt ? OpenAppend COORyd, PageWidth ? 30
Write tempt, yd, fffffffffffffffffffffffffff
Close tempt

?Writing new results to the SAVE text file to open later in MS Excel in
  order to graph relationships?
PutAppend p, b, qo, wr, wi, qdr, qdi, beta, c, SAVE
```

Appendix C:

C.1 Equilibrium of a water-filled tube resting on a Winkler foundation

Mathematica code

```
{?Variables defined:
    p?internal air pressure
   b?contact length of tube supporting surface
    qo?initial equilibrium membrane tension {located at origin}
     xe?horizontal coordinate
      ye?vertical coordinate
       theta_e??e?intial equilibrium angle measured from rigid surface to membrane
         theta_d??d?initial dynamic angle measured form the rigid surface
            to membrane
           qd?initial dynamic membrane tension {located at origin}
             w?frequency of vibrations about equilibrium shape
              u?tangential displacement
               beta???damping coefficient
                 c?multiplier to visually vary the dynamic shape about the
                  equilibrium shape
                  t?scaled arc length?}

{?Clearing variables for solving a set of new cells?}
Clear{c, h, b, qe, qd, gw, gqd, y1, y2, y3, y4, y5, y6, y7, yy1, yy2, yy3, yy4,
  yy5, yy6, yy7, t, u, w};
```

```
(*where y1=xe, y2=ye, y3=theta_e, y4=xd, y5=yd, y6=theta_d, y7=qd*)
(*Defining the constant ??*)
pi = N[?];
(*Setting the tangential displacement*)
u = 0.0001;
(*Specifying internal air pressure*)
p = 2.85;
(*Equilibrium values {b and qo} obtained from AirEquilibrium.nb*)
b = 1}}p = 1};
qo = 0.204100534959496;
(*Guessing frequency and initial dynamic membrane tension*)
gw = 8.13994962931331;
gqd = 0.0005;
(*Setting damping coefficient*)
beta = 1;
(*Defining imaginery number*)
i = (?1)^0.5;
(*Setting arbitrary amplitude multiplier*)
c = 500;
(*Naming output text file to contain dynamic properties*)
SAVE = "2.85AirVibDampNonsym3.txt";
(*Naming output directory*)
DIR = "2.85AirVibDampNonsym3";
(*Naming output text files to contain coordinate information*)
COORx = "x.txt";
COORy = "y.txt";
COORxd = "xd.txt";
COORyd = "yd.txt";

(*Resetting the directory in order to start at the top of the driectory chain*)
ResetDirectory[]];
(*Creating the directory DIR*)
CreateDirectory[DIR];
(*Setting the directory to DIR where files will finally be placed*)
SetDirectory[DIR];

(*Defining terms with equations taken from the derivation described in Chapter 3,
  Section 3.5*)
de[y2_, y3_, y4_, y5_, y6_, y7_, w_] :=
 {y1'[t] == (1 - b) Cos[y3[t]], y2'[t] == (1 - b) Sin[y3[t]],
  y3'[t] == (1 - b) (p Cos[y3[t]]) / (y2[t] + qo), y4'[t] == -(1 - b) y6[t] Sin[y3[t]],
  y5'[t] == (1 - b) y6[t] Cos[y3[t]],
  y6'[t] ==
   (1 - b) (
    (y7[t] - p Cos[y3[t]]) / (y2[t] + qo) - y6[t] Sin[y3[t]] -
     (w^2 - i beta w) (y4[t] Sin[y3[t]] - y5[t] Cos[y3[t]]) / (y2[t] + qo)),
  y7'[t] ==
   (1 - b) (
    y6[t] Cos[y3[t]] (w^2 - i beta w) y4[t] Cos[y3[t]] + y5[t] Sin[y3[t]])}
```

```
(*Defining initial boundary conditions*)
leftBC[qd_] := {y1[0] == 0, y2[0] == 0, y3[0] == 0, y4[0] == u, y5[0] == 0, y6[0] == 0,
  y7[0] == qd}

(*Numerically solving the defined derivatives above*)
soln := NDSolve[Flatten[Append[de[y2, y3, y4, y5, y6, y7, w], leftBC[qd]]],
  {y1, y2, y3, y4, y5, y6, y7}, {t, 0, 1}, MaxSteps == 20000]

(*Applying the end point boundary conditions*)
endpt[w_, qd_] :=
  {y1[t], y2[t], y3[t], y4[t], y5[t], y6[t], y7[t]} /.
    First[NDSolve[Flatten[Append[de[y2, y3, y4, y5, y6, y7, w], leftBC[qd]]],
      {y1[t], y2[t], y3[t], y4[t], y5[t], y6[t], y7[t]}, {t, 0, 1}, MaxSteps == 4000]] /.
   t == 1;

(*Displaying end point values solved above before iterations*)
endpt[gw, gqd]

{0.25974, 1.72056 10^6, 6.28319, 0.00108086 0.000434498,
 0.000885326 0.000254524, 0.0315593 0.0111179, 0.00685741 0.00208677}

Clear[w, qd]

(*Defining end point boundary conditions: [[5]]y5 condition,
 setting the percent to change guess values in order to iterate,
 setting the accuracy goal of 6, setting number of iterations*)
rts := FindRoot[{endpt[w, qd][[5]] == 0, endpt[w, qd][[6]] == 0}, {w, gw, 0.98 gw},
  {qd, gqd, 0.98 gqd}, AccuracyGoal == 6, MaxIterations == 7000]

(*Displaying end point values solved above after iterations*)
endpt[w /. rts, qd /. rts]

{0.25974, 1.7203 10^6, 6.28319,
 0.000100038 8.03009 10^9, 1.93667 10^9 5.01715 10^9,
 3.87937 10^8 2.28357 10^7, 0.000368098 5.36198 10^8}

(*Displaying results of above shooting method*)
w == w /. rts
qd == qd /. rts

8.13965 0.499985

0.000368026 6.04071 10^10

(*Separating real from imaginery values*)
wr == Re[w];
wi == Im[w];
qdr == Re[u];
qdi == Im[u];
```

```
{?Solving terms in order to plot?}
{yy1[t_], yy2[t_], yy3[t_], yy4[t_], yy5[t_], yy6[t_], yy7[t_]} ?
  {y1[t], y2[t], y3[t], y4[t], y5[t], y6[t], y7[t]}. First[soln];
F ? ParametricPlot[Evaluate[{Re[yy1[t]], Re[yy2[t]]}. soln]. rts], {t, 0, 1},
   PlotRange ? All, AspectRatio ? Automatic, PlotPoints ? 1000];
G ?
  ParametricPlot[
   Evaluate[{Re[yy1[t]] ? c ? Re[yy4[t]], Re[yy2[t]] ? c ? Re[yy5[t]]}]. soln]. rts],
   {t, 0, 1}, PlotRange ? All, AspectRatio ? Automatic, PlotPoints ? 1000];
{?Plotting both equilibrium shape F and dynamic shape G?}
H ? Show[F, G];
```

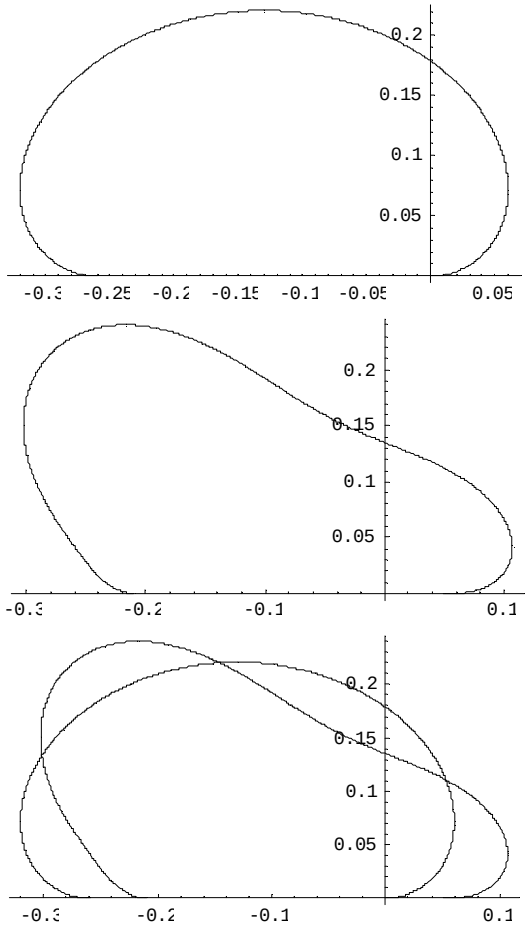

```
?Tabulating equilibrium x coordinate values in order to display shapes in Excel?
xe ? Table[Evaluate[{Re[yy1[t]]} /. soln] /. rts], {t, 0, 1, 1/300}];
?Tabulating equilibrium y coordinate values in order to display shapes in Excel?
ye ? Table[Evaluate[{Re[yy2[t]]} /. soln] /. rts], {t, 0, 1, 1/300}];
?Tabulating dynamic x coordinate values in order to display shapes in Excel?
xd ? Table[Evaluate[{Re[yy1[t]] ? c ? Re[yy4[t]]} /. soln] /. rts], {t, 0, 1, 1/300}];
?Tabulating dynamic y coordinate values in order to display shapes in Excel?
yd ? Table[Evaluate[{Re[yy2[t]] ? c ? Re[yy5[t]]} /. soln] /. rts], {t, 0, 1, 1/300}];
?Creating and opening COORx text file, Writing to COORx text file,
 Closing COORx text file?
tempt ? OpenAppend[COORx, PageWidth ? 30]
Write[tempt, xe, fffffffffffffffffffffffffff ]
Close[tempt]
tempt ? OpenAppend[COORy, PageWidth ? 30]
Write[tempt, ye, fffffffffffffffffffffffffff ]
Close[tempt]
tempt ? OpenAppend[COORxd, PageWidth ? 30]
Write[tempt, xd, fffffffffffffffffffffffffff ]
Close[tempt]
tempt ? OpenAppend[COORyd, PageWidth ? 30]
Write[tempt, yd, fffffffffffffffffffffffffff ]
Close[tempt]

?Writing new results to the SAVE text file to open later in MS Excel in
  order to graph relationships?
PutAppend[p, b, qo, wr, wi, qdr, qdi, beta, c, SAVE]
```

C.2 Symmetrical vibrations about equilibrium of a water-filled tube resting on a Winkler foundation

Mathematica code

```
(*Variables defined:
    h=internal pressure head
   hf=settlement of tube
    qe=initial equilibrium membrane tension (located at origin)
     k=soil stiffness coefficient
      xe=horizontal coordinate
       ye=vertical coordinate
        theta_e=e=intial equilibrium angle measured from rigid surface to membrane
          theta_d=d=initial dynamic angle measured form the rigid surface
             to membrane
            qd=initial dynamic membrane tension (located at origin)
              w=frequency of vibrations about equilibrium shape
               c=multiplier to visually vary the dynamic shape about the
                equilibrium shape
                t=scaled arc length=)

(*Clearing variables for solving a set of new cells=)
Clear[a, p, hf, gqd, gw, qe, k, pi, y1, y2, y3, y4, w];
(*where y1=xe, y2=ye, y3=e, y4=qe, y5=xd, y6=yd, y7=d, y8=qd=)
(*Defining the constant =)
pi = N[Pi];
(*Specifying internal pressure head and soil stiffness coefficient=)
h = 0.2;
k = 5;
(*Equilibrium values (hf and qe) obtained from equilibrium=)
hf = 0.0456997188262876;
qe = 0.0173971109710639;
(*Guessing frequency and initial dynamic membrane tension=)
gw = 1.86198205250768;
gqd = 0.0000157079792364172;
(*Setting arbitrary amplitude multiplier=)
c = 40;
g = 0;
(*Naming output text file to contain dynamic properties=)
SAVE = "0.2WaterWinkVib4.txt";
(*Naming output directory=)
DIR = "0.2WaterWinkVib4";
(*Naming output text files to contain coordinate information=)
COORx = "x.txt";
COORy = "y.txt";
COORrxd = "rxd.txt";
COORlxd = "lxd.txt";
COORryd = "ryd.txt";
COORlyd = "lyd.txt";
```

```
(*Resetting the directory in order to start at the top of the driectory chain*)
ResetDirectory[];
(*Creating the directory DIR*)
CreateDirectory[DIR];
(*Setting the directory to DIR where files will finally be placed*)
SetDirectory[DIR];

(*Defining terms about equations taken from the derivation described in Chapter 4,
 Section 4.5*)
de[y2_, y3_, y4_, y5_, y6_, y7_, y8_, w_] :=
 {y1'[t] == Cos[y3[t]], y2'[t] == Sin[y3[t]],
  y3'[t] == If[y2[t] == hf, h == hf == y2[t] == k == y2[t] == hf == Cos[y3[t]]][y4[t]],
    1 == y4[t] == h == hf == y2[t]], y4'[t] == If[y2[t] == hf, k == y2[t] == hf == Sin[y3[t]], 0],
  y5'[t] == == y7[t] == Sin[y3[t]], y6'[t] == y7[t] == Cos[y3[t]],
  y7'[t] ==
   If[y2[t] == hf,
    (y8[t] == h == hf == y2[t] == k == y2[t] == hf == Cos[y3[t]]][y4[t]] == k == y6[t] == Cos[y3[t]] ==
       k == y2[t] == hf == y7[t] == Sin[y3[t]] == y6[t] ==
        w^2 == y5[t] == Sin[y3[t]] == y6[t] == Cos[y3[t]]][y4[t]],
    (y8[t] == h == hf == y2[t]][y4[t] == y6[t] ==
        w^2 == y5[t] == Sin[y3[t]] == y6[t] == Cos[y3[t]][y4[t]],
  y8'[t] == If[y2[t] == hf, == w^2 == y5[t] == Cos[y3[t]] == y6[t] == Sin[y3[t]]] ==
     k == y2[t] == hf == y7[t] == Cos[y3[t]] == k == y6[t] == Sin[y3[t]],
    == w^2 == y5[t] == Cos[y3[t]] == y6[t] == Sin[y3[t]]]]]

(*Defining initial boundary conditions*)
leftBC[qd_] := y1[0] == 0, y2[0] == 0, y3[0] == 0, y4[0] == qe, y5[0] == 0,
  y6[0] == 0.0001, y7[0] == 0, y8[0] == qd

(*Numerically solving the defined derivatives above*)
soln := NDSolve[Flatten[Append[de[y2, y3, y4, y5, y6, y7, y8, w], leftBC[qd]]],
  {y1, y2, y3, y4, y5, y6, y7, y8}, {t, 0, 0.5}, MaxSteps == 8000]

(*Applying the end point boundary conditions*)
endpt[w_, qd_] :=
  {y1[t], y2[t], y3[t], y4[t], y5[t], y6[t], y7[t], y8[t]} /.
    First[NDSolve[Flatten[Append[de[y2, y3, y4, y5, y6, y7, y8, w], leftBC[qd]]],
      {y1[t], y2[t], y3[t], y4[t], y5[t], y6[t], y7[t], y8[t]}, {t, 0, 0.5},
      MaxSteps == 22000]] /. t == 0.5;

(*Displaying end point values solved above before iterations*)
endpt[gw, gqd]

{9.0636== 10^12, 0.210748, 3.14159, 0.012176,
 ==1.5857== 10^7, ==0.000193631, 3.6522== 10^6, 5.89487== 10^6}

Clear[w, qd]

(*Defining end point boundary conditions: [[5]]==y5 condition,
 setting the percent to change guess values in order to iterate,
 setting the accuracy goal of 5, setting number of iterations*)
rts := FindRoot[{endpt[w, qd][[5]] == 0, endpt[w, qd][[7]] == 0}, {w, {gw, 0.98== gw}},
  {qd, {gqd, 0.98== gqd}}, AccuracyGoal == 5, MaxIterations == 5000]
```

```
(*Displaying results of above shooting method*)
w = w /. rts
qd = qd /. rts
```

```
1.86219
```

```
0.0000157064
```

```
(*Displaying end point values solved above after iterations*)
endpt{w /. rts, qd /. rts}
```

```
{9.0636*10^12, 0.210748, 3.14159, 0.012176,
 -3.16236*10^11, -0.000193353, 1.87559*10^7, 6.02815*10^6}
```

```
(*Solving terms in order to plot*)
{yy1[t_], yy2[t_], yy3[t_], yy4[t_], yy5[t_], yy6[t_], yy7[t_], yy8[t_]} =
  {y1[t], y2[t], y3[t], y4[t], y5[t], y6[t], y7[t], y8[t]} /. First[soln];
F = ParametricPlot[Evaluate[{yy1[t], yy2[t]} /. hf /. soln /. rts], {t, 0, 0.5},
  PlotRange -> All, AspectRatio -> Automatic, PlotPoints -> 100]
G = ParametricPlot[Evaluate[{yy1[t] + c, yy5[t], yy2[t] + hf + c + yy6[t]}] /. soln /. rts],
  {t, 0, 0.5}, PlotRange -> All, AspectRatio -> Automatic, PlotPoints -> 100]
(*Plotting both right equilibrium shape F and right dynamic shape G*)
H = Show[F, G]
```

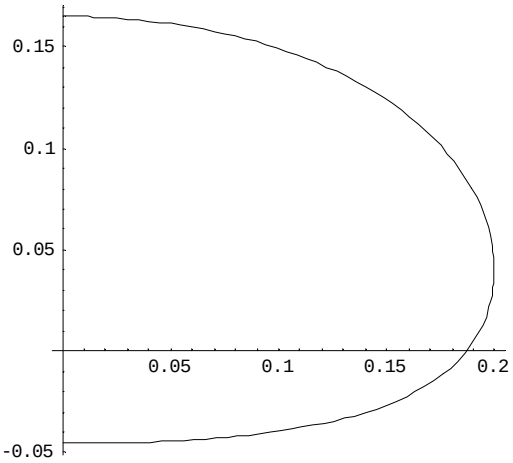


```
-Graphics-
```

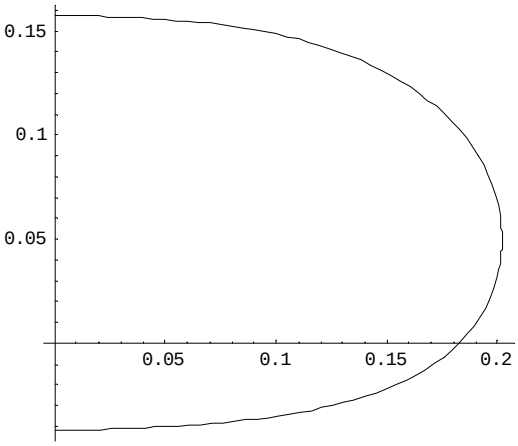

?Graphics??

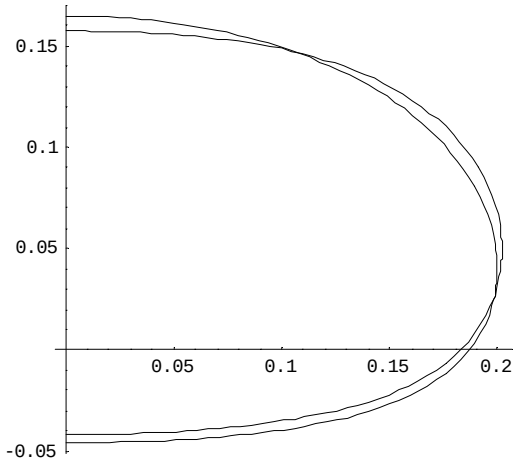

?Graphics??

```
M = ParametricPlot[{Evaluate[{{yy1[t], yy2[t]} = hf} /. soln /. rts], {t, 0, 0.5},
  PlotRange → All, AspectRatio → Automatic, PlotPoints → 100]
U = ParametricPlot[{Evaluate[{{yy1[t] → c yy5[t], yy2[t] → hf → c yy6[t]}} /. soln /. rts],
   {t, 0, 0.5}, PlotRange → All, AspectRatio → Automatic, PlotPoints → 100]
}?Plotting both left equilibrium shape M and left dynamic shape U?}
V = Show[M, U]
```

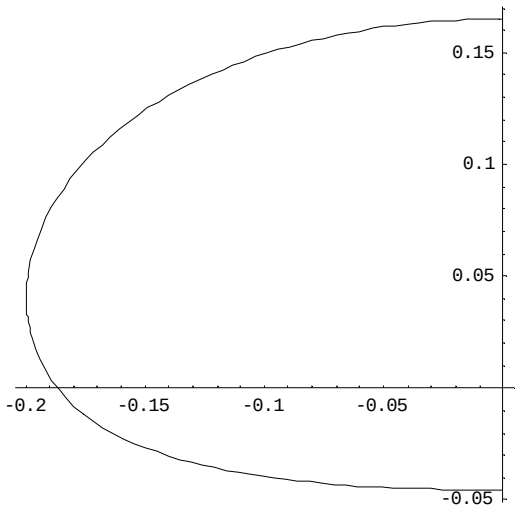

??Graphics??

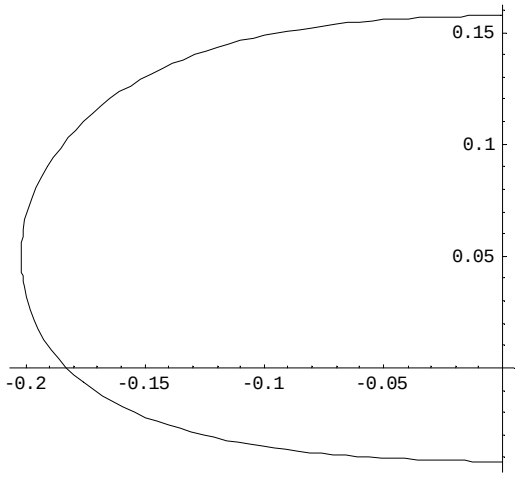

??Graphics??

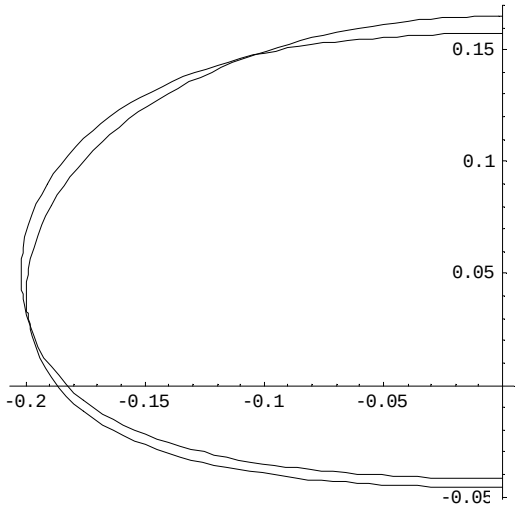

??Graphics??

```
W = Show[H, V]
```

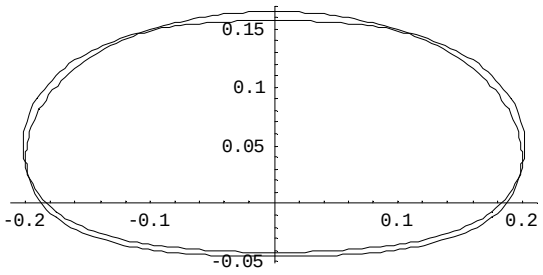


```
? Graphics
```

```
(?Tabulating equilibrium x coordinate values in order to display shapes in Excel?)
xe = Table[Evaluate[{yy1[t]} /. soln /. rts], {t, 0, 0.5, 1}, 300];
(?Tabulating equilibrium y coordinate values in order to display shapes in Excel?)
ye = Table[Evaluate[{yy2[t] + hf} /. soln /. rts], {t, 0, 0.5, 1}, 300];
(?Tabulating the right dynamic x coordinate values in order to display
  shapes in Excel?)
rxd = Table[Evaluate[{Re[yy1[t]] + c + Re[yy5[t]]} /. soln /. rts], {t, 0, 0.5, 1}, 300];
(?Tabulating the left dynamic x coordinate values in order to display
  shapes in Excel?)
lxd = Table[Evaluate[{Re[-yy1[t]] + c + Re[yy5[t]]} /. soln /. rts], {t, 0, 0.5, 1}, 300];
(?Tabulating the right dynamic y coordinate values in order to display
  shapes in Excel?)
ryd = Table[Evaluate[{Re[yy2[t]] + hf + c + Re[yy6[t]]} /. soln /. rts],
   {t, 0, 0.5, 1}, 300];
(?Tabulating the left dynamic y coordinate values in order to display
  shapes in Excel?)
lyd = Table[Evaluate[{Re[yy2[t]] + hf + c + Re[yy6[t]]} /. soln /. rts],
   {t, 0, 0.5, 1}, 300];
(?Creating and opening COORx text file, Writing to COORx text file,
 Closing COORx text file?)
tempt = OpenAppend[COORx, PageWidth → 30]
Write[tempt, xe, ffffffffffffffffffffffffffff]
Close[tempt]
tempt = OpenAppend[COORy, PageWidth → 30]
Write[tempt, ye, ffffffffffffffffffffffffffff]
Close[tempt]
tempt = OpenAppend[COORlxd, PageWidth → 30]
Write[tempt, lxd, ffffffffffffffffffffffffffff]
Close[tempt]
tempt = OpenAppend[COORrxd, PageWidth → 30]
Write[tempt, rxd, ffffffffffffffffffffffffffff]
Close[tempt]
tempt = OpenAppend[COORryd, PageWidth → 30]
Write[tempt, ryd, ffffffffffffffffffffffffffff]
Close[tempt]
tempt = OpenAppend[COORlyd, PageWidth → 30]
Write[tempt, lyd, ffffffffffffffffffffffffffff]
Close[tempt]

OutputStream[x.txt, 8]

x.txt

OutputStream[y.txt, 9]

y.txt

OutputStream[lxd.txt, 10]

lxd.txt
```

```
OutputStream[rxd.txt, 11]

rxd.txt

OutputStream[ryd.txt, 12]

ryd.txt

OutputStream[lyd.txt, 13]

lyd.txt

(?Writing new results to the SAVE text file to open later in MS Excel in
  order to graph relationships?)
PutAppend[h, k, hf, qe, w, qd, c, 0, 0, SAVE]
```

C.3 Nonsymmetrical vibrations about equilibrium of a water-filled tube resting on a Winkler foundation

Mathematica code

```
(?Variables defined:
    h?internal pressure head
   hf?settlement of tube
    qe?initial equilibrium membrane tension [located at origin]
     k?soil stiffness coefficient
      xe?horizontal coordinate
       ye?vertical coordinate
        theta_e??e?intial equilibrium angle measured from rigid
           surface to membrane
          theta_d??d?initial dynamic angle measured form the rigid
             surface to membrane
            qd?initial dynamic membrane tension [located at origin]
              w?frequency of vibrations arriving at equilibrium
                shape
               c?multiplier to visually vary the dynamic shape
                about the equilibrium shape
                t?scaled arc length?)
```

```
(*Clearing variables for solving a set of new cells*)
Clear[a, p, hf, gqd, gw, qe, k, pi, y1, y2, y3, y4, w];
(*where y1=xe, y2=ye,y3=e, y4=qe,y5=xd,y6=yd,y7=d,y8=qd*)
(*Defining the constant *)
pi = N[Pi];
(*Specifying internal pressure head and soil stiffness coefficient*)
h = 0.2;
k = 5;
(*Equilibrium values {hf and qe} obtained from equilibrium*)
hf = 0.0456997188262876;
qe = 0.0173971109710639;
(*Guessing frequency and initial dynamic membrane tension*)
gw = 2.30250392607331;
gqd = 0.0000332359689061022;
(*Setting arbitrary amplitude multiplier*)
c = 40;
(*Naming output text file to contain dynamic properties*)
SAVE = "0.2WaterWinkVib3.txt";


(*Defining terms about equations taken from the derivation described
  in Chapter 4, Section 4.5*)
de[y2_, y3_, y4_, y5_, y6_, y7_, y8_, w_] :=
 {y1'[t] = Cos[y3[t]], y2'[t] = Sin[y3[t]],
  y3'[t] = If[y2[t] = hf, (h = hf = y2[t] = k = y2[t] = hf = Cos[y3[t]])[[y4[t]]],
    1 (y4[t] = (h = hf = y2[t]))],
  y4'[t] = If[y2[t] = hf, k = y2[t] = hf = Sin[y3[t]], 0],
  y5'[t] = = y7[t] = Sin[y3[t]], y6'[t] = y7[t] = Cos[y3[t]]],
  y7'[t] =
   If[y2[t] = hf,
    (= y8[t] = h = hf = y2[t] = k = y2[t] = hf = Cos[y3[t]])[[y4[t]]] =
      k = y6[t] = Cos[y3[t]] = k = y2[t] = hf = y7[t] = Sin[y3[t]] = y6[t] =
      w^2 = y5[t] = Sin[y3[t]] = y6[t] = Cos[y3[t]])[[y4[t]]],
    (= y8[t] = h = hf = y2[t]) y4[t] = y6[t] =
      w^2 = y5[t] = Sin[y3[t]] = y6[t] = Cos[y3[t]])[[y4[t]]],
  y8'[t] = If[y2[t] = hf, = w^2 = y5[t] = Cos[y3[t]] = y6[t] = Sin[y3[t]]] =
    k = y2[t] = hf = y7[t] = Cos[y3[t]] = k = y6[t] = Sin[y3[t]],
   = w^2 = y5[t] = Cos[y3[t]] = y6[t] = Sin[y3[t]]]]

(*Defining initial boundary conditions*)
leftBC[qd_] := {y1[0] = 0, y2[0] = 0, y3[0] = 0, y4[0] = qe, y5[0] = 0,
  y6[0] = 0, y7[0] = 0.001, y8[0] = qd}

(*Numerically solving the defined derivatives above*)
soln := NDSolve[Flatten[Append[de[y2, y3, y4, y5, y6, y7, y8, w], leftBC[qd]]],
  {y1, y2, y3, y4, y5, y6, y7, y8}, {t, 0, 0.5}, MaxSteps = 8000]
```

```
(*Applying the end point boundary conditions*)
endpt[w_, qd_] :=
  {y1[t], y2[t], y3[t], y4[t], y5[t], y6[t], y7[t], y8[t]} /.
    First[NDSolve[Flatten[Append[de[y2, y3, y4, y5, y6, y7, y8, w], leftBC[qd]]],
      {y1[t], y2[t], y3[t], y4[t], y5[t], y6[t], y7[t], y8[t]}, {t, 0, 0.5},
      MaxSteps -> 22000]] /. t -> 0.5;

(*Displaying end point values solved above before iterations*)
endpt[gw, gqd]

{-7.20824*10^-9, 0.210748, 3.14159, 0.012176,
 -3.0917*10^-6, -3.30645*10^-6, -0.00244069, 0.0000190601}

Clear[w, qd]

(*Defining end point boundary conditions: {5} -y5 condition,
 setting the percent to change guess values in order to iterate,
 setting the accuracy goal of 5, setting number of iterations*)
rts := FindRoot[{endpt[w, qd][[5]] == 0, endpt[w, qd][[6]] == 0},
  {w, {gw, 0.98 gw}}, {qd, {gqd, 0.98 gqd}}, AccuracyGoal -> 5,
  MaxIterations -> 5000]

(*Displaying results of above shooting method*)
w -> w /. rts
qd -> qd /. rts

2.30423

0.0000334277

(*Displaying end point values solved above after iterations*)
endpt[w /. rts, qd /. rts]

{-7.26694*10^-9, 0.210748, 3.14159, 0.012176,
 -7.42424*10^-8, -1.52023*10^-7, -0.00244722, 0.0000223015}

(*Solving terms in order to plot*)
{yy1[t_], yy2[t_], yy3[t_], yy4[t_], yy5[t_], yy6[t_], yy7[t_], yy8[t_]} =
  {y1[t], y2[t], y3[t], y4[t], y5[t], y6[t], y7[t], y8[t]} /. First[soln];

F = ParametricPlot[Evaluate[{yy1[t], yy2[t] hf}] /. soln /. rts,
  {t, 0, 0.5}, PlotRange -> All, AspectRatio -> Automatic, PlotPoints -> 100]
G =
 ParametricPlot[
  Evaluate[{yy1[t] c, yy5[t], yy2[t] hf c, yy6[t]}] /. soln /. rts,
  {t, 0, 0.5}, PlotRange -> All, AspectRatio -> Automatic, PlotPoints -> 100]
(*Plotting both right equilibrium shape F and right dynamic shape G*)
H = Show[F, G]
```

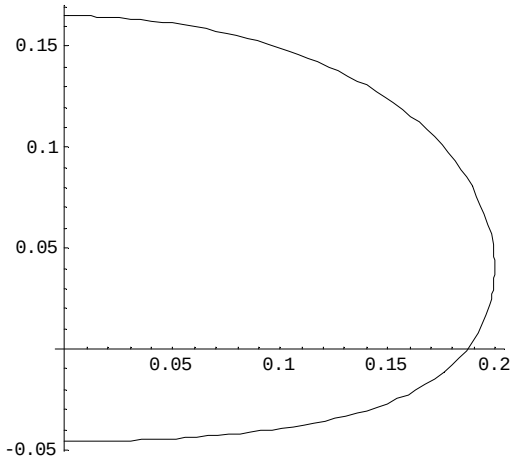

?? Graphics ??

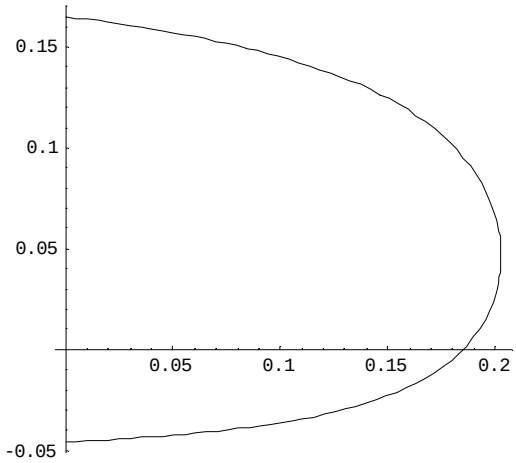

?? Graphics ??

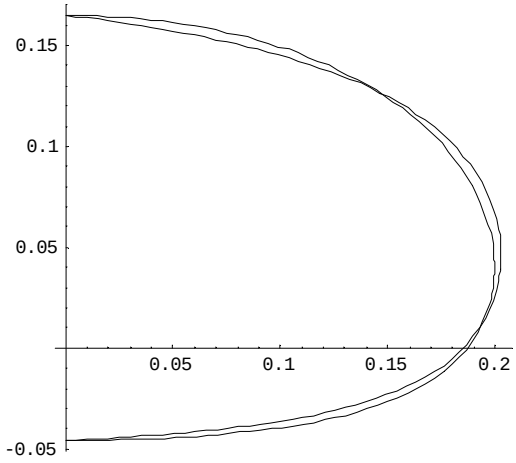

?? Graphics ??

```
M = ParametricPlot[Evaluate[{yy1[t], yy2[t] + hf} /. soln /. rts],
   {t, 0, 0.5}, PlotRange → All, AspectRatio → Automatic, PlotPoints → 100]
U =
 ParametricPlot[
  Evaluate[{yy1[t] + c + yy5[t], yy2[t] + hf + c + yy6[t]} /. soln /. rts],
   {t, 0, 0.5}, PlotRange → All, AspectRatio → Automatic, PlotPoints → 100]
];Plotting both left equilibrium shape M and left dynamic shape U;
V = Show[M, U]
```

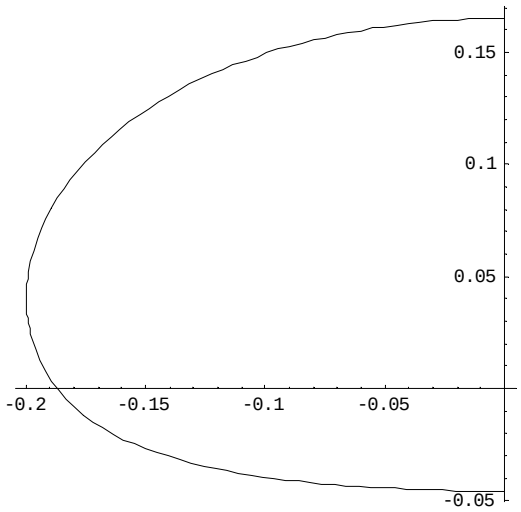

-Graphics-

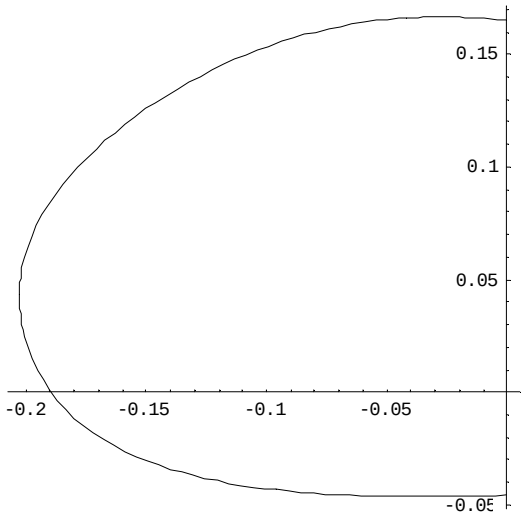

-Graphics-

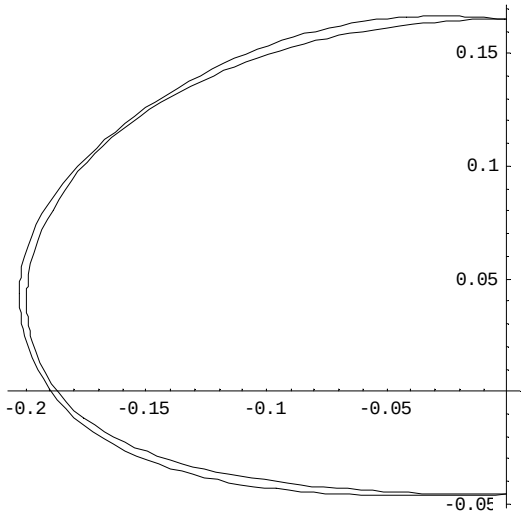

?? Graphics ??

```
W = Show[H, V]
```

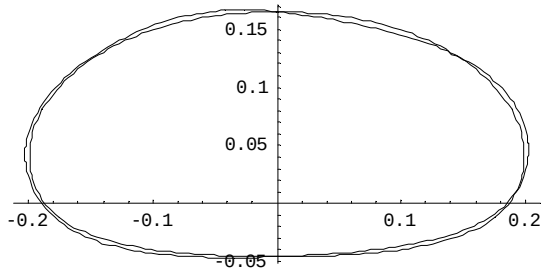

?? Graphics ??

```
]?Writing new results to the SAVE text file to open later in MS
  Excel in order to graph relationships?]
PutAppend[h, k, hf, qe, w, qd, c, 0, 0, SAVE]
```

Appendix D:

D.1 Equilibrium of a water-filled tube resting on a Pasternak foundation

Mathematica code

```
(*Variables defined:
    p=internal air pressure
   hf=settlement of tube
    qe=initial equilibrium membrane tension (located at origin)
     g=shear modulus
      k=soil stiffness coefficient
       xe=horizontal coordinate
        ye=vertical coordinate
         theta_e=e=intial equilibrium angle measured from rigid surface
            to membrane
            t=scaled arc length=)
(=Clearing variables for solving a set of new cells=)
Clear(h, ghf, gqe, qe, hf, k, pi, y1, y2, y3, y4);
(=where y1=xe, y2=ye, y3=e, y4=qe=)
(=Defining the constant ==)
pi = N(Pi);
(=Specifying internal air pressure, soil stiffness coefficient,
 and shear modulus=)
p = 2;
k = 40;
g = 0;
(=Guessing tube settlement and initial equilibrium membrane tension=)
ghf = 0.0714051272526214;
gqe = 0.158354937747283;
(=Naming output text file to contain dynamic properties=)
SAVE = "2AirPastEq200.txt";
(=Naming output directory=)
DIR = "2AirPastEq200";
(=Naming output text files to contain coordinate information=)
X = "EPastXe.txt";
Y = "EPastYe.txt";
(=Resetting the directory in order to start at the top of the driectory chain=)
(=ResetDirectory[]);
 (=Creating the directory DIR=)
 CreateDirectory[DIR];
 (=Setting the directory to DIR where files will finally be placed=)
 SetDirectory[DIR];=)
```

```
(*Defining terms with equations taken from the derivation described
  in Chapter 5, Section 5.8*)
de[y2_, y3_, y4_, hf_] := {y1'[t] == Cos[y3[t]], y2'[t] == Sin[y3[t]],
  y3'[t] == If[y2[t] == hf, {p == Cos[y3[t]] == k == y2[t] == hf == Cos[y3[t]]},
     {y4[t] == g == {Cos[y3[t]]}^2, {1 - y4[t]} == {p == Cos[y3[t]]}}],
  y4'[t] == If[y2[t] == hf, Sin[y3[t]] == k == y2[t] == hf == Sin[y3[t]] ==
     g == Sin[y3[t]] == Cos[y3[t]] == p == Cos[y3[t]] == k == y2[t] == hf == Cos[y3[t]]},
     {y4[t] == g == {Cos[y3[t]]}^2, Sin[y3[t]]}]

(*Defining initial boundary conditions*)
leftBC[qe_] := {y1[0] == 0, y2[0] == 0, y3[0] == 0, y4[0] == qe}

(*Numerically solving the defined derivatives above*)
soln := NDSolve[Flatten[Append[de[y2, y3, y4, hf], leftBC[qe]]],
  {y1, y2, y3, y4}, {t, 0, 0.5}, MaxSteps == 5000]

(*Applying the end point boundary conditions*)
endpt[hf_, qe_] :=
  {y1[t], y2[t], y3[t], y4[t]} /.
    First[NDSolve[Flatten[Append[de[y2, y3, y4, hf], leftBC[qe]]],
      {y1[t], y2[t], y3[t], y4[t]}, {t, 0, 0.5}, MaxSteps == 4000]] /. t == 0.5;

(*Displaying end point values solved above before iterations*)
endpt[ghf, gqe]

{1.97478 10^-9, 0.214738, 3.14159, 0.271121}

Clear[hf, qe]

(*Defining end point boundary conditions: {5} == y5 condition,
 setting the percent to change guess values in order to iterate,
 setting the accuracy goal of 5, setting number of iterations*)
rts := FindRoot[{endpt[hf, qe][[1]] == 0, endpt[hf, qe][[3]] == pi},
  {hf, {ghf, 0.95 ghf}}, {qe, {gqe, 0.95 gqe}}, AccuracyGoal == 2,
  MaxIterations == 3000]

(*Displaying results of above shooting method*)
hf == hf /. rts
qe == qe /. rts

0.0714051

0.158355

(*displaying maximum height of tube from origin*)
y == Evaluate[yy2[0.5]]

0.218942

endpt[hf /. rts, qe /. rts]

{4.29089 10^-10, 0.214738, 3.14159, 0.271121}

(*Solving terms in order to plot*)
{yy1[t_], yy2[t_], yy3[t_], yy4[t_]} ==
  {y1[t], y2[t], y3[t], y4[t]} /. First[soln];
```

```
?Plotting equilibrium shape?
ParametricPlot[Evaluate[{yy1[t], yy2[t]} ? hf] /. soln /. rts, {t, 0, 0.5},
 PlotRange ? All, AspectRatio ? Automatic, PlotPoints ? 100]
```

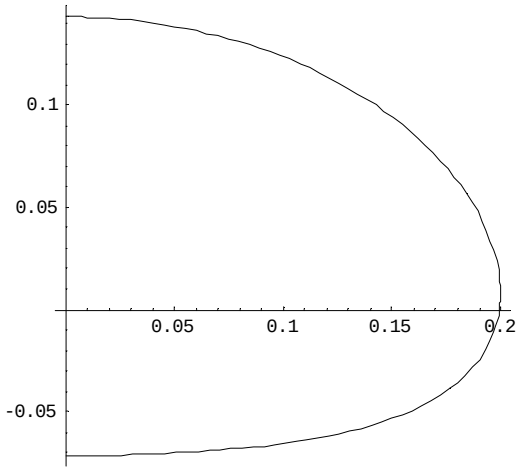


```
??Graphics??
```

```
?Tabulating equilibrium x coordinate values in order to display
  shapes in Excel?
xe ? Table[Evaluate[{yy1[t]} /. soln /. rts], {t, 0, 0.5, 1/300}];
?Creating and opening COORx text file, Writing to COORx text file,
 Closing COORx text file?
tempt ? OpenAppend[X, PageWidth ? 30]
Write[tempt, xe, fffffffffffffffffffffffffff]
Close[tempt]
```

```
OutputStream[EPastqe[k?40 g?0].txt, 43]
```

```
EPastqe[k?40 g?0].txt
```

```
?Tabulating equilibrium y coordinate values in order to display
  shapes in Excel?
ye ? Table[Evaluate[{yy2[t]} ? hf /. soln /. rts], {t, 0, 0.5, 1/300}];
?Creating and opening Y text file, Writing to Y text file,
 Closing Y text file?
tempt ? OpenAppend[Y, PageWidth ? 30]
Write[tempt, ye, fffffffffffffffffffffffffff]
Close[tempt]
```

```
OutputStream[EPastYe01.txt, 44]
```

```
EPastYe01.txt
```

```
?Tablulating xe?s[ in order to find max and min values to use for
  the calculation of the aspect ratio AR?]
 J ? Table[Evaluate[{yy1[t]} /. soln /. rts], {t, 0, 0.5, 1/300}];
K ? Table[Evaluate[{yy2[t]} /. soln /. rts], {t, 0, 0.5, 1/300}];
```

```
{?maximum x coordinate?}
xmax ? Max[J];
{?minimum x coordinate?}
xmin ? Min[J];
{?Aspect ratio?}
AR ? {2 ? xmax} } y
```

```
1.8238
```

```
{?Writing new results to the SAVE text file to open later in MS Excel
  in order to graph relationships?}
PutAppend[p, k, g, hf, qe, y, yhalf, AR, 0, SAVE]
```

D.2 Symmetrical vibrations about equilibrium of a water-filled tube resting on a Pasternak foundation

Mathematica code

```
{?Variables defined:
    h?internal pressure head
   hf?settlement of tube
    qe?initial equilibrium membrane tension }located at origin}
     g?shear modulus
      k?soil stiffness coefficient
       xe?horizontal coordinate
        ye?vertical coordinate
         theta_e??e?intial equilibrium angle measured from rigid
            surface to membrane
           theta_d??d?initial dynamic angle measured form the rigid
              surface to membrane
             qd?initial dynamic membrane tension }located at origin}
               w?frequency of vibrations about equilibrium shape
                c?multiplier to visually vary the dynamic shape about
                 the equilibrium shape
                 t?scaled arc length?}
```

```
{?Clearing variables for solving a set of new cells?}
Clear{h, a, p, hf, gqd, gw, qe, k, pi, y1, y2, y3, y4, w};
{?where y1?xe, y2?ye, y3??e, y4?qe,y5?xd,y6?yd,y7??d,y8?qd?}
{?Defining the constant ??}
pi ? N{Pi};
{?Specifying internal pressure head, soil stiffness coefficient,
 and shear modulus?}
h ? 0.3;
k ? 200;
g ? 1;
hf ? 0.000950711672369291;
qe ? 0.0212044924869494;
{?Guessing frequency and initial dynamic membrane tension?}
gw ? 0.872210876374265;
gqd ? 0.0000611188234067214;
{?Setting arbitrary amplitude multiplier?}
c ? 25;
{?Naming output text file to contain dynamic properties?}
SAVE ? "0.3WaterPast200Vib2.txt";
```

```
(*Defining terms about equations taken from the derivation described
  in Chapter 4, Section 4.10*)
de[y2_, y3_, y4_, y5_, y6_, y7_, y8_, w_] :=
 {y1'[t] == Cos[y3[t]], y2'[t] == Sin[y3[t]],
  y3'[t] == If[y2[t] == hf, (h*hf*y2[t] + k*(y2[t] - hf)*Cos[y3[t]])/
     (y4[t] + g*(Cos[y3[t]])^2), 1/(y4[t] + (h*hf*y2[t]))],
  y4'[t] ==
   If[y2[t] == hf, k*(y2[t] - hf)*Sin[y3[t]] +
     g*Sin[y3[t]]*Cos[y3[t]] + (h*hf*y2[t] + k*(y2[t] - hf)*Cos[y3[t]])/
      (y4[t] + g*(Cos[y3[t]])^2), 0], y5'[t] == y7[t]*Sin[y3[t]],
  y6'[t] == y7[t]*Cos[y3[t]],
  y7'[t] ==
   If[y2[t] == hf,
    (y8[t] - (h*hf*y2[t] + k*(y2[t] - hf)*Cos[y3[t]])/
       (y4[t] + g*(Cos[y3[t]])^2) - k*y6[t]*Cos[y3[t]] -
      k*(y2[t] - hf)*y7[t]*Sin[y3[t]]*y6[t] -
      (w^2 - (y5[t] - Sin[y3[t]])*y6[t]*Cos[y3[t]]))/
     (y4[t] + g*(Cos[y3[t]])^2),
    (y8[t] - (h*hf*y2[t])/y4[t]*y6[t] -
      (w^2 - (y5[t] - Sin[y3[t]])*y6[t]*Cos[y3[t]]))/y4[t]],
  y8'[t] == If[y2[t] == hf, (w^2 - (y5[t] - Cos[y3[t]])*y6[t]*Sin[y3[t]]) -
     k*(y2[t] - hf)*y7[t]*Cos[y3[t]]*k*y6[t]*Sin[y3[t]] -
     g*y7[t]*Cos[y3[t]]*Cos[y3[t]] -
     (h*hf*y2[t]*k*(y2[t] - hf)*Cos[y3[t]])/y4[t]*g*Cos[y3[t]])^2 -
     g*Sin[y3[t]]*
      Cos[y3[t]] -
      (y8[t] - (h*hf*y2[t]*k*(y2[t] - hf)*Cos[y3[t]])/
         (y4[t] + g*(Cos[y3[t]])^2) - k*y6[t]*Cos[y3[t]] -
        k*(y2[t] - hf)*y7[t]*Sin[y3[t]]*y6[t] -
        (w^2 - (y5[t] - Sin[y3[t]])*y6[t]*Cos[y3[t]]))/
       (y4[t] + g*(Cos[y3[t]])^2)*
       y7[t]*Sin[y3[t]] - (h*hf*y2[t] + k*(y2[t] - hf)*Cos[y3[t]])/
        (y4[t] + g*(Cos[y3[t]])^2),
    (w^2 - (y5[t] - Cos[y3[t]])*y6[t]*Sin[y3[t]])]}

(*Defining initial boundary conditions*)
leftBC[qd_] := {y1[0] == 0, y2[0] == 0, y3[0] == 0, y4[0] == qe, y5[0] == 0,
  y6[0] == 0.0001, y7[0] == 0, y8[0] == qd}

(*Numerically solving the defined derivatives above*)
soln := NDSolve[Flatten[Append[de[y2, y3, y4, y5, y6, y7, y8, w], leftBC[qd]]],
  {y1, y2, y3, y4, y5, y6, y7, y8}, {t, 0, 0.5}, MaxSteps == 8000]

(*Applying the end point boundary conditions*)
endpt[w_, qd_] :=
  {y1[t], y2[t], y3[t], y4[t], y5[t], y6[t], y7[t], y8[t]} /.
    First[NDSolve[Flatten[Append[de[y2, y3, y4, y5, y6, y7, y8, w], leftBC[qd]]],
      {y1[t], y2[t], y3[t], y4[t], y5[t], y6[t], y7[t], y8[t]}, {t, 0, 0.5},
      MaxSteps == 22000]] /. t == 0.5;
```

```
(*Displaying end point values solved above before iterations*)
endpt[gw, gqd]
```

```
{5.97848*10^-7, 0.221474, 3.1416, 0.0209228,
 5.11285*10^-8, 0.000508097, 7.35504*10^-7, -0.0000607664}
```

```
Clear[w, qd]
```

```
(*Defining end point boundary conditions: {{5}}*y5 condition,
 setting the percent to change guess values in order to iterate,
 setting the accuracy goal of 5, setting number of iterations*)
rts := FindRoot[{endpt[w, qd][[5]] == 0, endpt[w, qd][[7]] == 0},
  {w, {gw, 0.98*gw}}, {qd, {gqd, 0.98*gqd}}, AccuracyGoal -> 5,
  MaxIterations -> 5000]
```

```
(*Displaying results of above shooting method*)
w -> w /. rts
qd -> qd /. rts
```

```
0.872112
```

```
0.0000611132
```

```
endpt[w /. rts, qd /. rts]
```

```
{5.97848*10^-7, 0.221474, 3.1416, 0.0209228,
 8.75519*10^-10, 0.000508155, -1.22166*10^-8, -0.0000607653}
```

```
(*Solving terms in order to plot*)
{yy1[t_], yy2[t_], yy3[t_], yy4[t_], yy5[t_], yy6[t_], yy7[t_], yy8[t_]} =
  {y1[t], y2[t], y3[t], y4[t], y5[t], y6[t], y7[t], y8[t]} /. First[soln];
F = ParametricPlot[Evaluate[{yy1[t], yy2[t]} * hf] /. soln /. rts, {t, 0, 0.5},
   PlotRange -> All, AspectRatio -> Automatic, PlotPoints -> 100];
G = ParametricPlot[
   Evaluate[{yy1[t] * c * yy5[t], yy2[t] * hf * c * yy6[t]}] /. soln /. rts,
   {t, 0, 0.5}, PlotRange -> All, AspectRatio -> Automatic, PlotPoints -> 100];
(*Plotting both right equilibrium shape F and right dynamic shape G*)
H = Show[F, G];
```

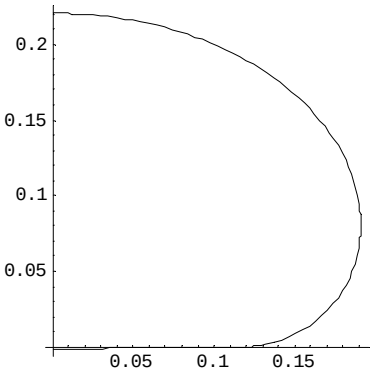

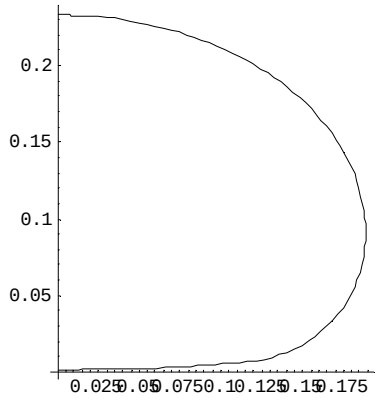

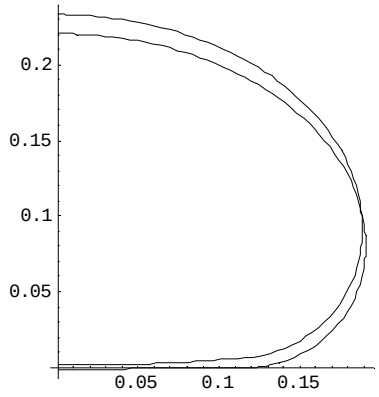


```
M = ParametricPlot[Evaluate[{yy1[t], yy2[t]} /. hf /. soln /. rts],
    {t, 0, 0.5}, PlotRange → All, AspectRatio → Automatic, PlotPoints → 100];
U = ParametricPlot[
    Evaluate[{yy1[t] + c yy5[t], yy2[t] + hf + c yy6[t]} /. soln /. rts],
    {t, 0, 0.5}, PlotRange → All, AspectRatio → Automatic, PlotPoints → 100];
{"Plotting both left equilibrium shape M and left dynamic shape U"}
V = Show[M, U];
```

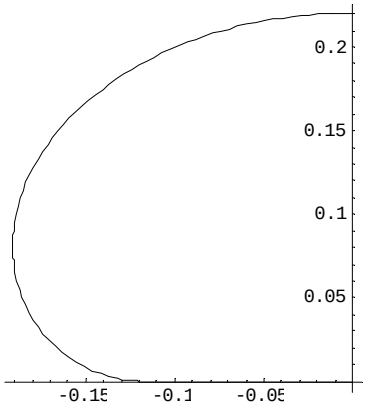

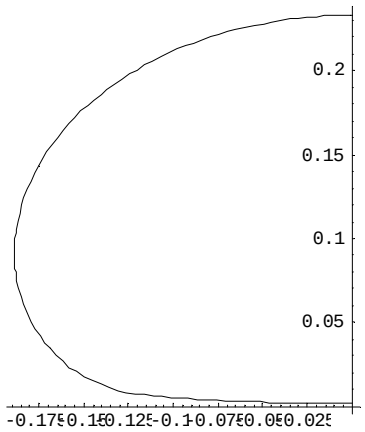

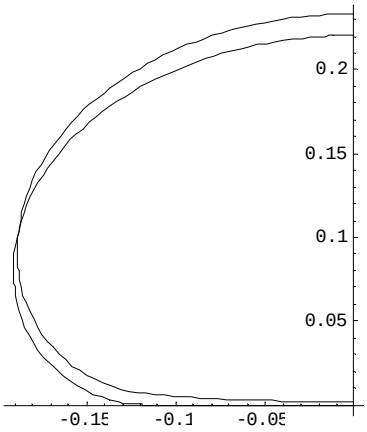


```
W ? Show{H, V}
```

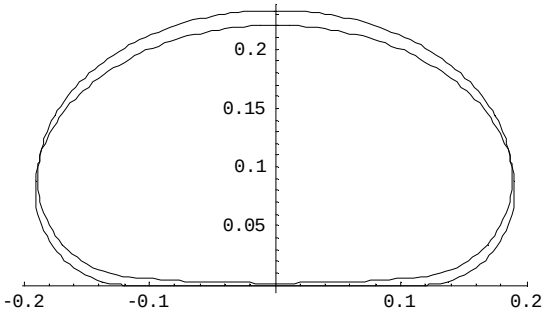


```
??Graphics??

}?Writing new results to the SAVE text file to open later in MS Excel
  in order to graph relationships?}
PutAppend{h, k, g, hf, qe, w, qd, c, 0, SAVE}
```

D.3 Nonsymmetrical vibrations about equilibrium of a water-filled tube resting on a Pasternak foundation

Mathematica code

```
(*Variables defined:
    h=internal pressure head
   hf=settlement of tube
    qe=initial equilibrium membrane tension (located at origin)
     g=shear modulus
      k=soil stiffness coefficient
       xe=horizontal coordinate
        ye=vertical coordinate
         theta_e=e=intial equilibrium angle measured from rigid
            surface to membrane
           theta_d=d=initial dynamic angle measured form the rigid
              surface to membrane
             qd=initial dynamic membrane tension (located at origin)
               w=frequency of vibrations about equilibrium shape
                c=multiplier to visually vary the dynamic shape about
                 the equilibrium shape
                 t=scaled arc length=)

(=Clearing variables for solving a set of new cells=)
Clear[a, p, hf, c, gqd, gw, qe, k, pi, y1, y2, y3, y4, w];
(=where y1=xe, y2=ye, y3=e, y4=qe, y5=xd, y6=yd, y7=d, y8=qd=)
(=Defining the constant =)
pi = N[Pi];
(=Specifying internal pressure head, soil stiffness coefficient,
 and shear modulus=)
h = 0.3;
k = 200;
g = 10;
(=Equilibrium values (hf and qe) obtained from equilibrium=)
hf = 0.000184850748034101;
qe = 0.0209766853108681;
(=Guessing frequency and initial dynamic membrane tension=)
gw = 2.651706600951475;
gqd = 0.00012762955461032396;
(=Setting arbitrary amplitude multiplier=)
c = 30;
(=Naming output text file to contain dynamic properties=)
SAVE = "0.3WaterPast200Vib5.txt";
```

```
(*Defining terms with equations taken from the derivation described
  in Chapter 4, Section 4.10*)
de[y2_, y3_, y4_, y5_, y6_, y7_, y8_, w_] :=
 {y1'[t] == Cos[y3[t]], y2'[t] == Sin[y3[t]],
  y3'[t] == If[y2[t] == hf, (h*hf*y2[t] + k*(y2[t] - hf)*Cos[y3[t]])/
     (y4[t] + g*(Cos[y3[t]])^2), 1/(y4[t] + (h*hf*y2[t]))],
  y4'[t] ==
   If[y2[t] == hf, k*(y2[t] - hf)*Sin[y3[t]] +
     g*Sin[y3[t]]*Cos[y3[t]] + (h*hf*y2[t] + k*(y2[t] - hf)*Cos[y3[t]])/
      (y4[t] + g*(Cos[y3[t]])^2), 0], y5'[t] == y7[t]*Sin[y3[t]],
  y6'[t] == y7[t]*Cos[y3[t]],
  y7'[t] ==
   If[y2[t] == hf,
    (y8[t] - (h*hf*y2[t] + k*(y2[t] - hf)*Cos[y3[t]])/
       (y4[t] + g*(Cos[y3[t]])^2) - k*y6[t]*Cos[y3[t]] -
      k*(y2[t] - hf)*y7[t]*Sin[y3[t]]*y6[t] -
      (w^2*(y5[t] - Sin[y3[t]])*y6[t]*Cos[y3[t]])/
       (y4[t] + g*(Cos[y3[t]])^2),
    (y8[t] - (h*hf*y2[t])/y4[t]*y6[t] -
      (w^2*(y5[t] - Sin[y3[t]])*y6[t]*Cos[y3[t]])/y4[t]),
  y8'[t] == If[y2[t] == hf, -(w^2*(y5[t] - Cos[y3[t]])*y6[t]*Sin[y3[t]]) -
     k*(y2[t] - hf)*y7[t]*Cos[y3[t]]*k*y6[t]*Sin[y3[t]] -
     g*y7[t]*Cos[y3[t]]*Cos[y3[t]] -
     (h*hf*y2[t]*k*(y2[t] - hf)*Cos[y3[t]])/y4[t]*g*Cos[y3[t]])^2 -
     g*Sin[y3[t]]*
      Cos[y3[t]] -
      (y8[t] - (h*hf*y2[t]*k*(y2[t] - hf)*Cos[y3[t]])/
         (y4[t] + g*(Cos[y3[t]])^2) - k*y6[t]*Cos[y3[t]] -
        k*(y2[t] - hf)*y7[t]*Sin[y3[t]]*y6[t] -
        (w^2*(y5[t] - Sin[y3[t]])*y6[t]*Cos[y3[t]])/
         (y4[t] + g*(Cos[y3[t]])^2)*
        y7[t]*Sin[y3[t]] - (h*hf*y2[t]*k*(y2[t] - hf)*Cos[y3[t]])/
         (y4[t] + g*(Cos[y3[t]])^2),
     -(w^2*(y5[t] - Cos[y3[t]])*y6[t]*Sin[y3[t]])]]


(*Defining initial boundary conditions*)
leftBC[qd_] := {y1[0] == 0, y2[0] == 0, y3[0] == 0, y4[0] == qe, y5[0] == 0,
  y6[0] == 0, y7[0] == 0.001, y8[0] == qd}

(*Numerically solving the defined derivatives above*)
soln := NDSolve[Flatten[Append[de[y2, y3, y4, y5, y6, y7, y8, w], leftBC[qd]]],
  {y1, y2, y3, y4, y5, y6, y7, y8}, {t, 0, 0.5}, MaxSteps == 8000]

(*Applying the end point boundary conditions*)
endpt[w_, qd_] :=
  {y1[t], y2[t], y3[t], y4[t], y5[t], y6[t], y7[t], y8[t]} /.
    First[NDSolve[Flatten[Append[de[y2, y3, y4, y5, y6, y7, y8, w], leftBC[qd]]],
      {y1[t], y2[t], y3[t], y4[t], y5[t], y6[t], y7[t], y8[t]}, {t, 0, 0.5},
      MaxSteps == 22000]] /. t == 0.5;
```

```
(*Displaying end point values solved above before iterations*)
endpt[gw, gqd]
```

```
{-1.02972 10^-6, 0.220717, 3.14159, 0.0209213,
 0.0003178, 0.000289656, -0.00615871, 0.000515158}
```

```
Clear[w, qd]
```

```
(*Defining end point boundary conditions: {{5}}=y5 condition,
 setting the percent to change guess values in order to iterate,
 setting the accuracy goal of 5, setting number of iterations*)
rts := FindRoot[{endpt[w, qd][[5]] == 0, endpt[w, qd][[6]] == 0},
  {w, {gw, 0.98 gw}}, {qd, {gqd, 0.98 gqd}}, AccuracyGoal -> 5,
  MaxIterations -> 5000]
```

```
(*Displaying results of above shooting method*)
w -> w /. rts
qd -> qd /. rts
```

```
2.59783
```

```
0.0000763263
```

```
endpt[w /. rts, qd /. rts]
```

```
{-1.30092 10^-6, 0.220718, 3.14159, 0.0209213,
 -2.00371 10^-7, -3.02087 10^-7, -0.00331124, 0.0000565823}
```

```
(*Solving terms in order to plot*)
{{yy1[t_], yy2[t_], yy3[t_], yy4[t_], yy5[t_], yy6[t_], yy7[t_], yy8[t_]} =
  {y1[t], y2[t], y3[t], y4[t], y5[t], y6[t], y7[t], y8[t]} /. First[soln]};
F = ParametricPlot[Evaluate[{yy1[t], yy2[t]} /. hf] /. soln /. rts,
  {t, 0, 0.5}, PlotRange -> All, AspectRatio -> Automatic, PlotPoints -> 100]
G =
 ParametricPlot[
  Evaluate[{yy1[t] -> c yy5[t], yy2[t] -> hf c yy6[t]}] /. soln /. rts,
  {t, 0, 0.5}, PlotRange -> All, AspectRatio -> Automatic, PlotPoints -> 100]
(*Plotting both right equilibrium shape F and right dynamic shape G*)
H = Show[F, G]
```

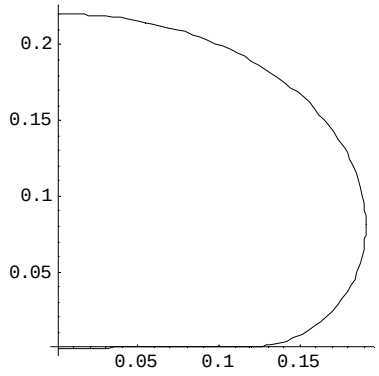


```
-Graphics-
```

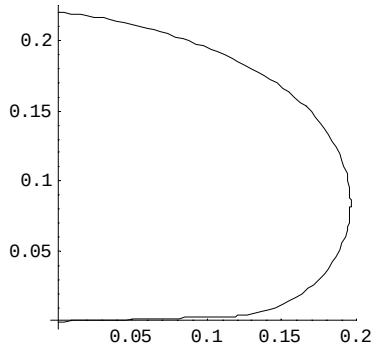

?Graphics??

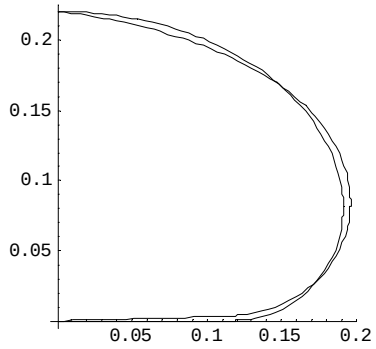

?Graphics??

```
M ? ParametricPlot[{Evaluate[{?yy1[t], yy2[t]} ? hf]}. soln}. rts],
   {t, 0, 0.5}, PlotRange ? All, AspectRatio ? Automatic, PlotPoints ? 100]
U ?
 ParametricPlot[
  Evaluate[{?yy1[t] ? c ? yy5[t], yy2[t]} ? hf ? c ? yy6[t]]}. soln}. rts],
   {t, 0, 0.5}, PlotRange ? All, AspectRatio ? Automatic, PlotPoints ? 100]
}?Plotting both left equilibrium shape M and left dynamic shape U?]
V ? Show[M, U]
```

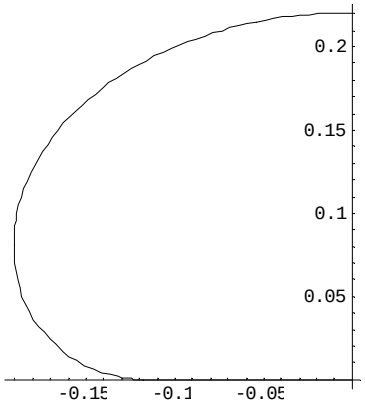

?Graphics??

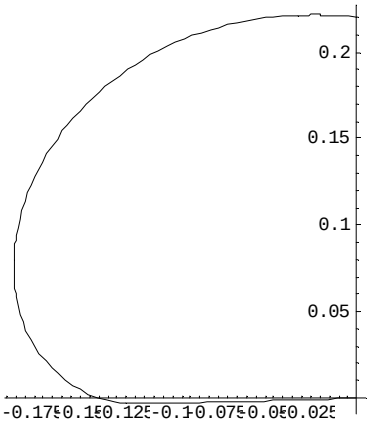

?Graphics??

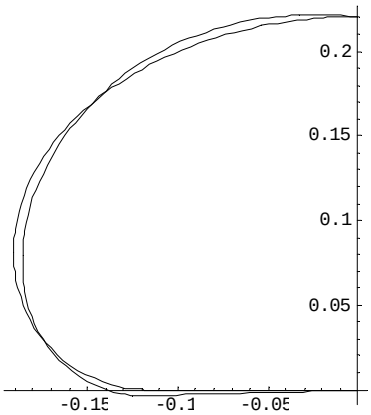

?Graphics??

```
W ? Show[H, V]
```

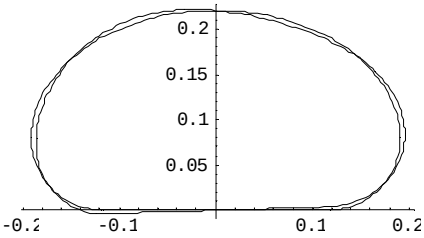

?Graphics??

```
]?Writing new results to the SAVE text file to open later in MS
  Excel in order to graph relationships?]
PutAppend[h, k, g, hf, qe, w, qd, c, 0, SAVE]
```

Appendix E:

E.1 Equilibrium of an air-filled tube resting on a Winkler foundation

Mathematica code

```
(*Variables defined:
    p=internal air pressure
   hf=settlement of tube
   qe=initial equilibrium membrane tension (located at origin)
    k=soil stiffness coefficient
     xe=horizontal coordinate
       ye=vertical coordinate
        theta_e=e=intial equilibrium angle measured from rigid surface
           to membrane
           t=scaled arc length=)

(*Clearing variables for solving a set of new cells=)
Clear[h, ghf, gqe, qe, hf, k, pi, y1, y2, y3, y4];
(*where y1=xe, y2=ye, y3=e, y4=qe=)
(*Defining the constant =)
pi = N[Pi];
(*Specifying internal air pressure and soil stiffness coefficient=)
p = 5;
k = 40;
(*Guessing tube settlement and initial equilibrium membrane tension=)
ghf = 0.0903225612678003;
gqe = 0.648423916254237;
(*Naming output text file to contain equilibrium properties=)
SAVE = "5AirWinkEq.txt";
(*Naming output directory=)
DIR = "5AirWinkEqk40";
(*Naming output text files to contain coordinate information=)
COORx = "x.txt";
COORy = "y.txt";

(*Resetting the directory in order to start at the top of the driectory chain=)
ResetDirectory[];
(*Creating the directory DIR=)
CreateDirectory[DIR];
(*Setting the directory to DIR where files will finally be placed=)
SetDirectory[DIR];
```

```
(*Defining terms with equations taken from the derivation described
  in Chapter 5, Section 5.3*)
de[y2_, y3_, y4_, hf_] := {y1'[t] == Cos[y3[t]], y2'[t] == Sin[y3[t]],
  y3'[t] == If[y2[t] == hf, {1, y4[t]} * {p * Cos[y3[t]] * k * {y2[t] * hf} * Cos[y3[t]]},
    {1, y4[t]} * {p * Cos[y3[t]]}],
  y4'[t] == If[y2[t] == hf, Sin[y3[t]] * k * {y2[t] * hf} * Sin[y3[t]], Sin[y3[t]]]}

(*Defining initial boundary conditions*)
leftBC[qe_] := {y1[0] == 0, y2[0] == 0, y3[0] == 0, y4[0] == qe}

(*Numerically solving the defined derivatives above*)
soln := NDSolve[Flatten[Append[de[y2, y3, y4, hf], leftBC[qe]]],
  {y1, y2, y3, y4}, {t, 0, 0.5}, MaxSteps == 5000]

(*Applying the end point boundary conditions*)
endpt[hf_, qe_] :=
  {y1[t], y2[t], y3[t], y4[t]} /.
    First[NDSolve[Flatten[Append[de[y2, y3, y4, hf], leftBC[qe]]],
      {y1[t], y2[t], y3[t], y4[t]}, {t, 0, 0.5}, MaxSteps == 4000]] /. t == 0.5;

(*Displaying end point values solved above before iterations*)
endpt[ghf, gqe]
```

```
{1.05164 * 10^-8, 0.283423, 3.14159, 0.768687}
```

```
Clear[hf, qe]
```

```
(*Defining end point boundary conditions: {{3}} == y3 condition,
 setting the percent to change guess values in order to iterate,
 setting the accuracy goal of 7, setting number of iterations*)
rts := FindRoot[{endpt[hf, qe][[1]] == 0, endpt[hf, qe][[3]] == pi},
  {hf, {ghf, 0.95 * ghf}}, {qe, {gqe, 0.95 * gqe}}, AccuracyGoal == 7,
  MaxIterations == 3000]

(*Displaying results of above shooting method*)
hf == hf /. rts
qe == qe /. rts
```

```
0.0903226
```

```
0.648424
```

```
(*Maximum tube height from origin*)
y == Evaluate[yy2[0.5]]
```

```
0.275199
```

```
endpt[hf /. rts, qe /. rts]
```

```
{-7.36935 * 10^-10, 0.283423, 3.14159, 0.768687}
```

```
(*Solving terms in order to plot*)
{yy1[t_], yy2[t_], yy3[t_], yy4[t_]} ==
  {y1[t], y2[t], y3[t], y4[t]} /. First[soln];
```

```
(*Plotting equilibrium shape to visualize foundation*)
ParametricPlot[Evaluate[{yy1[t], yy2[t]} /. hf /. soln /. rts], {t, 0, 0.5},
 PlotRange -> All, AspectRatio -> Automatic, PlotPoints -> 100]
```

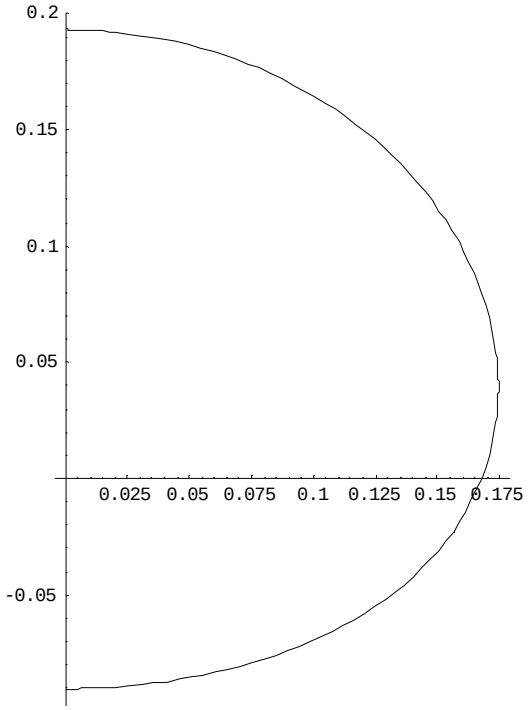


```
<<Graphics`
J = Table[Evaluate[{yy1[t]} /. soln /. rts], {t, 0, 0.5, 1/300}];
K = Table[Evaluate[{yy2[t]} /. soln /. rts], {t, 0, 0.5, 1/300}];
(*Location of left and right vertical tangent in order to compute
  aspect ratio below*)
xmin = Min[J]
xmax = Max[J]
```

```
7.36935*10^-10
```

```
0.174456
```

```
(*Aspect Ratio*)
AR = 2 xmax / y
```

```
1.26786
```

```
(*Writing new results to the SAVE text file to open later in MS Excel
  in order to graph relationships*)
PutAppend[p, k, hf, qe, y, AR, c, 0, 0, SAVE]
```

```
(?Tabulating equilibrium x coordinate values in order to display
  shapes in Excel?)
xe ? Table[Evaluate[{yy1[t]}. soln]. rts]], {t, 0, 0.5, 1} 300]];
(?Tabulating equilibrium y coordinate values in order to display
  shapes in Excel?)
ye ? Table[Evaluate[{yy2[t] ? hf}. soln]. rts]], {t, 0, 0.5, 1} 300]];
(?Creating and opening COORx text file, Writing to COORx text file,
 Closing COORx text file?)
tempt ? OpenAppend[COORx, PageWidth ? 30]
Write[tempt, xe, fffffffffffffffffffffffffff ]
Close[tempt]
tempt ? OpenAppend[COORy, PageWidth ? 30]
Write[tempt, ye, fffffffffffffffffffffffffff ]
Close[tempt]
```

```
OutputStream[x.txt, 39]
```

```
x.txt
```

```
OutputStream[y.txt, 40]
```

```
y.txt
```

E.2 Symmetrical vibrations about equilibrium of an air-filled tube resting on a Winkler foundation

Mathematica code

```
(?Variables defined:
    p?internal air pressure
   hf?settlement of tube
    qe?initial equilibrium membrane tension [located at origin]
     k?soil stiffness coefficient
      xe?horizontal coordinate
       ye?vertical coordinate
        theta_e??e?intial equilibrium angle measured from rigid surface
           to membrane
          theta_d??d?initial dynamic angle measured form the rigid
             surface to membrane
            qd?initial dynamic membrane tension [located at origin]
              w?frequency of vibrations about equilibrium shape
               c?multiplier to visually vary the dynamic shape about
                the equilibrium shape
                t?scaled arc length?)
```

```
(*Clearing variables for solving a set of new cells*)
Clear[a, p, hf, gqd, gw, qe, k, pi, qd, xe, ye, rxd, lxd, ryd, lyd, w, y1, y2,
  y3, y4, y5, y6, y7, y8, yy1, yy2, yy3, yy4, yy5, yy6, yy7, yy8];
(*where y1=xe, y2=ye, y3=e, y4=qe,y5=xd,y6=yd,y7=d,y8=qd*)
(*Defining the constant *)
pi = N[Pi];
(*Specifying internal air pressure and soil stiffness coefficient*)
p = 3;
k = 200;
(*Equilibrium values {hf and qe} obtained from AirWinkEq.nb*)
hf = 0.0195743165848826;
qe = 0.253376663315812;
(*Guessing frequency and initial dynamic membrane tension*)
gw = 3.69156324032477;
gqd = 0.00901185944639346;
(*Setting arbitrary amplitude multiplier*)
c = 5;
(*Naming output text file to contain dynamic properties*)
SAVE = "3AirWinkVib2.txt";
(*Naming output directory*)
DIR = "3AirWinkVib2k2001";
(*Naming output text files to contain coordinate information*)
COORx = "x.txt";
COORy = "y.txt";
COORrxd = "rxd.txt";
COORlxd = "lxd.txt";
COORryd = "ryd.txt";
COORlyd = "lyd.txt";

(*Resetting the directory in order to start at the top of the driectory chain*)
ResetDirectory[];
(*Creating the directory DIR*)
CreateDirectory[DIR];
(*Setting the directory to DIR where files will finally be placed*)
SetDirectory[DIR];
```

```
(*Defining terms about equations taken from the derivation described
  in Chapter 5, Section 5.5*)
de[y2_, y3_, y4_, y5_, y6_, y7_, y8_, w_] :=
 {y1'[t] == Cos[y3[t]], y2'[t] == Sin[y3[t]],
  y3'[t] == If[y2[t] == hf, k*y2[t] == hf*Cos[y3[t]] == p*Cos[y3[t]]][[y4[t]]],
    p*Cos[y3[t]]][[y4[t]]],
  y4'[t] == If[y2[t] == hf, k*y2[t] == hf*Sin[y3[t]] == Sin[y3[t]], Sin[y3[t]]],
  y5'[t] == y7[t]*Sin[y3[t]], y6'[t] == y7[t]*Cos[y3[t]],
  y7'[t] ==
   If[y2[t] == hf,
    k*y6[t]*Cos[y3[t]] == k*y2[t] == hf*y7[t]*Sin[y3[t]] ==
        y8[t][[y4[t]]] == k*y2[t] == hf*Cos[y3[t]][[y4[t]] ==
     y8[t] == p*Cos[y3[t]][[y4[t]] == y7[t]*Sin[y3[t]] ==
       w^2*y5[t]*Sin[y3[t]] == y6[t]*Cos[y3[t]]][[y4[t]],
    y8[t] == p*Cos[y3[t]][[y4[t]] == y7[t]*Sin[y3[t]] ==
      w^2*y5[t]*Sin[y3[t]] == y6[t]*Cos[y3[t]]][[y4[t]],
  y8'[t] == If[y2[t] == hf, k*y2[t] == hf*y7[t]*Cos[y3[t]] == k*y6[t]*Sin[y3[t]] ==
    y7[t]*Cos[y3[t]] == w^2*y5[t]*Cos[y3[t]] == y6[t]*Sin[y3[t]]],
    y7[t]*Cos[y3[t]] == w^2*y5[t]*Cos[y3[t]] == y6[t]*Sin[y3[t]]][[y4[t]]]}

(*Defining initial boundary conditions*)
leftBC[qd_] := {y1[0] == 0, y2[0] == 0, y3[0] == 0, y4[0] == qe, y5[0] == 0,
  y6[0] == 0.0001, y7[0] == 0, y8[0] == qd}

(*Numerically solving the defined derivatives above*)
soln := NDSolve[Flatten[Append[de[y2, y3, y4, y5, y6, y7, y8, w], leftBC[qd]]],
  {y1, y2, y3, y4, y5, y6, y7, y8}, {t, 0, 0.5}, MaxSteps == 8000]

(*Applying the end point boundary conditions*)
endpt[w_, qd_] :=
  {y1[t], y2[t], y3[t], y4[t], y5[t], y6[t], y7[t], y8[t]} /.
    First[NDSolve[Flatten[Append[de[y2, y3, y4, y5, y6, y7, y8, w], leftBC[qd]]],
      {y1[t], y2[t], y3[t], y4[t], y5[t], y6[t], y7[t], y8[t]}, {t, 0, 0.5},
      MaxSteps == 22000]] /. t == 0.5;

(*Displaying end point values solved above before iterations*)
endpt[gw, gqd]

{2.98675*10^7, 0.234224, 3.14159, 0.44929,
 3.9191*10^10, 0.00547465, 8.78379*10^10, 0.00292585}

Clear[w, qd]

(*Defining end point boundary conditions: {5}[[5]] == y5 condition,
 setting the percent to change guess values in order to iterate,
 setting the accuracy goal of 7, setting number of iterations*)
rts := FindRoot[{endpt[w, qd][[5]] == 0, endpt[w, qd][[7]] == 0}, {w, gw, 0.98*gw},
  {qd, gqd, 0.98*gqd}, AccuracyGoal == 7, MaxIterations == 5000]

(*Displaying results of above shooting method*)
w == w /. rts
qd == qd /. rts
```

```
3.69156

0.00901186

endpt[w /. rts, qd /. rts]

{2.98675 10^7, 0.234224, 3.14159, 0.44929,
 3.11447 10^12, 0.00547465, 1.88747 10^11, 0.00292585}

{Solving terms in order to plot}
{{yy1[t_], yy2[t_], yy3[t_], yy4[t_], yy5[t_], yy6[t_], yy7[t_], yy8[t_]} ->
  {y1[t], y2[t], y3[t], y4[t], y5[t], y6[t], y7[t], y8[t]}} /. First[soln];

F = ParametricPlot[Evaluate[{yy1[t], yy2[t]} hf] /. soln /. rts, {t, 0, 0.5},
  PlotRange -> All, AspectRatio -> Automatic, PlotPoints -> 100]
G =
 ParametricPlot[Evaluate[{yy1[t] c yy5[t], yy2[t] hf c yy6[t]}] /. soln /. rts,
  {t, 0, 0.5}, PlotRange -> All, AspectRatio -> Automatic, PlotPoints -> 100]
{Plotting both right equilibrium shape F and right dynamic shape G}
H = Show[F, G]
```

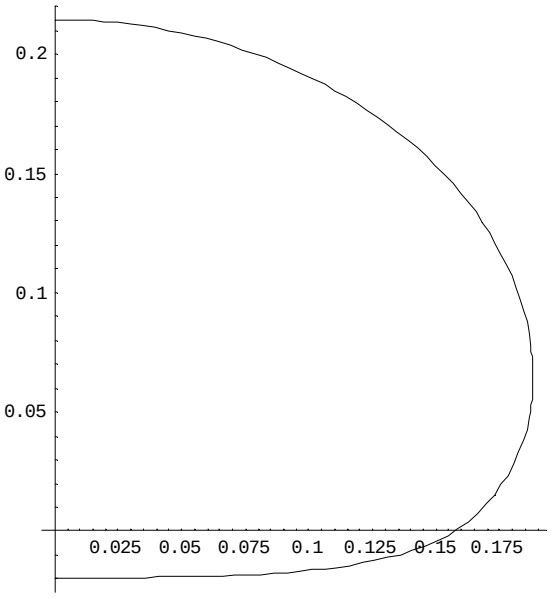


```
-Graphics-
```

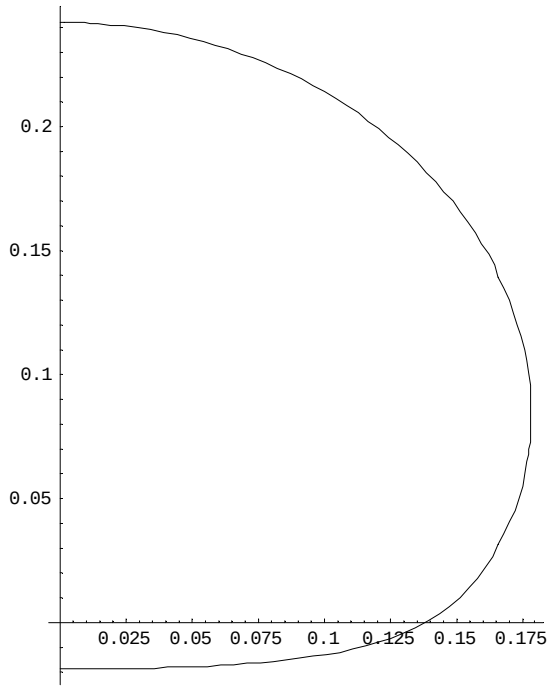

??Graphics??

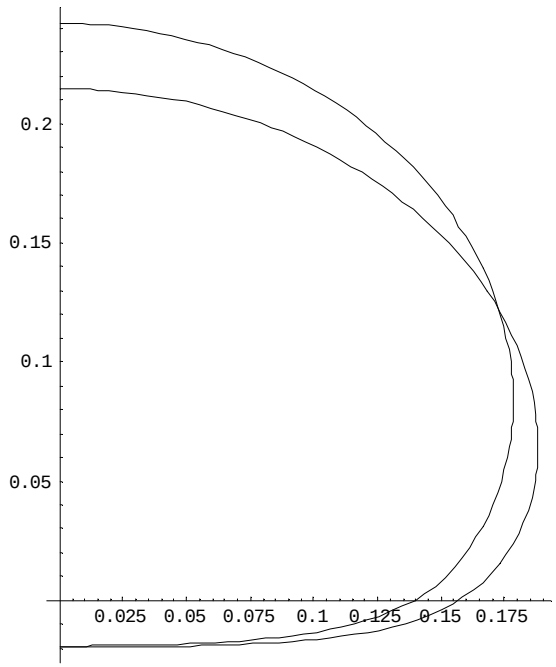

??Graphics??

```
M = ParametricPlot[Evaluate[{yy1[t], yy2[t]} & /. soln /. rts], {t, 0, 0.5},
  PlotRange → All, AspectRatio → Automatic, PlotPoints → 100]
U =
 ParametricPlot[
  Evaluate[{yy1[t] & c, yy5[t], yy2[t] & hf & c, yy6[t]} & /. soln /. rts],
   {t, 0, 0.5}, PlotRange → All, AspectRatio → Automatic, PlotPoints → 100]
];Plotting both left equilibrium shape M and left dynamic shape U;
V = Show[M, U]
```

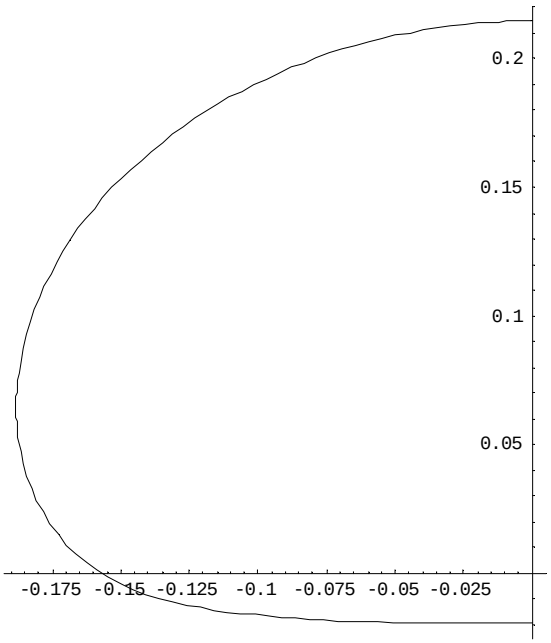


```
;;Graphics;;
```

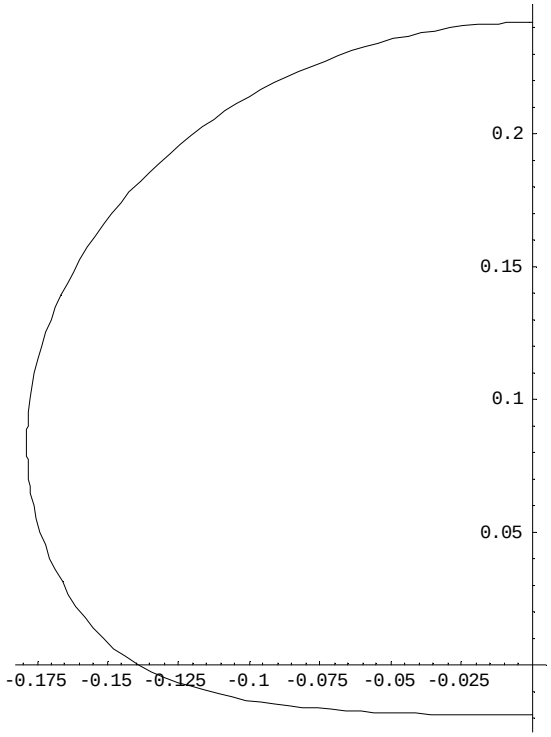

??Graphics??

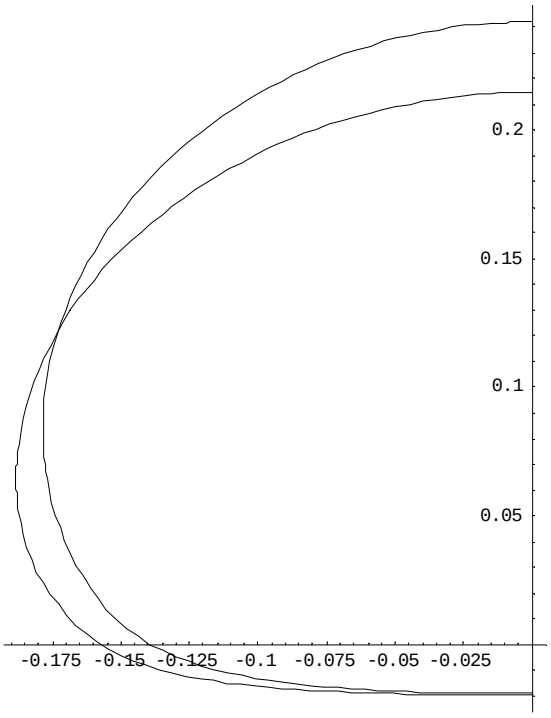

??Graphics??

W ? Show{H, V}

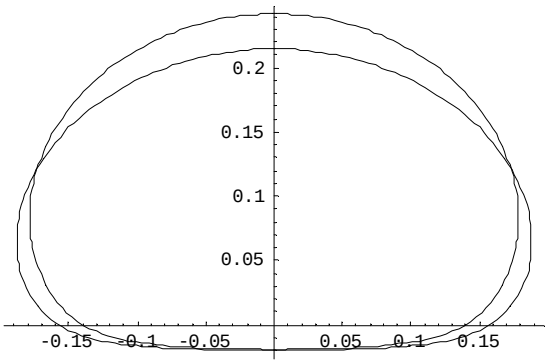

??Graphics??

```
(?Tabulating equilibrium x coordinate values in order to display
  shapes in Excel?)
xe ? Table[Evaluate[{yy1[t]}]. soln]. rts]}, {t, 0, 0.5, 1} 300]};
(?Tabulating equilibrium y coordinate values in order to display
  shapes in Excel?)
ye ? Table[Evaluate[{yy2[t] ? hf }]. soln]. rts]}, {t, 0, 0.5, 1} 300]};
(?Tabulating the right dynamic x coordinate values in order to display
  shapes in Excel?)
rxd ? Table[Evaluate[{Re[yy1[t]]} ? c ? Re[yy5[t]]} ]. soln]. rts]},
    {t, 0, 0.5, 1} 300]};
(?Tabulating the left dynamic x coordinate values in order to display
  shapes in Excel?)
lxd ? Table[Evaluate[{Re[?yy1[t]]} ? c ? Re[yy5[t]]} ]. soln]. rts]},
    {t, 0, 0.5, 1} 300]};
(?Tabulating the right dynamic y coordinate values in order to display
  shapes in Excel?)
ryd ? Table[Evaluate[{Re[yy2[t]]} ? hf ? c ? Re[yy6[t]]} ]. soln]. rts]},
    {t, 0, 0.5, 1} 300]};
(?Tabulating the left dynamic y coordinate values in order to display
  shapes in Excel?)
lyd ? Table[Evaluate[{Re[yy2[t]]} ? hf ? c ? Re[yy6[t]]} ]. soln]. rts]},
    {t, 0, 0.5, 1} 300]};
(?Creating and opening COORx text file, Writing to COORx text file,
 Closing COORx text file?)
tempt ? OpenAppend[COORx, PageWidth ? 30]
Write[tempt, xe, fffffffffffffffffffffffffff ]
Close[tempt]
tempt ? OpenAppend[COORy, PageWidth ? 30]
Write[tempt, ye, fffffffffffffffffffffffffff ]
Close[tempt]
tempt ? OpenAppend[COORlxd, PageWidth ? 30]
Write[tempt, lxd, fffffffffffffffffffffffffff ]
Close[tempt]
tempt ? OpenAppend[COORrxd, PageWidth ? 30]
Write[tempt, rxd, fffffffffffffffffffffffffff ]
Close[tempt]
tempt ? OpenAppend[COORryd, PageWidth ? 30]
Write[tempt, ryd, fffffffffffffffffffffffffff ]
Close[tempt]
tempt ? OpenAppend[COORlyd, PageWidth ? 30]
Write[tempt, lyd, fffffffffffffffffffffffffff ]
Close[tempt]

OutputStream[x.txt, 50]

x.txt

OutputStream[y.txt, 51]

y.txt
```

```
OutputStream[lxd.txt, 52]

lxd.txt

OutputStream[rxd.txt, 53]

rxd.txt

OutputStream[ryd.txt, 54]

ryd.txt

OutputStream[lyd.txt, 55]

lyd.txt

]?Writing new results to the SAVE text file to open later in MS Excel
  in order to graph relationships?]
PutAppend[p, k, hf, qe, w, qd, c, a, beta, SAVE]
```

E.3 Nonsymmetrical vibrations about equilibrium of an air-filled tube resting on a Winkler foundation

Mathematica code

```
]?Variables defined:
    p?internal air pressure
   hf?settlement of tube
    qe?initial equilibrium membrane tension ]located at origin]
     k?soil stiffness coefficient
      xe?horizontal coordinate
       ye?vertical coordinate
        theta_e??e?intial equilibrium angle measured from rigid
           surface to membrane
          theta_d??d?initial dynamic angle measured form the rigid
             surface to membrane
            qd?initial dynamic membrane tension ]located at origin]
              w?frequency of vibrations about equilibrium shape
               c?multiplier to visually vary the dynamic shape about
                the equilibrium shape
                t?scaled arc length?]
```

```
(?Clearing variables for solving a set of new cells?)
Clear[a, p, hf, gqd, gw, qe, k, pi, y1, y2, y3, y4, w];
(?where y1?xe, y2?ye, y3??e, y4?qe, y5?xd, y6?yd, y7??d, y8?qd?)
(?Defining the constant ??)
pi ? N[Pi];
(?Specifying internal air pressure?)
p ? 2;
k ? 200;
(?Equilibrium values [hf and qe] obtained from AirWinkEq.nb?)
hf ? 0.0149922449392862;
qe ? 0.106714875868214;
(?Guessing frequency and initial dynamic membrane tension?)
gw ? 9.66135117164242;
gqd ? 0.0153835248017288;
(?Setting arbitrary amplitude multiplier?)
c ? 5;
(?Naming output text file to contain dynamic properties?)
SAVE ? "2AirWinkVib5.txt";
(?Naming output directory for multiple files?)
DIR ? "2AirWinkVib5k200";
(?Naming output text files for graphing shapes later on?)
COORx ? "x.txt";
COORy ? "y.txt";
COORrxd ? "rxd.txt";
COORlxd ? "lxd.txt";
COORryd ? "ryd.txt";
COORlyd ? "lyd.txt";
(?Resetting the directory in order to start at the top of the
  driectory chain?)
ResetDirectory[];
(?Creating the directory DIR?)
CreateDirectory[DIR];
(?Setting the directory to DIR where files will finally be placed?)
SetDirectory[DIR];
```

```
(*Defining terms about equations taken from the derivation described
  in Chapter 5, Section 5.5*)
de[y2_, y3_, y4_, y5_, y6_, y7_, y8_, w_] :=
 {y1'[t] == Cos[y3[t]], y2'[t] == Sin[y3[t]],
  y3'[t] == If[y2[t] == hf, k*y2[t] == hf*Cos[y3[t]] == p*Cos[y3[t]]][y4[t]],
    p*Cos[y3[t]]][y4[t]],
  y4'[t] == If[y2[t] == hf, k*y2[t] == hf*Sin[y3[t]] == Sin[y3[t]], Sin[y3[t]]],
  y5'[t] == y7[t]*Sin[y3[t]], y6'[t] == y7[t]*Cos[y3[t]],
  y7'[t] ==
   If[y2[t] == hf,
    k*y6[t]*Cos[y3[t]] == k*y2[t] == hf*y7[t]*Sin[y3[t]] ==
        y8[t]*y4[t]] == k*y2[t] == hf*Cos[y3[t]]][y4[t] ==
     y8[t] == p*Cos[y3[t]]][y4[t] == y7[t]*Sin[y3[t]] ==
       w^2*y5[t]*Sin[y3[t]] == y6[t]*Cos[y3[t]]][y4[t],
    y8[t] == p*Cos[y3[t]]][y4[t] == y7[t]*Sin[y3[t]] ==
      w^2*y5[t]*Sin[y3[t]] == y6[t]*Cos[y3[t]]][y4[t]],
  y8'[t] == If[y2[t] == hf, k*y2[t] == hf*y7[t]*Cos[y3[t]] ==
     k*y6[t]*Sin[y3[t]] == y7[t]*Cos[y3[t]] ==
     w^2*y5[t]*Cos[y3[t]] == y6[t]*Sin[y3[t]]],
    y7[t]*Cos[y3[t]] == w^2*y5[t]*Cos[y3[t]] == y6[t]*Sin[y3[t]]]]]

(*Defining initial boundary conditions*)
leftBC[qd_] := {y1[0] == 0, y2[0] == 0, y3[0] == 0, y4[0] == qe, y5[0] == 0,
  y6[0] == 0, y7[0] == 0.001, y8[0] == qd}

(*Numerically solving the defined derivatives above*)
soln := NDSolve[Flatten[Append[de[y2, y3, y4, y5, y6, y7, y8, w], leftBC[qd]]],
  {y1, y2, y3, y4, y5, y6, y7, y8}, {t, 0, 0.5}, MaxSteps == 8000]

(*Applying the end point boundary conditions*)
endpt[w_, qd_] :=
  {y1[t], y2[t], y3[t], y4[t], y5[t], y6[t], y7[t], y8[t]} /.
    First[
     NDSolve[Flatten[Append[de[y2, y3, y4, y5, y6, y7, y8, w], leftBC[qd]]],
      {y1[t], y2[t], y3[t], y4[t], y5[t], y6[t], y7[t], y8[t]}, {t, 0, 0.5},
      MaxSteps == 22000]] /. t == 0.5;

(*Displaying end point values solved above before iterations*)
endpt[gw, gqd]

{0.000183006, 0.190957, 3.14192, 0.275198,
 2.45254*10^9, 5.99398*10^10, -0.0696017, 0.0160477}

Clear[w, qd]

(*Defining end point boundary conditions: {5}==y5 condition,
 setting the percent to change guess values in order to iterate,
 setting the accuracy goal of 5, setting number of iterations*)
rts := FindRoot[{endpt[w, qd][[5]] == 0, endpt[w, qd][[6]] == 0},
  {w, {gw, 0.98*gw}}, {qd, {gqd, 0.98*gqd}}, AccuracyGoal == 5,
  MaxIterations == 5000]
```

```
{?Displaying results of above shooting method?}
w ? w}. rts
qd ? qd}. rts
```

```
9.66135
```

```
0.0153835
```

```
{?Maximum tube height from origin?}
y ? Evaluate{yy2{0.5}}
```

```
0.190957
```

```
endpt{w}. rts, qd}. rts}
```

```
{?0.000183006, 0.190957, 3.14192, 0.275198,
 5.64319? 10^?11, ?7.29995? 10^?11, ?0.0696017, 0.0160477}
```

```
{?Solving terms in order to plot?}
{{yy1{t_}, yy2{t_}, yy3{t_}, yy4{t_}, yy5{t_}, yy6{t_}, yy7{t_}, yy8{t_}} ?
  {y1{t}, y2{t}, y3{t}, y4{t}, y5{t}, y6{t}, y7{t}, y8{t}}}. First{soln};
F ? ParametricPlot{Evaluate{{yy1{t}, yy2{t}} ? hf}}. soln}. rts},
  {t, 0, 0.5}, PlotRange ? All, AspectRatio ? Automatic, PlotPoints ? 100}
G ?
 ParametricPlot}
  Evaluate{{yy1{t} ? c ? yy5{t}, yy2{t}} ? hf ? c ? yy6{t}}}. soln}. rts},
  {t, 0, 0.5}, PlotRange ? All, AspectRatio ? Automatic, PlotPoints ? 100}
{?Plotting both right equilibrium shape F and right dynamic shape G?}
H ? Show{F, G}
```

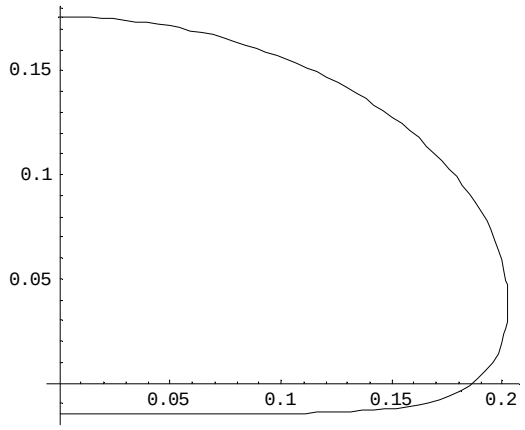


```
? ?Graphics??
```

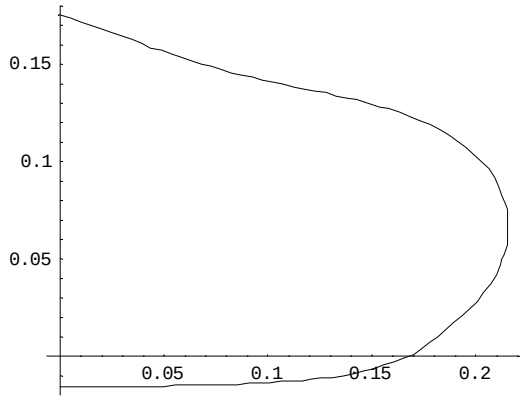

??Graphics??

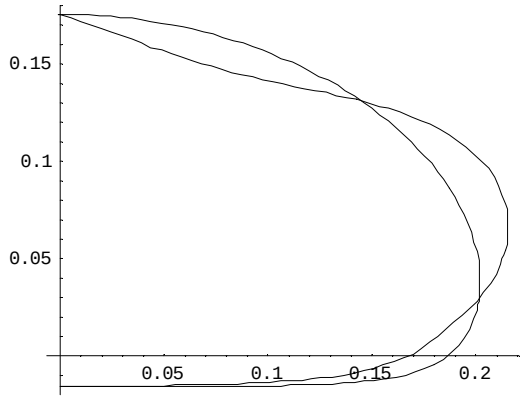

??Graphics??

```
M ? ParametricPlot[Evaluate[{?yy1[t], yy2[t]} ? hf] /. soln /. rts],
   {t, 0, 0.5}, PlotRange ? All, AspectRatio ? Automatic, PlotPoints ? 100]
U ?
 ParametricPlot[
  Evaluate[{?yy1[t] ? c ? yy5[t], yy2[t]} ? hf ? c ? yy6[t]}] /. soln /. rts],
   {t, 0, 0.5}, PlotRange ? All, AspectRatio ? Automatic, PlotPoints ? 100]
}?Plotting both left equilibrium shape F and left dynamic shape G?]
V ? Show[M, U]
```

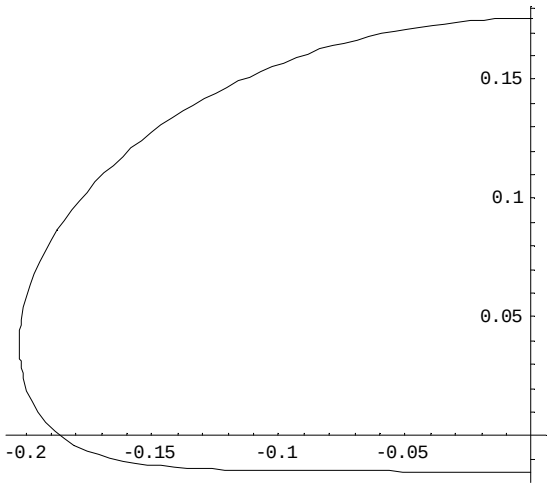

??Graphics??

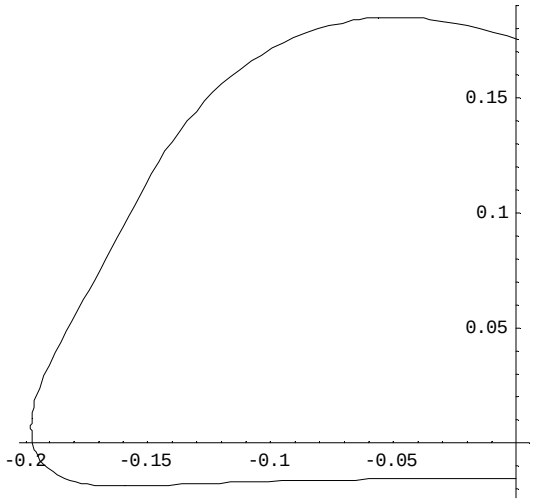

??Graphics??

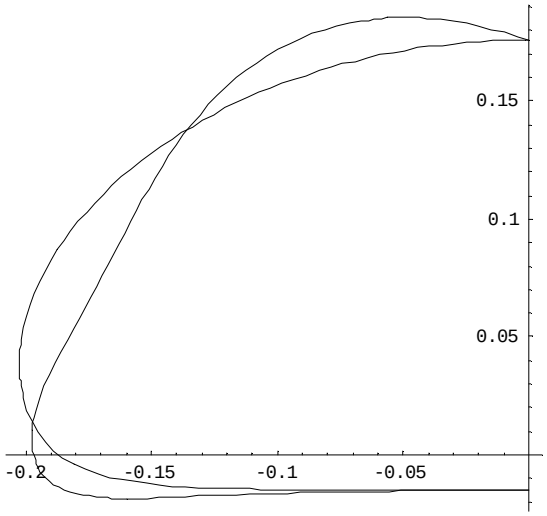

??Graphics??

```
W ? Show[H, V]
```

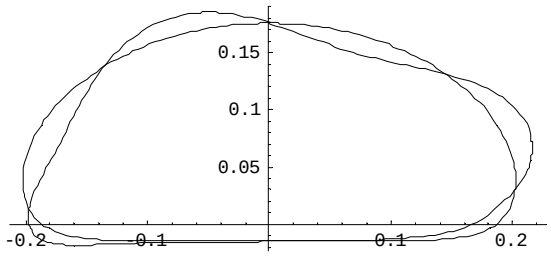


```
? Graphics
```

```
(*Tabulating equilibrium x coordinate values in order to display
  shapes in Excel*)
xe = Table[Evaluate[{yy1[t]}. soln. rts], {t, 0, 0.5, 1}300];
(*Tabulating equilibrium y coordinate values in order to display
  shapes in Excel*)
ye = Table[Evaluate[{yy2[t] + hf}. soln. rts], {t, 0, 0.5, 1}300];
(*Tabulating the right dynamic x coordinate values in order to
  display shapes in Excel*)
rxd = Table[Evaluate[{Re[yy1[t]] + c + Re[yy5[t]]}. soln. rts],
   {t, 0, 0.5, 1}300];
(*Tabulating the left dynamic x coordinate values in order to
  display shapes in Excel*)
lxd = Table[Evaluate[{Re[-yy1[t]] + c + Re[yy5[t]]}. soln. rts],
   {t, 0, 0.5, 1}300];
(*Tabulating the right dynamic y coordinate values in order to
  display shapes in Excel*)
ryd = Table[Evaluate[{Re[yy2[t]] + hf + c + Re[yy6[t]]}. soln. rts],
   {t, 0, 0.5, 1}300];
(*Tabulating the left dynamic y coordinate values in order to
  display shapes in Excel*)
lyd = Table[Evaluate[{Re[yy2[t]] + hf + c + Re[yy6[t]]}. soln. rts],
   {t, 0, 0.5, 1}300];
(*Creating and opening COORx text file, Writing to COORx text file,
 Closing COORx text file*)
tempt = OpenAppend[COORx, PageWidth → 30]
Write[tempt, xe, ffffffffffffffffffffffffffff]
Close[tempt]
tempt = OpenAppend[COORy, PageWidth → 30]
Write[tempt, ye, ffffffffffffffffffffffffffff]
Close[tempt]
tempt = OpenAppend[COORlxd, PageWidth → 30]
Write[tempt, lxd, ffffffffffffffffffffffffffff]
Close[tempt]
tempt = OpenAppend[COORrxd, PageWidth → 30]
Write[tempt, rxd, ffffffffffffffffffffffffffff]
Close[tempt]
tempt = OpenAppend[COORryd, PageWidth → 30]
Write[tempt, ryd, ffffffffffffffffffffffffffff]
Close[tempt]
tempt = OpenAppend[COORlyd, PageWidth → 30]
Write[tempt, lyd, ffffffffffffffffffffffffffff]
Close[tempt]
```

```
OutputStream[x.txt, 21]
```

x.txt

```
OutputStream[y.txt, 22]
```

y.txt

```
OutputStream[lxd.txt, 23]

lxd.txt

OutputStream[rxd.txt, 24]

rxd.txt

OutputStream[ryd.txt, 25]

ryd.txt

OutputStream[lyd.txt, 26]

lyd.txt

]?Writing new results to the SAVE text file to open later in MS
  Excel in order to graph relationships?]
PutAppend[p, k, hf, qe, w, qd, y, yhalf, c, SAVE]
```

Appendix F:

F.1 Equilibrium of an air-filled tube resting on a Pasternak foundation

Mathematica code

```
(?Variables defined:
    p?internal air pressure
   hf?settlement of tube
    qe?initial equilibrium membrane tension )located at origin(
     g?shear modulus
      k?soil stiffness coefficient
       xe?horizontal coordinate
        ye?vertical coordinate
         theta_e??e?intial equilibrium angle measured from rigid surface
            to membrane
            t?scaled arc length?)
(?Clearing variables for solving a set of new cells?)
Clear(h, ghf, gqe, qe, hf, k, pi, y1, y2, y3, y4);
(?where y1?xe, y2?ye, y3??e, y4?qe?)
(?Defining the constant ??)
pi ? N(Pi);
(?Specifying internal air pressure, soil stiffness coefficient,
 and shear modulus?)
p ? 2;
k ? 40;
g ? 0;
(?Guessing tube settlement and initial equilibrium membrane tension?)
ghf ? 0.0714051272526214;
gqe ? 0.158354937747283;
(?Naming output text file to contain dynamic properties?)
SAVE ? "2AirPastEq200.txt";
(?Naming output directory?)
DIR ? "2AirPastEq200";
(?Naming output text files to contain coordinate information?)
X ? "EPastXe.txt";
Y ? "EPastYe.txt";
(?Resetting the directory in order to start at the top of the driectory chain?)
((?ResetDirectory))];
 (?Creating the directory DIR?)
 CreateDirectory(DIR);
 (?Setting the directory to DIR where files will finally be placed?)
 SetDirectory(DIR);?)
```

```
(*Defining terms with equations taken from the derivation described
  in Chapter 5, Section 5.8*)
de[y2_, y3_, y4_, hf_] := {y1'[t] == Cos[y3[t]], y2'[t] == Sin[y3[t]],
  y3'[t] == If[y2[t] == hf, {p == Cos[y3[t]] == k == y2[t] == hf == Cos[y3[t]]},
     {y4[t] == g == {Cos[y3[t]]}^2, {1 - y4[t]} == {p == Cos[y3[t]]}}],
  y4'[t] == If[y2[t] == hf, Sin[y3[t]] == k == y2[t] == hf == Sin[y3[t]] ==
     g == Sin[y3[t]] == Cos[y3[t]] == {p == Cos[y3[t]]} == k == y2[t] == hf == Cos[y3[t]]},
     {{y4[t] == g == {Cos[y3[t]]}}^2, Sin[y3[t]]}]}

(*Defining initial boundary conditions*)
leftBC[qe_] := {y1[0] == 0, y2[0] == 0, y3[0] == 0, y4[0] == qe}

(*Numerically solving the defined derivatives above*)
soln := NDSolve[Flatten[Append[de[y2, y3, y4, hf], leftBC[qe]]],
  {y1, y2, y3, y4}, {t, 0, 0.5}, MaxSteps == 5000]

(*Applying the end point boundary conditions*)
endpt[hf_, qe_] :=
  {y1[t], y2[t], y3[t], y4[t]} /.
    First[NDSolve[Flatten[Append[de[y2, y3, y4, hf], leftBC[qe]]],
      {y1[t], y2[t], y3[t], y4[t]}, {t, 0, 0.5}, MaxSteps == 4000]] /. t == 0.5;

(*Displaying end point values solved above before iterations*)
endpt[ghf, gqe]

{1.97478*10^-9, 0.214738, 3.14159, 0.271121}

Clear[hf, qe]

(*Defining end point boundary conditions: {{5}}*y5 condition,
 setting the percent to change guess values in order to iterate,
 setting the accuracy goal of 5, setting number of iterations*)
rts := FindRoot[{endpt[hf, qe][[1]] == 0, endpt[hf, qe][[3]] == pi},
  {hf, {ghf, 0.95 ghf}}, {qe, {gqe, 0.95 gqe}}, AccuracyGoal == 2,
  MaxIterations == 3000]

(*Displaying results of above shooting method*)
hf == hf /. rts
qe == qe /. rts

0.0714051

0.158355

(*displaying maximum height of tube from origin*)
y == Evaluate[yy2[0.5]]

0.218942

endpt[hf /. rts, qe /. rts]

{4.29089*10^-10, 0.214738, 3.14159, 0.271121}

(*Solving terms in order to plot*)
{yy1[t_], yy2[t_], yy3[t_], yy4[t_]} =
  {y1[t], y2[t], y3[t], y4[t]} /. First[soln];
```

```
(?Plotting equilibrium shape?)
ParametricPlot(Evaluate((yy1(t), yy2(t) ? hf) /. soln /. rts), (t, 0, 0.5),
 PlotRange ? All, AspectRatio ? Automatic, PlotPoints ? 100)
```

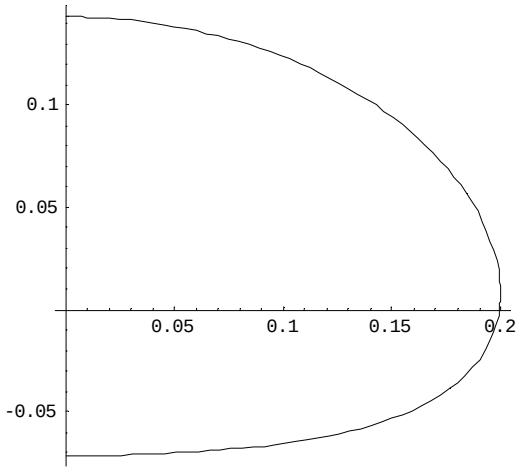


```
??Graphics??
```

```
(?Tabulating equilibrium x coordinate values in order to display
  shapes in Excel?)
xe ? Table(Evaluate((yy1(t) /. soln /. rts)), (t, 0, 0.5, 1(300)));
(?Creating and opening COORx text file, Writing to COORx text file,
 Closing COORx text file?)
tempt ? OpenAppend(X, PageWidth ? 30)
Write(tempt, xe, fffffffffffffffffffffffffff)
Close(tempt)
```

```
OutputStream(EPastqe(k?40 g?0).txt, 43)
```

```
EPastqe(k?40 g?0).txt
```

```
(?Tabulating equilibrium y coordinate values in order to display
  shapes in Excel?)
ye ? Table(Evaluate((yy2(t) ? hf /. soln /. rts)), (t, 0, 0.5, 1(300)));
(?Creating and opening Y text file, Writing to Y text file,
 Closing Y text file?)
tempt ? OpenAppend(Y, PageWidth ? 30)
Write(tempt, ye, fffffffffffffffffffffffffff)
Close(tempt)
```

```
OutputStream(EPastYe01.txt, 44)
```

```
EPastYe01.txt
```

```
(?Tablulating xe?s( in order to find max and min values to use for
  the calculation of the aspect ratio AR?)
 J ? Table(Evaluate((yy1(t) /. soln /. rts)), (t, 0, 0.5, 1(300)));
K ? Table(Evaluate((yy2(t) /. soln /. rts)), (t, 0, 0.5, 1(300)));
```

```
{?maximum x coordinate?}
xmax ? Max[J];
{?minimum x coordinate?}
xmin ? Min[J];
{?Aspect ratio?}
AR ? {2 ? xmax} } y
```

```
1.8238
```

```
{?Writing new results to the SAVE text file to open later in MS Excel
  in order to graph relationships?}
PutAppend[p, k, g, hf, qe, y, yhalf, AR, 0, SAVE]
```

F.2 Symmetrical vibrations about equilibrium of an air-filled tube resting on a Pasternak foundation

Mathematica code

```
{?Variables defined:
    p?internal air pressure
   hf?settlement of tube
    qe?initial equilibrium membrane tension [located at origin]
     g?shear modulus
      k?soil stiffness coefficient
       xe?horizontal coordinate
        ye?vertical coordinate
         theta_e??e?intial equilibrium angle measured from rigid
            surface to membrane
           theta_d??d?initial dynamic angle measured form the rigid
              surface to membrane
             qd?initial dynamic membrane tension [located at origin]
               w?frequency of vibrations about equilibrium shape
                c?multiplier to visually vary the dynamic shape about
                 the equilibrium shape
                 t?scaled arc length?]
```

```
(?Clearing variables for solving a set of new cells?)
Clear[a, p, hf, qe, qd, k, g, gqd, gw, qe, k, pi, y1, y2, y3, y4, w];
(?where y1?xe, y2?ye, y3??e, y4?qe, y5?xd, y6?yd,y7??d,y8?qd?)
(?Defining the constant ??)
pi ? N[Pi];
(?Specifying internal air pressure, soil stiffness coefficient,
 and shear modulus?)
p ? 3;
k ? 200;
g ? 30;
(?Equilibrium values {hf and qe} obtained from AirPastEq.nb?)
hf ? 0.00100523882359036;
qe ? 0.228077690014547;
(?Guessing frequency and initial dynamic membrane tension?)
gw ? 0.693006325799207;
gqd ? 0.0000266352329596943;
(?Setting arbitrary amplitude multiplier?)
c ? 100;
(?Naming output text file to contain dynamic properties?)
SAVE ? "3AirPastVib2k200.txt";
(?Naming output directory?)
DIR ? "3AirPastVib2k200";
(?Naming output text files to contain coordinate information?)
COORx ? "00x.txt";
COORy ? "00y.txt";
COORrxd ? "00rxd.txt";
COORlxd ? "00lxd.txt";
COORryd ? "00ryd.txt";
COORlyd ? "00lyd.txt";

(?Resetting the directory in order to start at the top of the driectory
  chain?)
ResetDirectory[]];
(?Creating the directory DIR?)
CreateDirectory[DIR];
(?Setting the directory to DIR where files will finally be placed?)
SetDirectory[DIR];
```

```
(*Defining terms about equations taken from the derivation described
  in Chapter 5, Section 5.10*)
de[y2_, y3_, y4_, y5_, y6_, y7_, y8_, w_] :=
 {y1'[t] == Cos[y3[t]], y2'[t] == Sin[y3[t]],
  y3'[t] == If[y2[t] == hf, {p*Cos[y3[t]] - k*(y2[t] - hf)*Cos[y3[t]]}/
     {y4[t]*g*(Cos[y3[t]])^2, 1/y4[t]*p*Cos[y3[t]]}],
  y4'[t] == If[y2[t] == hf, Sin[y3[t]]*k*(y2[t] - hf)*Sin[y3[t]] +
     g*Sin[y3[t]]*Cos[y3[t]] - p*Cos[y3[t]] + k*(y2[t] - hf)*Cos[y3[t]]]/
      (y4[t]*g*(Cos[y3[t]])^2), Sin[y3[t]]], y5'[t] == y7[t]*Sin[y3[t]]],
  y6'[t] == y7[t]*Cos[y3[t]],
  y7'[t] ==
   If[y2[t] == hf,
    k*y6[t]*Cos[y3[t]] - k*(y2[t] - hf)*y7[t]*Sin[y3[t]] -
     (y8[t]*g*y7[t]*Sin[2*y3[t]])/(y4[t]*g*(Cos[y3[t]])^2) -
      k*(y2[t] - hf)*Cos[y3[t]]*y7[t]*Sin[y3[t]]/(y4[t]*g*(Cos[y3[t]])^2) -
     (y8[t]*g*y7[t]*Sin[2*y3[t]])/(y4[t]*g*(Cos[y3[t]])^2) -
      p*Cos[y3[t]]*y7[t]*Sin[y3[t]]/(y4[t]*g*(Cos[y3[t]])^2) -
     w^2*y5[t]*Sin[y3[t]] - y6[t]*Cos[y3[t]]/(y4[t]*g*(Cos[y3[t]])^2),
    -(y8[t]*p*Cos[y3[t]])/y4[t] - y7[t]*Sin[y3[t]] -
     (w^2*y5[t]*Sin[y3[t]] - y6[t]*Cos[y3[t]])/y4[t]],
  y8'[t] ==
   If[y2[t] == hf, y7[t]*Cos[y3[t]] -
     (w^2*y5[t]*Cos[y3[t]] - y6[t]*Sin[y3[t]]) -
     k*(y2[t] - hf)*y7[t]*Cos[y3[t]] - k*y6[t]*Sin[y3[t]] -
     g*y7[t]*Cos[y3[t]]*Cos[y3[t]] -
     (k*(y2[t] - hf)*Cos[y3[t]]*p*Cos[y3[t]])/(y4[t]*g*(Cos[y3[t]])^2) -
     g*Sin[y3[t]] -
     Cos[y3[t]]*
      (k*y6[t]*Cos[y3[t]] - k*(y2[t] - hf)*y7[t]*Sin[y3[t]] -
       (y8[t]*g*y7[t]*Sin[2*y3[t]])/(y4[t]*g*(Cos[y3[t]])^2) -
       k*(y2[t] - hf)*Cos[y3[t]]*y7[t]*Sin[y3[t]]/(y4[t]*g*(Cos[y3[t]])^2) -
       (y8[t]*g*y7[t]*Sin[2*y3[t]])/(y4[t]*g*(Cos[y3[t]])^2) -
       p*Cos[y3[t]]*y7[t]*Sin[y3[t]]/(y4[t]*g*(Cos[y3[t]])^2) -
       w^2*y5[t]*Sin[y3[t]] - y6[t]*Cos[y3[t]]/(y4[t]*g*(Cos[y3[t]])^2) -
      y7[t]*Sin[y3[t]]*(k*(y2[t] - hf)*Cos[y3[t]] - p*Cos[y3[t]])/
       (y4[t]*g*(Cos[y3[t]])^2),
    y7[t]*Cos[y3[t]] - (w^2*y5[t]*Cos[y3[t]] - y6[t]*Sin[y3[t]])/y4[t]]]

(*Defining initial boundary conditions*)
leftBC[qd_] := {y1[0] == 0, y2[0] == 0, y3[0] == 0, y4[0] == qe, y5[0] == 0,
  y6[0] == 0.0001, y7[0] == 0, y8[0] == qd}

(*Numerically solving the defined derivatives above*)
soln := NDSolve[Flatten[Append[de[y2, y3, y4, y5, y6, y7, y8, w], leftBC[qd]]],
  {y1, y2, y3, y4, y5, y6, y7, y8}, {t, 0, 0.5}, MaxSteps -> 8000]
```

```
(*Applying the end point boundary conditions*)
endpt[w_, qd_] :=
  {y1[t], y2[t], y3[t], y4[t], y5[t], y6[t], y7[t], y8[t]} /.
    First[NDSolve[Flatten[Append[de[y2, y3, y4, y5, y6, y7, y8, w], leftBC[qd]]],
      {y1[t], y2[t], y3[t], y4[t], y5[t], y6[t], y7[t], y8[t]}, {t, 0, 0.5},
      MaxSteps -> 22000]] /. t -> 0.5;

(*Displaying end point values solved above before iterations*)
endpt[gw, gqd]

{0.000013522, 0.22608, 3.14153, 0.450166,
 9.72665*10^-7, 0.00011042, -6.19196*10^-6, 4.60463*10^-6}

Clear[w, qd]

(*Defining end point boundary conditions: {{5}} (*y5 condition,
 setting the percent to change guess values in order to iterate,
 setting the accuracy goal of 5, setting number of iterations*)
rts := FindRoot[{endpt[w, qd][[5]] == 0, endpt[w, qd][[7]] == 0},
  {w, {gw, 0.98 gw}}, {qd, {gqd, 0.98 gqd}}, AccuracyGoal -> 5,
  MaxIterations -> 5000]

(*Displaying results of above shooting method*)
w -> w /. rts
qd -> qd /. rts

0.69085

0.0000257385

endpt[w /. rts, qd /. rts]

{0.000013522, 0.22608, 3.14153, 0.450166,
 3.16654*10^-10, 0.000109572, -6.21069*10^-9, 2.86186*10^-6}

(*Solving terms in order to plot*)
{{yy1[t_], yy2[t_], yy3[t_], yy4[t_], yy5[t_], yy6[t_], yy7[t_], yy8[t_]} =
  {y1[t], y2[t], y3[t], y4[t], y5[t], y6[t], y7[t], y8[t]} /. First[soln];

F = ParametricPlot[Evaluate[{yy1[t], yy2[t]} = hf] /. soln /. rts,
  {t, 0, 0.5}, PlotRange -> All, AspectRatio -> Automatic, PlotPoints -> 100]
G =
 ParametricPlot[
  Evaluate[{yy1[t] = c = yy5[t], yy2[t] = hf = c = yy6[t]}] /. soln /. rts,
  {t, 0, 0.5}, PlotRange -> All, AspectRatio -> Automatic, PlotPoints -> 100]
(*Plotting both right equilibrium shape F and right dynamic shape G*)
H = Show[F, G]
```

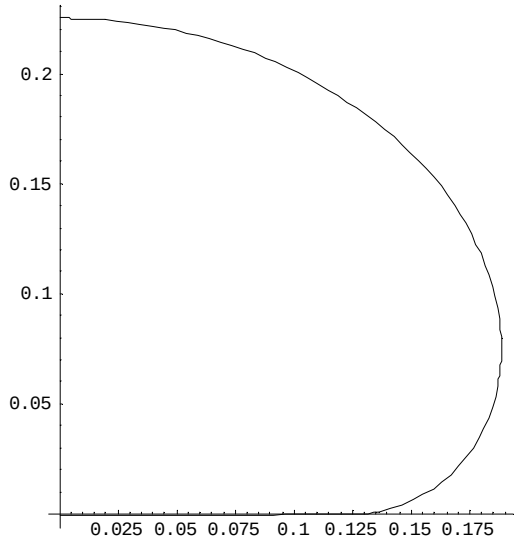

? ?Graphics??

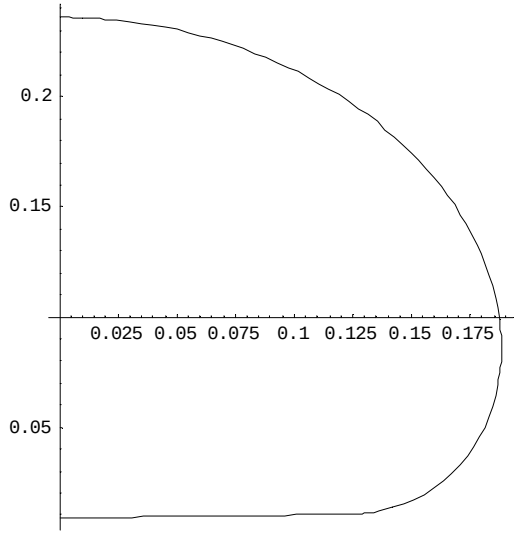

? ?Graphics??

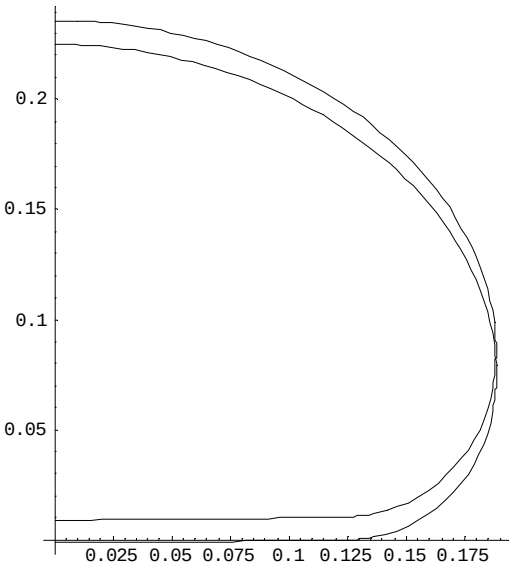

??Graphics??

```
M = ParametricPlot[Evaluate[{?yy1[t], yy2[t]} ? hf] /. soln /. rts],
   {t, 0, 0.5}, PlotRange → All, AspectRatio → Automatic, PlotPoints → 100]
U =
 ParametricPlot[
  Evaluate[{?yy1[t] ? c ? yy5[t], yy2[t]} ? hf ? c ? yy6[t]}] /. soln /. rts],
   {t, 0, 0.5}, PlotRange → All, AspectRatio → Automatic, PlotPoints → 100]
];?Plotting both left equilibrium shape M and left dynamic shape U?]
V = Show[M, U]
```

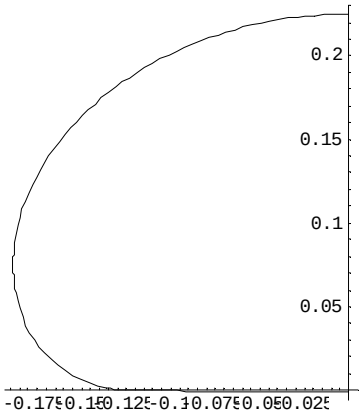

??Graphics??

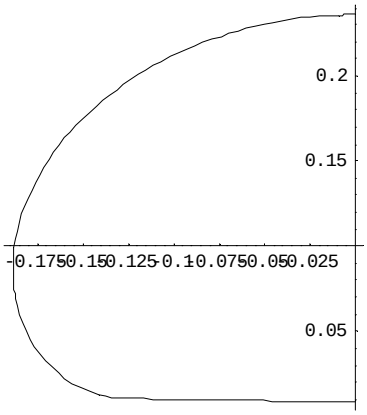

? Graphics

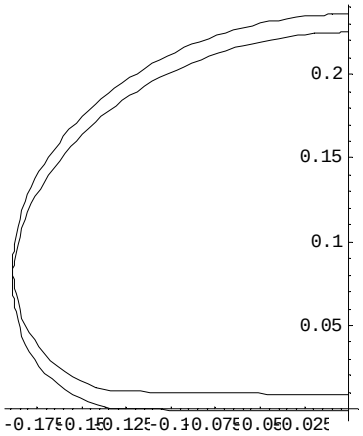

? Graphics

```
W = Show[H, V]
```

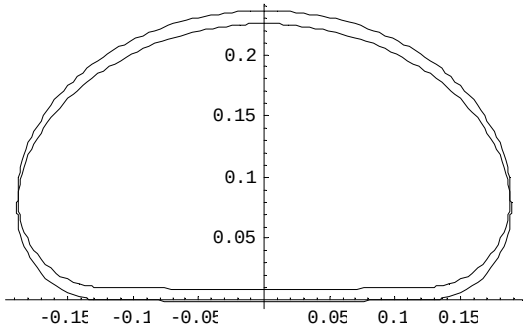

? Graphics

```
(?Tabulating equilibrium x coordinate values in order to display
  shapes in Excel?)
xe = Table[Evaluate[{yy1[t]}. soln. rts], {t, 0, 0.5, 1}300];
(?Tabulating equilibrium y coordinate values in order to display
  shapes in Excel?)
ye = Table[Evaluate[{yy2[t] ? hf}. soln. rts], {t, 0, 0.5, 1}300];
(?Tabulating the right dynamic x coordinate values in order to
  display shapes in Excel?)
rxd = Table[Evaluate[{Re[{yy1[t]}] ? c ? Re[yy5[t]]}. soln. rts],
    {t, 0, 0.5, 1}300];
(?Tabulating the left dynamic x coordinate values in order to display
  shapes in Excel?)
lxd = Table[Evaluate[{Re[{?yy1[t]}] ? c ? Re[yy5[t]]}. soln. rts],
    {t, 0, 0.5, 1}300];
(?Tabulating the dynamic y coordinate values in order to display
  shapes in Excel?)
yd = Table[Evaluate[{Re[{yy2[t]}] ? hf ? c ? Re[yy6[t]]}. soln. rts],
    {t, 0, 0.5, 1}300];
(?Creating and opening COORx text file, Writing to COORx text file,
 Closing COORx text file?)
tempt = OpenAppend[COORx, PageWidth = 30]
Write[tempt, xe, fffffffffffffffffffffffffff]
Close[tempt]
tempt = OpenAppend[COORy, PageWidth = 30]
Write[tempt, ye, fffffffffffffffffffffffffff]
Close[tempt]
tempt = OpenAppend[COORlxd, PageWidth = 30]
Write[tempt, lxd, fffffffffffffffffffffffffff]
Close[tempt]
tempt = OpenAppend[COORrxd, PageWidth = 30]
Write[tempt, rxd, fffffffffffffffffffffffffff]
Close[tempt]
tempt = OpenAppend[COORlyd, PageWidth = 30]
Write[tempt, lyd, fffffffffffffffffffffffffff]
Close[tempt]
tempt = OpenAppend[COORryd, PageWidth = 30]
Write[tempt, ryd, fffffffffffffffffffffffffff]
Close[tempt]

OutputStream[00x.txt, 15]

00x.txt

OutputStream[00y.txt, 16]

00y.txt

OutputStream[00lxd.txt, 17]

00lxd.txt
```

```
OutputStream[00rxd.txt, 18]

00rxd.txt

OutputStream[00lyd.txt, 19]

00lyd.txt

OutputStream[00ryd.txt, 20]

00ryd.txt

(*Writing new results to the SAVE text file to open later in MS
  Excel in order to graph relationships*)
PutAppend[p, k, g, hf, qe, w, qd, c, 0, SAVE]
```

F.3 Nonsymmetrical vibrations about equilibrium of an air-filled tube resting on a Pasternak foundation

Mathematica code

```
(*Variables defined:
    p=internal air pressure
   hf=settlement of tube
    qe=initial equilibrium membrane tension
      (located at origin)
     xe=horizontal coordinate
      ye=vertical coordinate
       theta_e=
       =e=intial equilibrium angle measured from
          rigid surface to membrane
        theta_d=
        =d=initial dynamic angle measured form
           the rigid surface to membrane
         qd=initial dynamic membrane tension
           (located at origin)
          w=frequency of vibrations about
           equilibrium shape
           c=multiplier to visually vary the
            dynamic shape about the equilibrium
            shape
            t=scaled arc length=)
```

```
(*Clearing variables for solving a set of new cells*)
Clear[a, p, hf, gqd, gw, qe, k, pi, y1, y2, y3, y4, w];
(*where y1=xe, y2=ye, y3=e, y4=qe, y5=xd, y6=yd,
 y7=d,y8=qd*)
(*Defining the constant *)
pi = N[Pi];
(*Specifying internal air pressure,
 soil stiffness coefficient, and shear modulus*)
p = 3;
k = 200;
g = 30;
(*Equilibrium values [hf and qe] obtained from
  AirPastEq.nb*)
hf = 0.00100523882359036;
qe = 0.228077690014547;
(*Guessing frequency and initial dynamic membrane
  tension*)
gw = 10.3330394381296;
gqd = 0.00104464252989462;
(*Setting arbitrary amplitude multiplier*)
c = 200;
(*Naming output text file to contain dynamic
  properties*)
SAVE = "3AirVibDampNonsym5.txt";
(*Naming output directory*)
DIR = "3AirVibDampNonsym5";
(*Naming output text files to contain coordinate
  information*)
COORx = "x.txt";
COORy = "y.txt";
COORrxd = "rxd.txt";
COORlxd = "lxd.txt";
COORryd = "ryd.txt";
COORlyd = "lyd.txt";
(*Resetting the directory in order to start at the
  top of the driectory chain*)
ResetDirectory[];
(*Creating the directory DIR*)
CreateDirectory[DIR];
(*Setting the directory to DIR where files will
  finally be placed*)
SetDirectory[DIR];
```

```
(*Defining terms about equations taken from the derivation described in Chapter 5,
 Section 5.10*)
de[y2_, y3_, y4_, y5_, y6_, y7_, y8_, w_] :=
 {y1'[t] == Cos[y3[t]], y2'[t] == Sin[y3[t]],
  y3'[t] == If[y2[t] == hf, (p*Cos[y3[t]] - k*(y2[t] - hf)*Cos[y3[t]])/(y4[t] - g*Cos[y3[t]]),
    (1 - y4[t]*p*Cos[y3[t]])/(y4[t]^2 - g*Cos[y3[t]])],
  y4'[t] == If[y2[t] == hf, Sin[y3[t]] == k*(y2[t] - hf)*Sin[y3[t]] ==
    g*Sin[y3[t]]*Cos[y3[t]] - p*Cos[y3[t]] - k*(y2[t] - hf)*Cos[y3[t]])/
     (y4[t] - g*Cos[y3[t]])^2, Sin[y3[t]]], y5'[t] == y7[t]*Sin[y3[t]]],
  y6'[t] == y7[t]*Cos[y3[t]],
  y7'[t] ==
   If[y2[t] == hf,
    (k*y6[t]*Cos[y3[t]] - k*(y2[t] - hf)*y7[t]*Sin[y3[t]] -
       (y8[t]*g*y7[t]*Sin[2*y3[t]])/(2*(y4[t] - g*Cos[y3[t]])^2)*k*(y2[t] - hf)*Cos[y3[t]])/
     (y4[t] - g*Cos[y3[t]])^2 -
     ((-(y8[t]*g*y7[t]*Sin[2*y3[t]])/(2*(y4[t] - g*Cos[y3[t]])^2))*p*Cos[y3[t]])/(y4[t] - g*Cos[y3[t]])^2 -
      (y7[t]*Sin[y3[t]]*w^2*y5[t]*Sin[y3[t]] - y6[t]*Cos[y3[t]])/(y4[t] - g*Cos[y3[t]])^2,
    (-y8[t]*p*Cos[y3[t]])/(y4[t] - y7[t]*Sin[y3[t]] -
      (w^2*y5[t]*Sin[y3[t]] - y6[t]*Cos[y3[t]])/(y4[t]),
  y8'[t] == If[y2[t] == hf, y7[t]*Cos[y3[t]] - w^2*y5[t]*Cos[y3[t]] - y6[t]*Sin[y3[t]]] -
    k*(y2[t] - hf)*y7[t]*Cos[y3[t]] - k*y6[t]*Sin[y3[t]] -
    g*y7[t]*Cos[y3[t]]*Cos[y3[t]]*k*(y2[t] - hf)*Cos[y3[t]] - p*Cos[y3[t]])/
     (y4[t] - g*Cos[y3[t]])^2 -
    g*Sin[y3[t]]*
     Cos[y3[t]]*
      (k*y6[t]*Cos[y3[t]] - k*(y2[t] - hf)*y7[t]*Sin[y3[t]] -
         (y8[t]*g*y7[t]*Sin[2*y3[t]])/(2*(y4[t] - g*Cos[y3[t]])^2)*k*
          (y2[t] - hf)*Cos[y3[t]])/(y4[t] - g*Cos[y3[t]])^2 -
       ((-(y8[t]*g*y7[t]*Sin[2*y3[t]])/(2*(y4[t] - g*Cos[y3[t]])^2))*p*Cos[y3[t]])/(y4[t] - g*Cos[y3[t]])^2 -
        (y7[t]*Sin[y3[t]]*w^2*y5[t]*Sin[y3[t]] - y6[t]*Cos[y3[t]])/(y4[t] - g*Cos[y3[t]])^2)/
     (y4[t] - g*Cos[y3[t]])^2,
    y7[t]*Cos[y3[t]]*w^2*y5[t]*Cos[y3[t]] - y6[t]*Sin[y3[t]]]]

(*Defining initial boundary conditions*)
leftBC[qd_] := {y1[0] == 0, y2[0] == 0, y3[0] == 0,
  y4[0] == qe, y5[0] == 0, y6[0] == 0, y7[0] == 0.001, y8[0] == qd}

(*Numerically solving the defined derivatives above*)
soln :=
 NDSolve[
  Flatten[{Append[de[y2, y3, y4, y5, y6, y7, y8, w],
    leftBC[qd]]}, {y1, y2, y3, y4, y5, y6, y7, y8},
  {t, 0, 0.5}, MaxSteps -> 8000]
```

```
(*Applying the end point boundary conditions*)
endpt[w_, qd_] :=
  {y1[t], y2[t], y3[t], y4[t], y5[t], y6[t], y7[t], y8[t]} /.
    First[
     NDSolve[Flatten[Append[de[y2, y3, y4, y5, y6, y7, y8, w],
        leftBC[qd]]], {y1[t], y2[t], y3[t], y4[t],
       y5[t], y6[t], y7[t], y8[t]}, {t, 0, 0.5},
      MaxSteps -> 22000]] /. t -> 0.5;

(*Displaying end point values solved above before
  iterations*)
endpt[gw, gqd]

{0.000013488, 0.22608, 3.14153, 0.450166,
 -2.30113*10^-7, -3.32466*10^-7, -0.00262719, 0.00094098}

Clear[w, qd]

(*Defining end point boundary conditions: {{5}}*)
  y5 condition, setting the percent to change guess
  values in order to iterate,
 setting the accuracy goal of 6,
 setting number of iterations*)
rts :=
 FindRoot[{endpt[w, qd][[5]] == 0, endpt[w, qd][[6]] == 0},
  {w, {gw, 0.98 gw}}, {qd, {gqd, 0.98 gqd}},
  AccuracyGoal -> 6, MaxIterations -> 5000]

(*Displaying results of above shooting method*)
w -> w /. rts
qd -> qd /. rts

10.3347

0.00104528

endpt[w /. rts, qd /. rts]

{0.0000134879, 0.22608, 3.14153, 0.450166,
 -1.71832*10^-9, 3.5835*10^-9, -0.00263047, 0.000946585}

(*Solving terms in order to plot*)
{{yy1[t_], yy2[t_], yy3[t_], yy4[t_], yy5[t_],
   yy6[t_], yy7[t_], yy8[t_]} =
  {y1[t], y2[t], y3[t], y4[t], y5[t], y6[t], y7[t], y8[t]} /.
   First[soln];
```

```
F = ParametricPlot[
  Evaluate[{yy1[t], yy2[t]} = hf] /. soln /. rts],
  {t, 0, 0.5}, PlotRange → All, AspectRatio → Automatic,
  PlotPoints → 100]
G = ParametricPlot[
  Evaluate[
   {yy1[t] = c yy5[t], yy2[t] = hf = c yy6[t]}] /. soln /. rts],
  {t, 0, 0.5}, PlotRange → All, AspectRatio → Automatic,
  PlotPoints → 100]
];Plotting both right equilibrium shape F and
  right dynamic shape G;
H = Show[F, G]
```

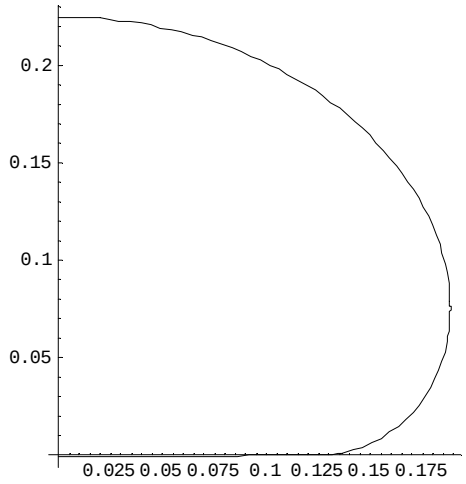

-Graphics-

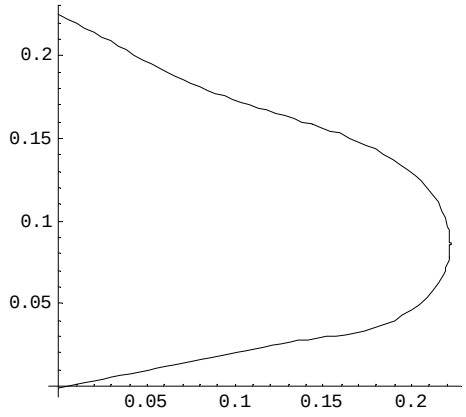

-Graphics-

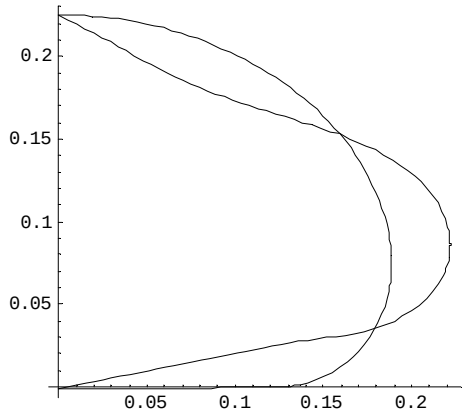

?Graphics??

```
M = ParametricPlot[
  Evaluate[{?yy1[t], yy2[t]} ? hf] /. soln /. rts],
  {t, 0, 0.5}, PlotRange ? All, AspectRatio ? Automatic,
  PlotPoints ? 100]
U = ParametricPlot[
  Evaluate[
   {?yy1[t] ? c ? yy5[t], yy2[t]} ? hf ? c ? yy6[t]}] /. soln /.
    rts], {t, 0, 0.5}, PlotRange ? All,
  AspectRatio ? Automatic, PlotPoints ? 100]
}?Plotting both left equilibrium shape M and left
  dynamic shape U?]
V = Show[M, U]
```

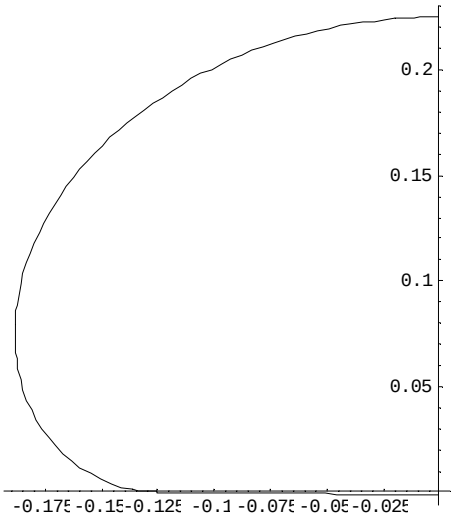

?Graphics??

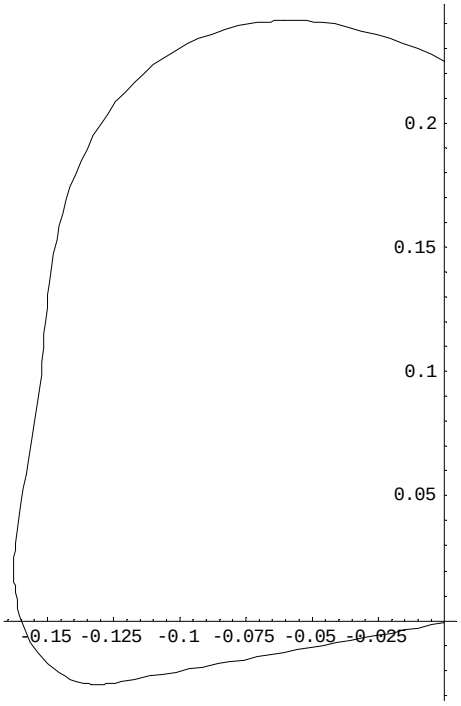

??Graphics??

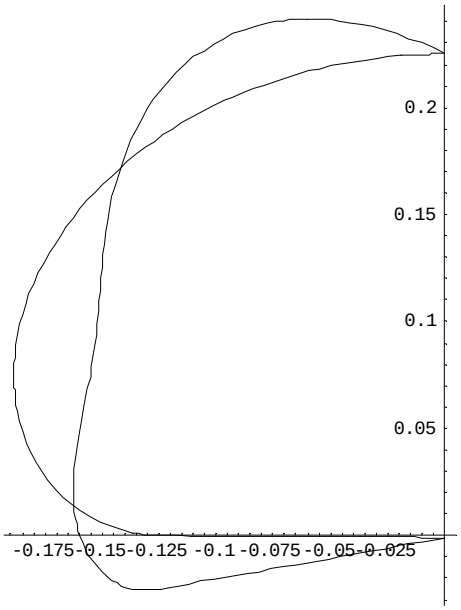

??Graphics??

W ? Show{H, V}

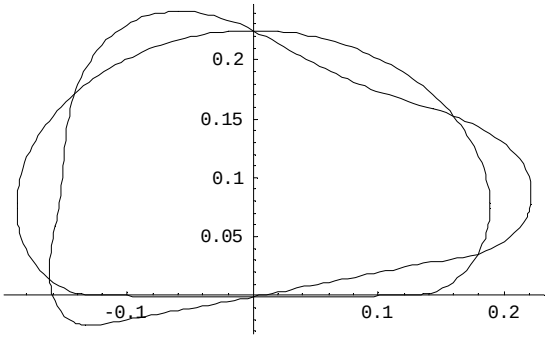

? Graphics

```
?Tabulating equilibrium x coordinate values in
  order to display shapes in Excel?
xe ? Table[Evaluate[{yy1[t]}. soln]. rts],
   {t, 0, 0.5, 1}, 300];
?Tabulating equilibrium y coordinate values in
  order to display shapes in Excel?
ye ? Table[Evaluate[{yy2[t] ? hf}. soln]. rts],
   {t, 0, 0.5, 1}, 300];
?Tabulating the right dynamic x coordinate values
  in order to display shapes in Excel?
rxd ? Table[Evaluate[{yy1[t] ? c ? yy5[t]}. soln]. rts],
   {t, 0, 0.5, 1}, 300];
?Tabulating the left dynamic x coordinate values
  in order to display shapes in Excel?
lxd ? Table[Evaluate[{?yy1[t] ? c ? yy5[t]}. soln]. rts],
   {t, 0, 0.5, 1}, 300];
?Tabulating the right dynamic y coordinate values
  in order to display shapes in Excel?
ryd ? Table[Evaluate[{yy2[t] ? hf ? c ? yy6[t]}. soln]. rts],
   {t, 0, 0.5, 1}, 300];
?Tabulating the left dynamic y coordinate values
  in order to display shapes in Excel?
lyd ? Table[Evaluate[{yy2[t] ? hf ? c ? yy6[t]}. soln]. rts],
   {t, 0, 0.5, 1}, 300];
?Creating and opening COORx text file,
 Writing to COORx text file, Closing COORx text file?
tempt ? OpenAppend[COORx, PageWidth ? 30]
Write[tempt, xe, fffffffffffffffffffffffffffff ]
Close[tempt]
tempt ? OpenAppend[COORy, PageWidth ? 30]
Write[tempt, ye, fffffffffffffffffffffffffffff ]
Close[tempt]
tempt ? OpenAppend[COORlxd, PageWidth ? 30]
Write[tempt, lxd, fffffffffffffffffffffffffffff ]
Close[tempt]
tempt ? OpenAppend[COORrxd, PageWidth ? 30]
Write[tempt, rxd, fffffffffffffffffffffffffffff ]
Close[tempt]
tempt ? OpenAppend[COORryd, PageWidth ? 30]
Write[tempt, ryd, fffffffffffffffffffffffffffff ]
Close[tempt]
tempt ? OpenAppend[COORlyd, PageWidth ? 30]
Write[tempt, lyd, fffffffffffffffffffffffffffff ]
Close[tempt]

OutputStream[x.txt, 8]

x.txt

OutputStream[y.txt, 9]
```

```
y.txt

OutputStream[lxd.txt, 10]

lxd.txt

OutputStream[rxd.txt, 11]

rxd.txt

OutputStream[ryd.txt, 12]

ryd.txt

OutputStream[lyd.txt, 13]

lyd.txt

]?Writing new results to the SAVE text file to open
  later in MS Excel in order to graph relationships?]
PutAppend[p, k, g, hf, qe, w, qd, c, 0, SAVE]
```

Vita

Stephen A. Cotton was born on January 4, 1979 to Danny B. Cotton and Linda M. Cotton of Arrington, TN. As a son of a career farmer, work ethic and love of nature were instilled at an early age. At Fred J. Page high school, an influential drafting teacher inspired ambition and drive to some day realizing his goal of becoming a practicing engineer.

Taking this inspiration, Stephen enrolled in Tennessee Technological University of Cookeville, TN in the fall of 1997. During his undergraduate career, three promising opportunities arose. One, being Tennessee Tech's American Society of Civil Engineering's student chapter president, taught him both leadership skills and patience. Two, after attending a research experience for undergraduates program at the University of Maine at Orono and benefiting from the guidance and knowledge of Dr. Eric Landis and Dr. William Davids, the thought of graduate school was planted. Lastly, working for the bridge design company Crouch Engineering, P.C., taught him both the role of a civil engineer and the hierarchy of communication.

In December 2001, Stephen received his Bachelor's degree in Civil Engineering, emphasizing structural engineering, from Tennessee Tech. Stephen was also granted his Engineering Intern License for the state of Tennessee in February, 2002. Within a month of graduating from Tennessee Tech, he relocated to Blacksburg, VA to pursue a Master's degree at Virginia Polytechnic Institute and State University emphasizing structural engineering. After graduation he will pursue his career as a civil engineer.